UNIVERSITAT DE BARCELONA

Modificación enzimática de la celulosa para la producción de biomateriales

Lourdes Verónica Cabañas Romero

Programa de doctorado de Biotecnología

Departamento de Genética, Microbiología y Estadística

Facultad de Biología

Modificación enzimática de la celulosa para la producción de biomateriales

Memoria presentada por Lourdes Verónica Cabañas Romero para optar al grado de Doctora por la Universidad de Barcelona

Directora y tutora

Dra. Susana V. Valenzuela

Doctoranda

Lourdes Verónica Cabañas Romero

El rollo de papiro supuso un fantástico avance. Tras siglos de búsqueda de soportes y de escritura humana sobre piedra, barro, madera o metal, el lenguaje encontró finalmente su hogar en la materia viva. El primer libro de la historia nació cuando las palabras, apenas aire escrito, encontraron cobijo en la médula de una planta acuática. Y, frente a sus antepasados inertes y rígidos, el libro fue desde el principio un objeto flexible, ligero, preparado para el viaje y la aventura.

…

Hablemos por un momento de ti, que lees estas líneas. Ahora mismo, con el libro abierto entre las manos, te dedicas a una actividad misteriosa e inquietante, aunque la costumbre te impide asombrarte por lo que haces. Piénsalo bien. Estás en silencio, recorriendo con la vista hileras de letras que tienen sentido para ti y te comunican ideas independientes del mundo que te rodea ahora mismo. Te has retirado, por decirlo así, a una habitación interior donde te hablan las personas ausentes, es decir, fantasmas visibles solo para ti (en este caso, mi yo espectral) y donde el tiempo pasa al compás de tu interés o aburrimiento. Has creado una realidad paralela parecida a la ilusión cinematográfica, una realidad que depende solo de ti. Tú puedes, en cualquier momento, apartar los ojos de estos párrafos y volver a participar en la acción y el movimiento del mundo exterior. Pero mientras tanto permaneces al margen, donde tú has elegido estar. Hay un aura casi mágica en todo esto.

¨El infinito en un junco¨

Irene Vallejo

La presente tesis fue patrocinada por una beca doctoral del Programa Nacional de Becas de Posgrado en el Exterior “Don Carlos Antonio López” (Ministerio de Hacienda, Paraguay)

Agradecimientos

Cuando comencé a escribir la tesis pensé que esta parte sería la más sencilla, pero no ha sido así. Escribir esta sección requiere hacer una retrospectiva, lo cual lleva tiempo, considerando que han sido cuatro años intensos.

Me siento enormemente agradecida a todos los que me han acompañado durante estos cuatro años que en general han pasado volando. Siento que estos agradecimientos se quedan cortos frente a la inmensa gratitud que siento hacia todos.

Quiero agradecer a mi directora y tutora de tesis, la Dra. Susana Valenzuela por el apoyo durante toda la tesis y lo mucho que he aprendido de ella, tanto sobre las enzimas como de la vida. A la Dra. Josefina Martínez, tutora de mi trabajo final de máster y que durante toda la tesis siempre ha estado pendiente de mi trabajo, especialmente en la parte más complicada y difícil que ha sido esta última etapa. Al Dr. Javier Pastor por confiar en mí para la tesis, por todas las siempre pertinentes aportaciones para los experimentos y los artículos. A la Dra. Pilar Diaz, desde el máster sus aportes han sido esclarecedores. En el lab 2 siempre me he sentido como en casa y esto sólo ha sido posible por el brillante y muy humano equipo de trabajo.

Muchas gracias al grupo CELBIOTECH, a la Dra. Blanca Roncero y a la Dra. Cristina Valls por recibirme en su laboratorio. Gracias a Julia, Noelia y a Antonio que siempre me ayudaron. He aprendido un montón.

À l'équipe BIA NANO du INRAE, merci beaucoup pour m'ouvrir vos portes sans à peine me connaître. Dès le premier jour je me suis sentie accueillie et part de votre équipe. Je suis spécialement reconnaissant au Dr. Ana Villares por sa guide pendant mon séjour là. Merci Margaux et Lisa pour tout, je ne sais pas ce que j'aurai fait sans votre aide. On se voit à Barcelone (ou Nantes)!

A mamá y papá. En casa nunca faltó el cariño, los libros, viajes y miles de anécdotas. Desde que tengo memoria me enseñaron a ser responsable, a trabajar (aunque si te gusta lo que haces no es trabajo, es puro *deleite*) y valorar los pequeños detalles de la

vida. Sin duda son mi mayor ejemplo. Quiero ser como ustedes. A Edu, ¨*che hermano*¨ sos un ejemplo de persona buena y de corazón puro. A toda mi familia que siempre me apoyó incondicionalmente, allá donde estuviera.

A los chicos del lab2 que han llenado el laboratorio de compañerismo y complicidad: Gala, Vivi, Melina, Marina, Noelia, Arnau, Marc y Maricarmen. Gracias a todo el equipo del lab5, mi otra casa, gracias especialmente a Laura y Sara, he aprendido muchísimo de ustedes, gracias por el apoyo constante, no olvido la *playlist* de los viernes tarde cuando no quedaba un alma en los laboratorios. Muchas gracias por las risas cuando más lo necesitaba.

Y desde luego, la hermana que me dio el lab2, Carol. *Sis*, me he sentido muchas veces muy perdida (como pimiento en sangría, como Tarzán en la discoteca) y siempre me enseñaste con toda la paciencia del mundo (tienes de verdad vocación de enseñar), gracias por esto y por hacer estos años más llevaderos. Nuestras anécdotas no cabrían en un solo libro. Hoy por hoy tenemos la tarea de seguir recorriendo de punta a punta Barcelona.

A mis amigas del alma (JdA), Whitney, Jesi y Ale. Estemos donde estemos, esparcidas por el mundo o juntas bajo una noche estrellada en la casa de alguna. Cada vez que hablamos es como si no hubiese pasado el tiempo. Son ejemplos de mujeres a las que admiro un montón.

A mis amigas del cole: Fati, Hilse, Belén y Paula. Siempre están presentes en mis pensamientos. ¡Nos vemos pronto con un tereré bien frío (o una *caipirinha*)!

Muchas gracias a Fati y Toni, grandes amigos que me dio Barcelona. Gracias por el apoyo, los viajes y los encuentros *random* de un domingo por la mañana que empezaban en un sitio de la ciudad y acababan en la otra punta horas después.

Avei aguyje *Consejo directivo grupo del grupo* Vy'a Paraguay-pe: Claudia, Vero, Sara, Karen, Gladis ha Edi akóinte oñangarekóva orerehe ha orembopiro'ýva. Umi polka

paraguaya jeroky chemoñeñandu hi'aguîve ógagui (ángante ajeroky porãveta). Maricarmen, aguyjevete peẽme pene angirũ rehe (pya'e jajohechata).

Sofi y Alba, del team *festivaleras* y *excursionistas*. Sofi, nuestra amistad comenzó hace muchos años gracias a *aquel máster* y hoy eres de mis personas favoritas, gracias por todas las charlas, los viajes, las excursiones, y, como no, los libros, la música, pelis y series.

A los *chochis*, Jon, Nathy y Jose. Son los mejores amigos que una persona puede tener. Como la pequeña familia que somos hemos pasado por muchas cosas juntas, muchísimas cosas buenas y otras no tanto, pero siempre nos hemos apoyado. Amistades como esta no tienen precio y son mi pequeño tesoro. Vic, gracias por tu preciosa amistad, las charlas, los *brunch* y los *podcasts* que nos mandamos siempre. *You are my sunshine*. Andressa, llenaste de alegría la casa, y, aunque no te guste el *feijão*, sos mi brasileña favorita.

A la prof. Celia Vázquez, no olvidaré todo el apoyo que siempre nos diste en aquellas clases de Fisicoquímica de los sábados. Creíste en nosotros, tus inquietos estudiantes, siempre nos motivaste a soñar y gracias a ti me permití soñar y hoy estoy aquí.

En fin, este camino no hubiese sido el mismo sin todas estas maravillosas personas. Mi eterno agradecimiento a todos.

Vero

Índice

Lista de abreviaturas

AA – Actividad auxiliar

BC – *Bacterial cellulose* (Celulosa bacteriana)

BC-ChI – Nanocomposición (*Nanocomposite*) de celulosa bacteriana con chitosán añadido por inmersión

BC-ChM - *Nanocomposite* de celulosa bacteriana con chitosan añadido por impregnación en masa

BC/Ag/TT – Soporte de papel de celulosa bacteriana con plata y tratamiento térmico

BC-ox/Ag/TT – Soporte de papel de celulosa bacteriana oxidada, con plata y tratamiento térmico

BED - *Backscattered electron detector* (detector de electrones retrodispersados)

C1 – Carbono 1

C4 – Carbono 2

CAZy - *Carbohydrate-Active enZYmes* (Enzimas activas sobre carbohidratos)

CBM – *Carbohydrate binding module* (Módulo de unión a carbohidratos)

EDS - *Energy-Dispersive X-ray Spectroscopy* (Espectroscopia de rayos X de energía dispersiva)

eu/Ag/TT – Soporte de papel de eucalipto con plata y tratamiento térmico

eu-ox/Ag/TT – Soporte de papel de eucalipto oxidado, con plata y tratamiento térmico

HPSEC- MALLS - *High-performance size exclusion chromatography (HPSEC) coupled with multi-angle laser light scattering detection (MALLS)* (Cromatografía de exclusión por tamaño de alto rendimiento (HPSEC) acoplado a la detección de dispersión de luz láser multiángulo (MALLS)

LPMO - *Lytic Polysaccharide Monooxygenase* (Monooxigenasa lítica de polisacáridos

MALDI-TOF - *Matrix-assisted Laser Desorption/Ionization-Time of Flight*

M_w - Masa molar promedio ponderada

M_n - Masa molar promedio en número

SEM - *Scanning Electron Microscopy* (Microscopía electronica de barrido)

PASC – *Phosporic acid swollen cellulose* (Celulosa hinchada con ácido fosfórico)

QCM-D - *Quartz crystal microbalance with dissipation* (Microbalanza de cristal de cuarzo con disipación)

Abstract

The growing concern for sustainability and the environmental impact of petroleum derivatives has driven the development of new materials based on renewable and eco-friendly sources. Among these materials, natural polymers like cellulose have emerged as one of the most promising alternatives to replace plastics and other polluting polymers. Cellulose, the most abundant polymer on Earth, has proven to be a valuable resource due to its biodegradable, renewable, and insoluble nature in many solvents, attributed to its hydrogen bonds and crystalline structure.

This thesis focuses on the modification of cellulose with two different purposes. Firstly, functionalization of cellulose was explored, aiming to impart new properties to the material. Secondly, the use of cellulases as biorefining agents for paper production was studied.

In the first functionalization, a biopolymer called chitosan was added to bacterial cellulose. Nanocomposites of bacterial cellulose and chitosan were produced using two different methods: immersing bacterial cellulose paper in an aqueous chitosan solution (BC−ChI) and impregnating bacterial cellulose pulp with chitosan before paper production (BC−ChM). These nanocomposites were investigated to evaluate their physical characteristics, antimicrobial and antioxidant properties, as well as their ability to inhibit biofilm formation on their surface. Both nanocomposites retained the hydrophobic character and barrier properties of bacterial cellulose. Additionally, they exhibited antimicrobial activity against *Staphylococcus aureus* and *Pseudomonas aeruginosa*, as well as *Candida albicans*. Furthermore, the incorporation of chitosan increased the antioxidant activity of bacterial cellulose.

The second functionalization focused on the enzymatic modification of bacterial and plant-origin cellulose using the oxidative enzyme SamLPMO10C, a lytic polysaccharide monooxygenase (LPMO). Bacterial and plant-origin celluloses were functionalized through enzymatic oxidation, which increased the number of carboxyl groups in both. Subsequently, a silver nitrate solution was added, and paper supports containing silver nanoparticles were produced, allowing interaction between silver ions and hydroxyl or carboxyl groups of the celluloses. The formation of silver nanoparticles occurred through thermal reduction. These silver-functionalized paper supports exhibited antibacterial activity against *Staphylococcus aureus*.

SamLPMO10C demonstrated its potential as a cellulose-modifying enzyme, prompting research into expression strategies to produce these enzymes more efficiently, rapidly, and economically. Two active LPMOs, SamLPMO10C and ShaLPMO10A, were successfully produced in *Escherichia coli* and *Streptomyces lividans*. Additionally, both enzymes showed oxidative activity across a wide temperature range, making them promising candidates for industrial applications. The effect of these enzymes on the molar mass of cellulose throughout the oxidation reaction was studied, showing that the molar mass decreases as the reaction progresses. SamLPMO10C and ShaLPMO10A bound firmly to bacterial cellulose which showed mass change due to the enzymatic activity very early at the beginning of the reaction.

The second cellulose modification involved evaluating the potential of the enzyme Cel6D, a recently discovered exocellulase, as a biorefining agent for flax pulp. Its effects were compared with another enzyme, Cel9B, and a combination of both. The results indicated that treatments with Cel6D and Cel9B, either separately or combined, improved the air permeability of flax pulp sheets. Moreover, the enzymes had varied effects on the mechanical properties of the handsheets, such as tensile strength index, tear resistance index, and tensile index, suggesting that exocellulases and endocellulases may have different applications in biorefining processes and other biotechnological applications.

Resumen

La creciente preocupación por la sostenibilidad y el impacto ambiental de los derivados del petróleo ha impulsado el desarrollo de nuevos materiales basados en fuentes renovables y amigables con el medio ambiente. Entre estos materiales, los polímeros naturales, como la celulosa, han surgido como una de las alternativas más prometedoras para reemplazar los a los plásticos y otros polímeros contaminantes. La celulosa, que es el polímero más abundante en la tierra, ha demostrado ser un recurso valioso debido a su carácter biodegradable, renovable e insoluble en muchos solventes, atribuido a sus enlaces de hidrógeno y su estructura cristalina.

Esta tesis se enfoca en la modificación de la celulosa con dos propósitos diferentes. Primeramente, se exploró la funcionalización de la celulosa, es decir dotar este material de nuevas propiedades. Luego, se estudió el uso de celulasas como agentes biorefinadores para la producción de papel.

La primera funcionalización consistió en añadir a la celulosa bacteriana un biopolímero, el quitosano. Se produjeron nanocomposites de celulosa bacteriana y quitosano mediante dos métodos diferentes: sumergiendo hojas de celulosa bacteriana en una solución acuosa de quitosano (BC−ChI) y empapando la pulpa de celulosa bacteriana con quitosano antes de producir hojas de papel (BC−ChM). Estos nanocomposites se investigaron para evaluar sus características físicas, sus propiedades antimicrobianas y antioxidantes, así como su capacidad para inhibir la formación de biofilms en su superficie. Ambos nanocomposites conservaron el carácter hidrofóbico y las propiedades de barrera de la celulosa bacteriana. Además, los nanocomposites mostraron actividad antimicrobiana contra *Staphylococcus aureus* y *Pseudomonas aeruginosa*, así como contra la levadura *Candida albicans*. También se encontró que la incorporación de quitosano aumentó la actividad antioxidante de la celulosa bacteriana.

La segunda funcionalización se centró en la modificación enzimática de la celulosa bacteriana y vegetal mediante el uso de la enzima oxidativa SamLPMO10C, una monooxigenasa lítica de polisacáridos (LPMO). La celulosa bacteriana y vegetal fueron funcionalizadas por oxidación enzimática, lo que aumentó la cantidad de grupos carboxilo en ambas. A continuación, se añadió una solución de nitrato de plata y se produjeron soportes de papel que contenían

nanopartículas de este metal, lo que permitió la interacción entre los iones de plata y los grupos hidroxilo o carboxilo de las celulosas. La formación de nanopartículas de plata se dio mediante reducción térmica. Estos soportes de papel funcionalizados con plata exhibieron propiedades antibacterianas contra *Staphylococcus aureus*.

SamLPMO10C demostró su potencial como enzima modificadora de celulosa y, por tanto, impulsó la investigación de estrategias de expresión que permitieran producir este tipo de enzimas de manera más eficiente, rápida y económica. Se ha producido exitosamente dos LPMOs activas, SamLPMO10C y ShaLPMO10A, en *Escherichia coli* y *Streptomyces lividans*. El efecto de estas enzimas en la masa molar de la celulosa a lo largo de la oxidación enzimática se estudió demostrando que la masa molar de la celulosa disminuye a medida que la reacción avanza. SamLPMO10C y ShaLPMO10A se unieron firmemente a la celulosa bacteriana y ambas enzimas mostraron cambios de masa debido a la acción enzimática al principio de la reacción. Seguidamente, se observó que ambas mostraron actividad oxidativa en un amplio rango de temperaturas, lo que las convierte en candidatas prometedoras para ser utilizadas a nivel industrial.

La segunda modificación de la celulosa consistió en la evaluación del potencial de la enzima Cel6D, una exocelulasa recientemente descubierta, como agente biorefinador para la pasta de lino. Se compararon los efectos de Cel6D con otra enzima, Cel9B, y una combinación de ambas. Los resultados mostraron que los tratamientos con las enzimas Cel6D y Cel9B, tanto por separado como combinadas, mejoraron la permeabilidad al aire de las hojas de pasta de lino. Además, las enzimas tuvieron efectos variados en las propiedades mecánicas de las hojas de papel, como el índice de resistencia a la tensión, el índice de resistencia a la tracción y el índice de resistencia al rasgado, lo que sugiere que las exocelulasas y endocelulasas pueden tener aplicaciones diferenciadas en procesos de biorefinado y en otras aplicaciones biotecnológicas.

1. INTRODUCCIÓN

La influencia del petróleo y sus derivados como los plásticos en nuestro día a día es innegable. Los combustibles fósiles son la fuente de energía para el transporte y la industria y se utilizan para generar calor y electricidad, contribuyendo con alrededor del 80 % de las emisiones de gases de efecto invernadero producidas a nivel mundial (Antar *et al*., 2021). Aunque la producción de plásticos a gran escala solo data de la década de 1950, ésta se ha incrementado de 2 a 380 megatoneladas entre 1950 y 2015 (Geyer *et al*., 2017). Junto con el volumen de producción y consumo mundial de plásticos, crecen las diversas preocupaciones sobre su impacto en el ecosistema y la salud humana. Una de las estrategias para mitigar los efectos nocivos de los plásticos es su sustitución por materiales sostenibles y ecológicos que utilicen materias primas renovables y biodegradables provenientes, por ejemplo, de plantas, algas o quitina (Rosenboom *et al*., 2022; Tanpichai *et al*., 2022; Tennakoon *et al*., 2023). Sin embargo, para que esto sea factible es necesario que estos biomateriales adquieran nuevas propiedades fisicoquímicas que permitan aumentar su rango de aplicabilidad. Por otro lado, en la producción industrial intervienen procesos muy exigentes desde el punto de vista energético y contaminantes. La intervención de la actividad enzimática en algunos de estos procesos puede suponer, como ha sido ampliamente demostrado, una reducción de costes energéticos y en la generación de residuos perjudiciales para el medio ambiente (Gil *et al*., 2009).

La presente tesis doctoral se enfoca en la modificación de la celulosa, el biopolímero más abundante de la Tierra, siguiendo dos enfoques principales. Por un lado, se ha funcionalizado la celulosa y se han producido nuevos materiales. Por otro lado, se ha llevado a cabo su digestión enzimática parcial con el objetivo de producir papeles con propiedades mecánicas mejoradas. Se han realizado dos tipos de funcionalizaciones: la primera consistió en añadir quitosano, un derivado de la quitina con propiedades antimicrobianas y antioxidantes, a la celulosa bacteriana. La otra funcionalización consistió en oxidar enzimáticamente la celulosa con una monooxigenasa lítica de polisacáridos, LPMO (*Lytic Polysaccharide Monooxigenase*) por sus siglas en inglés, para a continuación añadir iones de plata, como modelo de ligando, a la matriz de celulosa. Las LPMOs son enzimas recientemente descubiertas capaces de romper el enlace glucosídico que une las glucosas de la cadena de celulosa mediante un mecanismo oxidativo. Su interés biotecnológico sigue creciendo por sus aplicaciones para la producción de biocombustibles, nuevos materiales y *building blocks* y ha motivado a que en esta tesis se estudie con profundidad a dos LPMOs, SamLPMO10C, una LPMO previamente clonada y expresada en el grupo de investigación y, la ShaLPMO10A, caracterizada por primera vez en este trabajo. Finalmente, la digestión enzimática parcial de pastas papeleras se ha llevado a cabo con celulasas, un grupo de enzimas que pertenecen a la familia las glucosil hidrolasas y

son responsables de la hidrólisis de los enlaces β-1,4 de la celulosa. Tienen múltiples aplicaciones en la industria alimenticia, textil, biorefinerías y en esta tesis concretamente se han utilizado las celulasas Cel6D y la Cel9B de *Paenibacillus barcinonensis* como potenciales agentes de biorefino de pastas papeleras y se han estudiado las propiedades fisicomecánicas de los papeles resultantes. En los siguientes apartados se tratan todos estos elementos para un mejor entendimiento.

1.1. La pared celular vegetal

La pared celular vegetal es una matriz extracelular muy compleja que encierra a la célula vegetal. Tiene como función restringir la presión de turgencia, proteger a la célula contra patógenos y herbívoros y brindar coherencia estructural a la planta como una interfaz adhesiva entre las células. La composición de la pared celular y las proporciones de sus diferentes constituyentes pueden variar ampliamente entre diferentes tipos de células, especies y etapas de desarrollo. Está compuesta principalmente por celulosa, hemicelulosas, pectinas y glicoproteínas, y en ocasiones se encuentra reforzada por polímeros aromáticos como la lignina (Jordan *et al*., 2012; Pedersen *et al*., 2023). La pared celular de los vegetales tiene una estructura común compuesta de una pared primaria, una pared secundaria y la lámina media (Fig.1A). A medida que crece una célula, primero se secreta la pared primaria, compuesta de fibras de celulosa en una matriz de hemicelulosa y pectina; la hemicelulosa se une a la superficie de las microfibrillas de celulosa, mientras que la pectina retícula las moléculas de hemicelulosa de las microfibrillas adyacentes. Una vez que el crecimiento celular se detiene, la pared ya no necesita ser extensible por lo que a veces la pared primaria se mantiene sin modificaciones importantes, pero, más comúnmente, se produce una pared celular secundaria rígida cuyo polímero adicional más común es la lignina. Finalmente, la lámina media, la parte más externa de la pared celular, es la región especializada que une las paredes de las células adyacentes (Pedersen *et al*., 2023).

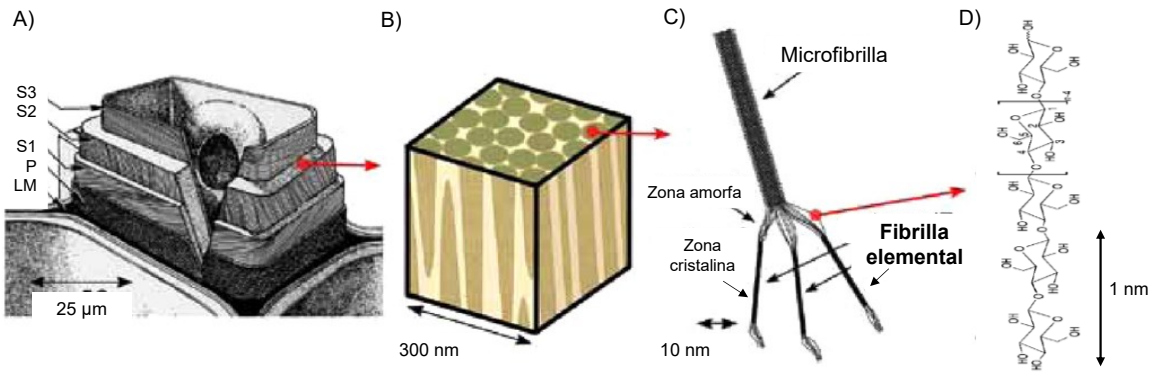

Figura 1 Organización jerárquica de la pared celular. A) Estructura de la pared celular B) Matriz de estructura de fibrillas C) Estructura de la microfibrilla D) Celulosa. LM = lámina media, P = pared celular primaria, S1, S2, S3 = capas de la pared celular secundaria. Imagen modificada de Postek *et al*., (2011).

1.2. Celulosa

En 1838 el químico francés Anselme Payen aisló una sustancia extraída de diversos tejidos vegetales con ácidos y amoníaco, seguida de una extracción posterior con agua, alcohol y éter. Determinó que la fórmula molecular de dicha sustancia era $C_6H_{10}O_5$ por medio de un análisis elemental y observó su isomería con el almidón. Llamó a esta sustancia, que encontró en abundancia en las paredes celulares de todas las plantas que estudió, celulosa (Payen, 1838).

La celulosa es el biopolímero más abundante en la tierra y es el componente principal de la pared celular vegetal. La producción de biomasa celulósica ocurre principalmente a través de la fotosíntesis realizada por algas y plantas superiores. Sin embargo, también hay organismos no fotosintéticos que producen celulosa, como ciertas especies bacterianas, algunos invertebrados marinos, hongos, gusanos de seda, amebas y tunicados (Tanpinchai *et al*., 2021). La celulosa es un polímero biodegradable, renovable e insoluble en la mayoría de los solventes debido a sus enlaces de hidrógeno y su cristalinidad (Klemm *et al*., 2005). Su estructura molecular está compuesta por unidades de 500-1500 residuos de glucosa unidas por enlaces O-glucosídicos β (1→4). Estos residuos contiguos de glucosa han girado 180º unas respecto a otras a lo largo del eje molecular y en torno a él formando largas cadenas lineales. Es esta "base" de celobiosa (dos residuos de glucosa contiguos que han girado 180º una respecto a otra) la que permite que las cadenas de celulosa formen redes de enlaces de hidrógeno intramoleculares e intermoleculares que dan como resultado tramos cristalinos fuertes e insolubles (Deligey *et al*.,

2022). La cadena de celulosa consta de un extremo de una unidad de D-glucosa con un grupo C4-OH original (el extremo no reductor); el otro extremo termina con un grupo C1-OH original, que está en equilibrio con la estructura del aldehído (extremo reductor) (Fig. 2).

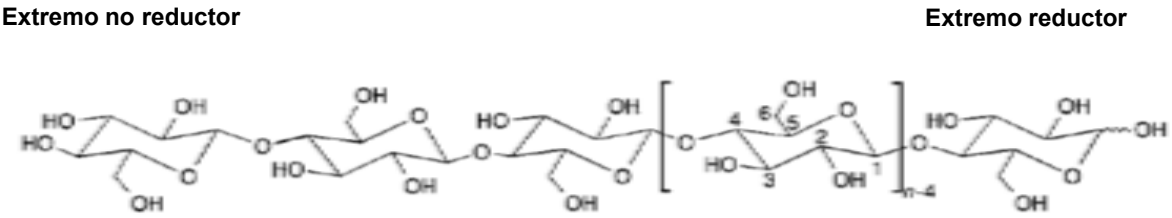

Figura 2 Estructura molecular de la celulosa. *n*= grado de polimerización. Imagen modificada de Klemm *et al*. (2005).

Las cadenas de celulosa se unen mediante puentes de hidrógeno y fuerzas de van der Waals para formar microfibrillas, que contienen varias fibrillas elementales con diámetros de 5 a 50 nm y longitudes de varios micrómetros (Deligey *et al*., 2022; Moon *et al*., 2011).

La biosíntesis de la microfibrilla de celulosa ocurre en varios pasos y es muy específica para los diferentes organismos productores de celulosa. Las variaciones en su síntesis determinarán su grado de polimerización, morfología y estructura cristalina (Polko and Kieber, 2019). La celulosa es el principal componente de la pared celular de las plantas, sin embargo, un solo componente, la celulosa sintasa (CESA, *cellulose synthase),* se ha identificado como responsable de biosíntesis de la celulosa. Las proteínas CESA están compuestas por una región N-terminal citosólica, un gran bucle central citoplasmático que contiene las regiones catalíticas y de unión al sustrato, seis dominios transmembrana adicionales y, finalmente, un dominio C-terminal intracelular (Fig. 3 A). La Fig. 3B muestra que dieciocho proteínas CESA se agrupan para formar el denominado complejo de celulosa sintasa (CSC, *cellulose synthase complex*). Cada enzima CESA sintetiza una fibrilla elemental de celulosa, por tanto 18 fibrillas formarán una microfibrilla (Polko and Kieber, 2019). Estudios de modelado examinaron diferentes formas de organización de la celulosa dentro de una microfibrilla de 18 cadenas demostrando que el modelo ¨234432¨ es más probable, es decir, las cadenas de celulosa se apilan en la microfibrilla en una disposición de dos cadenas, seguido de tres cadenas, seguido de cuatro cadenas, etc. como se muestra en la Fig. 3C Yang y Kubicki, (2020).

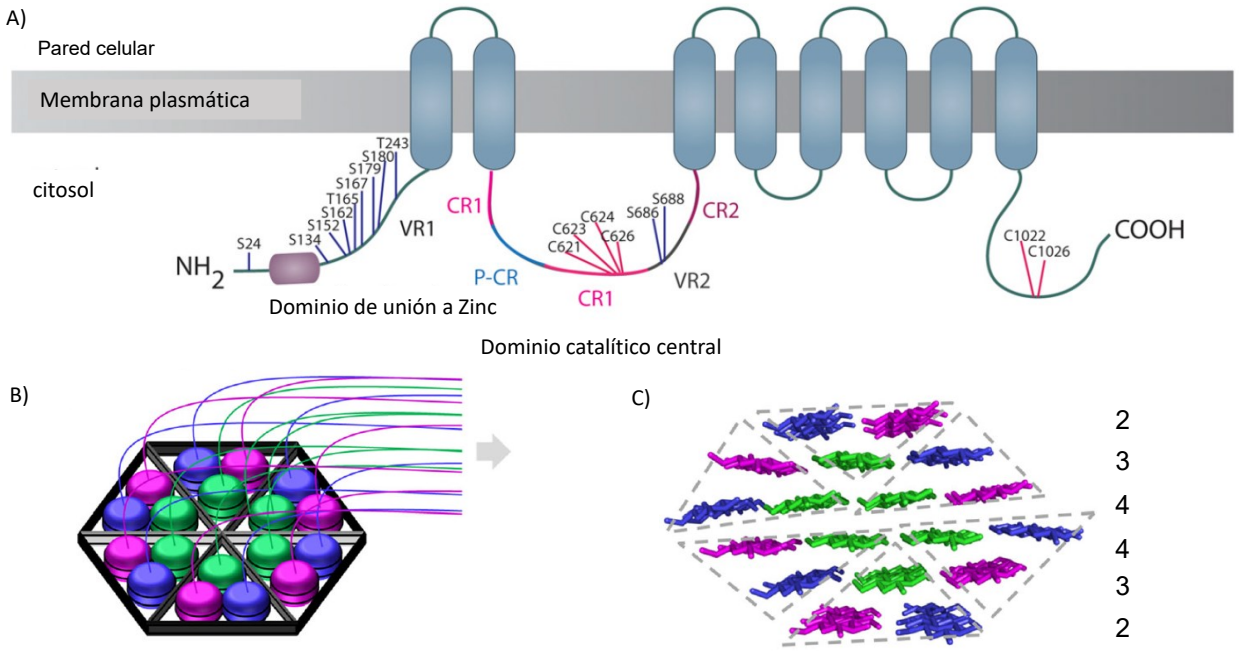

Figura 3 A) Estructura de una proteína CESA. B) Representación esquemática de un CSC que consta de 18 proteínas CESA individuales. C) Modelo de una microfibrilla de celulosa que consta de cinco capas de cadenas de celulosa en un arreglo "234432". Imagen modificada de (Polko and Kieber, 2019; Yang and Kubicki, 2020).

1.2.1. Celulosa bacteriana

La celulosa bacteriana (CB) fue descrita por primera vez por Brown (1886) cuando encontró una membrana gelatinosa flotando sobre el vinagre. Desde entonces, su popularidad ha crecido debido a sus excelentes propiedades y se han llevado a cabo varios estudios de su biosíntesis, producción industrial y aplicaciones (Klemm *et al*., 2021).

La CB es producida por varias bacterias, incluidos los géneros *Komagataeibacter*, *Agrobacterium*, *Pseudomonas*, *Rhizobium*, *Sarcina, Azotobacter* y *Lactibacillus* (Matthysse *et al*., 2005; Robledo *et al*., 2012; Saleh *et al*., 2022; Torres *et al*., 2019). Se han planteado diversas hipótesis para explicar la producción de CB por parte de las bacterias. Estas hipótesis son las siguientes: en primer lugar, para mantener una mayor proximidad a la superficie del medio de cultivo donde la concentración de oxígeno es más elevada; en segundo lugar, para protegerse contra los efectos de la luz ultravioleta; y, en tercer lugar, para protegerse contra los efectos de los iones de metales pesados y mejorar el transporte de nutrientes por difusión (Lee *et al*., 2014)

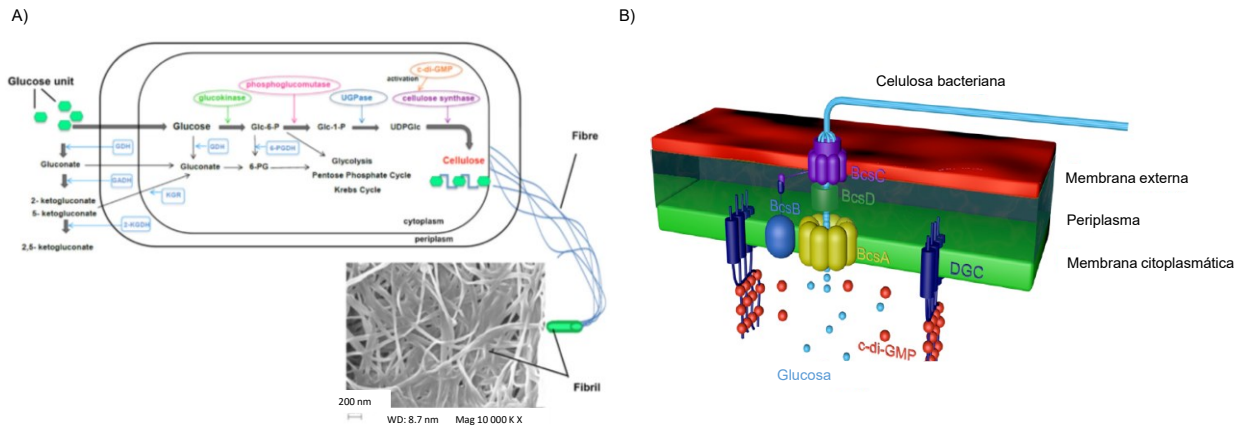

Figura 4 A) Esquema de la síntesis de CB en *K. xylinus*. Imagen tomada de (Lee *et al*., 2014). B) Representación esquemática de la organización del complejo celulosa sintasa en las membranas interna y externa de *K. xylinum*. Imagen modificada de (Manan *et al*., 2022).

De manera general se puede decir que la biosíntesis de CB ocurre en tres pasos: 1) polimerización de las unidades de glucosa que se unen mediante enlaces glucosídicos para formar la cadena β-(1-4)- glucano, 2) transporte extracelular al medio de la cadena β-(1-4)-glucano y, 3) cristalización de las fibras de celulosa, formación de los puentes de hidrógeno intra e intermolecular entre las fibras elementales y su organización en estructuras altamente ordenadas (Manan *et al*., 2022).

Komagataeibacter, anteriormente conocida como *Gluconacetobacter* (Yamada *et al*., 2012) es el género de referencia para la investigación de la biosíntesis de la CB. Son bacterias gram-negativas, aerobias estrictas, no son patógenos y se encuentran comúnmente en frutas y en vinagres (Klemm *et al*., 2005). La bacteria productora de celulosa más estudiada es *Komagataeibacter xylinus*, ya que es una de las pocas cepas capaces de producir CB a niveles comerciales (Lee *et al*., 2014). *K. xylinus* es capaz de sintetizar celulosa a partir de diversas fuentes de carbono, tales como glucosa, sacarosa, glicerol, manitol o arabitol (Ishihara *et al*., 2002; Keshk, 2014).

La biosíntesis de CB está a cargo de un complejo enzimático llamado celulosa bacteriana sintasa (Bcs) a partir de UDP-glucosa (Fig. 4A). Para obtener UDP-glucosa las etapas enzimáticas se resumen en los siguientes pasos: 1) fosforilación de la glucosa a glucosa-6-fosfato (G6P) por una glucoquinasa, 2) isomerización de G6P a glucosa-1-fosfato (G1P) por

una fosfoglucomutasa (PGM), y, 3) la enzima UDP-glucosa pirofosforilasa convierte G1P a uridina difosfato-glucosa (UDP-glucosa) que será sustrato de la Bcs (Jacek *et al*., 2019).

El complejo Bcs está formado por varias subunidades, sin embargo, cuatro subunidades llamadas BcsA, BcsB, BCsC y BcsD (Fig. 4B), son las más estudiadas y se encuentran codificadas por tres (*bcsAB*, *bcsC* y *bcsD*) o cuatro (*bcsA*, *bcsB*, *bcsC* y *bcsD*) genes (Jacek *et al*., 2019; Ross *et al*., 1991). BcsA y BcsB están ancladas a la membrana plasmática y son importantes para la producción de CB tanto *in vivo* como *in vitro* (Omadjela *et al*., 2013). La subunidad BcsA está asociada con la membrana citoplasmática a través de 8 hélices transmembrana y en su región citosólica se encuentra el dominio catalítico con actividad glucosiltransferasa (GT) que utiliza la UDP-Glucosa como precursor para la síntesis de la cadena de β-1,4-glucano. La subunidad BcsB se encuentra mayormente en el periplasma mientras que su extremo C-terminal se encuentra embebido en la membrana plasmática y contiene dos copias repetidas del dominio de unión a carbohidratos (CBD) fusionado con un dominio de flagroxina (FD). BcsB participa en el transporte de la cadena de β-1,4-glucano recién sintetizada desde el citoplasma a través del espacio periplásmico. Por otro lado, BcsC, una subunidad cuyo extremo C-terminal tiene una estructura en β-barril característica de las proteínas localizadas en la membrana celular externa tiene como función exportar al exterior de la célula el polisacárido recién sintetizado (Jacek *et al*., 2019; Manan *et al*., 2022). BcsD es un octámero con una estructura cilíndrica con un túnel que permite que las cadenas de celulosa debido a la interacción entre ellas se reorganicen, creando una región cristalina con una estructura estrictamente definida (Hu *et al*., 2010). Otros genes se han encontrado en *K. xylinus*, pero sus funciones no se conocen aún (Römling and Galperin, 2015).

Las cadenas de celulosa expulsadas al medio por BcsC se unen para formar protofibrillas de unos 2-4 nm de diámetro. A partir de estas protofibrillas se forman las microfibrillas en forma de cinta de aproximadamente 80 nm (Lee *et al*., 2014). Estas microfibrillas formarán una red tridimensional que darán a la CB características únicas: gran área superficial, alta cristalinidad, porosidad y estabilidad mecánica (Klemm *et al*., 2021). En condiciones de cultivo estático, se forma una película o membrana en la interfaz entre el aire y el líquido, mientras que, en condiciones de cultivo agitado, se generan masas esféricas irregulares (Hestrin and Schramm, 1954) (Fig.5).

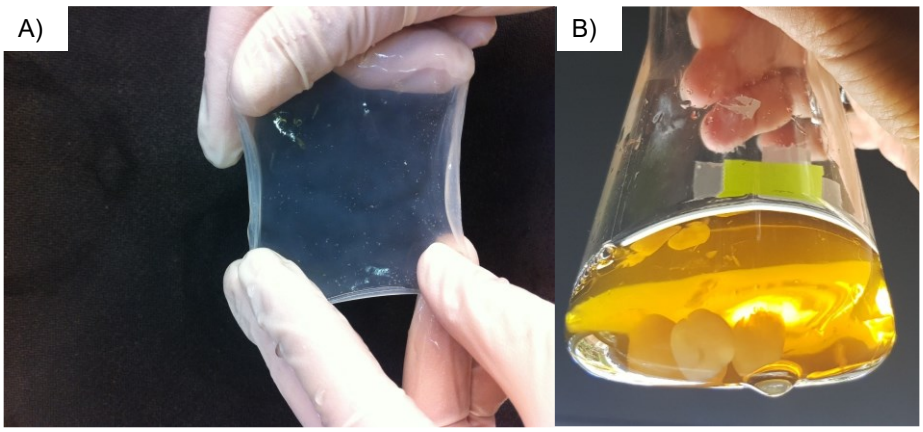

Figura 5 CB producida por *K. intermedius* JF2, A) Membrana de CB limpia, producida en un cultivo en condiciones estáticas, B) Masas esféricas de CB producidas en condiciones de agitación.

1.2.2. Aplicaciones de la celulosa

La producción mundial anual de biomasa lignocelulósica en la naturaleza se estima en 181.500 millones de toneladas. De esto, se calcula que actualmente solo se utilizan 8200 millones de toneladas de biomasa, de las cuales 7000 millones de toneladas provienen de bosques, agricultura y pastos mientras que 1200 millones de toneladas provienen de residuos agrícolas. Tradicionalmente esta biomasa lignocelulósica es utilizada para generar calor, en la industria textil y para producir cartón y papel (Ashokkumar *et al*., 2022). En España, en 2021 la producción fue de 6,7 millones de toneladas de papel y 1,8 millones de toneladas de celulosa para otros usos, con un incremento en papel del 6,2% y del 7,7% en celulosa respecto al año anterior. Sin embargo, en el primer cuatrimestre del 2022 los altos costes de energía y transporte supusieron un incremento en la producción del papel de solo un 0.4% mientras que la producción de celulosa para otros usos ha bajado un 8.3% (Álvarez and de Santos, 2022).

El alto coste de la energía y las preocupaciones del cambio climático procedentes del uso de derivados fósiles hacen imperativo la búsqueda de opciones más económicas y amigables con el medio ambiente. En este contexto, la biomasa lignocelulósica es reconocida como una fuente de materiales para reemplazar, en algún momento, a los derivados del petróleo. Con el avance de las tecnologías y la gestión de la biomasa es posible la obtención de bioetanol de segunda generación a partir de la fermentación de glucosa derivada de la celulosa (Merino and Cherry, 2007; Roukas and Kotzekidou, 2022). Además, la materia prima lignocelulósica puede valorizarse en otros bioproductos industriales útiles (Tanpichai *et al*., 2022).

En cuanto a la CB, aunque idéntica a la celulosa de origen vegetal en términos de fórmula molecular, sus características son bastante diferentes. El grado de polimerización es muy alto. La cristalinidad también es alta, con valores de 60 a 90% (Lee *et al*., 2014; Yano *et al*., 2005). La CB se caracteriza por su alta pureza debido a que no está asociada con sustancias acompañantes como hemicelulosas, lignina o pectina. Debido a estas propiedades, en los últimos años ha aumentado el interés por las aplicaciones comerciales de la CB. Ejemplos importantes incluyen soportes para proteínas, cultivos celulares y microorganismos, productos de uso cosmético, reemplazo de tejidos, aplicación como material para membranas de auriculares y altavoces, dispositivos móviles, embalaje de alimentos y películas comestibles, reciclaje y restauración de hojas de papel dañados (Lee *et al*., 2014). Sin embargo, los productos de CB comercializados son de alto valor añadido debido a los altos costos de producción ya que se requiere sistemas de fermentación eficientes que aumenten la productividad de CB. Adicionalmente, el medio de cultivo de la cepa productora de celulosa requiere grandes cantidades de fuente de carbono (sacarosa, glucosa o fructosa) si se desea obtener un alto rendimiento de producción. El aumento del rendimiento de la producción de CB es uno de los grandes desafíos y las estrategias actuales para conseguirlo se enfocan en: selección de cepas productoras de CB que tengan alto rendimiento, selección de la técnica fermentativa (estática, en agitación o biorreactor) y, por último, selección del medio de cultivo como por ejemplo el uso de residuos agrícolas como fuente de carbono para disminuir costos de la fuente de carbono (Fernandes *et al*., 2020; Revin *et al*., 2018).

1.2.3. Funcionalización de la celulosa

La funcionalización es el proceso de agregar nuevas funciones, características, capacidades o propiedades a un material. En el caso de la celulosa, esta funcionalización puede obtenerse al añadir una sustancia o compuesto cuyas propiedades se combinarían con las de la celulosa: alta porosidad y área superficial, no es tóxica, y lo más importante, es biodegradable. Otra alternativa de funcionalización de la celulosa consiste en aprovechar uno de los tres grupos hidroxilos libres que ésta posee y modificar químicamente la cadena celulósica, añadiendo residuos que posean las propiedades de interés (Rol *et al*., 2019; Vasconcelos *et al*., 2020). Una de las nuevas características que se puede aportar a la matriz celulósica, de gran interés en el sector sanitario es, por ejemplo, capacidad antimicrobiana (Morena *et al*., 2019).

En el campo de la nanotecnología, el desarrollo de nanocristales de celulosa es especialmente interesante por las aplicaciones que se puede dar a este material: agentes de refuerzo para

materiales diversos, para inmovilización de enzimas, catálisis verde, biodetección y administración de fármacos (Lam *et al*., 2012; Liu *et al*., 2021; Roman *et al*., 2009). Recientemente se han desarrollado nanocristales de celulosa a partir de CB, únicamente a través de tratamientos enzimáticos como alternativa al tradicional método de hidrólisis ácida (Buruaga-Ramiro *et al*., 2022).

Entre los ligandos que pueden añadirse se encuentran otros biopolímeros como el quitosano. Recientemente el interés por el quitosano se ha incrementado debido a sus excelentes propiedades que comentan más abajo. En esta tesis se ha utilizado este biopolímero para funcionalizar la CB y se han obtenido *nanocomposites* de CB-quitosano que combinan las propiedades de ambos biopolímeros. El quitosano es un amino polisacárido obtenido por la desacetilación alcalina de la quitina, que se extrae del mar a partir de fuentes naturales como las conchas de crustáceos. Químicamente, el quitosano es un copolímero compuesto de β-(1,4)-glucosamina y N-acetil-unidades de D-glucosamina (Fig. 6). Es biodegradable, no tóxico y posee grupos amino reactivos. Además, el quitosano muestra actividad antimicrobiana intrínseca, que depende del peso molecular y el grado de desacetilación del polímero, así como en el tipo de microorganismo (Viana *et al*., 2018). Además, el quitosano se considera un antioxidante secundario porque puede unir los iones metálicos involucrados en la catálisis de una reacción de oxidación debida a la presencia de hidroxilo activo y grupos amino en las cadenas poliméricas (Crouvisier-Urion *et al*., 2016). Debido a sus propiedades, el quitosano es considerado un material versátil que participa en múltiples aplicaciones, que incluyen la formación de películas, mezclas, revestimientos, compuestos y nanocompuestos biodegradables; como agente floculante en el tratamiento de aguas residuales; en la generación de membranas a base de quitosano para la purificación del agua; como aditivo para envases de alimentos o bien para su preservación; y en vendajes para heridas (Bordenave *et al*., 2010; Fortunati *et al*., 2017, 2019; Lin *et al*., 2013; Wahid *et al*., 2019).

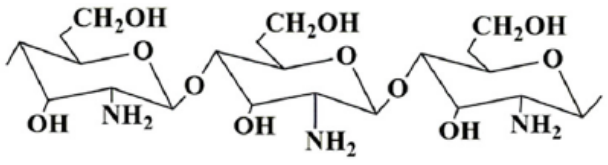

Figura 6 Estructura química del quitosano. Extraído de (Wahid *et al*., 2019).

El conjunto de todas estas propiedades hace que el interés en la biomasa (vegetal o de origen bacteriano) sea de máxima actualidad e interés. En consecuencia, esta tesis se centra en el estudio de la celulosa para su revalorización como posible sustituyente de los derivados del petróleo.

1.3. Enzimas que actúan sobre la celulosa

En el entorno natural, se encuentran diversos organismos que dependen de la descomposición de la biomasa para su supervivencia. Estos organismos suelen formar un consorcio complejo de hongos, bacterias y protozoos que trabajan en sinergia secretando enzimas para descomponer la pared celular de las plantas (Merino and Cherry, 2007).

Tradicionalmente las enzimas que degradan la celulosa están agrupadas en tres tipos (Fig. 7): 1) endoglucanasas que cortan aleatoriamente la celulosa generando cadenas más cortas que pueden ser susceptibles a ser otra vez hidrolizadas, 2) exo-glucanasas o celobiohidrolasas (CBHs) que hidrolizan los extremos de la celulosa dando como producto principal a la celobiosa y, 3) β-glucosidasas, que degradan la celobiosa a glucosa (Horn *et al*., 2012). Las expansinas, otro tipo de modificadoras de la pared celular vegetal, son proteínas que causan la expansión y relajación de la pared celular como respuesta al crecimiento de la planta (Cosgrove *et al*., 2002). Más recientemente, un nuevo tipo de enzima, la monooxigenasa lítica de polisacáridos, denominada, por sus siglas en inglés, LPMO (*Lytic Polysacharide Monoxigenase*), fue descubierta cambiando el paradigma respecto a las enzimas disruptoras de celulosa (Vaaje-Kolstad *et al*., 2010). En esta tesis son objeto de estudio las endoglucanasas, exoglucanasas y las LPMOs y sus respectivos potenciales biotecnológicos para el reaprovechamiento de la biomasa vegetal.

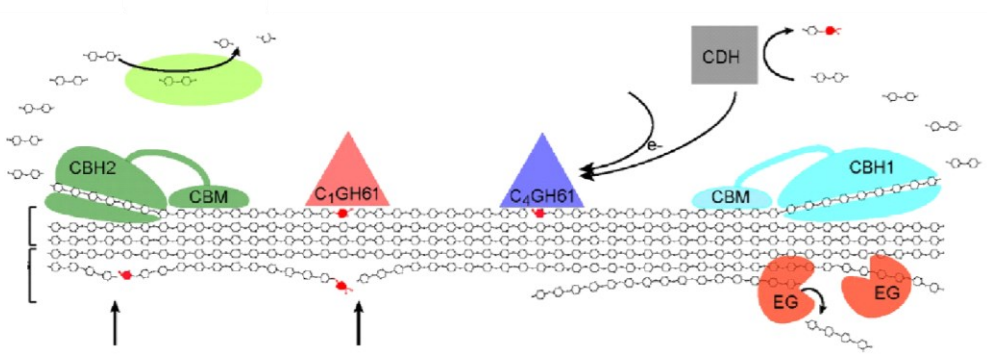

Figura 7 Enzimas disruptivas de celulosa. Imagen modificada de (Horn *et al*., 2012). Abreviaciones: EG, endoglucanasa; CBH, celobiohidrolasa; CDH, celobiosa deshidrogenasa; CBM, módulo de unión carbohidratos. C1GH61 y C1GH61, LPMOs que oxidan el C_1 y C_4 de la cadena de celulosa.

1.3.1. Celulasas

Las celulasas son glucosil hidrolasas cuyo mecanismo de acción consiste en una catálisis ácido-base con inversión o retención del carbono anomérico de la glucosa (Davies and Henrissat, 1995). De acuerdo con la base de datos de enzimas activas sobre carbohidratos CAZy (*Carbohydrate active enzymes*) hay, hasta la fecha, 180 familias de glucosil hidrolasas. Este sistema de clasificación en familias está basado en la secuencia aminoacídica y se aplica a módulos catalíticos, módulos de unión a carbohidratos, enzimas que hidrolizan, modifican o crean enlaces glucosídicos (Drula *et al*., 2022).

Las endoglucanasas (EC 3.2.1.4) tienen preferencia por la región amorfa de la celulosa y pueden ser procesivas o no procesivas. Las enzimas procesivas se unen a la celulosa hasta que ésta queda totalmente hidrolizada. Por lo general, el sitio activo de las endoglucanasas suele estar abierto y por tal razón, se unen al azar a su sustrato hidrolizando el enlace β-1-4-glucosídico. Las celobiohidrolasas (CBHs) (EC 3.2.1.91) se clasifican en CBHI y CBHII según actúen en el extremo reductor o no reductor de la celulosa, respectivamente, y son enzimas procesivas. El sitio activo de las CBHs por lo general tiene forma de túnel lo que le permite unirse al extremo de la cadena celulósica (Sukharnikov *et al*., 2011).

Muchas glucosil hidrolasas son enzimas multidominio que además del dominio catalítico, que suele ser el más grande, tienen otros dominios como el de unión a carbohidratos, CBMs, por sus siglas en inglés (*Carbohydrate binding module*) que está unido al dominio catalítico a través de un enlazador o *linker* flexible (Sukharnikov *et al*., 2011). Los CBMs no se encuentran únicamente en las celulasas sino también en xilanasas, glucosidasas, expansinas, LPMOs y otras proteínas. Los CBM, de manera general pueden tener una de estas funciones: 1) un efecto de proximidad, 2) una función de orientación y 3) una función disruptiva, siendo la primera la más habitual, es decir, el CBM al unirse al polisacárido permite que las enzimas se concentren sobre el sustrato creando un efecto de proximidad lo cual lleva a una mayor degradación de este (Boraston *et al*., 2004). Los CBMs se clasifican en familias acuerdo a la similitud de su secuencia aminoacídica y, hasta la fecha hay 97 familias en la base de datos CAZy.

Otro tipo de dominios que pueden ser encontrados en las glucosil hidrolasas son los módulos tipo Fibronectina 3 (Fn3) que poseen una pequeña estructura en β-sándwich. Aunque se sabe poco sobre las funciones específicas de los dominios Fn3, parece ser que desempeñan funciones estructurales como espaciadores entre los CBMs, el dominio catalítico y/o de anclaje a la membrana (Attia and Brumer, 2021; Sidar *et al*., 2020).

1.3.1.1. Aplicaciones industriales de las celulasas

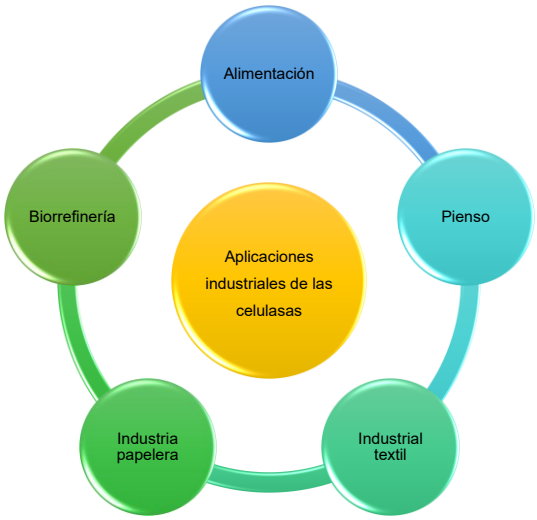

Figura 8 Aplicaciones industriales de las celulasas.

Las celulasas son unas de las enzimas más utilizadas en la industria (Fig. 8). Cócteles de celulasas y pectinasas se utilizan para mejorar la extracción y clarificación de zumos (Bhat and Bhat, 1997). En la industria cervecera, el uso de celulasas aumenta los azúcares fermentables mejorando el rendimiento de la fermentación. También, clarifican la cerveza y facilitan el proceso de filtración. El uso de celulasas junto con hemicelulasas y pectinasas en la elaboración del vino resulta en una notable extracción de color, proporciona una mejor clarificación y filtración, y mejora la calidad y estabilidad del vino (Chakraborty *et al*., 2016; Singh *et al*., 2021). La extracción de aceite de oliva puede mejorar en cuanto a rendimiento y en cuanto a calidad y claridad con el uso de cócteles enzimáticos como Olivex que contiene celulasas y pectinasas (Singh *et al*., 2021).

Se utilizan celulasas y hemicelulasas en la industria de alimentos para animales ya que el pretratamiento de piensos de cereales con estas enzimas puede mejorar su valor nutricional y proporcionar enzimas digestivas complementarias, como proteasas, amilasas y glucanasas (Dhiman *et al*., 2002; Lewis *et al*., 1996).

Los biocombustibles de segunda generación se producen a partir de la biomasa vegetal. Para obtener bioetanol, estos sustratos necesitan un pretratamiento que puede ser químico, fisicoquímico y biológico. A continuación, la biomasa pretratada es hidrolizada a glucosa

(sacarificación ácida y/o enzimática utilizando cócteles de celulasas) que, a su vez, será sustrato de microorganismos productores de bioetanol (Kucharska *et al*., 2018; Singh *et al*., 2021).

En la industria textil, se aplican celulasas para biolavado de vaqueros para así eliminar el exceso de tinte y dar un aspecto gastado a la prenda. En el biopulido de fibras textiles se consigue la mejora de absorbancia y suavizado de prendas (Bhat and Bhat, 1997).

En detergentes, se utilizan enzimas provenientes de especies del género *Humicola* que son activas a altas temperaturas y condiciones alcalinas. Estas enzimas facilitan el lavado de prendas sin dañarlas y eliminan eficientemente la suciedad (Sukumaran *et al*., 2005).

En la industria papelera, la aplicación de enzimas que modifican la superficie de las fibras puede potenciar los mecanismos de cohesión entre fibras y aumentar las propiedades mecánicas del papel. En este contexto, el uso de celulasas antes del refinado mecánico puede facilitar este proceso y por lo tanto reducir sus costos energéticos (Gil *et al*., 2009). La evaluación de las celulasas como auxiliares de refinado ha producido resultados muy diferentes. Pere *et al*., 1995 encontraron que la aplicación de endoglucanasas de *Trichoderma reesei* puede deteriorar las propiedades mecánicas del papel. Continuando con la investigación de enzimas de *Trichoderma reesei* como agentes de biorefinado, describieron que la celobiohidrolasa CBHI, como etapa anterior al refinado mecánico, conduce a ahorros de energía de hasta un 20% con mejoras en las propiedades de resistencia en pulpas termoquímicas (Pere *et. al*., 2000). Desde entonces, varios trabajos exploraron el potencial de las celulasas de diferentes orígenes para mejorar las propiedades mecánicas de los papeles con diversos resultados (Kmiotek *et al*., 2021; Nagl *et al*., 2021). Las celulasas han demostrado su potencial como agentes para el biorefinado, sin embargo, este efecto depende del tipo de enzima, sustrato, condiciones y tiempo de aplicación. Por ello, la identificación y desarrollo de nuevas celulasas que modifiquen las fibras celulósicas y aporten propiedades únicas a los productos obtenidos es de gran importancia tecnológica. Además, pueden reducir el consumo de energía y el impacto ambiental de la industria papelera.

1.3.1.2. Fabricación de papel

La palabra ¨papel¨ deriva del término griego *πάπυρος* papiros, que en latín es *papyrus*. En el antiguo Egipto sirvió como material de escritura al unir finas láminas del tallo de la planta del papiro (*Cyperus papyrus*) (Panyella, 2005). Sin embargo, el auténtico papel fue inventado en

China (siglo I d.C.) a partir de la corteza de la morera (*Broussonetia papyrifera*) (Colom *et. al.*, 1984).

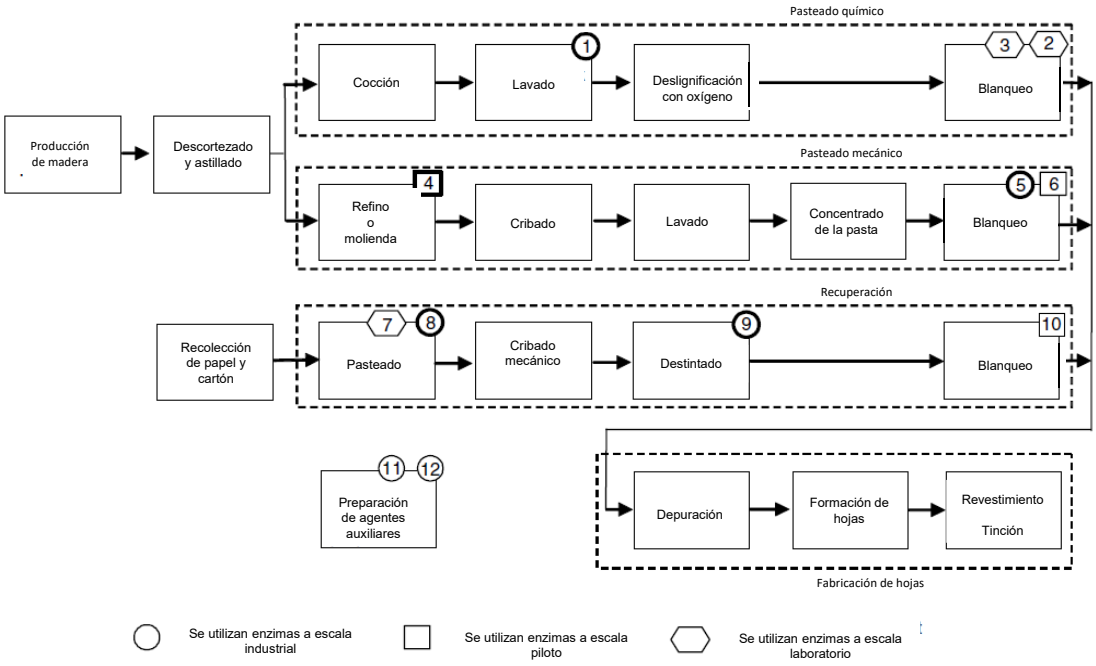

Figura 9 Principales procesos en la industria de la pulpa y el papel con indicación de los puntos donde se utilizan enzimas como coadyuvantes. Modificado de (Skals *et al*., 2008).

La norma española UNE 4046-14 define al papel como ¨una hoja constituida especialmente por fibras celulósicas de origen natural, afieltradas y entrelazadas. Por encima de cierto gramaje (250 g/m^2) y de cierta rigidez, el papel se denominará cartón¨. De manera resumida, la mayoría de los diseños de procesos para la producción de papel tienen como unidades básicas al pasteado, preparación de la pasta, formación de hojas y un paso de acabado (Fig. 9). El proceso de fabricación de pasta de papel es conocido como pasteado o cocción. El pasteado consiste en una serie de operaciones mecánicas y/o químicas para obtener una suspensión de fibras celulósicas (pasta del papel) a partir de materias primas lignocelulósicas (madera, papel recuperado o incluso plantas anuales). La mayor parte de la producción mundial de pasta de papel proviene de la fabricación de pulpa Kraft. Este proceso implica la eliminación de la lignina de las astillas de madera utilizando una mezcla de productos químicos alcalinos para la cocción (hidróxido de sodio y sulfuro sódico) que permite obtener pastas con una resistencia mecánica

excepcional, al tiempo que degrada una gran cantidad de lignina (Sewsynker-Sukai *et al*., 2020). Las cantidades residuales de lignina y los grupos cromóforos restantes se eliminan eficientemente mediante procesos de blanqueo, dando lugar a pastas con un alto grado de blancura.

El blanqueo es esencial para obtener papeles de elevada blancura. Este paso es necesario para la fabricación de papeles para impresión, tisús, papeles de uso sanitario, etc. Durante muchos años el blanqueo ha sido un proceso químico donde utilizaban compuestos a base de cloro e hipoclorito que reaccionaban con la lignina y los grupos cromóforos de la pasta. Sin embargo, la producción de clorofenoles y otros compuestos organoclorados altamente tóxicos y no biodegradables junto con las normativas ambientales ha motivado a la industria a buscar alternativas como por ejemplo la sustitución del cloro elemental por dióxido de cloro. A la pasta blanqueada de esta manera se conoce como pasta ECF, *elemental chlorine free pulp*. Con la pasta TCF (*total chlorine free*) en lugar del cloro elemental, se utilizan métodos de blanqueo alternativos, como el blanqueo con oxígeno, ozono o peróxido de hidrógeno. Estos métodos son menos impactantes a nivel medioambiental y generan menos residuos tóxicos (Roncero and Vidal, 2007). Sin embargo, el blanqueo ECF es el proceso dominante ya que produce la pulpa más fuerte y brillante (Reeve, 2012; Sharma *et al*., 2020).

A escala de laboratorio, los pasos para la elaboración del papel se resumen en la Fig. 10. Algunas fibras celulósicas muy largas necesitan un paso previo al refino, el pre-refino, que permite acortar las fibras (Fig. 10 A). A continuación, la suspensión de celulosa se filtra para eliminar el exceso de agua (Fig. 10 B). La formación de las hojas de papel se realiza en el equipo Rapid-Köthen (ISO-5269) con una suspensión de fibras de celulosa (Fig. 10 C y D). Finalmente, las hojas húmedas son secadas mediante una aplicación de vacío, presión y calor (Fig. 10 E) hasta obtener el producto final (Fig. 10 F).

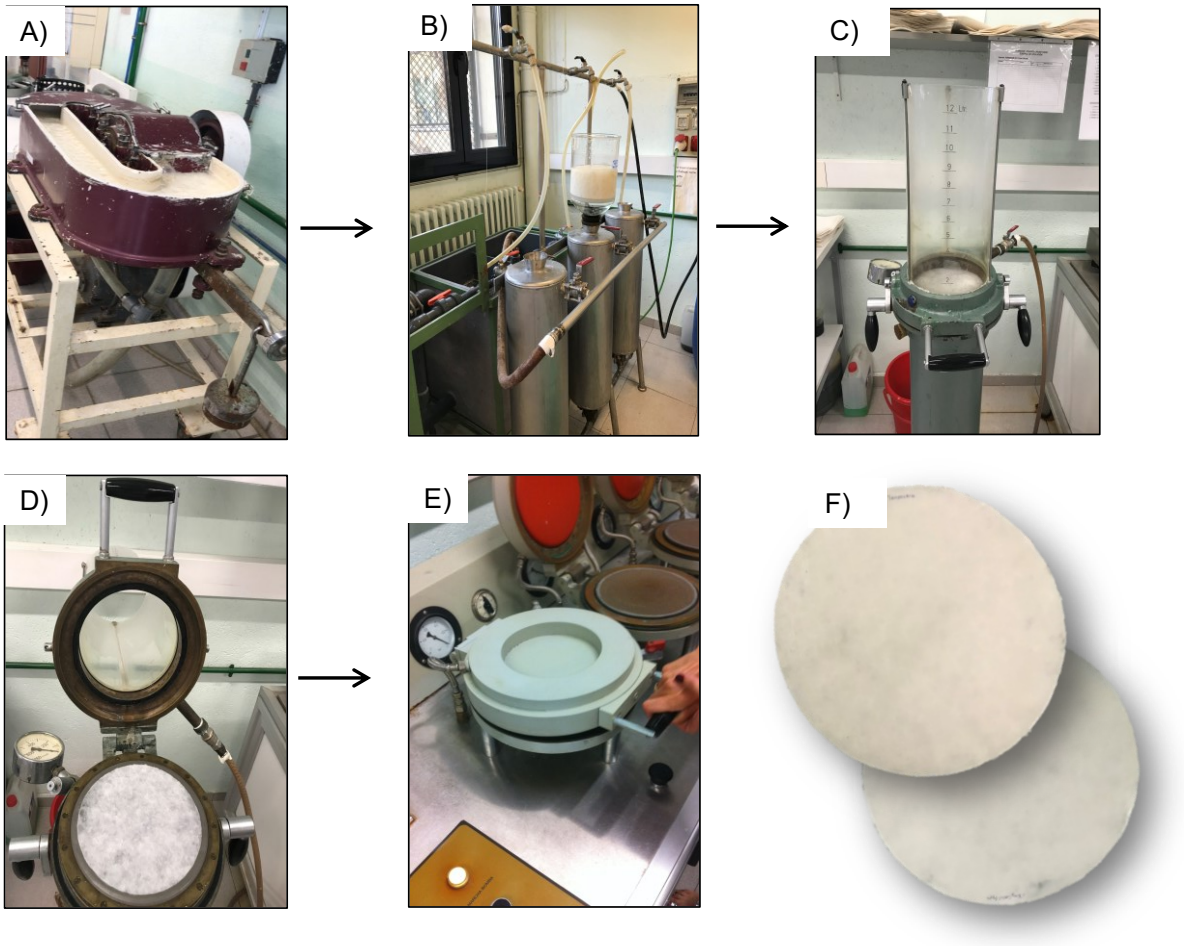

Figura 10 Proceso de elaboración del papel en el laboratorio.

1.3.1.2.1. Refinado

Enmarcado en la etapa de preparación de la pasta papelera se encuentra el refinado que consiste en un tratamiento mecánico de la pulpa mediante el uso de un equipo especial llamado refino. Los propósitos principales del refino son: 1) obtener papeles de mayor resistencia y mejor calidad para la impresión a través del aumento de la capacidad de unión entre las fibras, y 2) acortar las fibras demasiado largas para mejorar la formación (homogeneidad de la hoja) y desarrollar propiedades de la hoja tales como absorbancia, porosidad y opacidad (Torres *et al*., 2012).

En el proceso de refinado las fibras están bajo compresión y fuerzas de corte que están causando varios cambios en las fibras. Los cambios resultantes del refinado dependerán de las

propiedades iniciales de la fibra, la consistencia de la pulpa (peso en gramos de fibra secada al horno en 100 g de mezcla de pulpa y agua) y la especificación del refino (Gharehkhani *et al*., 2015).

El aparato donde se realiza el refinado se llama refino y está basado en un elemento fijo (estator) y otro de rotación (rotor) (Fig. 11). Tanto el estator como el rotor están equipados con cuchillas metálicas. En el proceso de refinado la primera es la etapa de recogida, las fibras se acumulan y quedan atrapadas entre los bordes de las barras (Fig. 11 A). En el siguiente paso, las fibras atrapadas son comprimidas por las superficies de las barras móviles y estacionarias (Fig. 11 B). En la etapa final, las fibras se ven afectadas por las fuerzas de corte. En esta etapa, las fibras también golpean las barras en la superficie hasta el borde y nuevamente de borde a borde. Durante el cruce de las barras actúan sobre las fibras dos fuerzas diferentes, una debida al contacto fibra con barra y otra debida al contacto fibra con fibra (Fig. 11 C).

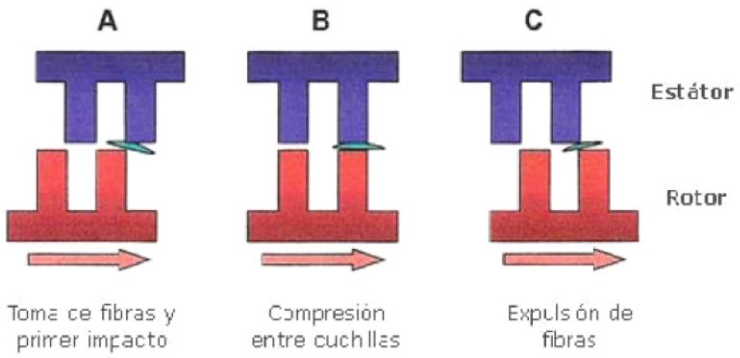

Figura 11 Proceso de refinado. Imagen modificada de (Gharehkhani *et al*., 2015).

Durante el proceso de refinado las paredes primarias y secundarias de la fibra se rompen y se eliminan parcialmente lo que hace posible que el agua penetre dentro de la pared secundaria de la celulosa y la fibra se hinche. El refinado afecta de muchas maneras a las fibras de celulosa (Fig. 12). Los efectos más importantes son los siguientes (Gharehkhani *et al*., 2015; Lin *et al*., 2018; Lumiainen, 2000):

- Fibrilación externa: consiste en el desprendimiento de fibrillas de la superficie de la fibra, dejándolas adheridas a la superficie de dicha fibra. Estas fibrillas pueden muy delgadas y aumentan notablemente la superficie capaz de interactuar con otras fibras, compuestos y partículas en la suspensión de pulpa.

- Fibrilación interna: es el resultado de la ruptura de los puentes de hidrógeno que se encuentran entre las microfibrillas. Esto provoca un incremento en la absorción de agua, el volumen específico y la flexibilidad de la fibra.
- Generación de finos: son cortes de la pared primaria y secundaria de la pared vegetal de tamaño menores a 0.3 mm. Tienen gran área superficial y aumentan la unión entre fibras.
- Corte y acortamiento de fibras: es el efecto que tienen las cuchillas del refino sobre las fibras, éstas, por tanto, disminuyen su longitud. Esto promueve que las fibras se hinchen, sin embargo, un exceso de fibras cortas afecta a la unión entre fibras causando disminución de la fuerza del papel resultante.

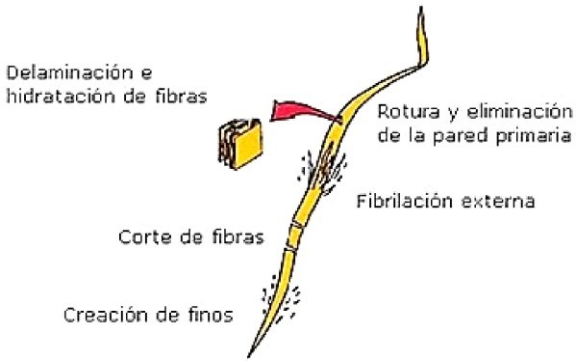

Figura 12 Efectos del refinado sobre la fibra de celulosa. Extraído de (Torraspapel, 2009).

Los efectos del refinado están dirigidos a que causar fibrilación, cortes y que las fibras absorban agua y por tanto se hinchen. Las paredes primaria y secundaria de la fibra vegetal quedan expuestas y los grupos hidroxilo de la hemicelulosa atraen a las moléculas de agua lo que resulta en una mayor hinchazón. La hinchazón de las fibras es importante porque de esta manera se incrementa el área superficial de las fibras, por tanto, éstas están más compactas lo que resulta en mejores propiedades fisicomecánicas del papel (Gharehkhani *et al*., 2015; Lin *et al*., 2018).

1.3.1.2.2. Fibras papeleras no madereras

Hay dos tipos de materia prima en la industria papelera: las fibras madereras (eucalipto, acacia, etc.) y las no madereras también conocidas como plantas herbáceas o plantas anuales (banana, bambú, algodón, cáñamo, lino, etc.). Aunque la mayoría de la materia prima

papeleras proviene de fibras madereras, el interés por las fibras no madereras ha crecido rápidamente debido a su abundancia, bajo costo de producción y fácil disponibilidad, lo cual es de especial interés para los países con escasez de madera (Abd El-Sayed *et al*. 2020).

El lino es originario de Asia y se cultiva por su semilla y su fibra. Esta planta, perteneciente a la familia de las plantas dicotiledóneas, es una angiosperma y, entre todas las especies de lino, el *Linum usitatissimum* es la única que se cultiva con fines comerciales.

La semilla oleaginosa produce un aceite secante utilizado en pintura y derivados que entran en la fabricación de linóleo. La fibra de lino es muy utilizada en industria textil. Las fibras de lino tienen propiedades que permiten la fabricación de papeles duros, resistentes, densos y permanentes. También es posible fabricar papeles de bajo gramaje como cigarrillos, papeles para libros especiales y papel moneda (del Río *et al*. 2011; García Hortal 1986).

1.3.1.3. *Paenibacillus barcinonensis*

P. barcinonensis es un bacilo gram-positivo anaerobio facultativo endoesporulado aislado de suelos de arrozales del Delta del Ebro (Fig. 13) que crece en un amplio rango de temperaturas y pHs. Esta cepa fue escogida para su estudio debido a su gran capacidad xilanolítica y celulolítica (Blanco and Pastor, 1993).

Muchas de sus enzimas identificadas degradadoras de xilano y celulosa fueron caracterizadas y demostraron potencial biotecnológico para su uso en la industria papelera, tal y como se muestra en la Tabla 1. Por el lado de las xilanasas, Xyn10A demostró su efectividad para el bioblanqueo de pasta de eucalipto (Blanco *et al*., 1995) mientras que Xyn30D es efectiva para la eliminación de ácidos hexenurónicos de pastas papeleras (Valenzuela *et al*. 2014a). En cuanto a las celulasas, Cel9B se ha aplicado sobre pastas papeleras como eucalipto y lino y ha demostrado ser un agente biorefinador muy eficaz además de lograr reducir el consumo de energía durante el refino (Cadena *et al*., 2010; Garcia-Ubasart *et al*., 2013).

Los buenos resultados obtenidos con Cel9B guiaron la exploración de otra celulasa de *P. barcinonensis*, Cel6D, como candidata para el tratamiento de la biomasa vegetal, específicamente para la evaluación de su capacidad como coadyuvante para el refinado de pastas papeleras y la obtención de nuevos materiales celulósicos con propiedades mejoradas.

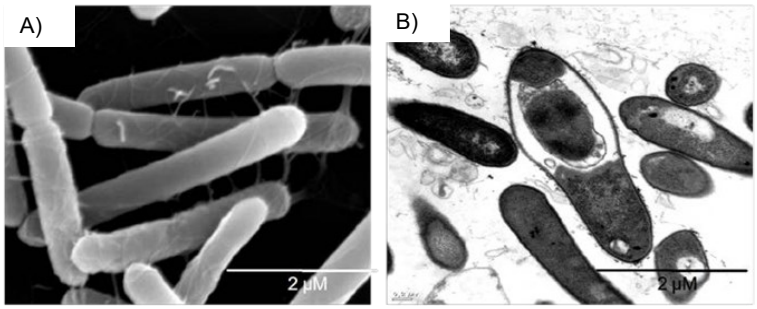

Figura 13 *P. barcinonensis*: A) imagen tomada con microscopio electrónico de barrido (SEM), B) imagen de una célula endoesporulada tomada con microscopio electrónico de transmisión (TEM). Imágenes tomadas de (Sánchez *et al*., 2005).

Tabla 1 Enzimas lignocelulósicas caracterizadas de *P. barcinonensis.*

Xilanasas		***Celulasas***		***Otras enzimas***	
Xyn10A	(Blanco *et al.* 1995)	Cel5A	(Blanco *et al*. 1998)	Rex8A	(Valenzuela *et al*. 2016)
Xyn10B	(Gallardo *et al*. 2010)	Cel48C	(Sánchez *et al*. 2003)	EstA	(Prim *et al*. 2000)
Xyn10C	(Sainz-Polo *et al*. 2015)	Cel9B	(Chiriac *et al*. 2010)	Est23	(Infanzón *et al*. 2014)
Xyn30D	(Valenzuela *et al.* 2014a)	Cel6D	(Cerda-Mejía *et al*. 2017)	Lic16A	(Cerda *et al*. 2016)
Xyn11E	(Valenzuela *et al*. 2014b)				

1.3.2. Monooxigenasas líticas de polisacáridos (LPMOs)

En 2005 Vaaje-Kolstad *et al*. describieron una proteína ¨no hidrolítica¨ (CBP21) que se unía a quitina y en cuya presencia la eficiencia de degradación de quitina por parte de quitinasas se incrementaba. Más adelante descubrirían que esta proteína se trataba de un nuevo tipo de enzima oxidativa no descrita antes (Vaaje-Kolstad *et al*. 2010). Esta enzima dependiente de cobre sería bautizada como Monooxigenasa lítica de polisacáridos, LPMO, y fue reclasificada, junto con otras proteínas similares, en la base de datos CAZy como proteínas de actividad auxiliar, ¨AA¨, en las familias AA9−11 y AA13−17. Las familias de LPMO más estudiadas son AA9 y AA10. Mientras que las LPMO AA9 solo se distribuyen en hongos, las LPMO AA10 se encuentran principalmente en bacterias. Tras el descubrimiento de LPMOs activas sobre quitina se han descrito que varias de estas enzimas tienen actividad sobre otros polisacáridos como celulosa, hemicelulosas y almidón (Agger *et al*., 2014; Forsberg *et al*., 2011; Frommhagen *et al*., 2015; Vu *et al*., 2014). Hoy día, las LPMOs forman parte de los cocteles enzimáticos para el tratamiento industrial de la biomasa lignocelulósica, sin embargo, estudios

recientes han demostrado que estas enzimas están muy distribuidas taxonómicamente y son responsables de aspectos tan diversos como el desarrollo celular y la virulencia (Fig. 14) (Askarian *et al*., 2021; Chiu *et al*., 2015; Sabbadin *et al*., 2018; Vandhana *et al*., 2022).

Una característica estructural peculiar de las LPMOs es la presencia de una superficie de unión plana en su centro catalítico en la que dos histidinas conservadas, una de ellas en el extremo N-terminal, coordinan el ion Cu^{2+} y forman un ¨brazo de histidina¨ (Ciano *et al*., 2018; Quinlan *et al*., 2011). El tercer residuo del sitio catalítico suele ser una fenilalanina para la mayoría de la familia AA10 (Forsberg *et al*., 2014) (Fig. 15). Las LPMO pueden actuar sobre las superficies de sustratos insolubles, mejorando así la accesibilidad de las hidrolasas (quitinasas y celulasas, por ejemplo) a las partes más recalcitrantes del sustrato que, de otro modo, se habrían degradado mucho más lentamente o no se degradarían en absoluto (Moon *et al*., 2022).

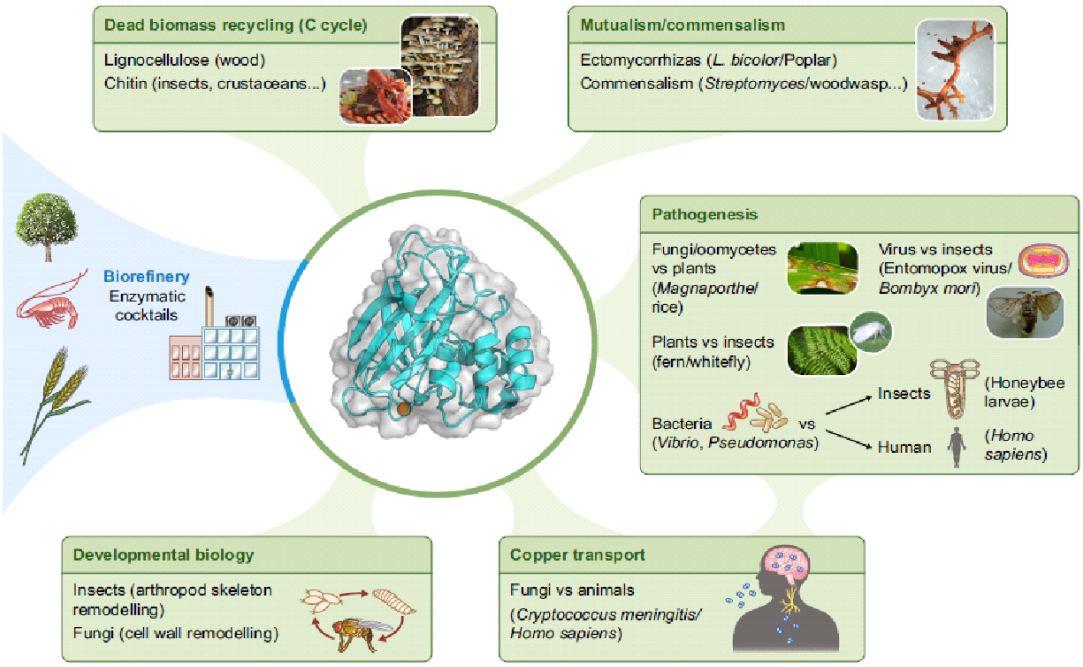

Figura 14 Descripción general de la diversidad de funciones biológicas de las LPMOs. Tradicionalmente, las LPMO se han utilizado en biorrefinería (zona azul) y, por lo tanto, se han estudiado principalmente como degradadoras de la biomasa y el reciclaje de carbono. Recientemente se ha observado que las LPMOs desempeñan un papel crucial en la patogénesis de plantas, insectos y humanos, al mismo tiempo que permiten algunos comportamientos mutualistas y comensales. Otro papel emergente es su presunta contribución a la remodelación de la pared celular durante las etapas de desarrollo de los artrópodos y los hongos. Imagen tomada de (Vandhana *et al*., 2022).

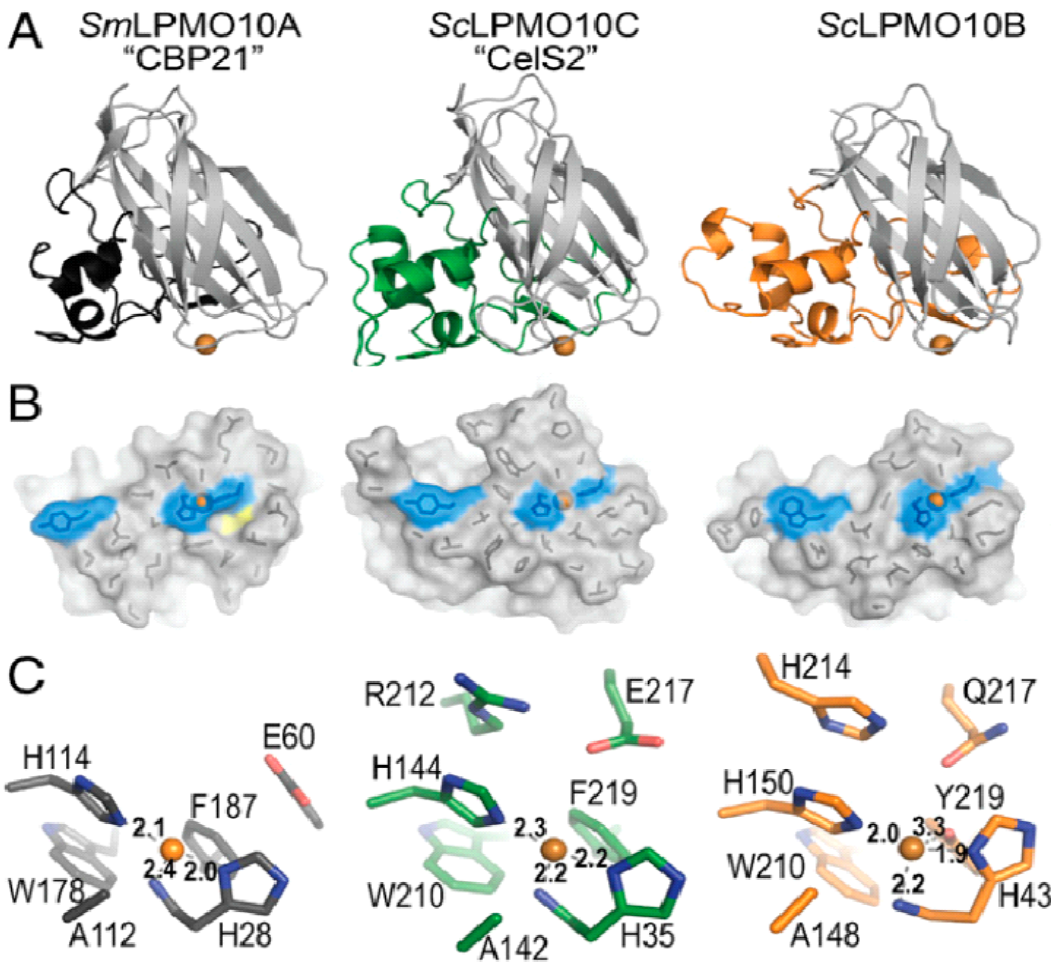

Figure 15 Estructura de tres LPMOs de la familia AA10: A) CBP21 (negro: superficie de unión a quitina, oxida en C1, 2) CelS2 (verde: superficie de unión a celulosa, oxida en C1) y ScLPMO10B (naranja: superficie de unión a sustratos celulósicos y quitina, oxidando en C1 y C4 y en C1, respectivamente). Las esferas naranjas corresponden a los iones de cobre tipo (II). B) Proyección de la superficie del área de unión del sustrato, supone una rotación de 90 º alrededor del eje horizontal de los planos anteriores. En azul se muestran los residuos de histidina y los residuos con anillos aromáticos. C) Centros activos de las LPMO. Modificado de (Forsberg *et al*., 2014).

El escenario catalítico original propuesto por Vaaje-Kolstad *et al*., 2010 es una reacción tipo monooxigenasa que involucra dos electrones, dos protones y oxígeno molecular (R-H + 2e- + 2H+ O_2 => R-OH + H_2O). Bissaro *et al*., 2017 demostraron que al añadir H_2O_2 los productos oxidados por las LPMOs incrementaron notablemente y sugirieron que el H_2O_2 es el verdadero cosustrato de las LPMOs. De hecho, propusieron que las LPMOs son en realidad peroxigenasas (R-H + H_2O_2 => R-OH + H_2O) y que estas enzimas deberían llamarse por tanto

LPPO (*Lytic polysaccharide peroxigenase*), es decir, peroxigenasas líticas de polisacáridos, una hipótesis que ha suscitado debate en la comunidad científica (Bissaro and Eijsink, 2023; Hangasky *et al*., 2018; Kommedal *et al*., 2023). Hasta la fecha, en la literatura científica todavía se las sigue llamando LPMOs y será el nombre que se utilizará a lo largo de la tesis.

En un entorno acuoso, la oxidación del C1 conduce a la formación de una lactona que, de manera espontánea, se convierte en un ácido aldónico a través de la hidrólisis del anillo. Por otro lado, la oxidación del C4 resulta en la formación de una cetoaldosa que, de manera espontánea, se transforma en un grupo diol en dicho carbono. Si ambos carbonos (C1 y C4) experimentan oxidación, se genera un grupo diol en el extremo no reductor y un ácido glucónico en el extremo reductor (Fig. 16) (Aachmann *et al*., 2012; Forsberg *et al*., 2011; Quinlan *et al*., 2011; Vaaje-Kolstad *et al*., 2017). Estas enzimas requieren un donante de electrones como ascorbato, celobiosa deshidrogenasa, fenoles, glucosa-metanol-colina oxidorreductasas o pigmentos fotosintéticos como las clorofilas (Eijsink *et al*., 2019; Kracher *et al*., 2016). También se ha descrito que la actividad de dos LPMOs fúngicas podría potenciarse drásticamente agregando clorofilina, un pigmento fotosintético, y luz, junto al reductor, ácido ascórbico (AscA) (Cannella *et al*., 2016). Recientemente se ha demostrado que la irradiación con luz de la lignina promueve su oxidación y la generación de H_2O_2, éste último sirve de cosustrato a la LPMO. El uso de lignina y luz ofrece una alternativa barata y por tanto muy atractiva para la aplicación industrial de estas novedosas enzimas (Kommedal *et al*., 2023).

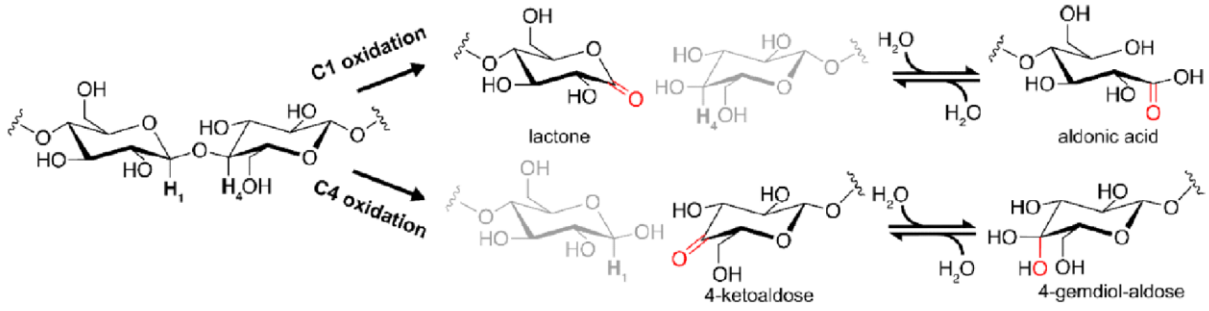

Figura 16 Producto de oxidación de la celulosa generados por LPMOs. Imagen tomada de (Chylenski *et al*., 2019).

1.3.2.1. Producción de LPMOs

La producción de grandes cantidades de enzimas activas es uno de los principales objetivos de la biotecnología. *Pichia pastoris* para las LPMO fúngicas y *Escherichia coli* para las LPMO bacterianas son ejemplos de los sistemas de expresión de mayor preferencia (Eijsink *et al*., 2019).

E. coli ofrece varias ventajas para la producción de proteínas recombinantes. En primer lugar, es un organismo de fácil cultivo y crecimiento rápido en medios de cultivo sencillos y económicos lo cual permite la producción escalable y rentable de proteínas. En segundo lugar, es uno de los sistemas de expresión más ampliamente estudiados y mejor comprendidos desde el punto de vista genético. Además, debido a su amplio uso en investigación y aplicaciones biotecnológicas existen numerosas herramientas, vectores de expresión y sistemas de clonación disponibles específicamente diseñados para la expresión de proteínas en *E. coli*. Finalmente, aunque *E. coli* no tiene todas las rutas metabólicas necesarias para llevar a cabo todas las modificaciones postraduccionales, es capaz de realizar la formación de enlaces disulfuro y la glicosilación simple, entre otras (Rosano and Ceccarelli, 2014; Zhang *et al*., 2022).

Sin embargo, en el sistema tradicional de *E. coli*, con frecuencia se forman cuerpos de inclusión insolubles que dificultan el procesamiento posterior. Además, el uso de antibióticos aumenta los costos de producción y aumenta las preocupaciones relacionadas con la resistencia a los antibióticos (Chen, 2012). Ante tales disyuntivas se requieren estrategias alternativas de producción de proteínas. Otros huéspedes bacterianos utilizados con éxito para la producción de LPMOs son *Bacillus subtilis* y la cianobacteria *Synechococcus elongatus* (Russo *et al*., 2019; Yu *et al*., 2016).

En este contexto, *Streptomyces* actualmente es un sistema de expresión prometedor, ya que ha demostrado un alto rendimiento en la producción de proteínas que son secretadas al medio de cultivo, lo que a su vez facilita el proceso de purificación posterior. Entre las diferentes especies de *Streptomyces*, *S. lividans* es la cepa preferida para la expresión de proteínas por su baja capacidad proteolítica respecto a otras cepas de *Streptomyces* spp. (Vrancken and Anné, 2009) y se ha implementado con éxito para la producción de enzimas como amilasas, xilanasas, β-glucosidasas y fosfatasas (Díaz *et al*., 2008; Sevillano *et al*., 2017; Sianidis *et al*., 2006).

Una vez producida la LPMO, el siguiente paso su purificación. Una de las técnicas de expresión de proteínas recombinantes más habitual consiste en incluir una cola de histidinas en uno de los extremos de la proteína para su posterior purificación por afinidad de estas histidinas por metales como el níquel (Bornhorst and Falke, 2000). Sin embargo, debido a que la histidina N-terminal participa de la unión al cobre y la catálisis, las opciones de expresión de LPMOs se ven limitadas. Por tanto, para producir LPMOs activas, no es recomendable utilizar colas de histidina en el extremo N-terminal a menos que se eliminen eficientemente después de la purificación, dado el papel crítico de esta histidina N-terminal. Aun así, eliminar la cola de histidinas N-terminal y mantener la enzima intacta y activa encarece los costes de producción. Aunque una alternativa es unir la cola de histidinas en el extremo C-terminal de la enzima se ha observado que su uso puede complicar el análisis de la enzima debido a su afinidad por los iones metálicos, incluyendo el cobre (Eijsink *et al*., 2019; Hemsworth *et al*., 2018). En el grupo de investigación se ha desarrollado un método rápido de purificación por afinidad a Avicel. Este método además es económico y no requiere la modificación de la secuencia de aminoácidos, (Valenzuela *et al*., 2017) por tanto es una excelente alternativa para la purificación de LPMOs para usos industriales.

1.3.2.2. SamLPMO10C y ShaLPMO10A

Dentro del reino bacteriano, el género *Streptomyces* es bien conocido por su importante papel en la descomposición de la biomasa (Kirby, 2005; Pinheiro *et al*., 2017). De ahí el interés en investigar los sistemas degradadores de biomasa de los diferentes miembros de este género para aplicaciones en biotecnología.

En esta tesis se han estudiado dos LPMOs pertenecientes al género *Streptomyces*: SamLPMO10C y ShaLPMO10A (Fig. 17). SamLPMO10C es una enzima de *S. ambofaciens* que oxida el C1 de la celulosa (Valenzuela *et al*., 2017). ShaLPMO10A es una enzima de *S. halstedii* JM8, una cepa celulolítica aislada de la paja (Fernández-Abalos *et al*., 1992). ShaLPM010A, denominada inicialmente como p40, fue descrita inicialmente como una proteína ancestral que probablemente había perdido su capacidad hidrolítica ya que no hidrolizaba ningún sustrato (Garda *et. al*., 1997) pero que tenía gran afinidad por Avicel (un tipo de celulosa de laboratorio).

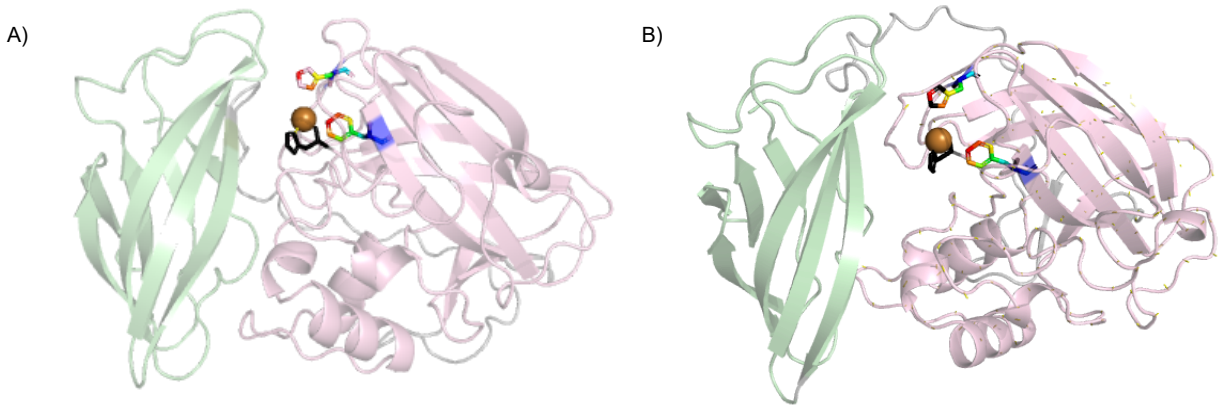

Figura 17 A) Representación de SamLPMO10C y B) ShaLPMO10A usando AlphaFold2. Las enzimas se muestran en complejo con cobre. Los residuos de la histidina N-terminal catalíticos están representados por barras negras, mientras que los otros dos posibles aminoácidos catalíticos (histidina y fenilalanina) se muestran con barras de colores. Estos residuos están en el dominio catalítico dentro de los 4 Å de sus respectivos iones metálicos (medidos usando PyMOL). Los dominios catalíticos se representan en rosa, los dominios CBM2 se muestran en verde y los enlazadores o *linkers,* en gris.

El hallazgo de las LPMOs y la búsqueda de enzimas con potencial aplicación biotecnológica ha impulsado el resurgimiento de la proteína p40, casi relegada al olvido. Mediante análisis bioinformáticos, se propuso que p40 podría ser una LPMO perteneciente a la familia AA10, lo cual finalmente se confirmó experimentalmente en esta tesis. Las características moleculares de ambas enzimas pueden verse en la tabla 2.

Tabla 2 Características de las LPMOs estudiadas en esta tesis.

Enzima	**Tamaño (AA)**	**pI**	**Peso molecular (kDa)**	**Sustrato**	**Mecanismo de oxidación**
SamLPMO10C*	364	5.03	34.69	Celulosa	C1
ShaLPMO10A**	365	5.95	38.29	Celulosa	C1

*Extraído de (Valenzuela *et al*., 2017)

** Esta tesis

2. OBJETIVOS

Esta tesis doctoral se ha llevado a cabo en el grupo de Enzimas microbianas de aplicación industrial y ambiental de la Universidad de Barcelona. Este grupo de investigación trabaja en la biotransformación de polímeros naturales, incluyendo el desarrollo de enzimas que catalizan su modificación, hidrólisis y/o síntesis para el desarrollo de nuevos materiales biotecnológicos amigables con el medio ambiente. En este contexto, esta tesis se ha centrado en el estudio de la celulosa como matriz para su funcionalización y valorización, la caracterización de un tipo nuevo de enzimas que sobre ella actúan: las LPMOs, incluyendo la búsqueda de estrategias para conseguir grandes cantidades de esta enzima y el uso de celulasas como agentes biorefinadores de pastas celulósicas papeleras.

Los objetivos específicos son:

1. Funcionalización de celulosa de origen vegetal y bacteriano para que el nuevo biomaterial adquiera nuevas y mejores propiedades que la materia prima original.

1.1 Funcionalización de celulosa bacteriana con quitosano.

1.2 Funcionalización de celulosa vegetal y bacteriana mediante oxidación enzimática con SamLPMO10C seguido de la adición de plata y generación de nanopartículas de plata.

1.3 Estudio de las propiedades de los nuevos biomateriales obtenidos.

2. Caracterización de nuevas enzimas modificadoras de celulosa.

2.1 Expresión homóloga de SamLPMO10C.

2.2 Expresión homóloga y heteróloga de una nueva LPMO: ShaLPMO10A.

2.3 Caracterización SamLPMO10C y ShaLPMO10A en relación con sus respectivas actividades a diferentes temperaturas, cambios en la masa molecular celulósica por la acción oxidativa enzimática y evaluación en tiempo real de la interacción enzima-sustrato.

3. Evaluación de celulasas Cel9B y Cel6D, utilizadas individualmente y en conjunto, en la modificación de fibras de lino y en el proceso de biorefino de pasta de lino.

3.1 Análisis del efecto de estas enzimas en la modificación de propiedades físicas y resistencia mecánica de los productos papeleros obtenidos.

3.INFORMES

3.1 Listado de publicaciones

La doctoranda tiene dos artículos publicados, uno como primera autora y otro como coautora. Otros tres artículos, donde es la autora principal, se encuentran en preparación. Los artículos mencionados son los siguientes:

1. **Cabañas-Romero, L.V.**, Valls, C., Valenzuela, S. V., Roncero, M.B., Pastor, F. I. J., Diaz, P., & Martínez, J. (2020). Bacterial Cellulose−Chitosan Paper with Antimicrobial and Antioxidant Activities. *Biomacromolecules*, *21*, 1568−1577. https://dx.doi.org/10.1021/acs.biomac.0c00127

2. Buruaga-Ramiro, C., Fernández-Gándara, N., **Cabañas-Romero, L.V.**, Valenzuela, S.V., Pastor, F.I. J., Diaz, P. & Martínez, J. Lytic polysaccharide monooxygenases and cellulases on the production of bacterial cellulose nanocrystals. *European Polymer Journal*, 163, 110939. https://doi.org/10.1016/j.eurpolymj.2021.110939

3. **Cabañas-Romero, L.V.**, Martínez, J. & Valenzuela, S.V. Lytic polysaccharide monooxygenase-mediated cellulose functionalization for paper supports with enhanced properties. *Cellulose*. En curso.

4. **Cabañas-Romero, L.V.**, Buruaga-Ramiro, C., Javier Pastor, F.I., Villares, A., Grellier, G., Santamaría, R.I., Díaz, M. & Valenzuela, S.V. Lytic polysaccharide monooxygenases low-cost expression strategies and insights into the enzyme-substrate interactions. *ACS Sustainable Chemistry & Engineering*. En curso.

5. **Cabañas-Romero, L.V.**, Buruaga-Ramiro, C., Roncero, M.B., & Valenzuela, S. V. Flax biorefining for paper production. *Cellulose*. En curso.

3.2 Informe sobre el factor de impacto

Los artículos que forman parte de la memoria de la tesis doctoral presentada por Lourdes Verónica Cabañas Romero han sido publicados o están en preparación para su publicación en revistas internacionales indexadas en el Journal Citation Reports ® tal y como se detalla a continuación:

1. **Cabañas-Romero, L.V.**, Valls, C., Valenzuela, S. V., Roncero, M.B., Pastor, F. I. J., Diaz, P., & Martínez, J. (2020). Bacterial Cellulose−Chitosan Paper with Antimicrobial and Antioxidant Activities. *Biomacromolecules*, 21, 1568−1577. https://dx.doi.org/10.1021/acs.biomac.0c00127

Esta revista se encuentra incluida en el primer cuartil del área temática de: bioquímica y biología molecular (56/285), química orgánica (3/52) y ciencias de polímeros (6/86), con un factor de impacto para el año 2022 de 6.2.

2. Buruaga-Ramiro, C., Fernández-Gándara, N., **Cabañas-Romero, L.V.**, Valenzuela, S. V., Díaz, P., & Martínez, J. Lytic polysaccharyde monooxigenases and cellulases on the production of bacterial cellulose nanocrystals. *European Polymer Journal*, 163, 110939. https://doi.org/10.1016/j.eurpolymj.2021.110939

Esta revista se encuentra incluida en el primer cuartil del área temática de ciencias de polímeros (7/86) con un factor de impacto para el año 2022 de 6.0.

3. **Cabañas-Romero, L.V.**, Martínez, J. & Valenzuela, S.V. Lytic polysaccharide monooxygenase-mediated cellulose functionalization for paper supports with enhanced properties. En curso.

Este trabajo ha sido enviado a la revista *Cellulose* que se encuentra incluida en el primer cuartil del área temática de ciencias de polímeros (1/21), ciencia de materiales y textiles (2/25) y ciencia de polímeros (10/86) con un factor de impacto para el año 2022 de 5.7.

4. **Cabañas-Romero, L.V.**, Buruaga-Ramiro, C., Javier Pastor, F.I., Villares, A., Grellier, G., Santamaría, R.I., Díaz, M. & Valenzuela, S.V. Lytic polysaccharide monooxygenases low-cost expression strategies and insights into the enzyme-substrate interactions. *ACS Sustainable Chemistry & Engineering*. En curso.

Este trabajo ha sido enviado a la revista *ACS Sustainable Chemistry & Engineering*, que se encuentra incluida en el primer cuartil del área temática de: química (32/178), ingeniería química (13/140) y ciencias de polímeros (6/86), con un factor de impacto para el año 2022 de 8.7.

5. **Cabañas-Romero, L.V.**, Buruaga-Ramiro, C., Roncero, M.B., & Valenzuela, S. V. Flax biorefining for paper production. *Cellulose*. En curso.

Este trabajo ha sido enviado a la revista *Cellulose* que se encuentra incluida en el primer cuartil del área temática de ciencias de polímeros (1/21), ciencia de materiales y textiles (2/25) y ciencia de polímeros (10/86) con un factor de impacto para el año 2022 de 5.7.

Dra. Susana Valenzuela
Directora y tutora de tesis

3.3 Informe de participación en las publicaciones

La doctoranda L. Verónica Cabañas Romero ha participado en los artículos que forman parte de su tesis doctoral de la manera que se detalla a continuación:

1. **Cabañas-Romero, L.V.**, Valls, C., Valenzuela, S. V., Roncero, M.B., Pastor, F. I. J., Diaz, P., & Martínez, J. (2020). Bacterial Cellulose−Chitosan Paper with Antimicrobial and Antioxidant Activities. Biomacromolecules, 21, 1568−1577. https://dx.doi.org/10.1021/acs.biomac.0c00127

La doctoranda llevó a cabo la parte del trabajo experimental y redacción del manuscrito.

2. Buruaga-Ramiro, C., Fernández-Gándara, N., **Cabañas-Romero, L.V.**, Valenzuela, S. V., Díaz, P., & Martínez, J. Lytic polysaccharide monooxigenases and cellulases on the production of bacterial cellulose nanocrystals. *European Polymer Journal*, 163, 110939. https://doi.org/10.1016/j.eurpolymj.2021.110939

La doctoranda llevó a cabo parte del trabajo experimental (expresión, purificación y ensayos de actividad de la enzima SamLPMO10C).

3. **Cabañas-Romero, L.V.**, Martínez, J. & Valenzuela, S.V. Lytic polysaccharide monooxygenase-mediated cellulose functionalization for paper supports with enhanced properties. *Cellulose*. En curso.

La doctoranda llevó a cabo la parte de los experimentos y redacción del manuscrito.

4. **Cabañas-Romero, L.V.**, Buruaga-Ramiro, C., Javier Pastor, F.I., Villares, A., Grellier, G., Santamaría, R.I., Díaz, M. & Valenzuela, S.V. Lytic polysaccharide monooxygenases low-cost expression strategies and insights into the enzyme-substrate interactions. *ACS Sustainable Chemistry & Engineering*. En curso.

La doctoranda llevó a cabo la mayor parte del trabajo experimental, participó activamente en el diseño experimental y en la redacción del manuscrito.

5. **<u>Cabañas-Romero, L.V.</u>**, Buruaga-Ramiro, C., Roncero, M.B., & Valenzuela, S. V. Flax biorefining for paper production. *Cellulose*. En curso.

La doctoranda llevó a cabo la parte experimental, participó activamente en el diseño experimental y en la redacción del manuscrito.

El artículo ¨ Lytic polysaccharyde monooxigenases and cellulases on the production of bacterial cellulose nanocrystals¨ ha sido utilizado como parte de la tesis doctoral de la autora principal de dicho artículo. En cuanto a los demás artículos, ninguno ha sido utilizado como parte de la tesis doctoral de los coautores.

Dra. Susana Valenzuela
Directora y tutora de tesis

4. ARTÍCULOS

4. Artículos

4.1 Capítulo 1. Funcionalización de la celulosa

4.1.1 Artículo 1: Bacterial Cellulose−Chitosan Paper with Antimicrobial and Antioxidant Activities

4.1.2 Artículo 2: Lytic polysaccharide monooxygenase-mediated cellulose functionalization for paper supports with enhanced properties

Papel de celulosa bacteriana y quitosano con propiedades antimicrobianas y Antioxidantes

La producción de *nanocomposites* de celulosa bacteriana−quitosano (BC−Ch) en soportes tipo papel se llevó a cabo siguiendo dos enfoques diferentes. En el primero, se produjeron papeles de CB y luego se sumergieron en una solución acuosa de quitosano (BC−ChI); en el segundo, la pulpa de CB se impregnó con quitosano antes de la producción de hojas de papel (BC−ChM). Se investigaron los *nanocomposites* BC−Ch en términos de características físicas, propiedades antimicrobianas y antioxidantes, y su capacidad para inhibir la formación de biofilms en su superficie. Los dos tipos de *nanocomposites* BC−Ch mantuvieron el carácter hidrofóbico, las propiedades de barrera de aire y la alta cristalinidad propias de la CB.

Sin embargo, BC−ChI mostró una superficie con una red de fibras más densa y poros más pequeños que los de BC−ChM. Solo el 5% del quitosano se filtró de los *nanocomposites* BC−Ch después de 96 horas de incubación en un medio acuoso, lo que indica que fue retenido por la matriz de papel BC. Los *nanocomposites* BC−Ch mostraron actividad antimicrobiana, inhibiendo el crecimiento y teniendo un efecto bactericida contra las bacterias *Staphylococcus aureus* y *Pseudomonas aeruginosa*, así como contra la levadura *Candida albicans*. Además, los papeles BC−Ch mostraron actividad contra la formación de biofilms en su superficie. La incorporación de quitosano aumentó la actividad antioxidante del papel de CB. Los *nanocomposites* BC−Ch basados en papel combinaron las propiedades físicas del papel BC y las actividades antimicrobianas, antibiofilm y antioxidantes del quitosano.

BioMACROMOLECULES

pubs.acs.org/Biomac

Article

Bacterial Cellulose–Chitosan Paper with Antimicrobial and Antioxidant Activities

L. Verónica Cabañas-Romero, Cristina Valls, Susana V. Valenzuela, M. Blanca Roncero, F. I. Javier Pastor, Pilar Diaz, and Josefina Martínez*

Cite This: *Biomacromolecules* 2020, 21, 1568–1577

Read Online

ACCESS | Metrics & More | Article Recommendations

ABSTRACT: The production of paper-based bacterial cellulose–chitosan (BC–Ch) nanocomposites was accomplished following two different approaches. In the first, BC paper sheets were produced and then immersed in an aqueous solution of chitosan (BC–ChI); in the second, BC pulp was impregnated with chitosan prior to the production of paper sheets (BC–ChM). BC–Ch nanocomposites were investigated in terms of physical characteristics, antimicrobial and antioxidant properties, and the ability to inhibit the formation of biofilms on their surface. The two types of BC–Ch nanocomposites maintained the hydrophobic character, the air barrier properties, and the high crystallinity of the BC paper. However, BC–ChI showed a surface with a denser fiber network and with smaller pores than those of BC–ChM. Only 5% of the chitosan leached from the BC–Ch nanocomposites after 96 h of incubation in an aqueous medium, indicating that it was well retained by the BC paper matrix. BC–Ch nanocomposites displayed antimicrobial activity, inhibiting growth of and having a killing effect against bacteria *Staphylococcus aureus* and *Pseudomonas aeruginosa* and yeast *Candida albicans*. Moreover, BC–Ch papers showed activity against the formation of a biofilm on their surface. The incorporation of chitosan increased the antioxidant activity of the BC paper. Paper-based BC–Ch nanocomposites combined the physical properties of BC paper and the antimicrobial, antibiofilm, and antioxidant activities of chitosan.

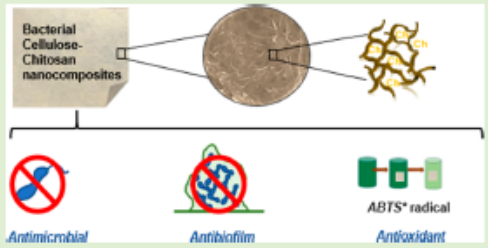

INTRODUCTION

Bacterial cellulose (BC) is a polysaccharide, synthesized and extruded outside the cell by some microorganisms, especially from the genera Komagataeibacter. The biopolymer is composed of units of glucose linearly linked by $\beta(1 \rightarrow 4)$-glycosidic bonds. Although identical to cellulose of a plant origin in terms of molecular formula, BC presents unique properties that make it superior for many applications. Unlike vegetable cellulose, which is always bound to hemicellulose and lignin requiring subsequent refining treatments, BC is synthesized chemically pure. BC displays a high degree of polymerization and crystallinity, great mechanical strength, and a high water-holding capacity.[1] BC is also biodegradable and biocompatible.[2] Microorganisms produce cellulose as a three-dimensional open porous network of nanofibers, providing a large surface area. Moreover, cellulose contains available hydroxyl groups on its surface that facilitate the possibility of molecular adsorption by the formation of hydrogen bonds and electrostatic interactions. These structural and mechanical features are important for the practical application of BC as the supporting matrix for the preparation of new composite materials.[3,4] Because of these properties, in recent years, there has been an increased interest in commercial applications of bacterial cellulose. Important examples include supports for proteins, cell cultures, and microorganisms; products for temporary skin and tissue replacement; materials for headphone and loudspeaker membranes, food packing, and edible films.[1,5,6]

Chitosan is an amino polysaccharide obtained by the alkaline deacetylation of chitin, which is extracted from marine natural sources such as crustacean shells. Chemically, chitosan is a copolymer composed of β-(1,4)-glucosamine and *N*-acetyl-D-glucosamine units. It is biodegradable, nontoxic, and possesses reactive amino groups. Moreover, chitosan displays intrinsic antimicrobial activity, which depends on the molecular weight and the degree of deacetylation of the polymer as well as on the type of microorganism.[7] Also, chitosan is considered a secondary antioxidant because it can chelate the metal ions involved in the catalysis of an oxidizing

Received: January 28, 2020
Revised: March 9, 2020
Published: March 12, 2020

https://dx.doi.org/10.1021/acs.biomac.0c00127
Biomacromolecules 2020, 21, 1568–1577

reaction due to the presence of active hydroxyl and amino groups in the polymer chains.[8] Owning to its properties, chitosan is considered a versatile material that participates in multiple applications, which include the formation of biodegradable films, blends, coatings, composites, and nanocomposites; as a flocculating agent in wastewater treatment; in the generation of chitosan-based membranes for water purification; as an additive for food packages or food preservation; and in wound dressing.[4,9−14]

The blending of polymers to produce composites materials with new properties has received extensive attention as a strategy for supporting new applications.[4,15−17] The combination of chitosan with BC has been successfully described for biomedical and packaging applications.[4,9,10] In these works, the matrix of BC was in the form of a native never-dried membrane or in the form of a film. Recently, the production of paper from BC pulp has been reported.[18] BC paper sheets combine the attributes of BC nanofibers with the stiffness and physical properties of paper, showing remarkable mechanical characteristics and barrier properties to water and oil.[18] Some studies have shown how chitosan-coated vegetable paper has impaired paper properties, such as its resistance to water or steam transfer.[11,19] However, to our knowledge, no work has yet been reported regarding the combination of BC paper and chitosan.

The aim of this work was to compare two different procedures to blend BC with chitosan to obtain a novel nanocomposite based on BC paper and investigate its physical characteristics and its antimicrobial, antioxidant, and antibiofilm properties. The study is framed in the research area of bioactive papers with potential applicability in the design of biomedical devices and in the field of packaging of food and high value goods.

EXPERIMENTAL SECTION

Microbial Strains. The cellulose producing strain was *Komagataeibacter xylinus* CECT 7351. Antimicrobial activity was tested against *Staphylococcus aureus* CECT 234, *Pseudomonas aeruginosa* PAO1 CR32, and *Candida albicans* CECT 1001. Strains were obtained from the Spanish Type Culture Collection (CECT).

Production of Bacterial Cellulose. To produce bacterial cellulose, *K. xylinus* was grown on the Hestrin and Schramm (HS) medium, containing 20 g/L glucose, 20 g/L peptone, 10 g/L yeast extract, 1.15 g/L citric acid, and 6.8 g/L Na_2HPO_4, pH 6.[20] Suspensions of *K. xylinus* were used to inoculate 10 cm Petri dishes containing 40 mL of HS medium that were statically incubated at 25−28 °C for 7 days. After incubation, bacterial cellulose pellicles generated in the air/liquid interface of the culture media were harvested, rinsed with water, and incubated in NaOH (1%) at 70 °C overnight to remove the bacteria. Finally, the BC pellicles were thoroughly washed in deionized water until the pH reached neutrality. To obtain the BC pulp, pellicles were mechanically cut into small pieces (1 cm^2 approximately) and disrupted with a homogenizer (CAT Unidrive X1000 Homogenizer, Germany) at 20 000 rpm for 10 m.

Preparation of Bacterial Cellulose/Chitosan Nanocomposites. To obtain the composites of BC paper containing chitosan, two approaches were followed: the formation of BC paper followed by impregnation by immersion of paper sheets with chitosan; and the impregnation in mass of the BC pulp with chitosan followed by the formation of paper sheets.

Impregnations were carried out with the water-soluble derivative methyl glycol chitosan (FUJIFILM Wako Pure Chemical Corporation, MW: $(375.2)_n$) with a ratio of 0.3 mg of chitosan/mg of dry bacteria cellulose.

The impregnation of the previously produced BC paper was done by immersing pieces of 1 cm^2 of paper in 3 mg/mL aqueous solution at pH 6 and incubating overnight at room temperature. After incubation, the paper sheets were washed with deionized water to remove poorly attached chitosan. To perform the impregnation in mass, BC pulp and chitosan at 3 mg/mL (final concentration) were mechanically mixed in a blender (proBlend6 3D, Philips, Spain) until homogenization (500 rpm, 5 m). The mixture was incubated overnight at room temperature and, after incubation, washed with deionized water. The pulp of BC impregnated with chitosan was then used to produce paper sheets.

Paper sheets were produced following the ISO−5269:2004 standard method using a Rapid−Köthen laboratory former (Frank-PTI, Germany). The sheets were sterilized by an autoclave at 121 °C for 20 min, dried at 45 °C, and stored at room temperature until further use. Three types of papers were obtained: bacterial cellulose (BC), bacterial cellulose−chitosan nanocomposite by immersion (BC−ChI), and bacterial cellulose−chitosan nanocomposite by impregnation in mass (BC−ChM).

Physical and Barrier Properties. Paper sheets were conditioned at 23 °C and 50% of relative humidity for at least 24 h before physical testing, as indicated in ISO 187 (1990). Basic physical and barrier properties were measured according to standards indicated in parentheses as follows: grammage (ISO 536:2012), thickness (ISO 534:2005), density (ISO 534:2005), Bendtsen roughness (ISO 8791-2:2013), Bendtsen air permeance (ISO 5636-5:2003), and water drop test (WDT) (Tappi T835 om-08). At least five measurements per sample were made and averaged. Statistical analysis of the results was performed. To determinate the water absorption capacity (WAC), BC and BC−chitosan nanocomposites were immersed in deionized water for 24 h at room temperature. Then, the weight of the swollen pieces was measured.

Water absorption capacity was calculated as follows

$$\text{water absorption capacity} = \frac{W_f - W_i}{W_i}$$

where W_i is the initial weight of the dried sample and W_f is the weight of the sample in the swollen state.

Scanning Electron Microscopy (SEM). Surface morphology of BC−chitosan nanocomposites was analyzed by SEM (JEOL JSM 7100 F, Tokyo, Japan) using a light-emitting diode (LED) filter. Samples were graphite-coated using an EMITECH K950X vacuum evaporator, France.

X-ray Diffraction (XRD). X-ray diffraction patterns of the samples were obtained with a PANalytical X'Pert PRO MPD Alpha1 powder diffractometer (Malvern Panalytical B.V., Netherlands) in Bragg−Brentano $\theta/2\theta$ geometry of 240 mm radius. The radiation was Cu $K\alpha_1$ (λ = 1.5406 Å) at 45 kV and 40 mA, focalizing a Ge(111) primary monochromator, with sample spinning at 2 revolutions per second, and a fixed divergence slit of 0.25° was used. The measurement range (2θ) was from 2 to 50° with a step size of 0.033° and a measuring time of 100 s per step. The samples were placed, over zero-background silicon single-crystal sample holders, keeping them as flat as possible, using when necessary silicon paste and/or small scotch pieces. The crystallinity index (CrI) of the samples was calculated from the XRD spectra using the following equation, based on the peak height method.[21]

$$\text{CrI}\ (\%) = \frac{I_{002} - I_{AM}}{I_{002}} \times 100$$

where I_{002} is the maximum intensity of the lattice diffraction and I_{AM} is the minimum intensity at 2θ between 18 and 19°, which corresponds to the amorphous part of cellulose.

Fourier Transform Infrared (FTIR) Spectroscopy. The infrared spectra of samples were obtained using FTIR spectroscopy (PerkinElmer Frontier Fourier transform IR spectrometer, Waltham, MA). Spectra were obtained at wave numbers ranging from 4000 to 400 cm^{-1} recorded at 4 cm^{-1} resolution.

Antimicrobial Activity. The antimicrobial activity of BC−Ch composites was tested against the Gram-positive bacteria *S. aureus*, Gram-negative bacteria *P. aeruginosa*, and yeast *C. albicans*. To obtain

https://dx.doi.org/10.1021/acs.biomac.0c00127
Biomacromolecules 2020, 21, 1568−1577

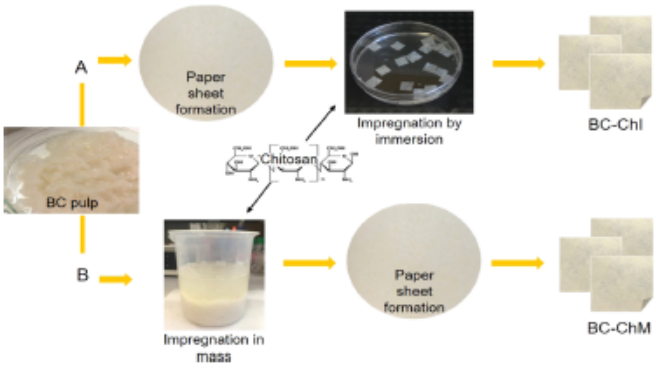

Figure 1. Scheme of the production of BC−Ch nanocomposites with the methods: (A) impregnation by immersion and (B) impregnation in mass. Black arrows indicate when chitosan was added.

the inoculum for the antimicrobial tests, the strains were grown overnight in Luria−Bertani (LB) broth at 37 °C in shaking conditions. Then, these cultures were centrifuged for 5 min at 18 407 RCF and the pellets were resuspended in 0.3 mM KH_2PO_4 to remove the culture medium. BC−chitosan nanocomposites were cut in squares of 1 cm^2 and sterilized prior to the assay. Two antimicrobial tests were performed, the drop over paper test and the dynamic contact condition test.

Drop Over Paper Test. Three microliters of the corresponding microbial suspension (about 10^5 microorganisms per mL) was inoculated over the 1 cm^2 BC−chitosan composite placed on the surface of tryptic soy agar (TSA) medium plates. The growth over a sample of BC paper was used as a positive control. After overnight incubation at 37 °C, the samples of composites and BC paper were submerged in 1 mL of 0.3 mM KH_2PO_4 and the microorganisms were detached by intense shaking. The metabolic activity of the resuspension was measured by the resazurin assay. In a medium with viable cells, resazurin is reduced to resorufin and this reduction can be quantified by a fluorometer.[22]

For the assay, 30 μL of resazurin (7-hydroxy-3*H*-phenoxazin-3-one-10-oxide) was added to 100 μL of each microbial resuspension in a 96-well plate. The plate was incubated at 37 °C in dark conditions until the solution turned pink (approximately 10 min). Fluorescence was measured (λ_{ex} = 570 nm, λ_{em} = 600 nm) with a Varian Cary Eclipse fluorescence spectrophotometer (Varian Iberica, Spain). The difference between the metabolic activity of the microorganisms grown on BC−chitosan composites and BC paper was used to calculate the percentage of growth inhibition.

Dynamic Contact Condition Test. This procedure was adapted from ASTM E2149-01:2001 (standard test method for determining the antimicrobial activity agents under dynamic contact conditions). Nine 1 cm^2 pieces of the BC−chitosan composites were immersed in 5 mL of a suspension of a known concentration of microorganisms (approximately 10^7 UFC/mL) and incubated at room temperature while stirring. In each case, a control was run with BC paper under the same conditions. The viable cells on the suspension were determined at different times (0, 1, 4, and 24 h). The percentage of reduction was calculated by the following equation

$$\text{reduction (\%)} = \frac{\text{viable CFU at}t_0 - \text{viable CFU at}t_x}{\text{viable CFU at}t_0} \times 100$$

where t_0 is the time 0 h and t_x is the time at which the percentage of reduction is calculated.

Antibiofilm Activity. Antibiofilm properties of BC−Ch nanocomposites were assayed with *P. aeruginosa*, a well-known biofilm producer. Aliquots (1 mL) of a 1:100 dilution of an overnight culture of *P. aeruginosa* (about 10^6 bacteria) were pipetted into a 24-well plate where samples of BC−Ch and BC paper were previously placed. After overnight incubation at 37 °C, the medium was removed and the samples were rinsed 3 times with phosphate-buffered saline (PBS). The resazurin assay and SEM analysis were carried out on BC−Ch nanocomposites and BC paper.

Antioxidant Activity. The antioxidant activity was assessed by a procedure that allows us to determine the antioxidant capacity of insoluble components by the quantification of the inhibition of 2,20-azino-bis(3-ethylbenzothiazoline-6sulphonic acid) radical ($ABTS^{\cdot+}$).[23−25] First, 7 mM ABTS was oxidized by 2.45 mM of potassium persulfate obtaining the $ABTS^{\cdot+}$ radical. Then, 1 cm^2 samples of BC−chitosan nanocomposites and BC paper were placed in Eppendorf tubes and 1 mL of $ABTS^{\cdot+}$ was added. A tube without the sample was used as a blank. The next step was vortexing the tubes, centrifuging at 3381g, and incubating them in dark conditions for 30 min. Finally, 900 μL of liquid was pipetted in a cuvette and the final absorbance at 730 nm was measured in a T92+ UV spectrophotometer (PG Instruments, U.K.). The antioxidant activity of the samples was expressed by the following equation

$$ABTS^{\cdot+}\text{inhib (\%)} = \frac{A_i - A_f}{A_i} \times 100$$

where A_i is the absorbance value of the blank and A_f the absorbance value of the sample.

Determination of the Concentration of Chitosan. The method to measure chitosan was adapted from Badawy.[26] Briefly, samples were incubated with 0.5 M $NaNO_2$ at 80 °C for 30 m to complete the depolymerization−deamination reaction. Then, after raising the pH to 8, a 0.04 M thiobarbituric acid solution was added and the mix was incubated a second time at 80 °C for 10 m. Finally, the absorbance was measured at 555 nm and the concentration of chitosan was calculated based on a calibration curve.

RESULTS AND DISCUSSION

Production of Bacterial Cellulose−Chitosan Nanocomposites. Figure 1 schematizes the two approaches followed to produce BC−chitosan nanocomposites: impregnation by immersion (BC−ChI) and impregnation in mass (BC−ChM). The produced paper sheets were dried and storage at room temperature, maintaining their properties for, at least, 12 months (results not shown). The amount of chitosan in the composites was estimated by subtracting the concentration of chitosan in the solution before and after the impregnation procedure. The amount of chitosan in the wash liquids was considered in the calculations. BC−ChI and BC−ChM contained 625 ± 1.3 and 668 ±1.2 μg of chitosan per

https://dx.doi.org/10.1021/acs.biomac.0c00127
Biomacromolecules 2020, 21, 1568−1577

cm^2 of paper, respectively (A and B, Figure 1). These values correspond to 104 and 106 μg of chitosan absorbed per gram of cellulosic matrix (dry weight) for BC−ChI and BC−ChM, respectively, indicating that the ratio BC/Ch on the composites was about 10:1 and suggesting that chitosan was well incorporated into the nanofibers of cellulose network structure. In the mass impregnation process, the BC fibers were suspended in water, which would facilitate the access of the chitosan and favor its interaction with the cellulose molecules. In contrast, in the impregnation by immersion procedure, the molecules of cellulose could be less accessible to chitosan since BC fibers were compacted and dried during the process of papermaking. However, not substantial differences were found in the amount of chitosan loaded throughout the two approaches, suggesting that chitosan in BC−ChI composites not only coated the paper surface but also penetrated the porous matrix of fibers of BC.

To assess whether the two types of composites had different retention capacities, the migration of chitosan from the cellulosic matrices was evaluated. BC−ChI and BC−ChM nanocomposites were immersed in distilled water and, at different times up to 96 h, aliquots samples were withdrawn and assayed for the presence of chitosan. No disintegration or erosion of the BC−Ch composites was observed during the migration experiments. Results indicated that after 96 h in water both types of nanocomposites retained more than 90% of chitosan (Figure 2). Most of the release of chitosan took

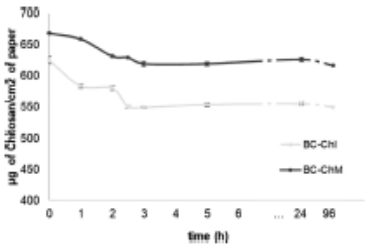

Figure 2. Retention of chitosan on the BC−Ch nanocomposites immersed in water. Results are expressed in micrograms of chitosan that remained per square centimeters of paper. The dark gray line corresponds to the BC−Ch nanocomposite by impregnation in mass and the light gray line to the BC−Ch nanocomposite by immersion. Values were expressed as mean ± standard deviations and were analyzed statistically by analysis of variance (ANOVA); $p \leq 0.05$ was considered statistically significant.

place during the first 2 h on contact with the aqueous solution and could be attributed to the molecules that were loosely attached to the BC nanofibers. Less chitosan migrated from BC−ChM (3%) than from BC−ChI (7%), suggesting that in the course of the impregnation in mass chitosan is trapped more effectively in the dense network of nanofibrils of BC than during the impregnation by immersion of the preformed paper sheet. Regardless, the results indicated that both BC matrices strongly retained the molecules of chitosan. Under these experimental conditions, the interactions between chitosan and BC can be explained by the overall opposite charge between cellulose (negative) and chitosan (positive)[27] as well as by the three-dimensional network of BC nanofibers that would entrap the molecules of chitosan. It is worth noting that the stabilization of chitosan into the BC matrices was achieved without the addition of chemical cross-linkers that could compromise the applicability of the composites by increasing their brittleness[28,29] or by weakening their antimicrobial ability.[28]

Bacterial cellulose membranes embedded with antimicrobial agents, such as chitosan, have been proposed for wound healing applications on the basis of their progressive migration from the BC matrix toward the skin.[30,31] BC paper is a different kind of matrix that allowed the retention of chitosan and could expand the applicability of the BC−Ch composites. For example, chitosan has been proposed as a carrier for protein and enzyme immobilization owning to the availability of numerous amino and hydroxyl groups.[32] The strong interaction between chitosan and the BC matrix would ensure permanent immobilization of the carrier and consequently would prevent the leaking of the bioactive molecules. In the packaging industry, one of the most appreciated properties is the retention of additives, preventing the transfer of active compounds from packaging materials to packaged goods. Furthermore, since chitosan is biocompatible, nontoxic, and biodegradable, BC−Ch nanocomposites could be interesting for applications having to be in contact with food or pharmaceutical products.[33−35]

Characterization of the BC−Chitosan Nanocomposites. *FTIR Analysis.* FTIR spectra obtained from BC and BC−Ch nanocomposites are shown in Figure 3. The molecular

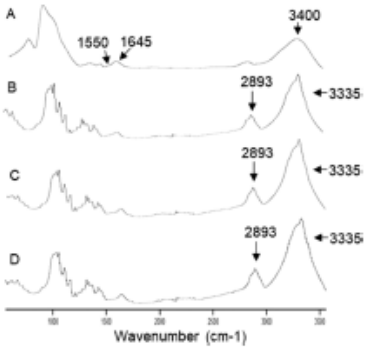

Figure 3. FTIR spectra of (A) chitosan, (B) BC, (C) BC−ChI, and (D) BC−ChM.

structures of bacterial cellulose and chitosan are very similar; therefore, for chitosan, BC paper, and BC−Ch nanocomposites, characteristic peaks at 2893 cm^{-1} were attributed to the aliphatic C−H stretching vibration.[10] The absorption band of chitosan at 1554 cm^{-1} was assigned to the N−H bending of amide II. The strong band between 3500 and 3200 cm^{-1} corresponds to N−H and O−H stretching.[28,36] The band at 1645 cm^{-1} is due to amide I. The spectra of the BC−Ch nanocomposites are dominated by the cellulose component.

Structural Analysis by SEM. SEM images of BC paper and BC nanocomposites are shown in Figure 4. Figure 4A shows the typical fibril network of BC with spaces randomly distributed through the matrix. The highly interweaved nanofiber network provides a large surface area, and the porous structure of the BC facilitates the bounding and entrapment of molecules. The images of BC−Ch nano-

https://dx.doi.org/10.1021/acs.biomac.0c00127
Biomacromolecules 2020, 21, 1568−1577

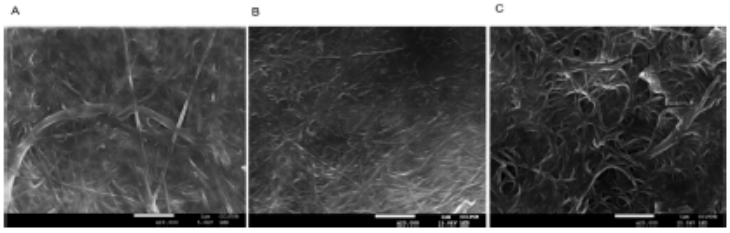

Figure 4. SEM images of (A) BC, (B) BC−Ch nanocomposite by immersion, (C) BC−Ch nanocomposite by impregnation in mass. Magnification, 20 000×.

composites (Figure 4B,C) revealed a homogeneous surface without aggregations, suggesting a correct dispersion of chitosan. Figure 4B,C exhibits a layer coating the nanofibers of BC that could be attributed to the presence of chitosan molecules interacting with the BC fibers. Moreover, the addition of chitosan by the immersion method (BC−ChI; Figure 4B) rendered matrices with smaller pores, in agreement with what has been previously described for bacterial cellulose membranes.[10,36] The effect of chitosan on the surface of the BC matrix was more evident in the case of the nanocomposites obtained by the immersion method, which suggests that when impregnation is performed after paper formation chitosan molecules bind to a greater extent to the fibers of the surface of the paper.

Physical and Barrier Properties. Table 1 summarizes the effect of the incorporation of chitosan into the network

Table 1. Physical and Barrier Properties of BC Paper and BC−Chitosan Nanocomposites

property	BC	BC−ChI	BC−ChM
grammage (g/m^2)	50.67 (±0.6)	60.10 (±1.5)	63.08 (±3.9)
thickness (μm)	171 (±16)	172 (±14)	171 (±10)
density (g/cm^3)	0.295 (±0.004)	0.359 (±0.031)	0.369 (±0.042)
Bendtsen roughness (mL/min)	4.3 (±0.6)	3.1 (±0.8)	3.6 (±0.8)
Bendtsen air permeance ($\mu m/Pa{\cdot}s^{-1}$)	1.24 (±0.19)	0.92 (±0.14)	1.19 (±0.13)
water drop test (WDT) (min)	34 (±3)	34 (±4)	32 (±4)

structure of the BC on certain physical and barrier properties of the resulting nanocomposite. No significant differences were observed between the results obtained for the BC−ChI and the BC−ChM composites (Table 1), suggesting that the two approaches to obtain the BC−Ch nanocomposites rendered similar matrices in terms of the characteristics assayed. However, some changes were observed on BC paper after the binding of chitosan. As expected, the grammage, defined as the weight in grams of 1 m^2 of paper, and the density of the BC−Ch composites were higher than those of BC paper, indicating a more closed structure. Chitosan also provided a slight increase in the smoothness of the paper surface, more obvious in the case of BC−ChI probably due to the differences on the methodology to produce the nanocomposites. In the case of BC−ChI, the chitosan was coated on the paper surface, being placed in the surface pores of the composite. Paperlike supports made of bacterial cellulose are characterized by excellent barrier properties to air, water, and oil,[18,37] which is important for applications that need impermeability, as for the packaging material.[11] Results showed that the blend of chitosan and BC increased the impermeability to the air, indicated by the lower value in air permeance of the BC−Ch nanocomposites.

Hydrophylicity is a characteristic inherent to most matrices of polysaccharides. Bordenave et al.[11] reported that the association of paper produced from vegetal cellulose with chitosan was water-sensitive and they improved the hydrophobic character of chitosan-coated vegetal papers after chemical modification of chitosan and bonding with fatty acids. However, BC paper features water and vapor barrier properties without the need for the addition of hydrophobic components or the chemical modification of the molecule.[18,37] The results obtained in this work indicated that the presence of chitosan did not increase the wettability of the resulting BC−Ch nanocomposites estimated by WDT (Table 1), suggesting that the BC paper maintained its hydrophobic character.

Water absorption capacity (WAC) of BC−Ch nanocomposites was evaluated and compared with that of the BC paper. The WAC of BC paper was about 6.5 times its dry weight, while the WAC of BC−ChI and BC−ChM nanocomposites were 38 and 25% less, respectively, indicating that the addition of chitosan decreased the capacity of water absorption (Figure 5). The variation in the WAC between BC and BC−Ch papers could be explained by the electrostatic interaction between the amino groups of chitosan and hydroxyl groups of cellulose. Consequently, there are less hydroxyl

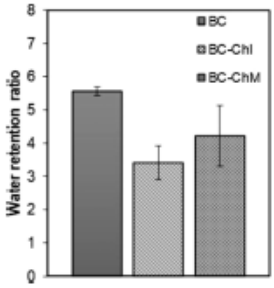

Figure 5. Water absorption ratio of BC paper and BC−Ch nanocomposites. Values were expressed as mean ± standard deviations and were analyzed statistically by analysis of variance (ANOVA); $p \leq 0.05$ was considered statistically significant.

https://dx.doi.org/10.1021/acs.biomac.0c00127
Biomacromolecules 2020, 21, 1568−1577

groups available to interact with water molecules, affecting the absorption behavior of the nanocomposites.[38]

X-ray Diffraction (XRD). To compare the microstructural changes in the BC produced after impregnation with chitosan, X-ray diffraction was used. The XRD diffraction patterns of the paperlike supports are shown in Figure 6. The determination of

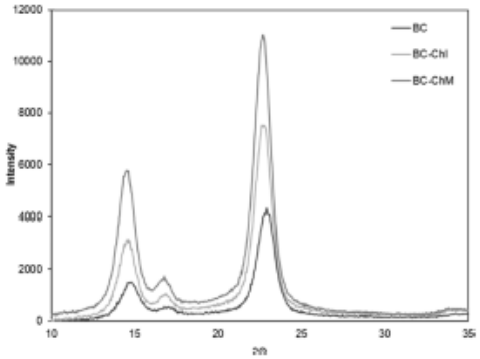

Figure 6. X-ray diffraction (XRD) patterns of BC, BC−ChI, and BC−ChM nanocomposites.

crystallinity by the XRD using the peak height method described by Segal et al.[21] was chosen because it is one of the most widely used methods to obtain semiquantitative amounts of amorphous and crystalline cellulosic components' crystallinity index reference. The values of crystallinity obtained were 94.5% for BC, 94.1% for BC−ChI, and 93.9% for BC−ChM. When chitosan is added, the crystallinity of the bacterial cellulose does not significantly change. Results on crystallinity suggested that the blending of BC and chitosan rendered composites of a homogeneous structure, probably due to the high compatibility of both materials.[39]

Antimicrobial Activity of the BC−Chitosan Nanocomposites. The capability of the BC−chitosan composites to inhibit the microbial growth by direct contact of the microorganism with their surface was assayed by the drop over paper test. Results showed that the three strains assayed were able to grow over BC paper; however, when an equivalent inoculum was incubated over the BC−Ch nanocomposites, the activity declined (Table 2). The results indicated that the chitosan bound to the cellulose fibers forming the paper had a negative effect on the growth of the three strains assayed.

The yeast *C. albicans* showed less sensitivity to chitosan than the bacterial strains. Moreover, chitosan was more active against Gram-positive (*S. aureus*) than Gram-negative (*P. aeruginosa*) bacteria. The differences in the effectiveness of chitosan can be explained by its varied mechanisms of action as well as by the differences in the structure of the cell envelopes of the three microorganisms.[7] However, the exact mechanism of chitosan antimicrobial action is not totally understood. Factors such as MW and degree of acetylation of chitosan and the pH of the medium may influence its antimicrobial action. Results suggested that the external lipidic membrane in Gram-negative could confer some protection, hindering the access of chitosan to the cell. Nevertheless, in the literature, there is not a general agreement regarding the degree of susceptibility of Gram-positive, Gram-negative, and fungi to the chitosan.[40] While we could expect more chitosan to accumulate on the surface of the compounds obtained by the immersion procedure than on those obtained by mass impregnation, the results indicated that BC−ChM was more effective in preventing microbial growth on their surface. The SEM images of the BC−Ch nanocomposites (Figure 4) revealed that BC−ChM presented a less compact surface that would allow better contact of the bacteria with the nanofibers, facilitating the action of chitosan.

Table 2. Inhibition of Microbial Growth over BC−Ch Nanocomposite Surfaces

	inhibitory rate (%)[a]	
strain	BC−ChI	BC−ChM
Staphylococcus aureus	63	83
Pseudomonas aeruginosa	55	75
Candida albicans	18	38

[a]Results expressed as the percentage of reduction of the microbial activity with respect to the activity over BC paper.

One aspect to consider was that results stated above indicated that BC−Ch nanocomposites had less water absorption capacity than that of BC paper (Figure 5). Moreover, SEM analysis showed that chitosan covered the nanofibers and could be filling the matrix pores. These circumstances could be limiting the diffusion of water and nutrients dissolved in water during the drop over paper test analysis and artificially increase the results of antimicrobial activity. To preclude this possibility, the biocidal ability of the BC−chitosan composites was assayed under dynamic liquid conditions. Suspensions of the microorganisms on the 0.3 mM KH_2PO_4 solution were incubated in contact with the BC−Ch composites and BC paper, at room temperature and slight agitation. Viable cell counts were determined at different times, and the percentage of cell viability reduction was calculated (Table 3). Suspensions of the microorganisms in contact with samples of BC paper did not exhibit a decrease of viability over 24 h incubation time (results not shown). However, the microorganisms in contact with BC−Ch nanocomposites showed a remarkable diminution of viability after 1 h of incubation and the reduction of viability was 100% after 24 h (Table 3). These results indicated that BC−Ch composites not only inhibited the microbial growth but also exhibited strong biocidal activity against the tested strains. Moreover, the antimicrobial effectiveness of the two types of nanocomposites was similar, suggesting that this property did not depend on the procedure followed for the production of the nanocomposites.

BC paper is a matrix with great mechanical resistance and does not disintegrate in water, which allows its reusability. An interesting characteristic of the composites produced was to know whether after keeping in an aqueous environment for a period and then drying retained their antimicrobial activity for further applications. To do this, samples of BC−Ch and BC paper were incubated in water at room temperature for 24 h. Then, the papers were dried and the drop over paper test was performed with a suspension of *S. aureus*. Both nanocomposites still showed antimicrobial activity after being in contact with water for 24 h and then dried (Table 4). BC−ChM and BC−ChI nanocomposites maintained 63 and 51% of its antimicrobial capacity, respectively, compared to its initial antimicrobial activity (t_0, Table 4). BC paper did not show a

https://dx.doi.org/10.1021/acs.biomac.0c00127
Biomacromolecules 2020, 21, 1568−1577

Table 3. Viable Cell Counts (CFU/mL) and Cell Viability Reduction (%) of Microorganisms in Dynamic Contact with BC−ChI and BC−ChM Composites

		strains					
		S. aureus		*P. aeruginosa*		*C. albicans*	
type of nanocomposite	time (h)	CFU (mL)	% of reduction	CFU (mL)	% of reduction	CFU (mL)	% of reduction
BC−ChI	t_0	9.70×10^7	0	9.25×10^7	0	4.05×10^7	0
	t_1	4.20×10^7	57	5.90×10^7	36	2.06×10^7	49
	t_4	8.35×10^6	91	3.15×10^6	97	9.10×10^6	78
	t_{24}	0	100	0	100	0	100
BC−ChM	t_0	7.95×10^7	0	5.00×10^7	0	2.75×10^6	0
	t_1	2.27×10^7	71	2.95×10^7	41	9.75×10^5	65
	t_4	4.40×10^6	94	2.00×10^6	96	4.30×10^5	84
	t_{24}	0	100	0	100	0	100

Table 4. Reduction of Activity (%) of *S. aureus* in Contact with Both Types of BC−Ch Nanocomposites before (t_0) and after Being Immersed in Water for 24 h (t_{24})

time (h)	BC−ChI	BC−ChM
t_0	63	83
t_{24}	32	52

reduction of activity (results not shown). Differences in the results of the two types of composites were consistent with the fact that BC−ChM showed less migration of chitosan from the BC matrix than BC−ChI.

Antibiofilm Activity of the BC−Ch Nanocomposites. Biofilms are microbial communities embedded in a self-produced matrix of extracellular polymers strongly attached to the surface of organic and inorganic materials. Biofilms increase the resistance of microorganisms to antimicrobial drugs and the immune system activity and are difficult to eradicate with cleaning agents.[41,42] The prevention of biofilm formation is an important issue in the development of new materials for biomedical, pharmaceutical, and packaging applications. Hence, the activity of the BC−Ch nanocomposites against the generation of biofilms on their surface was evaluated. To do that, samples of the BC−Ch nanocomposites and BC paper were immersed in a suspension of *P. aeruginosa* and incubated at 37 °C, optimal growth temperature for the strain. After 24 h, samples were rinsed, dried, and analyzed by SEM. SEM images of the surface of the BC−Ch composites and BC paper are shown in Figure 7. It can be observed that BC paper, which did not contain chitosan, is covered by a material compatible with the existence of a biofilm (Figure 7A). However, in the images of BC−Ch nanocomposites, the typical network of BC nanofibers can be distinguished, suggesting that chitosan inhibited the generation of the biofilm on the surface of the nanocomposites. Interestingly, this effect was more evident for BC−ChI than for BC−ChM, probably related to the higher smoothness of the surface of BC−ChI, which could hinder the adhesion of bacteria.

The microbial activity of the samples was measured by the resazurin assay as an indicator of the growth of Pseudomonas on their surfaces and to confirm that the material observed in SEM images could have a biological origin.

Results indicated the presence of microbial activity on the surface of the three types of analyzed samples: BC−ChI and BC−ChM composites and BC (Figure 8). However, BC−Ch nanocomposites displayed less activity than that of the BC paper, in concordance with the presence of the biofilm observed by SEM images. The reduction in activity was 68% for the BC−ChI nanocomposite and 81% for the BC−ChM nanocomposite. These results were in agreement with the

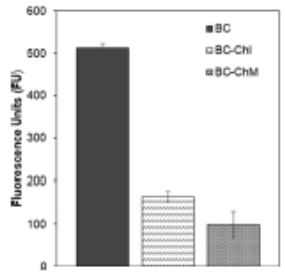

Figure 8. Microbial activity (FU) of the biofilm formed on the surface of BC−Ch and BC paper. Values were expressed as mean ± standard deviations and were analyzed statistically by analysis of variance (ANOVA); $p \leq 0.05$ was considered statistically significant.

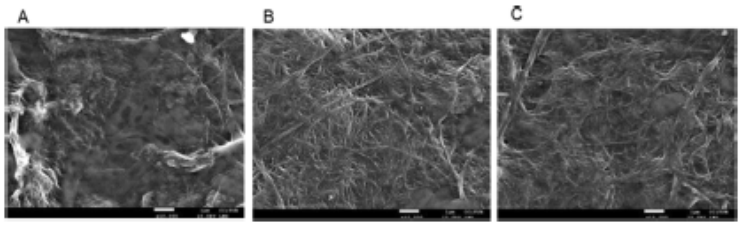

Figure 7. SEM images of biofilm on the surface of (A) BC paper, (B) BC−ChI, and (C) BC−ChM. Magnification, 10 000×.

https://dx.doi.org/10.1021/acs.biomac.0c00127
Biomacromolecules 2020, 21, 1568−1577

inhibition of *S. aureus* obtained by the drop over paper test and suggested that BC−ChM has enhanced antimicrobial activity, but it is less efficient in controlling biofilm formation than BC−ChI. The effectiveness of chitosan against biofilms has been documented.[43,44] The results of SEM analysis and microbial activity obtained in this work indicated that chitosan incorporated into the BC−Ch nanocomposites had a strong negative effect on biofilm formation on their surface.

Antioxidant Activity of the BC−Chitosan Nanocomposites. Antioxidant properties of BC paper and BC composites containing chitosan were tested. As shown in Figure 9, the BC

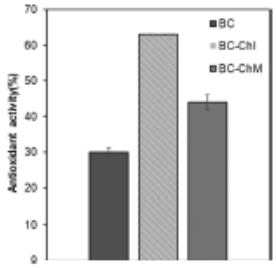

Figure 9. Antioxidant activity of the BC−chitosan nanocomposites. Values were expressed as mean ± standard deviations and were analyzed statistically by analysis of variance (ANOVA); $p \leq 0.05$ was considered statistically significant.

paper showed some antioxidant activity. Previous studies have reported the presence of aldehyde groups in BC[18] and the antioxidant capability of them.[45] Moreover, when chitosan is impregnated with BC, the antioxidant activity in both types of BC−Ch nanocomposites increased. BC−ChI showed more antioxidant activity than that of BC−ChM, probably because the immersion method causes a greater chitosan load on the surface of the composite, favoring its exposure to the surrounding environment. Chitosan antioxidant activity is mainly attributed to NH_2 residues and secondarily to OH groups of chitosan that have the capacity to scavenge radicals.[8] One of the characteristics that make chitosan interesting for applications in medicine or in the food packaging industry is its antioxidant activity;[46] therefore, BC−Ch nanocomposites can be a suitable material for these kinds of applications.

CONCLUSIONS

In this work, the combination of BC and chitosan rendered composites of paper with improved physical, chemical, and biological characteristics. The two impregnation methods tested allowed a stable binding of chitosan to the BC matrix without the requirement of cross-linking molecules and produced BC−Ch nanocomposites with similar characteristics. BC−Ch nanocomposites had the consistency and stiffness of paper and showed great durability, retaining their properties for a long time without the need for special storage in terms of temperature or humidity. They had good resistance to the passage of air and water. They exhibited antimicrobial activity against bacteria and yeasts and prevented the formation of biofilms on their surfaces. Moreover, BC−Ch paper showed scavenging capacity of oxidizing radicals. The BC−Ch composites developed in this work generated paperlike supports, which can expand the previously described biomedical applications for chitosan embedded in a never-dried BC membrane and BC film. Their physical and biological properties, and the organic nature of its components, make them suitable to be part of the design of environmentally friendly materials in the area of bioactive papers.

AUTHOR INFORMATION

Corresponding Author

Josefina Martínez − *Department of Genetics, Microbiology and Statistics, Faculty of Biology, University of Barcelona, 08028 Barcelona, Spain; Institute of Nanoscience and Nanotechnology (IN2UB), 08028 Barcelona, Spain;* orcid.org/0000-0002-2411-8818; Phone: +34 934034625; Email: jmartinez@ub.edu; Fax: +34 934034629

Authors

L. Verónica Cabañas-Romero − *Department of Genetics, Microbiology and Statistics, Faculty of Biology, University of Barcelona, 08028 Barcelona, Spain*

Cristina Valls − *CELBIOTECH_Paper Engineering Research Group, EGE Department, Universitat Politècnica de Catalunya, Barcelona Tech, 08222 Terrassa, Spain*

Susana V. Valenzuela − *Department of Genetics, Microbiology and Statistics, Faculty of Biology, University of Barcelona, 08028 Barcelona, Spain; Institute of Nanoscience and Nanotechnology (IN2UB), 08028 Barcelona, Spain*

M. Blanca Roncero − *CELBIOTECH_Paper Engineering Research Group, EGE Department, Universitat Politècnica de Catalunya, Barcelona Tech, 08222 Terrassa, Spain;* orcid.org/0000-0002-2694-2368

F. I. Javier Pastor − *Department of Genetics, Microbiology and Statistics, Faculty of Biology, University of Barcelona, 08028 Barcelona, Spain; Institute of Nanoscience and Nanotechnology (IN2UB), 08028 Barcelona, Spain*

Pilar Diaz − *Department of Genetics, Microbiology and Statistics, Faculty of Biology, University of Barcelona, 08028 Barcelona, Spain; Institute of Nanoscience and Nanotechnology (IN2UB), 08028 Barcelona, Spain*

Complete contact information is available at: https://pubs.acs.org/10.1021/acs.biomac.0c00127

Notes

The authors declare no competing financial interest.

ACKNOWLEDGMENTS

This work was financed by the Spanish Ministry of Economy, Industry and Competitiveness, Grants CTQ2017-84966-C2-2-R, FILMBIOCEL CTQ2016-77936-R (funding also from the "Fondo Europeo de Desarrollo Regional FEDER"), and MICROBIOCEL CTQ2017-84966-C2-1-R; the Pla de Recerca de Catalunya, Grant 2017SGR-30; and Generalitat de Catalunya, "Xarxa de Referència en Biotecnologia" (XRB). L.V.C.-R. acknowledges a doctoral fellowship from Programa Nacional de Becas de Posgrado en el Exterior "Don Carlos Antonio López" del Ministerio de Hacienda del Paraguay. Special thanks are due to the Serra Húnter Programme to C.V.

REFERENCES

(1) Klemm, D.; Heublein, B.; Fink, H.-P.; Bohn, A. Cellulose: Fascinating Biopolymer and Sustainable Raw Material. *Angew. Chem., Int. Ed.* **2005**, *44*, 3358−3393.

https://dx.doi.org/10.1021/acs.biomac.0c00127
Biomacromolecules 2020, 21, 1568−1577

(2) Klemm, D.; Kramer, F.; Moritz, S.; Lindström, T.; Ankerfors, M.; Gray, D.; Dorris, A. Nanocelluloses: A New Family of Nature-Based Materials. *Angew. Chem., Int. Ed.* **2011**, *50*, 5438−5466.
(3) Lee, K.-Y.; Buldum, G.; Mantalaris, A.; Bismarck, A. More Than Meets the Eye in Bacterial Cellulose: Biosynthesis, Bioprocessing, and Applications in Advanced Fiber Composites. *Macromol. Biosci.* **2014**, *14*, 10−32.
(4) Torres, F. G.; Arroyo, J. J.; Troncoso, O. P. Bacterial Cellulose Nanocomposites: An All-Nano Type of Material. *Mater. Sci. Eng. C* **2019**, *98*, 1277−1293.
(5) Viana, R. M.; Sá, N. M. S. M.; Barros, M. O.; Borges, M. d. F.; Azeredo, H. M. C. Nanofibrillated Bacterial Cellulose and Pectin Edible Films Added with Fruit Purees. *Carbohydr. Polym.* **2018**, *196*, 27−32.
(6) Lin, S.-P.; Loira Calvar, I.; Catchmark, J. M.; Liu, J.-R.; Demirci, A.; Cheng, K.-C. Biosynthesis, Production and Applications of Bacterial Cellulose. *Cellulose* **2013**, *20*, 2191−2219.
(7) Rabea, E. I.; Badawy, M. E. T.; Stevens, C. V.; Smagghe, G.; Steurbaut, W. Chitosan as Antimicrobial Agent: Applications and Mode of Action. *Biomacromolecules* **2003**, *4*, 1457−1465.
(8) Crouvisier-Urion, K.; Bodart, P. R.; Winckler, P.; Raya, J.; Gougeon, R. D.; Cayot, P.; Domenek, S.; Debeaufort, F.; Karbowiak, T. Biobased Composite Films from Chitosan and Lignin: Antioxidant Activity Related to Structure and Moisture. *ACS Sustainable Chem. Eng.* **2016**, *4*, 6371−6381.
(9) Wahid, F.; Hu, X.; Chu, L.; Jia, S.; Xie, Y.; Zhong, C. Development of Bacterial Cellulose/Chitosan Based Semi-Interpenetrating Hydrogels with Improved Mechanical and Antibacterial Properties. *Int. J. Biol. Macromol.* **2019**, *122*, 380−387.
(10) Lin, W.-C.; Lien, C.-C.; Yeh, H.-J.; Yu, C.-M.; Hsu, S. Bacterial Cellulose and Bacterial Cellulose−Chitosan Membranes for Wound Dressing Applications. *Carbohydr. Polym.* **2013**, *94*, 603−611.
(11) Bordenave, N.; Grelier, S.; Coma, V. Hydrophobization and Antimicrobial Activity of Chitosan and Paper-Based Packaging Material. *Biomacromolecules* **2010**, *11*, 88−96.
(12) Carvalho, T.; Guedes, G.; Sousa, F. L.; Freire, C. S. R.; Santos, H. A. Latest Advances on Bacterial Cellulose-Based Materials for Wound Healing, Delivery Systems, and Tissue Engineering. *Biotechnol. J.* **2019**, *14*, No. 1900059.
(13) Fortunati, E.; Mazzaglia, A.; Balestra, G. M. Sustainable Control Strategies for Plant Protection and Food Packaging Sectors by Natural Substances and Novel Nanotechnological Approaches. *J. Sci. Food Agric.* **2019**, *99*, 986−1000.
(14) Fortunati, E.; Giovanale, G.; Luzi, F.; Mazzaglia, A.; Kenny, J.; Torre, L.; Balestra, G. Effective Postharvest Preservation of Kiwifruit and Romaine Lettuce with a Chitosan Hydrochloride Coating. *Coatings* **2017**, *7*, No. 196.
(15) Chen, C. H.; Wang, F. Y.; Mao, C. F.; Liao, W. T.; Hsieh, C. D. Studies of Chitosan: II. Preparation and Characterization of Chitosan/Poly(Vinyl Alcohol)/Gelatin Ternary Blend Films. *Int. J. Biol. Macromol.* **2008**, *43*, 37−42.
(16) Grande, C. J.; Torres, F. G.; Gomez, C. M.; Troncoso, O. P.; Canet-Ferrer, J.; Martinez-Pastor, J. Development of Self-Assembled Bacterial Cellulose−Starch Nanocomposites. *Mater. Sci. Eng. C* **2009**, *29*, 1098−1104.
(17) Bonilla, J.; Fortunati, E.; Atarés, L.; Chiralt, A.; Kenny, J. M. Physical, Structural and Antimicrobial Properties of Poly Vinyl Alcohol−Chitosan Biodegradable Films. *Food Hydrocolloids* **2014**, *35*, 463−470.
(18) Morena, A. G.; Roncero, M. B.; Valenzuela, S. V.; Valls, C.; Vidal, T.; Pastor, F. I. J.; Díaz, P.; Martínez, J. Laccase/TEMPO-Mediated Bacterial Cellulose Functionalization: Production of Paper-Silver Nanoparticles Composite with Antimicrobial Activity. *Cellulose* **2019**, *26*, 8655−8668.
(19) Kjellgren, H.; Gällstedt, M.; Engström, G.; Järnström, L. Barrier and Surface Properties of Chitosan-Coated Greaseproof Paper. *Carbohydr. Polym.* **2006**, *65*, 453−460.
(20) Hestrin, S.; Schramm, M. Synthesis of Cellulose by *Acetobacter xylinum*. 2. Preparation of Freeze-Dried Cells Capable of Polymerizing Glucose to Cellulose. *Biochem. J.* **1954**, *58*, 345−352.
(21) Segal, L.; Creely, J. J.; Martin, A. E.; Conrad, C. M. An Empirical Method for Estimating the Degree of Crystallinity of Native Cellulose Using the X-Ray Diffractometer. *Text. Res. J.* **1959**, *29*, 786−794.
(22) Mariscal, A.; Lopez-Gigosos, R.; Carnero-Varo, M.; Fernandez-Crehuet, J. Fluorescent Assay Based on Resazurin for Detection of Activity of Disinfectants against Bacterial Biofilm. *Appl. Microbiol. Biotechnol.* **2009**, *82*, 773−783.
(23) Serpen, A.; Capuano, E.; Fogliano, V.; Gökmen, V. A New Procedure To Measure the Antioxidant Activity of Insoluble Food Components. *J. Agric. Food Chem.* **2007**, *55*, 7676−7681.
(24) Valls, C.; Roncero, M. B. Antioxidant Property of TCF Pulp with a High Hexenuronic Acid (HexA) Content. *Holzforschung* **2013**, *67*, 257−263.
(25) Cusola, O.; Valls, C.; Vidal, T.; Roncero, M. B. Conferring Antioxidant Capacity to Cellulose Based Materials by Using Enzymatically-Modified Products. *Cellulose* **2015**, *22*, 2375−2390.
(26) Badawy, M. E. I. A New Rapid and Sensitive Spectrophotometric Method for Determination of a Biopolymer Chitosan. *Int. J. Carbohydr. Chem.* **2012**, *2012*, No. 139328.
(27) Fernandes, S. C. M.; Oliveira, L.; Freire, C. S. R.; Silvestre, A. J. D.; Neto, C. P.; Gandini, A.; Desbriéres, J. Novel Transparent Nanocomposite Films Based on Chitosan and Bacterial Cellulose. *Green Chem.* **2009**, *11*, 2023−2029.
(28) Liang, J.; Wang, R.; Chen, R. The Impact of Cross-Linking Mode on the Physical and Antimicrobial Properties of a Chitosan/Bacterial Cellulose Composite. *Polymers* **2019**, *11*, No. 491.
(29) Aryaei, A.; Jayatissa, A. H.; Jayasuriya, A. C. Nano and Micro Mechanical Properties of Uncross-Linked and Cross-Linked Chitosan Films. *J. Mech. Behav. Biomed. Mater.* **2012**, *5*, 82−89.
(30) Wei, B.; Yang, G.; Hong, F. Preparation and Evaluation of a Kind of Bacterial Cellulose Dry Films with Antibacterial Properties. *Carbohydr. Polym.* **2011**, *84*, 533−538.
(31) Kingkaew, J.; Kirdponpattara, S.; Sanchavanakit, N.; Pavasant, P.; Phisalaphong, M. Effect of Molecular Weight of Chitosan on Antimicrobial Properties and Tissue Compatibility of Chitosan-Impregnated Bacterial Cellulose Films. *Biotechnol. Bioprocess Eng.* **2014**, *19*, 534−544.
(32) Orelma, H.; Filpponen, I.; Johansson, L. S.; Laine, J.; Rojas, O. J. Modification of Cellulose Films by Adsorption of Cmc and Chitosan for Controlled Attachment of Biomolecules. *Biomacromolecules* **2011**, *12*, 4311−4318.
(33) VandeVord, P. J.; Matthew, H. W. T.; DeSilva, S. P.; Mayton, L.; Wu, B.; Wooley, P. H. Evaluation of the Biocompatibility of a Chitosan Scaffold in Mice. *J. Biomed. Mater. Res.* **2002**, *59*, 585−590.
(34) Baldrick, P. The Safety of Chitosan as a Pharmaceutical Excipient. *Regul. Toxicol. Pharmacol.* **2010**, *56*, 290−299.
(35) Fortunati, E. Multifunctional Films, Blends, and Nanocomposites Based on Chitosan: Use in Antimicrobial Packaging. *Antimicrobial Food Packaging*; Elsevier Inc, 2016; pp 467−477.
(36) Phisalaphong, M.; Jatupaiboon, N. Biosynthesis and Characterization of Bacteria Cellulose-Chitosan Film. *Carbohydr. Polym.* **2008**, *74*, 482−488.
(37) Fillat, A.; Martinez, J.; Valls, C.; Cusola, O.; Valenzuela, S. V.; et al. Bacterial Cellulose for Increasing Barrier Properties of Paper Products. *Cellulose* **2018**, *25*, 6093−6105.
(38) Requies, J.; Gabilondo, N.; Urbina, L.; Corcuera, M. A.; Retegi, A.; Guaresti, O.; Eceiza, A. Design of Reusable Novel Membranes Based on Bacterial Cellulose and Chitosan for the Filtration of Copper in Wastewaters. *Carbohydr. Polym.* **2018**, *193*, 362−372.
(39) Mishima, T.; Hisamatsu, M.; York, W. S.; Teranishi, K.; Yamada, T. Adhesion of β-D-Glucans to Cellulose. *Carbohydr. Res.* **1998**, *308*, 389−395.
(40) Goy, R. C.; Britto, D. D.; Assis, O. B. G. A Review of the Antimicrobial Activity of Chitosan. *Polim.: Cienc. Tecnol.* **2009**, *19*, 241−247.

https://dx.doi.org/10.1021/acs.biomac.0c00127
Biomacromolecules 2020, 21, 1568−1577

(41) Flemming, H.-C.; Wingender, J. The Biofilm Matrix. *Nat. Rev. Microbiol.* **2010**, *8*, 623−633.
(42) Costerton, J. W. Bacterial Biofilms: A Common Cause of Persistent Infections. *Science* **1999**, *284*, 1318−1322.
(43) Martinez, L. R.; Mihu, M. R.; Han, G.; Frases, S.; Cordero, R. J. B.; Casadevall, A.; Friedman, A. J.; Friedman, J. M.; Nosanchuk, J. D. The Use of Chitosan to Damage Cryptococcus Neoformans Biofilms. *Biomaterials* **2010**, *31*, 669−679.
(44) Campana, R.; Biondo, F.; Mastrotto, F.; Baffone, W.; Casettari, L. Chitosans as New Tools against Biofilms Formation on the Surface of Silicone Urinary Catheters. *Int. J. Biol. Macromol.* **2018**, *118*, 2193−2200.
(45) Zhang, L.; Ge, H.; Xu, M.; Cao, J.; Dai, Y. Physicochemical Properties, Antioxidant and Antibacterial Activities of Dialdehyde Microcrystalline Cellulose. *Cellulose* **2017**, *24*, 2287−2298.
(46) Coma, V. Polysaccharide-Based Biomaterials with Antimicrobial and Antioxidant Properties. *Polim.: Ciênc. Tecnol.* **2013**, *20*, 287−297.

https://dx.doi.org/10.1021/acs.biomac.0c00127
Biomacromolecules 2020, 21, 1568−1577

Monooxigenasas líticas de polisacáridos para la producción de nanocristales de celulosa bacteriana

Los nanocristales de celulosa son un biomaterial renovable con propiedades a nivel nanométrico que tienen aplicaciones útiles. En este estudio, se realizó un tratamiento enzimático, un enfoque mucho más respetuoso con el medio ambiente que la tradicional hidrólisis ácida agresiva, para obtener nanocristales de celulosa bacteriana (BCNC, por sus siglas en inglés). La combinación de una oxidación mediante una monooxigensa lítica de polisacárido (LPMO, por sus siglas en inglés) y una hidrólisis con una mezcla de glicosil hidrolasas resultó efectiva para producir nanocristales a partir de la celulosa bacteriana. La morfología y el tamaño se confirmaron mediante microscopía electrónica y difracción láser, respectivamente. La estabilidad térmica también se midió y determinó que era mayor en comparación con la celulosa bacteriana nativa. Además, se descubrió que las cargas negativas generadas por la LPMO aumentaron la dispersión de los nanocristales en solución acuosa, medida mediante el potencial zeta. Los BCNC se utilizaron para recubrir materiales celulósicos preexistentes. Los compuestos obtenidos mostraron propiedades mecánicas mejoradas, una capacidad elevada de retención de agua e impermeabilidad al aceite. Estas características atractivas podrían llevar a los nanocompuestos de polímeros que contienen BCNC a tener un impacto en el campo de los materiales de embalaje biocompatibles y biodegradables.

European Polymer Journal 163 (2022) 110939

Contents lists available at ScienceDirect

European Polymer Journal

journal homepage: www.elsevier.com/locate/europolj

Lytic polysaccharide monooxygenases and cellulases on the production of bacterial cellulose nanocrystals

Carolina Buruaga-Ramiro [a,b], Noelia Fernández-Gándara [a], L. Verónica Cabañas-Romero [a,b], Susana V. Valenzuela [a,b], F.I. Javier Pastor [a,b], Pilar Diaz [a,b], Josefina Martinez [a,b,*]

[a] Department of Genetics, Microbiology and Statistics, Faculty of Biology, University of Barcelona, Av. Diagonal 643, 08028 Barcelona, Spain
[b] Institute of Nanoscience and Nanotechnology (IN2UB), Universitat de Barcelona, Spain

ARTICLE INFO

Keywords:
Bacterial cellulose
Bacterial cellulose nanocrystals
Nanocomposites, cellulose enzymatic hydrolysis
Lytic polysaccharide monooxygenases

ABSTRACT

Cellulose nanocrystals are a renewable biomaterial with nanoscale properties which have useful applications. In this study, an enzymatic treatment, an approach much more environmentally friendly than the traditional harsh acid hydrolysis, was performed to obtain bacterial cellulose nanocrystals (BCNC). The combination of an oxidation by a lytic polysaccharide monooxygenase (LPMO) and a hydrolysis with a mixture of glycosyl hydrolases was effective to produce nanocrystals from bacterial cellulose. Morphology and size were confirmed by electron microscopy and laser diffraction, respectively. Thermal stability was also measured and determined to be higher relative to native bacterial cellulose. Additionally, it was found that the negative charges generated by the LPMO increased the dispersion of the nanocrystals in aqueous solution, measured by the zeta potential. The BCNC were used to coat pre-existing cellulosic materials. The obtained composites displayed improved mechanical properties, an elevated water retention capacity, and impermeability to oil. These attractive features could lead BCNC-containing polymer nanocomposites to make an impact in the field of biocompatible and biodegradable packaging materials.

1. Introduction

There is a need to create a sustainable material that could replace traditional plastic packaging. In order to reduce packaging waste created by non-degradable petroleum based packaging materials, in the last decades, there has been a rising effort to produce various biodegradable polymers for the development of edible films [1]. However, these biopolymer edible films have some limitations regarding their mechanical properties and water sensitivity. An alternative to overcome them is the use of nanomaterials, which can reinforce biopolymers by the formation of nanocomposites [2]. Nanocomposites are defined as the combination of two types of individual materials: the matrix and the material imbedded on it, being at least one of the two of nanometre-sized dimension [3]. The reinforcement provided by the nanomaterial provides improved mechanical, thermal, optical, and physicochemical properties in comparison to the polymer alone [2,4], even at very low fractions [5]. Thus, the nanometric size and the increased surface area of the reinforcing material provides this new nanocomposite unique properties [6].

From the wide range of natural resources, cellulose is the most abundant macromolecule on Earth, and it is seen as an exciting alternative to fossil-fuel plastics. In fact, cellulose nanocrystals (CNC) obtained from plant sources are commonly used as nanomaterials [7]. These CNC are highly crystalline and exhibit excellent properties like high tensile strength [8]. The conversion of cellulose fibres into nanocrystals results in the formation of the well-known whiskers, rod-like or ribbon-like shape with large aspect ratio, mainly due to their nanoscale dimensions. When compared to cellulose fibres, CNC possess many advantages apart from their appealing intrinsic nanoscale dimension such as high surface area, unique morphology, low density, renewability, biodegradability and high mechanical strength [9-11]. According to their structure, CNC have an abundance of hydroxyl groups on the active surface, which allows both, the hydrogen bonding with the fibres [12] and further functionalization [13]. The applications of CNC can be of

* Corresponding author at: Department of Genetics, Microbiology and Statistics, Faculty of Biology, Universitat de Barcelona, Av. Diagonal 643, 08028 Barcelona, Spain.
E-mail addresses: buruaga.cbr@ub.edu (C. Buruaga-Ramiro), noeliafdzgandara@gmail.com (N. Fernández-Gándara), veronica.cabanas@ub.edu (L.V. Cabañas-Romero), susanavalenzuela@ub.edu (S.V. Valenzuela), fpastor@ub.edu (F.I.J. Pastor), pdiaz@ub.edu (P. Diaz), jmartinez@ub.edu (J. Martinez).

https://doi.org/10.1016/j.eurpolymj.2021.110939
Received 23 September 2021; Received in revised form 30 November 2021; Accepted 7 December 2021
Available online 10 December 2021

two types. On the one hand, they suppose a suitable material for a wide range of applications such as synthesis of antimicrobial materials, enzyme immobilization, green catalysis, biosensing and drug delivery [14-16]. On the other hand, CNC can act as a reinforcing agent [5], with potential uses ranging from barrier films to pH sensors [17-20]. Nevertheless, bacterial cellulose (BC) is more preferred over plant cellulose for CNC obtention as it is available in relatively pure form and has better physic-chemical properties than plant cellulose [21]. BC is produced mainly by bacteria from the genera *Komagataeibacter* as an exopolysaccharide. Even though in terms of chemical structure BC is identical to the vegetal one, it is synthetized chemically pure as it does not present hemicelluloses or lignin [22]. Consequently, it does not need to be purified, reducing the economic and the environmental impact. In addition, BC displays a higher degree of crystallinity, a higher tensile strength, a higher water-holding capacity and a finer three-dimensional nanofibre network [23,24]. BC is a versatile biomaterial with numerous biotechnological applications [25]. Besides, its addition to other celluloses is well known to decrease porosity, improving barrier properties, which is interesting in packaging applications [26]. Nanocrystals derived from bacterial cellulose (BCNC) can be physically incorporated into various polymer matrices to form polymer nanocomposites [27].

CNC suspensions can be obtained by submitting native cellulose to a harsh sulfuric acid hydrolysis, often followed by ultrasound treatments, as Rånby et al. described [28]. Under this acid treatment, the amorphous regions that interconnect the crystalline regions are removed and finally, the rod-like cellulose nanocrystals are isolated [29,30]. Even if the acid hydrolysis has been improved in terms of time of hydrolysis, choice of acid and its concentration, the principle of existing technologies for conversion of cellulosic biomass into CNC has barely changed until the date. It should be noted that this method requires many hazardous chemicals, which give alarming negative impacts to the environment. Furthermore, it can affect the final properties of the CNC, compromising their potential applications [31]. Thus, it is necessary to search for new processes to produce high quality CNC, with low environmental impact and without compromising their technological or health applications. In this direction, enzymatic hydrolysis offers the potential for higher selectivity, lower energy costs and milder operating conditions than chemical processes [32]. For instance, the inclusion of an enzymatic pretreatment in the process of preparation of microfibrillated cellulose is a feasible approach, at least from kraft pulp, as Lopez-Rubio et al. [33] and Svagan et al. [34] confirmed. In the enzymatic hydrolysis of cellulose, the main involved enzymes are the cellobiohydrolases (CBH) or cellulases. To digest efficiently crystalline cellulose at least three types of CBH are known to cooperate: (1) endoglucanases (EC 3.2.1.4) that cut cellulose chains in random locations; (2) exoglucanases (EC 3.2.1.91) which peel cellulose in a processive manner on the reducing or non-reducing ends of cellulose polysaccharide chains and (3) beta - glucosidases (bGLs) (EC 3.2.2.21) which hydrolyse cellobiose and various soluble cellodextrins into glucose [31,35]. Synergistic phenomena are widely observed in cellulose hydrolysis, with many forms reported and proposed [32,36,37]. However, the accessibility of the cellobiohydrolases to the crystalline regions was difficult to understand, and authors hypothesized for decades about a "a non-hydrolytic component" that, in nature, could disrupt the cellulosic substrate, increasing its accessibility for the hydrolytic enzymes [38]. It was not until 2010 that the oxidative cleavage of cellulose glycosidic bonds was described, performed by a new type of enzyme, the lytic polysaccharide monooxygenases (LPMO) [39]. LPMOs cleave cellulose leading to the formation of aldonic acids when the C1 is oxidized and/or 4-ketoaldoses at the C4 position [40]. Since then, they have extensively been reported to promote the efficiency of cellulases during cellulose digestion [39,41,42]. They are thought to act in first place, making crystalline cellulose accessible to glycosyl hydrolases [43,44].

In this study BCNC were obtained by an environmentally friendly technique based on an exclusively enzymatic treatment of native BC. First, BC paste was treated with the enzyme SamLPMO10C, a LPMO identified and cloned in the research group [44]. Then, it was digested with a commercially available preparation of cellobiohydrolases. The obtained BCNC were characterized in terms of morphology and chemical structure by electron microscopy and X-ray diffraction, respectively, and their dispersive and thermal properties measured. Finally, BCNC were used as reinforcing agent onto pre-existing eucalyptus sheets, and the mechanical and barrier properties of the obtained composites were evaluated.

2. Methods

2.1. BC synthesis and preparation of BC

Komagataeibacter intermedius JP2, a bacterial cellulose producer previously isolated in the laboratory [45], was grown on the Hestrin and Schramm (HS) medium, containing 20 g/L glucose, 20 g/L peptone, 10 g/L yeast extract, 1.15 g/L citric acid, 6.8 g/L Na_2HPO_4, pH 6. The cultures were statically incubated at 25–28 °C for 7 days. After that time, bacterial cellulose membranes generated in the air/liquid interface of the culture media were harvested, rinsed with water and incubated in 1% (w/v) NaOH at 70 °C 18 h. Then, the BC membranes were thoroughly washed in deionized water until neutrality was reached. Membranes were mechanically disrupted with a blender and homogenized (Homogenizing System UNIDRIVE X1000) to obtain a BC paste containing a suspension of BC fibres. The amount of BC was determinated by drying samples of known weight at 60 °C until constant weight.

2.2. Expression and purification of SamLPMO10C

Escherichia coli BL21 star (DE3) harvesting pET11/SamLPMO10C [44] was cultured in LB medium supplemented with 50 μ/mL kanamycin at 37 °C, and induced by 0,5 mM isopropyl β-D-1-thiogalactopyranoside (IPTG) at O.D. 600 nm = 0.8. After cultivation at 21 °C for 18 h, cell pellets were collected by centrifugation and resuspended in 50 mM Tris-HCl pH 7. Cells were lysed using PANDA GEA 2000 homogenizer at 800 bar. Soluble fraction of the cleared cell extracts were mixed with 5% (w/v) Avicel® PH-101 (Fluka) with gentle rotary shaking for 1 h at 4 °C. Following, samples of SamLPMO10C were purified by polysaccharide-binding as described previously [44], with some modifications: to collect bound proteins, a centrifugation of 5 min at 14,000 × g was used to separate the pellet of insoluble polysaccharides with adsorbed enzymes. The pellets were sequentially washed 3 times with fresh buffer and centrifuged to remove non-specific protein binding. Pellets were washed with 3 volumes of 1 M glucose, for 30 min each, at 4 °C with gentle rotary shaking in order to elute adsorbed enzymes. Then, samples were centrifuged at 14,000 × g for 5 min to separate supernatants (with eluted SamLPMO10C) from pellet. Homogeneity of samples were analysed by sodium dodecyl sulphate polyacrylamide gel electrophoresis (SDS-PAGE).

2.2.1. Copper saturation

Purified SamLPMO10C (Uniprot, A3KKC4) was saturated with copper by incubation with a 4-fold molar excess of $CuSO_4$ for 30 min at room temperature as described elsewhere [40]. Excess copper and glucose were removed by desalting the proteins using a PD-10 desalting columns (GE Healthcare) equilibrated with 20 mM MES buffer, pH 5.5. The concentration of desalted Cu^{2+} - saturated SamLPMO10C was measured with NanoDrop® ND-1000 (NanoDrop Technologies, Inc), using an extinction coefficient (ε) at 280 nm of 75.775 M_1 cm_1. The enzyme solution was stored at −20 °C before used.

2.2.2. LPMO activity

Standard reactions were carried out by mixing 1% (dry weight) of substrate with 5 μM of Cu^{2+} - saturated SamLPMO10C, 2 mM ascorbic acid and 20 μM of H_2O_2 if necessary. Reactions were performed in 50 mM of ammonium acetate pH 5.5 with PASC (Phosphoric Acid Swollen

Cellulose) and H_2O_2, and BC, and incubated at 50 °C with shaking for 72 h and 24 h, respectively. PASC was obtained from crystalline cellulose Avicel ® PH-101 (Fluka) treated with 70% of H_3PO_4 according to Wood [46], using centrifugation for the sedimentation of the cellulose instead of decantation during the washing process. Control reactions without LPMO were run in the same way. All reactions were performed in duplicates at least three times. Soluble fractions generated in the degradation reactions were analysed by matrix-assisted laser desorption/ionization time of flight mass spectrometry (MALDI-TOF MS) for the analysis of oxidized products. Reaction samples (3 μl) were mixed with 7 μl of acetonitrile. 1 μl of this solution was mixed with 1 μl of matrix solution (10 mg/ml of 2,5-dihydroxybenzoic acid dissolved in acetonitrile–water [1:1, vol/vol], 0.1% [wt/vol] trifluoroacetic acid)0.1 μl of the mixture was spotted in duplicated onto the MALDI-TOF MS plate and allowed to dry before the analysis. Positive mass spectra were collected with a 4800 Plus MALDI TOF/TOF (ABSciex 2010) spectrometer with an Nd:YAG 200-Hz laser operated at 355 nm.

2.3. Cellulase cocktail activity

Enzymatic product MetZyme® BRILA™ (cellulase cocktail C2) was kindly supplied by MetGen Oy (Finland) [47]. Reducing sugars resulting from glycosil hydrolase activity were quantified by the DNS reagent method [48]. Standard assays were performed at 50 °C in 50 mM potassium acetate buffer at pH 5. Solid material was removed by centrifugation at 12.000 × *g* for 5 min and cleared supernatant was analysed. One unit of enzymatic activity was defined as the amount of enzyme that releases 1 μmol of reducing sugar equivalent per min. A standard curve of glucose was used to calculate activity units. All determinations were made in triplicate at least two times.

2.4. Enzymatic preparation of bacterial cellulose nanocrystals (BCNC)

Enzymatic hydrolysis of the BC paste was run using the enzymes SamLPMO10C and the cellulose cocktail C2. Bacterial cellulose paste (1% dry weight) was mixed with Cu^{2+} - saturated SamLPMO10C and 2 mM ascorbic acid in 50 mM ammonium acetate pH 5.5. The mixture was kept in 50 °C for 24 h. Then, 12.5 U g^{-1} odp (oven-dried pulp) of C2 was added and the mixture was incubated at 60 °C for 18 h. For control reaction, the same dried weight of bacterial cellulose paste was incubated in all the buffer components at the same conditions. All reactions were incubated with shaking in a water bath. Hydrolysis was stopped by heating up the reaction to 100 °C for 10 min. The obtained suspensions were homogenized by ultrasonication (80 W, 0.8 s) in a Labsonic 1510 sonicator (B.Braun) for 5 min and kept at 4 °C.

2.5. Characterisation of BCNC

2.5.1. Scanning electron microscopy (SEM)

Water suspensions of BCNC were analysed by SEM (JSM 7100F) using a LED filter. Samples were graphite coated using a Vacuum Evaporator EMITECH K950X221. EDS analysis was carried out to verify their chemical composition. The diameter of the fibres was measured using the ImageJ software.

2.5.2. Transmission electron microscopy (TEM)

Suspensions of BCNC were negatively stained with 2% uranyl acetate, after dropping them on a Cu grid covered with formvar and a thin carbon film, and allowed to dry at room temperature. The diameter and length of BCNC were obtained using a transmission electron microscope (TEM) model JEOL 1010. Images were taken at an accelerated voltage of 80 kV. The length (L) and width (D) were determined from at least 100 measurements using the ImageJ software.

2.5.3. X-ray diffraction

X-ray diffraction patterns of dried samples of BCNC were obtained with a PANalytical X'Pert PRO MPD Alpha1 powder diffractometer. The samples were analysed at the radiation wavelength of 1.5418 Å and scanned from 2 ° to 50°, 2θ range. Samples were fixed over a zero background Silicon single crystal sample holder (pw1817/32), and the ensembles were mounted in a PW1813/32 sample holder. The same Silicon holder was used to measure all the replicates of each sample. Eq. (1) [49] was used to calculate the crystallinity index (CI) of bacterial cellulose:

$$CI(\%) = \frac{I_c - I_{am}}{I_c} \times 100 \quad (1)$$

where I_c is the maximum intensity of the lattice diffraction and I_{am} is the height of the intensity at the minimum at 2θ between 18 ° and 19 °, which corresponds to the amorphous part of cellulose.

2.6. Zeta potential

BCNC suspensions and BC were previously diluted in distilled water to a 1:5 and 1:10 sample:water ratio (v/v), respectively. Zeta potential was then measured in a Zetasier NanoZS (Malvern Instruments, UK), in triplicate.

2.7. Particle size determination

2.7.1. Light scattering (LS)

The particle size of BCNC was measured by laser diffraction in the range of 0.375–20000 μm in a Particle Size Analyzer (Beckman Coulter LS 13320), using the Micro Liquid Module in aqueous suspension and Fraunhofer optical model.

2.7.2. Filtration

After the enzymatic hydrolysis was complete, the final reaction containing the BCNC was filtered by several filters with a decreasing diameter pore size (50 μm, 6 μm, 3 μm, 0.4 μm and 0.2 μm, Nangtong FilterBio Membrane Co., Ltd). Then, the filters were left to dry at 80 °C for 24 h and the retained biomass was weighted.

2.8. Thermogravity analysis (TGA)

The thermal stability of BCNC was measured by TGA on TGA/SDTA851^e (Mettler Toledo). The experimental conditions were as follows: the test sample was heated at a rate of 10 °C / min to a maximum of 700 °C in nitrogen inert medium at a flow rate of 50 mL/min. The weight of the dry sample was about 1 mg.

2.9. Composites formation and characterisation

Eucalyptus/BCNC nanocomposites were obtained by a modification of the solving casting technique [50,51]. BCNC were added at different concentrations to preformed 10% (w/v) eucalyptus sheets on a 0.2 μm pore size filter while applying vacuum. Finally, they were left to dry at room temperature for 72 h under pressure. Water permeability was measured by the water drop test (WDT) according to TAPPI standard T835 om-08. The WDT involved placing a drop of deionized water on the surface of paper and recording the time needed for complete absorption, which was signalled by vanishing of the drop specular gloss. Ten measurements per sample were made and averaged. Grease resistance was determined by the standard UNE 5707174, where silica sand was placed on the composite before dyed turpentine was added, and the time needed to penetrate it was counted. Atomic force microscopy (AFM) – Peak Force (PF) Quantitative Nanomechanical Mapping (QNM) mode – was used to determine the tensile properties. Measurements were done with an Antimony (n) doped Si from Bruker, model RTESPA-525 with the characteristics: nominal tip radius 8 nm, cantilever length of 25 μm, resonant frequency 375–675 kHz.

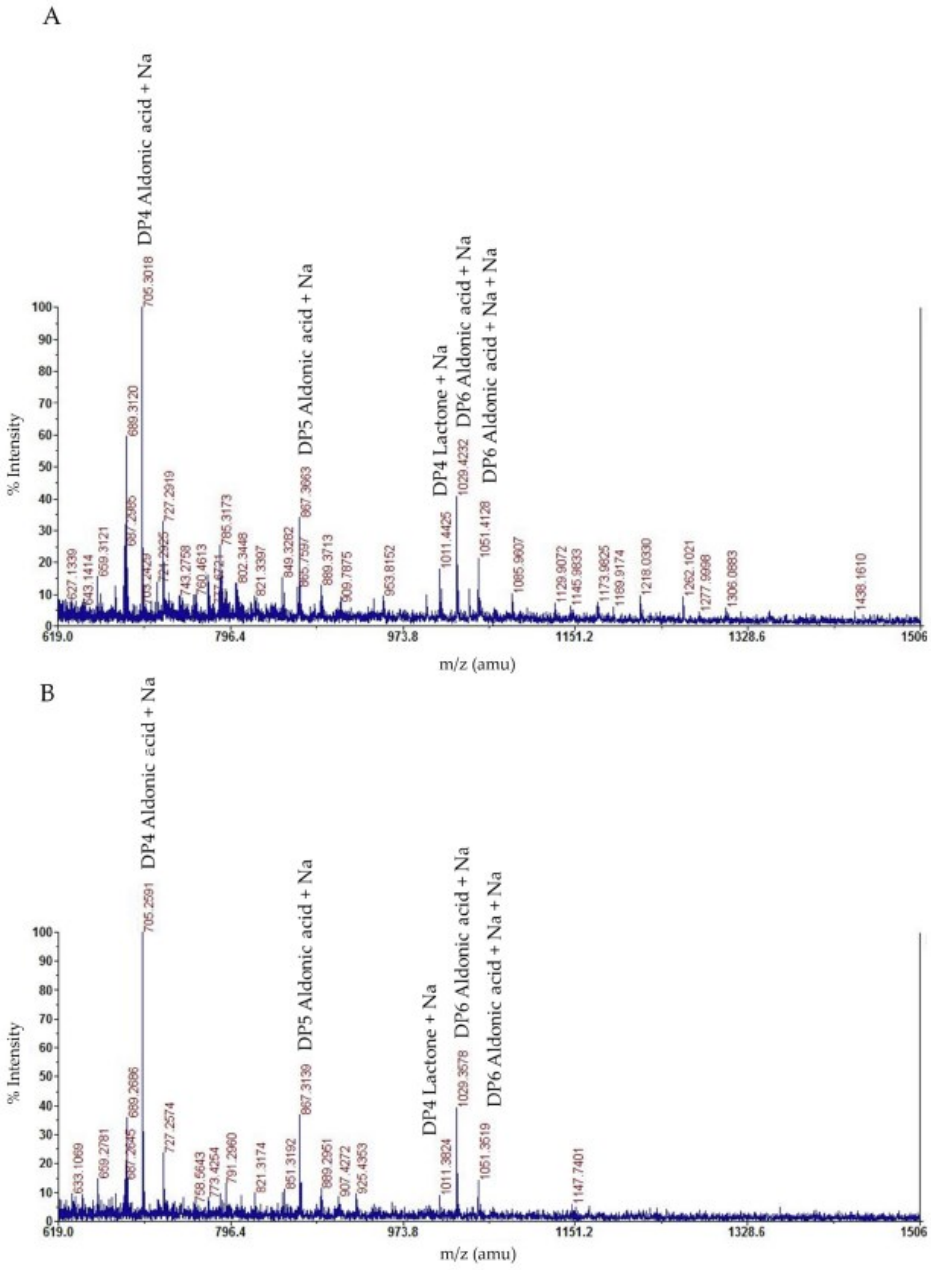

Fig. 1. MALDI-TOF MS analysis of soluble oxidized products from **(A)** PASC and **(B)** BC.

2.10. Statistical analysis

All determinations were performed after two replicas. In the case of enzyme activity, two replicas of triplicates (six determinations per sample) were measured. Experimental data were expressed as means ± standard deviations and were analysed statistically by the paired Student's *t*-test method and analysis of variance (ANOVA) if there were more than two groups in STATGRAPHICS Centurion XVIII software

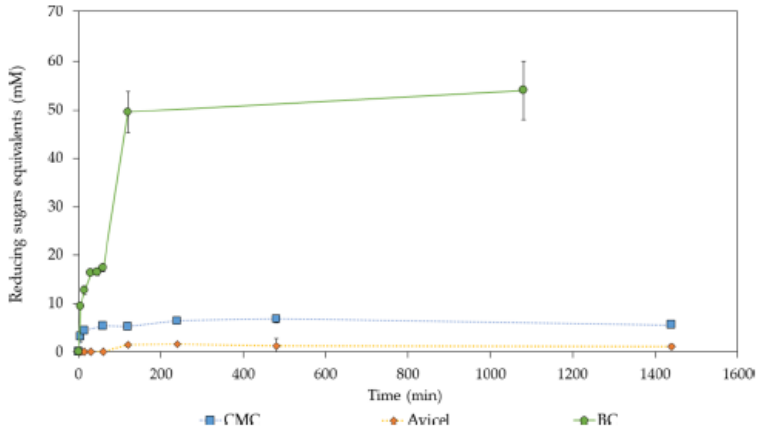

Fig. 2. Activity per mM reducing sugars equivalents of the industrial cellulolytic cocktail over time on different substrates: CMC (squares line), Avicel (rhombus line) and BC (dots line).

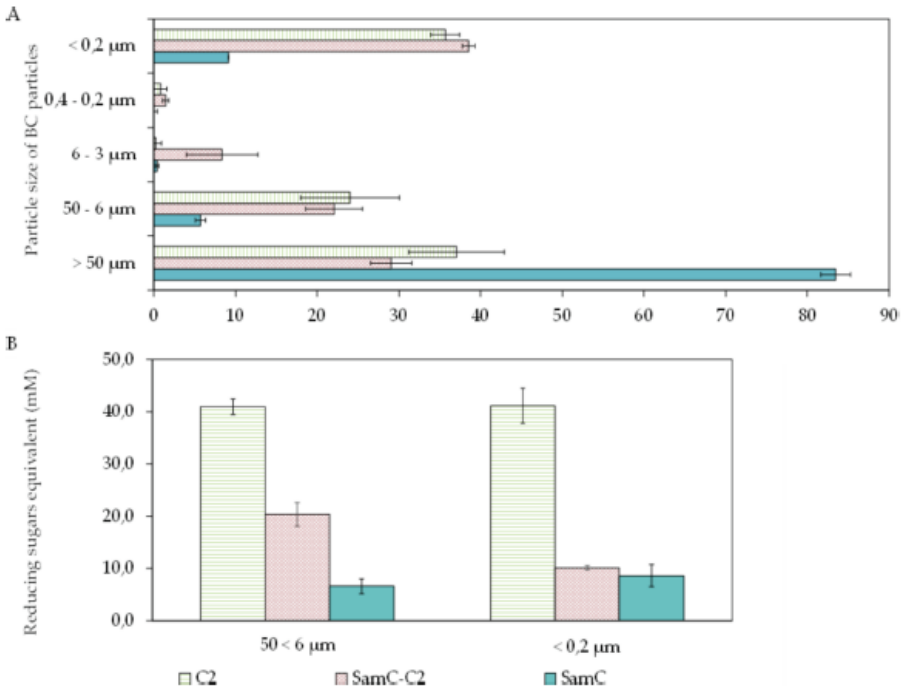

Fig. 3. BCNC length distribution by filtration **(A)** and reducing sugars content **(B)** after the enzymatic treatment.

(Statgraphics.Net, Madrid). Scheffe's multiple range test was used to detect differences among mean values. A value of $p \leq 0.05$ was considered statistically significant. Homogeneity of variance for all samples was tested with Bartlett's test. Residues normal distribution was assumed after performing the Shapiro-Wilk test.

3. Results and discussion

3.1. SamLPMO10C and cellulase activity onto bacterial cellulose

Prior to bacterial cellulose nanocrystals obtention by enzymatic hydrolysis, the activities of purified SamLPMO10C, hereinafter SamC, and cellulase cocktail C2 activities were tested. SamC standard reactions were performed with PASC, routinely considered as the preferred

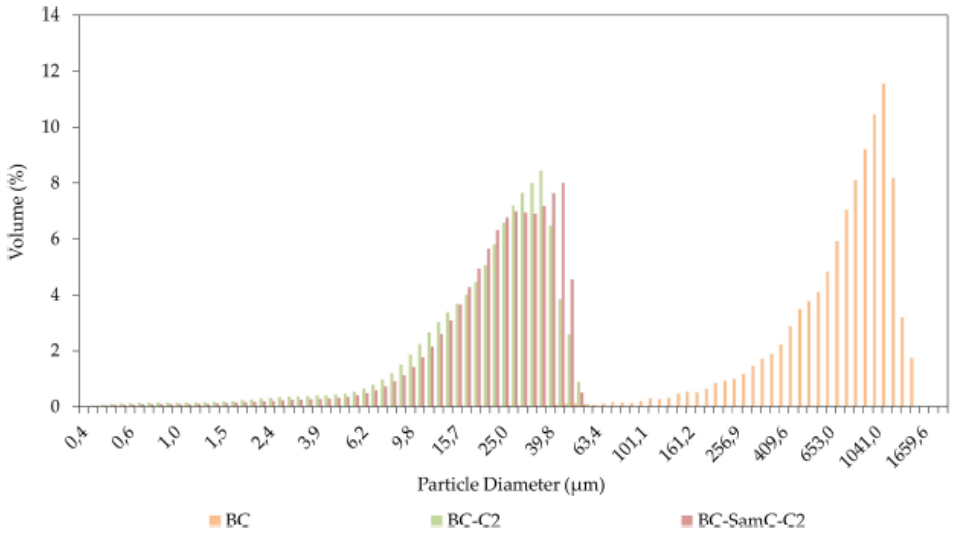

Fig. 4. Particle size distribution of native BC and after enzymatic treatments.

substrate of cellulose active LPMOs [44], and BC. MALDI-TOF MS detection of the soluble oxidized products from SamC activity is shown in Fig. 1. The analysis of the reaction products revealed that, under the reaction conditions used, SamC was active in both substrates, generating oxidized cellooligosaccharides with different degrees of polymerization (DP), of 4–7 in the case of PASC, and 4–6 for BC, in accordance with previous results from the research group [44,52]. In all cases, the peak assignment was in agreement to the size of C1-oxidized fragments from released aldonic acid oligosaccharides.

Glycosyl hydrolase activity of C2 was measured by the reducing sugars method on three crystalline cellulosic substrates: soluble cellulose (CMC, carboxymethyl cellulose), insoluble microcrystalline cellulose (Avicel) and BC, the most crystalline among them. As shown in Fig. 2, the amount of reducing sugars increased over time until a threshold was reached after 2 h of incubation, indicating, cellobiohydrolase activity. However, the activity for BC was notably higher indicating that, likewise SamC, C2 had preference for crystalline substrates as BC, the source of nanocrystals of this work.

3.2. Bacterial cellulose nanocrystals obtention and size distribution

To obtain BCNC, the BC paste was first treated with SamC and then with cellulases C2. Reactions with only SamC or C2 were also run in parallel. Mass spectrometry analysis were performed to detect soluble oxidized products from SamC activity onto BC, as well as to discard LPMO activity from the commercial cocktail C2 (Fig. A1). The particle size distribution of the enzymatically treated samples was attempted by filtering them through a series of membranes of decreasing pore diameter. As can be seen in Fig. 3A, there was a significant shift towards lower fibre sizes after cellulase hydrolysis of BC, in both cases, with and without prior action of SamC. However, more than 80% of the biomass of BC treated only with SamC is retained by 50 µm, while only 37% of the biomass subjected to the action of cellulases exceeds that size, corroborating that cellulases are the main responsible for the digestion of BC. Considering particles < 50 µm, the yield of BCNC obtained by C2 digestion would be of 62.9%, whereas for the pretreatment of SamC followed by C2 cellulase activity would increase it up to 70.9%. Interestingly, with the combined SamC-C2 treatment, more particles between 3 µm and 400 nm were obtained than with only C2 digestion [57], besides that for the bigger fractions all bars are smaller. These results would suggest that with LPMOs the obtained BCNC would have a larger length than those obtained with cellulases alone, which is in disagreement with the generally accepted role of auxiliary activity of LPMO [43,44,53]. This enzyme is thought to make crystalline cellulosic substrates, as BC, more accessible to the glycoside hydrolases, boosting their activity [44]. However, the reported pattern was found again after measuring the reducing sugars of the filtrates 50 < 6 µm and < 200 nm of each treatment (Fig. 3B). The value of reducing sugars after the combined SamC-C2 treatment was higher than those presented by the samples treated only with SamC, indicating that cellulase digestion has been effective. When comparing the two filtrates (50 < 6 µm and < 200 nm) after C2 treatment, there are no apparent differences between them, which could mean that the obtained particles are of small size, with a low degree of polymerization. Nevertheless, for SamC-C2 treatment, the value of reducing sugars is more elevated in the 50 < 6 µm filtration than in the < 200 nm one, reinforcing the prior hypothesis that a previous treatment with SamC before the cellulases digestion resulted in larger particles. Moreover, recent studies have reported severe impeding effects of C1-oxidizing LPMOs on the activity of reducing-end cellobiohydrolases [54]. Even though not knowing the underlying mechanism of this impeding effect, we justify the use of SamLPMO10C for the dispersive properties of the obtained BCNC.

Fig. 4 shows the results of laser diffraction (LS) technique by light scattering, which enabled determination of particle size, based on the diffraction of incident light on a sample. Again, it is clearly visible the effect of C2 onto the BC. In both treatments, SamC-C2 and C2, a shift towards smaller sizes particles could be observed. However, it can be noticed that particles obtained after SamC-C2 treatment had higher percentages of higher diameters than those obtained without previous SamC treatment. The high amount of particles of size greater than 2 µm observed in Fig. 4 could be easily attributed to agglomeration [55]. Similar results were observed by other authors who explain this tendency to agglomerate with presence of strong OH^- intermolecular bonds occurring in cellulose [51]. It should be noted that this technique assumes that the analysed particles are spheres [12], and cellulose nanocrystals are rod-like particles, not spherical. Nevertheless, these results corroborated the effect of the combination of SamC and cellulases treatment on the size of BCNC found by the filtration method.

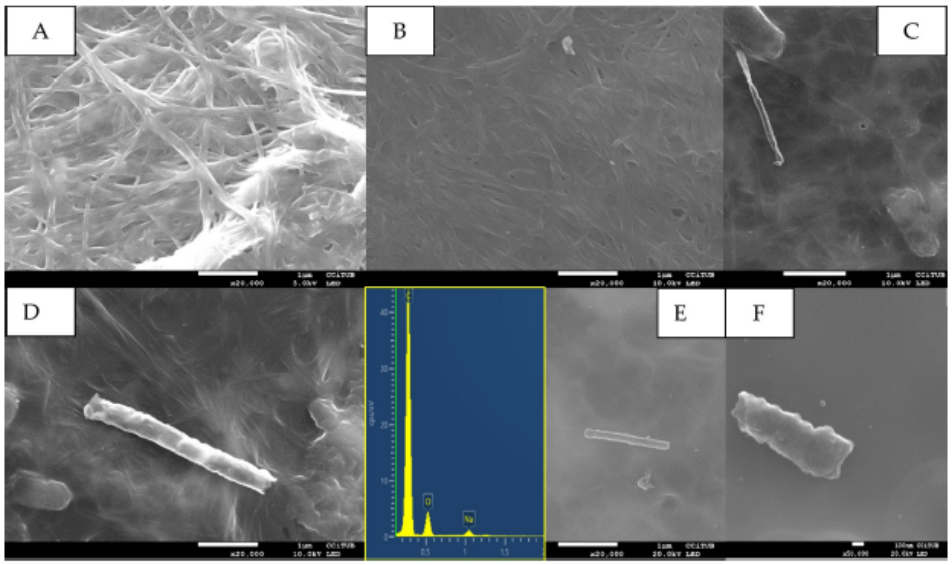

Fig. 5. Electron microscopy images obtained by SEM: BC (**A**), BC-SamC (**B**), BCNC (**C-F**). The insert in (E) represents the energy dispersive X-ray spectrometer (EDS) spectrum of BCNC.

3.3. BCNC characterisation

3.3.1. Morphology

Electron microscopy images of BCNC are shown in Fig. 5 and Fig. 6. Scanning electron microscopy (SEM) pictures of the native BC and oxidized BC by SamC (Fig. 5A, B) show the typical reticulated structure consisting of ultrafine cellulose fibrils with a diameter of about 50 – 70 nm and a length exceeding 20 μm, consistent with previous results [3,56]. Treatment with SamC did not noticeably change the cellulose structure, in agreement with other authors who oxidized BC with SamLPMO10C [52] or 2,2,6,6-tetramethyl-1- piperidinoxyl (TEMPO) [57]. In images of samples of BC enzymatically treated (Fig. 5C-F), rod-like structures compatible with BCNC were observed, with a length (L) in the range 80 nm – 2 μm. Energy Dispersive X-ray spectroscopy (EDS) confirmed that these structures were composed of cellulose.

Transmission electron microscopy (TEM) micrographs of BCNC allowed a more detail analysis (Fig. 6A). The observed flat, rod-like particles had a small number of laterally associated elementary crystallites, usually from 3 to 5, as it has been previously described [28,58]. In TEM negatively stained preparations (Fig. 6B-G), the accumulation of stain around the narrower parts of the nanocrystals suggested an alternation of narrow and wide parts along the BCNC, indicating that they would have a ribbon-like shape and that a homogeneous twist occur [59]. This twist (Fig. 6H-I), which is rarely directly observed [59], is especially clearly observed in well-dispersed ribbon-shaped bacterial cellulose [60], even if it is not clear its origin. It could be attributed to a rotational movement of bacteria or enzyme complexes or to the chiral nature of cellulose, or a combination of both [59]. BCNC had a length ranging from 80 to 2000 nm and a width ranging from 3 to 12 nm, which represented an average length (L) and width (D) of 711 ± 154 nm and 9 ± 5 nm, respectively. These sizes are in line with those reported for BCNC obtained by acid hydrolysis by others. [61-65]. BCNC are usually larger in dimension compared to those obtained from vegetal cellulose as wood and cotton [66,67], hence there are lower fractions of amorphous regions that need to be cleaved resulting in the production of larger nanocrystals [11]. Moreover, these dimensions lead to a higher ratio of length to diameter (L/D). The aspect ratio L/D of the BCNC here obtained was 80.1. The geometrical aspect ratio of cellulose nanocrystals is very important in defining their reinforcing capability in polymer matrices. Generally, nanocrystals exhibiting a ratio L/D greater than 13 results in improved reinforcement properties of the final polymer nanocomposites [11,68].

3.3.2. Crystallinity

Regarding chemical structure, XRD patterns were measured. Fig. 7 showed diffraction peaks at 2θ angles around 18.5 θ and 22.7 θ, corresponding to the typical profile of cellulose in crystalline form [69]. The estimated degree of crystallinity index (Eq. (1)) of the native BC was 97% and 95% for oxidized BC. For BCNC, obtained by SamC-C2 treatment, or only by C2 treatment, the crystallinity index barely changed, with a value of 85%. It should be noted that BC is one of the most crystalline cellulosic substrates [52], and in this work an enzymatic digestion has been performed. Consequently, some of the BC could have been completely hydrolysed, reflected in this slight decrease in crystallinity. In fact, it has been described that severe hydrolysis conditions can result in a likely change in the orientation of the cellulose chains [70]. However, the obtained BCNC displayed high crystallinity, even higher than BCNC obtained by acid hydrolysis [70-72], suggesting that the enzymatic treatment did not modify characteristics as mechanical strength and interfacial properties of the cellulose fibre [73].

3.3.3. Dispersion stability

The zeta potential was measured to evaluate the dispersion stability of BCNC suspensions in water (Fig. 8), where less negative the values are, better is the stability [74]. Interestingly, suspensions of BCNC where SamC was applied presented a zeta potential modulus much higher than suspensions of BCNC obtained without SamC treatment (-6.5 mV and −21.4 mV, respectively), indicating that SamC treatment was necessary for their stability. These results suggested that after SamC mediated oxidation, the negatively charged carboxylic groups would promote electrostatic repulsion and prevent the aggregation of the nanocrystals. CNC obtained by sulphuric acid hydrolysis often acquire a negatively

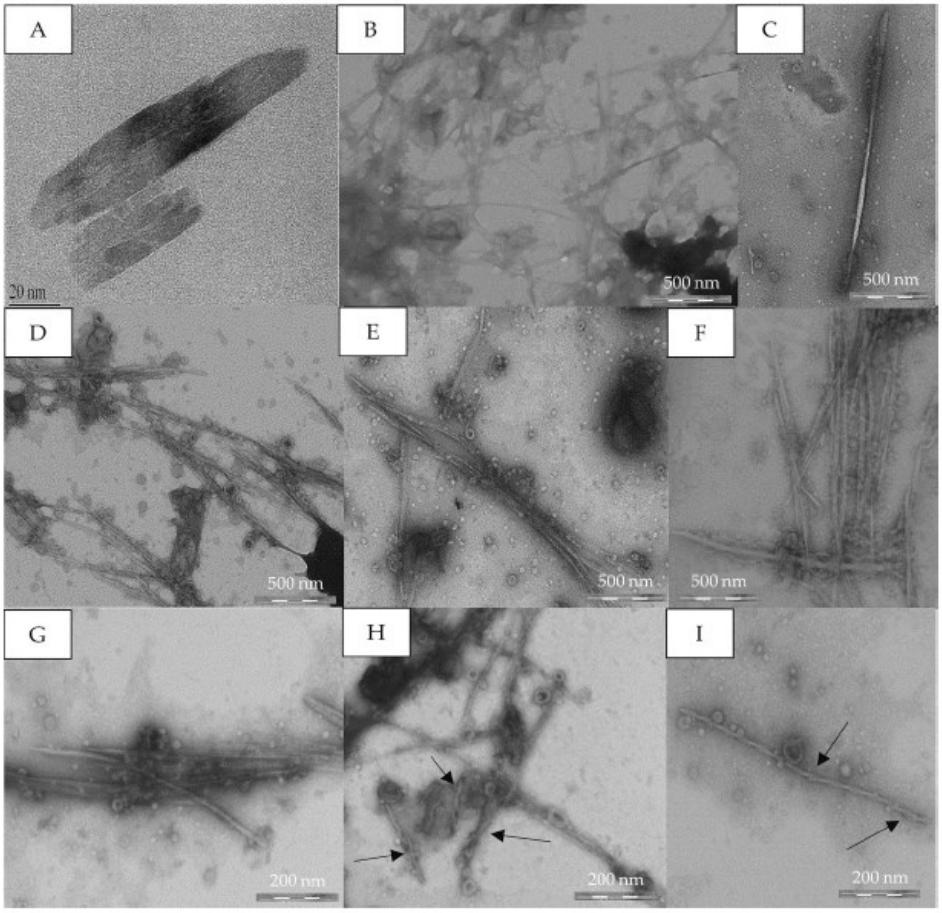

Fig. 6. Electron microscopy images of BCNC obtained by TEM **(A)** and negative stain TEM **(B-I)**. The arrows in (H) and (I) highlight the twist.

charged surface which promotes uniform dispersion in aqueous solution due to electrostatic repulsions [75]. However, even if this sulfonation results in a highly stable colloidal suspension, the obtained CNC are prone to have a lower thermal stability as compared to the native cellulose [76]. On the other hand, without these negative charges, CNC are prone to aggregate because of their strong hydrogen bonding between surface hydroxyl groups [64]. Consequently, this uniform dispersion provided by sulphate groups is a challenge when more environmentally friendly treatments, as the enzymatic ones, are applied. One of the more efficient pretreatments to cellulose is the oxidation mediated by TEMPO, as some authors have reported in the case of the obtention of oxidized nanofibrillated bacterial cellulose [57]. Alternatively, LPMOs have proved to contribute to a more sustainable production of cellulose nanofibrils [41,52], and they could also have a key role, as oxidative enzymes, in giving dispersion stability to BCNC obtained exclusively by enzymatic treatment.

3.4. Thermostability

Thermal stability of cellulose often is drastically changed due to acid hydrolysis during the process of cellulose nanocrystals obtention [76]. Therefore, it is important to establish whether the enzymatic treatments have a similar effect. For this purpose, the thermal degradation profiles of BC and BCNC were assessed by thermogravimetric analysis (TGA). Fig. 9 represents the three mass loss events that can be observed during TGA: the first event corresponds to the evaporation of residual water, while the second is characterized by a series of degradation reactions of cellulose [70,77]. This major degradation step is, though, associated with a high loss of mass of cellulosic material, which is characterized by the onset temperature (T_O, the temperature at 5% weight loss). The third thermal event is related to the unburnable residue. As stated in Table 1, a maximum decomposition point was observed for BC and BC-SamC around 140 °C, even if they had slightly different onset temperatures. Interestingly, enhanced thermal stability was noticed for BCNC, as the maximum degradation rate was registered at a higher temperature: 211,3 and 237,1 °C for those obtained with C2 only and SamC and C2, respectively. These differences could be related to the different defibrillation conditions [78,79]: in comparison with BCNC, BC and BC treated with SamC have a more compact structure for the same weight, leading to a better heat transference and therefore to a higher degradation rate. BCNC with high thermal stability can be used, for instance, for nanocomposites preparation where the polymers blending process

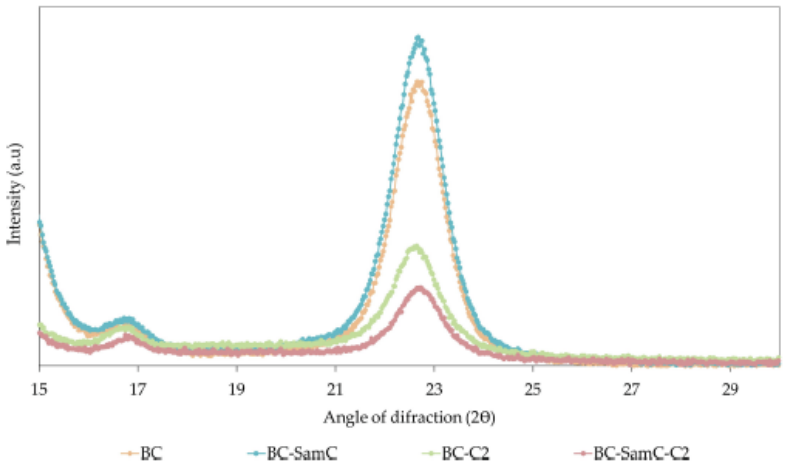

Fig. 7. XRD pattern of BC, BC-SamC and BCNC (BC-C2 and BC-SamC-C2).

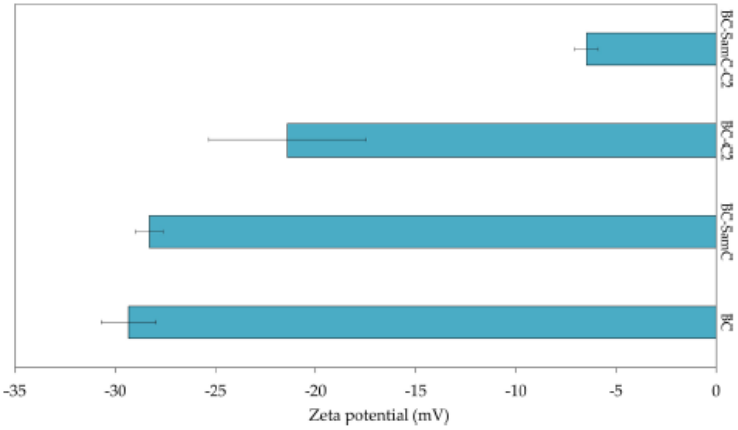

Fig. 8. Results from zeta potential of suspensions of BC, BC treated with SamC (BC-SamC) and with C2 cellulases (BC-C2 and BC-SamC-C2).

requires high temperature.

3.5. Eucalyptus /BCNC nanocomposites

When a polymer is reinforced with a nanomaterial, a polymer nanocomposite is obtained. The nanometric size and the increased surface area of the reinforcing material provides this new nanocomposite unique properties. Their incorporation in many polymers, even at very low volume fractions, can significantly improve the mechanical performance, thermal stability, and barrier and optical properties due to its elevated crystallinity and better interfacial interactions, probably due to high interfacial interactions [5,80]. For this purpose, to assure a good adhesion between the coating and the cellulosic sheet, in this study BCNC were physically incorporated in different doses to prepared 10% (w/v) eucalyptus sheets by casting and water evaporation, one of the most common and effective techniques to produce nanocomposite films on a laboratory scale [11]. As described by other authors, CNC obtained without sulphuric acid often reaggregate [64]. For this reason, CNC are usually chemically modified to improve their dispersion [12]. Nevertheless, the BCNC obtained in this study were negatively charged due to SamC treatment, and as stated by the determination of z potential, they were well dispersed. Overmore, their ratio L/D indicated a high reinforcing capability. Consequently, the obtained composites were homogeneous, no holes or big agglomerates were present in comparison to those coated with BCNC obtained without oxidation. According to literature, Xiang et al. [81] and Yuan et al. [82] proved that getting a homogeneous distribution of BCNC matrix is a key for successfully reinforcing paper in the paper industry. In further studies, these BCNC could serve as a matrix for active compounds immobilization, and the resultant nanocomposites could have special properties, as antimicrobial, antioxidant or catalytic ones [83-86]. They could also provide functionality to biodegradable packages and ability to control microbial population in the food, in the industry of food packaging [12].

3.5.1. Water permeability

All the nanocomposites showed an increased water impermeability in comparison to the eucalyptus sheet (Fig. 10). Interestingly, water retention time reached a threshold over 7 min at 4% BCNC addition.

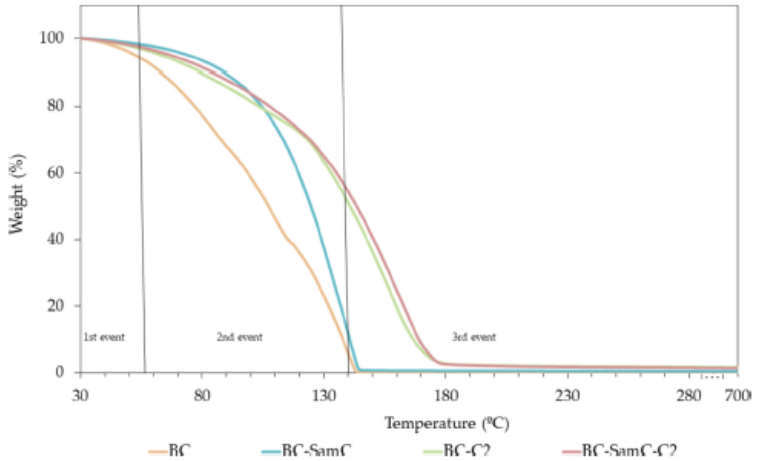

Fig. 9. Thermogravimetric curve of native BC, BC-SamC and after enzymatic treatments with cellulases (BC-C2) and SamC and cellulases (BC-SamC-C2).

Table 1
TGA results for BC, BC-SamC and BCNC after enzymatic treatments with cellulases (BC-C2) and SamC and cellulases (BC-SamC-C2).

	Onset temperature degradation (T_o) (°C)	Maximum degradation temperature (Td) (°C)
BC	63	141.7
BC-SamC	89.3	142.7
BC-C2	85.7	211.3
BC-SamC-C2	107	237.1

This effect can be easily attributed to the low hygroscopicity of highly crystalline BCNC [64]. The water transmission preferentially occurs through the amorphous areas of cellulose and their absence leads in an increase of the time that the water drop is retained on the surface of the nanocomposite. Overmore, the negative charged BCNC contribute to this decrease in water permeability.

3.5.2. Oil impermeability

Regarding barrier properties, a threshold was reached again at 4% of BCNC addition. As shown in Fig. 11, from this concentration the nanocomposite was able to hold the trementine solution for more than 30 min, indicating that it was grease resistant. This enhancement in barrier properties is probably due to the reduction of eucalyptus sheets porosity [12]. According to other authors, the high aspect ratio aspect of BCNC would give this reinforcing effect, ensuring percolation, event at low loadings [80,87]. Materials with low permeability to moisture and oil are very much needed in food and biomedical packaging areas [88].

3.5.3. Mechanical properties

Loading of BCNC resulted in improved mechanical resistance. The

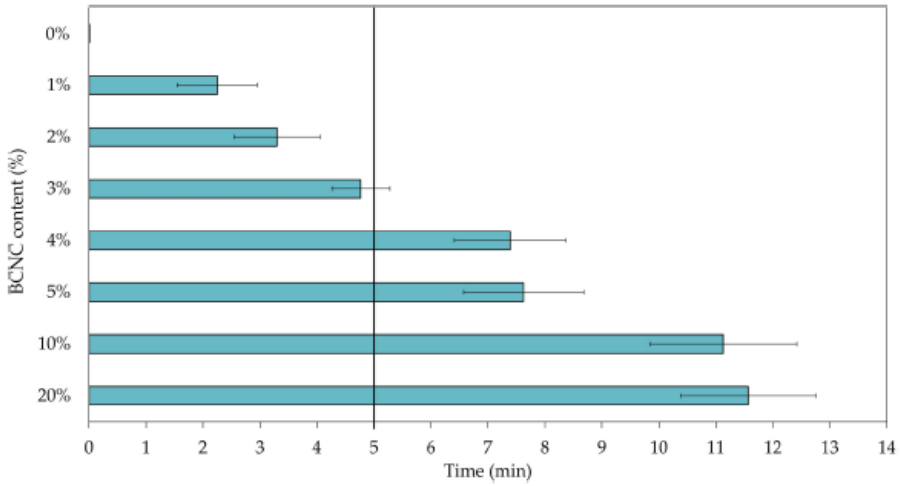

Fig. 10. Water drop test values of the BCNC-eucalyptus composites with different loadings of BCNC. The black line represents the 5 min threshold according to TAPPI standard T835 om-08.

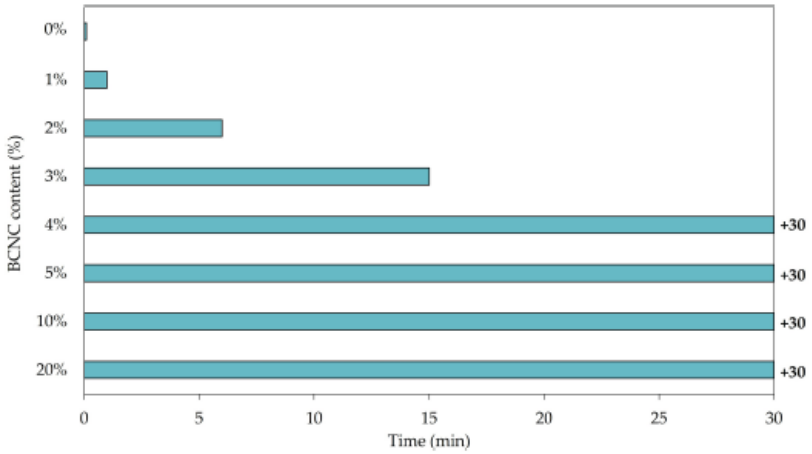

Fig. 11. Barrier properties to oil of the BCNC-eucalyptus composites with different loadings of BCNC.

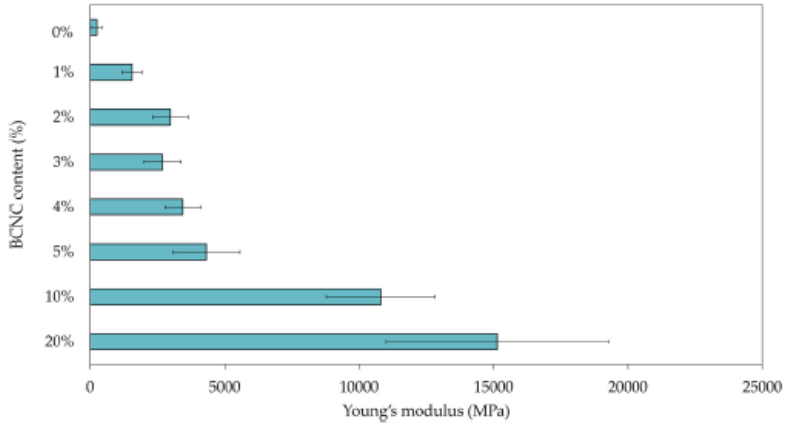

Fig. 12. Young's modulus parameters obtained for the tested composites with the addition of different BCNC loadings onto eucalyptus sheets.

highest values of Young's modulus (YM) were observed for composites with 20% loading of BCNC (Fig. 12). The addition of BCNC onto eucalyptus sheets lead to a increase of the yield strength, almost 15 times when BCNC were added at 20%, from 246.42 ± 190.1 MPa to 15.15 ± 4.1 GPa. However, in the literature is very often reported that composites with the smallest amount of filler are characterized by the highest values of strength parameters, resulting from their better dispersion [89-91]. Surprisingly, in our study, further increase of BCNC resulted in improvement of YM parameters, as it has been also recently described elsewhere [55,92].

4. Conclusions

In this work, bacterial cellulose nanocrystals have been obtained using a green procedure. A pretreatment with the enzyme SamLPMO10C, followed by digestion with a mixture of cellulases, led to the obtention of nanocrystals with high aspect ratio, high crystallinity index and excellent thermal properties. The oxidative action of LPMO generated negative charges on the cellulose chains on the surface of the nanocrystals that prevented aggregation and allowed good stability in an aqueous environment. Eucalyptus cellulose sheets coated with a low percentage of bacterial cellulose nanocrystals acquired water and oil impermeability and improved mechanical properties. The properties of the nanocrystals obtained by this enzymatic process make predictable a wide range of applications.

Funding

This work was financed by the Spanish Ministry of Economy, Industry and Competitiveness, grant CTQ2017-84966-C2-2-R, by the Pla de Recerca de Catalunya, grant 2017SGR-30, and by the Generalitat de Catalunya, "Xarxa de Referència en Biotecnologia" (XRB). C. Buruaga-Ramiro acknowledges an APIF predoctoral grant from the University of Barcelona.

Declaration of Competing Interest

The authors declare that they have no known competing financial

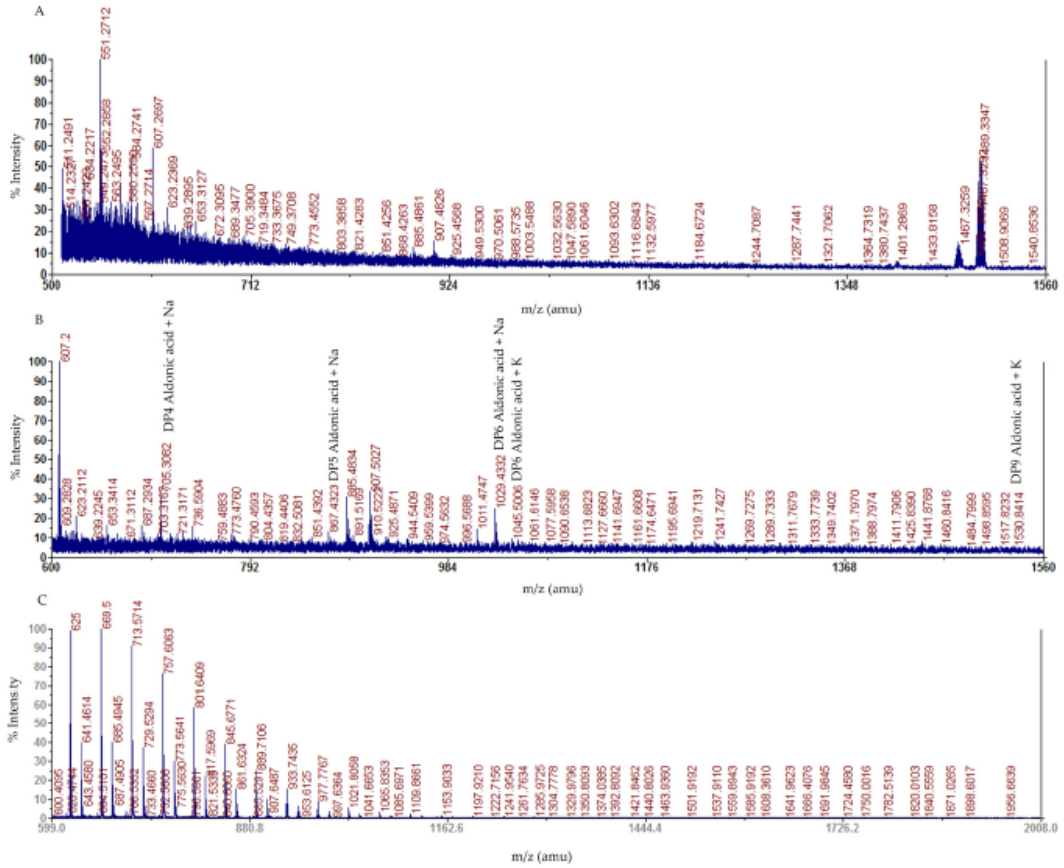

Fig. A1. MALDI-TOF MS analysis of soluble oxidized products from (a) BC negative control, (b) BC-SamLPMO10C and (c), BC-SamLPMO10C-Cel.

interests or personal relationships that could have appeared to influence the work reported in this paper.

Acknowledgements

We thank the Serveis Cientifico-Tecnics of the University of Barcelona (CCiTUB) for technical support in: electron microscopy; X-ray diffraction; laser diffraction; TGA analysis and AFM, and Institut de Ciències de Materials de Barcelona (ICMAB-CSIC) for z potential measure. We are grateful to MetGen Oy (Finland) for supplying enzyme products. M. Vieiros is acknowledged for technical assistance.

Data availability

The raw/processed data required to reproduce these findings cannot be shared at this time due to technical or time limitations.

Appendix

References

[1] R.N. Tharanathan, Biodegradable films and composite coatings: Past, present and future, Trends Food Sci. Technol. 14 (2003) 71–78, https://doi.org/10.1016/S0924-2244(02)00280-7.
[2] A. Dufresne, Comparing the mechanical properties of high performances polymer nanocomposites from biological sources, J. Nanosci. Nanotechnol. 6 (2006) 322–330, https://doi.org/10.1166/jnn.2006.906.
[3] C. Buruaga-Ramiro, S.V. Valenzuela, C. Valls, M.B. Roncero, F.I.J. Pastor, P. Díaz, J. Martínez, Bacterial cellulose matrices to develop enzymatically active paper, Cellulose 27 (2020) 3413–3426, https://doi.org/10.1007/s10570-020-03025-9.
[4] C. Zinge, B. Kandasubramanian, Nanocellulose based biodegradable polymers, Eur. Polym. J. 133 (2020), 109758, https://doi.org/10.1016/j.eurpolymj.2020.109758.
[5] J. George, S.N. Sabapathi, Cellulose nanocrystals: Synthesis, functional properties, and applications, Nanotechnol. Sci. Appl. 8 (2015) 45–54, https://doi.org/10.2147/NSA.S64386.
[6] M. Ghorbani, L. Roshangar, J. Soleimani Rad, Development of reinforced chitosan/pectin scaffold by using the cellulose nanocrystals as nanofillers: An injectable hydrogel for tissue engineering, Eur. Polym. J. 130 (2020), 109697, https://doi.org/10.1016/j.eurpolymj.2020.109697.
[7] S.J. Eichhorn, A. Dufresne, M. Aranguren, N.E. Marcovich, J.R. Capadona, S. J. Rowan, C. Weder, W. Thielemans, M. Roman, S. Renneckar, W. Gindl, S. Veigel, J. Keckes, H. Yano, K. Abe, M. Nogi, A.N. Nakagaito, A. Mangalam, J. Simonsen, A. S. Benight, A. Bismarck, L.A. Berglund, T. Peijs, Review: current international research into cellulose nanofibres and nanocomposites, J. Mater. Sci. 45 (2010) 1–33, https://doi.org/10.1007/s10853-009-3874-0.
[8] A.J. Uddin, J. Araki, Y. Gotoh, Toward "Strong" green nanocomposites: Polyvinyl alcohol reinforced with extremely oriented cellulose whiskers, Biomacromolecules 12 (2011) 617–624, https://doi.org/10.1021/bm101280f.

[9] N. Dogan, T.H. McHugh, Effects of microcrystalline cellulose on functional properties of hydroxy propyl methyl cellulose microcomposite films, J. Food Sci. 72 (2007) E016–E22, https://doi.org/10.1111/j.1750-3841.2006.00237.x.

[10] C.M.O. Müller, J.B. Laurindo, F. Yamashita, Effect of cellulose fibers addition on the mechanical properties and water vapor barrier of starch-based films, Food Hydrocoll. 23 (2009) 1328–1333, https://doi.org/10.1016/j.foodhyd.2008.09.002.

[11] B.L. Peng, N. Dhar, H.L. Liu, K.C. Tam, Chemistry and applications of nanocrystalline cellulose and its derivatives: A nanotechnology perspective, Can. J. Chem. Eng. 89 (2011) 1191–1206, https://doi.org/10.1002/cjce.20554.

[12] A. Balea, E. Fuente, M. Concepcion Monte, N. Merayo, C. Campano, C. Negro, A. Blanco, Industrial application of nanocelluloses in papermaking: A review of challenges, technical solutions, and market perspectives, Molecules 25 (2020) 526, https://doi.org/10.3390/molecules25030526.

[13] D. Roy, M. Semsarilar, J.T. Guthrie, S. Perrier, Cellulose modification by polymer grafting: A review, Chem. Soc. Rev. 38 (2009) 2046–2064, https://doi.org/10.1039/b808639g.

[14] M. Roman, S. Dong, A. Hirani, Y.W. Lee, Cellulose nanocrystals for drug delivery, ACS Symp. Ser. 1017 (2009) 81–91, https://doi.org/10.1021/bk-2009-1017.ch004.

[15] E. Lam, K.B. Male, J.H. Chong, A.C.W. Leung, J.H.T. Luong, Applications of functionalized and nanoparticle-modified nanocrystalline cellulose, Trends Biotechnol. 30 (2012) 283–290, https://doi.org/10.1016/j.tibtech.2012.02.001.

[16] S. Liu, S.A. Qamar, M. Qamar, K. Basharat, M. Bilal, Engineered nanocellulose-based hydrogels for smart drug delivery applications, Int. J. Biol. Macromol. 181 (2021) 275–290, https://doi.org/10.1016/J.IJBIOMAC.2021.03.147.

[17] M. Nogi, S. Iwamoto, A.N. Nakagaito, H. Yano, Optically transparent nanofiber paper, Adv. Mater. 21 (2009) 1595–1598, https://doi.org/10.1002/adma.200803174.

[18] S. Belbekhouche, J. Bras, G. Siqueira, C. Chappey, L. Lebrun, B. Khelifi, S. Marais, A. Dufresne, Water sorption behavior and gas barrier properties of cellulose whiskers and microfibrils films, Carbohydr. Polym. 4 (2011) 1740–1748, https://doi.org/10.1016/J.CARBPOL.2010.10.036.

[19] L.J. Nielsen, S. Eyley, W. Thielemans, J.W. Aylott, Dual fluorescent labelling of cellulose nanocrystals for pH sensing, Chem. Commun. 46 (2010) 8929–8931, https://doi.org/10.1039/c0cc03470c.

[20] I. Kalashnikova, H. Bizot, B. Cathala, I. Capron, Modulation of cellulose nanocrystals amphiphilic properties to stabilize oil/water interface, Biomacromolecules 13 (2012) 267–275, https://doi.org/10.1021/bm201599j.

[21] K.W. Lin, H.Y. Lin, Quality characteristics of chinese-style meatball containing bacterial cellulose (nata), J. Food Sci. 69 (2004) SNQ107–SNQ111. https://doi.org/10.1111/j.1365-2621.2004.tb13378.x.

[22] P.R. Chawla, I.B. Bajaj, S.A. Survase, R.S. Singhal, Microbial cellulose: Fermentative production and applications, Food Technol. Biotechnol. 47 (2009) 107–124.

[23] K.-Y. Lee, G. Buldum, A. Mantalaris, A. Bismarck, More than meets the eye in bacterial cellulose: biosynthesis, bioprocessing, and applications in advanced fiber composites, Macromol. Biosci. 14 (2014) 10–32, https://doi.org/10.1002/mabi.201300298.

[24] H. Yano, J. Sugiyama, A.N. Nakagaito, M. Nogi, T. Matsuura, M. Hikita, K. Handa, Optically transparent composites reinforced with networks of bacterial nanofibers, Adv. Mater. 17 (2005) 153–155, https://doi.org/10.1002/adma.200400597.

[25] D.A. Gregory, L. Tripathi, A.T.R. Fricker, E. Asare, I. Orlando, V. Raghavendran, I. Roy, Bacterial cellulose: A smart biomaterial with diverse applications, Mater. Sci. Eng. R Reports. 145 (2021), 100623, https://doi.org/10.1016/J.MSER.2021.100623.

[26] S.M. Mazhari Mousavi, E. Afra, M. Tajvidi, D.W. Bousfield, M. Dehghani-Firouzabadi, Cellulose nanofiber/carboxymethyl cellulose blends as an efficient coating to improve the structure and barrier properties of paperboard, Cellulose 24 (2017) 3001–3014, https://doi.org/10.1007/s10570-017-1299-5.

[27] D. Klemm, K. Petzold-Welcke, F. Kramer, T. Richter, V. Raddatz, W. Fried, S. Nietzsche, T. Bellmann, D. Fischer, Biotech nanocellulose: A review on progress in product design and today's state of technical and medical applications, Carbohydr. Polym. 254 (2021), https://doi.org/10.1016/J.CARBPOL.2020.117313.

[28] B.G. Rånby III, Fibrous macromolecular systems. Cellulose and muscle. The colloidal properties of cellulose micelles, Discuss. Faraday Soc. 11 (1951) 158–164, https://doi.org/10.1039/DF9511100158.

[29] Y. Habibi, L.A. Lucia, O.J. Rojas, Cellulose nanocrystals: Chemistry, self-assembly, and applications, Chem. Rev. 110 (2010) 3479–3500, https://doi.org/10.1021/cr900339w.

[30] M.A.S. Azizi Samir, F. Alloin, A. Dufresne, Review of recent research into cellulosic whiskers, their properties and their application in nanocomposite field, Biomacromolecules 6 (2005) 612–626, https://doi.org/10.1021/bm0493685.

[31] Z. Karim, S. Afrin, Q. Husain, R. Danish, Necessity of enzymatic hydrolysis for production and functionalization of nanocelluloses, Crit. Rev. Biotechnol. 37 (2017) 355–370, https://doi.org/10.3109/07388551.2016.1163322.

[32] B. Yang, Z. Dai, S.Y. Ding, C.E. Wyman, Enzymatic hydrolysis of cellulosic biomass, Biofuels. 2 (2011) 421–449, https://doi.org/10.4155/bfs.11.116.

[33] A. López-Rubio, J.M. Lagaron, M. Ankerfors, T. Lindström, D. Nordqvist, A. Mattozzi, M.S. Hedenqvist, Enhanced film forming and film properties of amylopectin using micro-fibrillated cellulose, Carbohydr. Polym. 68 (2007) 718–727, https://doi.org/10.1016/j.carbpol.2006.08.008.

[34] A.J. Svagan, M.A.S. Azizi Samir, L.A. Berglund, Biomimetic polysaccharide nanocomposites of high cellulose content and high toughness, Biomacromolecules 8 (2007) 2556–2563, https://doi.org/10.1021/bm0703160.

[35] C. Boisset, C. Fraschini, M. Schülein, B. Henrissat, H. Chanzy, Imaging the enzymatic digestion of bacterial cellulose ribbons reveals the endo character of the cellobiohydrolase Cel6A from Humicola insolens and its mode of synergy with cellobiohydrolase Cel7A, Appl. Environ. Microbiol. 66 (2000) 1444–1452, https://doi.org/10.1128/AEM.66.4.1444-1452.2000.

[36] N.R. Gilkes, E. Jervis, B. Henrissat, B. Tekant, R.C. Miller, R.A.J. Warren, D. G. Kilburn, The adsorption of a bacterial cellulase and its two isolated domains to crystalline cellulose, J. Biol. Chem. 267 (1992) 6743–6749, https://doi.org/10.1016/s0021-9258(19)50488-4.

[37] M. Kostylev, D. Wilson, A distinct model of synergism between a processive endocellulase (TfCel9A) and an exocellulase (TfCel9A) from thermobifida fusca, Appl. Environ. Microbiol. 80 (2014) 339–344, https://doi.org/10.1128/AEM.02706-13.

[38] E.T. Reese, R.G.H. Siu, H.S. Levinson, The biological degradation of soluble cellulose derivatives and its relationship to the mechanism of cellulose hydrolysis, J. Bacteriol. 59 (1950) 485–497, https://doi.org/10.1128/JB.59.4.485-497.1950.

[39] S.J. Horn, G. Vaaje-Kolstad, B. Westereng, V.G.H. Eijsink, Novel enzymes for the degradation of cellulose, Biotechnol. Biofuels. 5 (2012) 45, https://doi.org/10.1186/1754-6834-5-45.

[40] Z. Forsberg, A.K. Mackenzie, M. Sørlie, Å.K. Røhr, R. Helland, A.S. Arvai, G. Vaaje-Kolstad, V.G.H. Eijsink, Structural and functional characterization of a conserved pair of bacterial cellulose-oxidizing lytic polysaccharide monooxygenases, Proc. Natl. Acad. Sci. U. S. A. 111 (2014) 8446–8451, https://doi.org/10.1073/pnas.1402771111.

[41] C. Valls, F.I. Javier Pastor, M. Blanca Roncero, T. Vidal, P. Díaz, J. Martínez, S. V. Valenzuela, Assessing the enzymatic effects of cellulases and LPMO in improving mechanical fibrillation of cotton linters, Biotechnol. Biofuels. 12 (2019) 161, https://doi.org/10.1186/s13068-019-1502-z.

[42] B. Bissaro, A. Várnai, Å.K. Røhr, V.G.H. Eijsink, Oxidoreductases and reactive oxygen species in conversion of lignocellulosic biomass, Microbiol. Mol. Biol. Rev. 82 (2018), https://doi.org/10.1128/mmbr.00029-18.

[43] K.S. Johansen, Lytic polysaccharide monooxygenases: the microbial power tool for lignocellulose degradation, Trends Plant Sci. 21 (2016) 926–936, https://doi.org/10.1016/j.tplants.2016.07.012.

[44] S.V. Valenzuela, G. Ferreres, G. Margalef, F.I.J. Pastor, Fast purification method of functional LPMOs from Streptomyces ambofaciens by affinity adsorption, Carbohydr. Res. 448 (2017) 205–211, https://doi.org/10.1016/j.carres.2017.02.004.

[45] J. Fernández, A.G. Morena, S.V. Valenzuela, F.I.J. Pastor, P. Díaz, J. Martínez, Microbial cellulose from a komagataeibacter intermedius strain isolated from commercial wine vinegar, J. Polym. Environ. 27 (2019) 956–967, https://doi.org/10.1007/s10924-019-01403-4.

[46] T.M. Wood, Preparation of crystalline, amorphous, and dyed cellulase substrates, Methods Enzymol. 160 (1988) 19–25, https://doi.org/10.1016/0076-6879(88)60103-0.

[47] K.R. Birikh, M.W. Heikkilä, A. Michine, A. Mialon, T. Grönroos, P. Ihalainen, A. Varho, V. Hämäläinen, A. Suonpää, S.-P. Rantanen, Metgen: Value from Wood - Enzymatic Solutions, in: G. de Gonzalo, P. Domingues de Maria (Eds.), Biocatalysis: An Industrial Perspective (Catalysis Series), The Royal Society of Chemistry, 2017, pp. 298–322.

[48] G.L. Miller, Use of dinitrosalicylic acid reagent for determination of reducing sugar, Anal. Chem. 31 (1959) 426–428, https://doi.org/10.1021/ac60147a030.

[49] L. Segal, J.J. Creely, A.E. Martin, C.M. Conrad, An empirical method for estimating the degree of crystallinity of native cellulose using the X-ray diffractometer, Text. Res. J. 29 (1959) 786–794, https://doi.org/10.1177/004051755902901003.

[50] P. Falamarzpour, T. Behzad, A. Zamani, Preparation of nanocellulose reinforced chitosan films, cross-linked by adipic acid, Int. J. Mol. Sci. 18 (2017) 396, https://doi.org/10.3390/ijms18020396.

[51] A. Dufresne, Nanocellulose: A new ageless bionanomaterial, Mater. Today. 16 (2013) 220–227, https://doi.org/10.1016/j.mattod.2013.06.004.

[52] S.V. Valenzuela, C. Valls, V. Schink, D. Sánchez, M.B. Roncero, P. Díaz, J. Martínez, F.I.J. Pastor, Differential activity of lytic polysaccharide monooxygenases on celluloses of different crystallinity. Effectiveness in the sustainable production of cellulose nanofibrils, Carbohydr. Polym. 207 (2019) 59–67. https://doi.org/10.1016/j.carbpol.2018.11.076.

[53] O.A. Ogunyewo, A. Randhawa, M. Gupta, V.C. Kaladhar, P.K. Verma, S.S. Yazdani, Synergistic action of a lytic polysaccharide monooxygenase and a cellobiohydrolase from penicillium funiculosum in cellulose saccharification under high-level substrate loading, Appl. Environ. Microbiol. 86 (2020) 1–21, https://doi.org/10.1128/AEM.01769-20.

[54] M.B. Keller, S.F. Badino, N. Røjel, T.H. Sørensen, J. Kari, B. McBrayer, K. Borch, B. M. Blossom, P. Westh, A comparative biochemical investigation of the impeding effect of C1-oxidizing LPMOs on cellobiohydrolases, J. Biol. Chem. 296 (2021), https://doi.org/10.1016/j.jbc.2021.100504.

[55] A. Grząbka-Zasadzińska, A. Skrzypczak, S. Borysiak, The influence of the cation type of ionic liquid on the production of nanocrystalline cellulose and mechanical properties of chitosan-based biocomposites, Cellulose 26 (2019) 4827–4840, https://doi.org/10.1007/s10570-019-02412-1.

[56] C. Buruaga-Ramiro, S.V. Valenzuela, C. Valls, M.B. Roncero, F.I.J. Pastor, P. Díaz, J. Martínez, Development of an antimicrobial bioactive paper made from bacterial cellulose, Int. J. Biol. Macromol. 158 (2020) 587–594, https://doi.org/10.1016/j.ijbiomac.2020.04.234.

[57] E.S. do Nascimento, A.L.S. Pereira, M. de O. Barroz, M.K. de A. Barrozo, H.L.S. Lima, M. de F. Borges, J.P. de A. Feitosa, H.M.C. de Azeredo, M. de F. Rosa, TEMPO oxidation and high-speed blending as a combined approach to dimassemble

bacterial cellulose, Cellulose. 26 (2019) 2291–2302. https://doi.org/10.1007/s10570-018-2208-2.
[58] R.H. Marchessault, F.F. Morehead, M.J. Koch, Some hydrodynamic properties of neutral suspensions of cellulose crystallites as related to size and shape, J. Colloid Sci. 16 (1961) 327–344, https://doi.org/10.1016/0095-8522(61)90033-2.
[59] S. Elazzouzi-Hafraoui, Y. Nishiyama, J.L. Putaux, L. Heux, F. Dubreuil, C. Rochas, The shape and size distribution of crystalline nanoparticles prepared by acid hydrolysis of native cellulose, Biomacromolecules 9 (2008) 57–65, https://doi.org/10.1021/bm700769p.
[60] Y. Van Daele, J.F. Revol, P. Gaill, G. Goffinet, Characterization and supramolecular architecture of the cellulose-protein fibrils in the tunic of the sea peach (Halocynthia papillosa, Ascidiacea, Urochordata), Biol. Cell. 76 (1992) 87–96, https://doi.org/10.1016/0248-4900(92)90198-A.
[61] A.B. Perumal, P.S. Sellamuthu, R.B. Nambiar, E.R. Sadiku, Development of polyvinyl alcohol/chitosan bio-nanocomposite films reinforced with cellulose nanocrystals isolated from rice straw, Appl. Surf. Sci. 449 (2018) 591–602, https://doi.org/10.1016/j.apsusc.2018.01.022.
[62] M. Salari, M. Sowti Khiabani, R. Rezaei Mokarram, B. Ghanbarzadeh, H., Samadi Kafil, Preparation and characterization of cellulose nanocrystals from bacterial cellulose produced in sugar beet molasses and cheese whey media, Int. J. Biol. Macromol. 122 (2019) 280–288, https://doi.org/10.1016/j.ijbiomac.2018.10.136.
[63] J. George, A.S. Bawa, Siddaramaiah, Synthesis and characterization of bacterial cellulose nanocrystals and their PVA nanocomposites, in: Adv. Mater. Res., Trans Tech Publications Ltd, 2010: pp. 383–386. https://doi.org/10.4028/www.scientific.net/AMR.123-125.383.
[64] J. George, Siddaramaiah, High performance edible nanocomposite films containing bacterial cellulose nanocrystals, Carbohydr. Polym. 87 (2012) 2031–2037, https://doi.org/10.1016/j.carbpol.2011.10.019.
[65] D. Klemm, F. Kramer, S. Moritz, T. Lindström, M. Ankerfors, D. Gray, A. Dorris, Nanocelluloses: A new family of nature-based materials, Angew. Chemie Int. Ed. 50 (2011) 5438–5466, https://doi.org/10.1002/anie.201001273.
[66] L. Heux, G. Chauve, C. Bonini, Nonflocculating and chiral-nematic self-ordering of cellulose microcrystals suspensions in nonpolar solvents, Langmuir 16 (2000) 8210–8212, https://doi.org/10.1021/la9913957.
[67] M.M. De Souza Lima, J.T. Wong, M. Paillet, R. Borsali, R. Pecora, Translational and rotational dynamics of rodlike cellulose whiskers, Langmuir 19 (2003) 24–29, https://doi.org/10.1021/la020475a.
[68] A. Dufresne, Nanocellulose, DE GRUYTER (2012), https://doi.org/10.1515/9783110254600.
[69] L. Chen, M. Zou, F.F. Hong, Evaluation of fungal laccase immobilised on natural nanostructured bacterial cellulose, Front. Microbiol. 6 (2015), https://doi.org/10.3389/fmicb.2015.01245.
[70] N.F. Vasconcelos, J.P.A. Feitosa, F.M.P. da Gama, J.P.S. Morais, F.K. Andrade, M. de S.M. de Souza Filho, M. de F. Rosa, Bacterial cellulose nanocrystals produced under different hydrolysis conditions: Properties and morphological features, Carbohydr. Polym. 155 (2017) 425–431. https://doi.org/10.1016/j.carbpol.2016.08.090.
[71] P. Singhsa, R. Narain, H. Manuspiya, Bacterial Cellulose Nanocrystals (BCNC) Preparation and Characterization from Three Bacterial Cellulose Sources and Development of Functionalized BCNCs as Nucleic Acid Delivery Systems, ACS Appl. Nano Mater. 1 (2018) 209–221, https://doi.org/10.1021/acsanm.7b00105.
[72] C.L. Pirich, R.A. de Freitas, M.A. Woehl, C.P. Picheth, D.F.S. Petri, M. R. Sierakowski, Bacterial cellulose nanocrystals: impact of the sulfate content on the interaction with xyloglucan, Cellulose 22 (2015) 1773–1787, https://doi.org/10.1007/s10570-015-0626-y.
[73] Y. Huang, C. Zhu, J. Yang, Y. Nie, C. Chen, D. Sun, Recent advances in bacterial cellulose, Cellulose 21 (2014) 1–30, https://doi.org/10.1007/s10570-013-0088-z.
[74] H. Mirhosseini, C.P. Tan, N.S.A. Hamid, S. Yusof, Effect of Arabic gum, xanthan gum and orange oil contents on ζ-potential, conductivity, stability, size index and pH of orange beverage emulsion, Colloids Surf. A Physicochem. Eng. Asp. 315 (2008) 47–56, https://doi.org/10.1016/J.COLSURFA.2007.07.007.
[75] J.F. Revol, H. Bradford, J. Giasson, R.H. Marchessault, D.G. Gray, Helicoidal self-ordering of cellulose microfibrils in aqueous suspension, Int. J. Biol. Macromol. 14 (1992) 170–172, https://doi.org/10.1016/S0141-8130(05)80008-X.
[76] M. Roman, W.T. Winter, Effect of sulfate groups from sulfuric acid hydrolysis on the thermal degradation behavior of bacterial cellulose, Biomacromolecules 5 (2004) 1671–1677, https://doi.org/10.1021/bm034519+.
[77] M.C.I.M. Amin, A.G. Abadi, H. Katas, Purification, characterization and comparative studies of spray-dried bacterial cellulose microparticles, Carbohydr. Polym. 99 (2014) 180–189, https://doi.org/10.1016/j.carbpol.2013.08.041.
[78] D.M. Panaitescu, A.N. Frone, I. Chiulan, A. Casarica, C.A. Nicolae, M. Ghiurea, R. Trusca, C.M. Damian, Structural and morphological characterization of bacterial cellulose nano-reinforcements prepared by mechanical route, Mater. Des. 110 (2016) 790–801, https://doi.org/10.1016/j.matdes.2016.08.052.
[79] P. Rämänen, P.A. Penttilä, K. Svedström, S.L. Maunu, R. Serimaa, The effect of drying method on the properties and nanoscale structure of cellulose whiskers, Cellulose 19 (2012) 901–912, https://doi.org/10.1007/s10570-012-9695-3.
[80] F.V. Ferreira, A. Dufresne, I.F. Pinheiro, D.H.S. Souza, R.F. Gouveia, L.H.I. Mei, L. M.F. Lona, How do cellulose nanocrystals affect the overall properties of biodegradable polymer nanocomposites: A comprehensive review, Eur. Polym. J. 108 (2018) 274–285, https://doi.org/10.1016/j.eurpolymj.2018.08.045.
[81] Z. Xiang, X. Jin, Q. Liu, Y. Chen, J. Li, F. Lu, The reinforcement mechanism of bacterial cellulose on paper made from woody and non-woody fiber sources, Cellulose 24 (2017) 5147–5156, https://doi.org/10.1007/s10570-017-1468-6.
[82] J. Yuan, T. Wang, X. Huang, W. Wei, Dispersion and beating of bacterial cellulose and their influence on paper properties, BioResources. 11 (2016) 9290–9301. https://doi.org/10.15376/biores.11.4.9290-9301.
[83] C. Aulin, G. Salazar-Alvarez, T. Lindström, High strength, flexible and transparent nanofibrillated cellulose-nanoclay biohybrid films with tunable oxygen and water vapor permeability, Nanoscale. 4 (2012) 6622–6628, https://doi.org/10.1039/c2nr31726e.
[84] C.J. Ridgway, P.A.C. Gane, Constructing NFC-pigment composite surface treatment for enhanced paper stiffness and surface properties, Cellulose 19 (2012) 547–560, https://doi.org/10.1007/s10570-011-9634-8.
[85] S.S. Nair, J. Zhu, Y. Deng, A.J. Ragauskas, High performance green barriers based on nanocellulose, Sustain. Chem. Process. 2 (2014), https://doi.org/10.1186/s40508-014-0023-0.
[86] F. Hoeng, A. Denneulin, J. Bras, Use of nanocellulose in printed electronics: A review, Nanoscale. 8 (2016) 13131–13154, https://doi.org/10.1039/c6nr03054h.
[87] N.L. Garcia de Rodriguez, W. Thielemans, A. Dufresne, Sisal cellulose whiskers reinforced polyvinyl acetate nanocomposites, Cellulose 13 (2006) 261–270, https://doi.org/10.1007/s10570-005-9039-7.
[88] J. Lange, Y. Wyser, Recent innovations in barrier technologies for plastic packaging - a review, Packag. Technol. Sci. 16 (2003) 149–158, https://doi.org/10.1002/pts.621.
[89] M.K.M. Haafiz, A. Hassan, Z. Zakaria, I.M. Inuwa, M.S. Islam, M. Jawaid, Properties of polylactic acid composites reinforced with oil palm biomass microcrystalline cellulose, Carbohydr. Polym. 98 (2013) 139–145, https://doi.org/10.1016/j.carbpol.2013.05.069.
[90] J. Ambrosio-Martín, A. Lopez-Rubio, M.J. Fabra, G. Gorrasi, R. Pantani, J. M. Lagaron, Assessment of ball milling methodology to develop polylactide-bacterial cellulose nanocrystals nanocomposites, J. Appl. Polym. Sci. 132 (2015), https://doi.org/10.1002/app.41605.
[91] M. Martínez-Sanz, M.A. Abdelwahab, A. Lopez-Rubio, J.M. Lagaron, E. Chiellini, T. G. Williams, D.F. Wood, W.J. Orts, S.H. Imam, Incorporation of poly (glycidylmethacrylate) grafted bacterial cellulose nanowhiskers in poly(lactic acid) nanocomposites: Improved barrier and mechanical properties, Eur. Polym. J. 49 (2013) 2062–2072, https://doi.org/10.1016/j.eurpolymj.2013.04.035.
[92] R. Kumar, S. Kumari, B. Rai, R. Das, G. Kumar, Effect of nano-cellulosic fiber on mechanical and barrier properties of polylactic acid (PLA) green nanocomposite film, Mater. Res. Express. 6 (2019), 125108, https://doi.org/10.1088/2053-1591/ab5755.

Funcionalización de celulosa mediada por monooxigenasa líticas de polisacáridos para soportes de papel con propiedades mejoradas

La celulosa proveniente de eucalipto y la celulosa bacteriana fueron funcionalizadas mediante oxidación con una monooxigenasa lítica de polisacárido, SamLPMO10C, para aumentar sus contenidos de grupos carboxilo en 2,4 y 2,7 veces, respectivamente. Las celulosas funcionalizadas se utilizaron para generar soportes de papel que contenían nanopartículas de plata. Se añadió una solución de nitrato de plata a las celulosas oxidadas como fuente de Ag^+ que permitió la interacción entre cationes de plata y grupos hidroxilo o carboxilo. A continuación, se produjeron los soportes de papel y la formación de nanopartículas de plata se indujo mediante reducción térmica. La presencia de nanopartículas de plata se validó mediante microscopía electrónica de barrido y espectroscopía de rayos X de dispersión de energía. Los análisis de espectrometría de emisión óptica acoplada inductivamente y espectrometría de masas con plasma acoplado inductivamente permitieron medir el contenido de plata en los soportes de papel, así como la lixiviación de plata en un medio acuoso. Los soportes de papel funcionalizados con Ag mostraron fuertes propiedades antibacterianas contra *Staphylococcus aureus*.

Barcelona, April 1st 2023

Dear Editor

Please consider the enclosed manuscript entitled “Lytic polysaccharide monooxygenase-mediated cellulose functionalization for paper supports with enhanced properties ", signed by Josefina Martínez, Susana V. Valenzuela and myself, for publication in the Cellulose Journal.

We propose here a cellulose functionalization methodology by increasing the carboxylic content using an enzymatic treatment only. We used two different cellulosic substrates: bacterial and eucalyptus cellulose proving the potential use of these enzymes in complex materials.

Following this, we add silver as a model of ligand to cellulose. The silver-functionalized paper supports showed strong antibacterial capacity against *Staphylococcus aureus*.

The use of lytic polysaccharide monooxygenases on different cellulosic substrates for the functionalization of paper supports has not been extensively explored, here we demonstrated that these enzymes could be used to produce environmentally friendly biomaterials.

We believe that the work presented here gives a new and valuable piece of information on potential applications of different cellulosic substrates that can replace at some point petroleum derivatives, an imperative need these days.

We also think that it can be of general interest to the large community of researchers working on the development of enzyme-functionalized cellulosic materials.

Hoping this manuscript meets the criteria for publication in Cellulose.

Yours sincerely,

L. Verónica Cabañas-Romero

Lytic polysaccharide monooxygenase-mediated cellulose functionalization for paper supports with enhanced properties

L. Verónica Cabañas-Romero[a,b] *, Josefina Martínez[a,b], Susana V. Valenzuela[a,b]

[a] Department of Genetics, Microbiology, and Statistics, Faculty of Biology, Universitat de Barcelona, Av. Diagonal 643, 08028, Barcelona, Spain

[b] Institute of Nanoscience and Nanotechnology (IN^{2}UB), Universitat de Barcelona, Spain

veronica.cabanas@ub.edu

jmartinez@ub.edu

susanavalenzuela@ub.edu

* Corresponding author at Department of Genetics, Microbiology, and Statistics, Faculty of Biology, Universitat de Barcelona, Av. Diagonal 643, 08028, Barcelona, Spain.

Abstract

Eucalyptus and bacterial celluloses were functionalized by oxidation with a lytic polysaccharide monooxygenase, SamLPMO10C, to increase their contents in carboxyl groups by 2.4 and 2.7-fold, respectively. The functionalized celluloses were used to generate paper supports containing silver nanoparticles. A solution of silver nitrate was added to oxidized celluloses as a source of Ag^+ which allowed the interaction between silver cations and hydroxyl or carboxyl groups. Following, paper supports were produced, and the formation of silver nanoparticles was induced by heat reduction. The presence of silver nanoparticles was validated by scanning electron microscope and energy-dispersive X-ray spectroscopy. Inductively coupled plasma-optical emission spectrometry and inductively coupled plasma mass spectrometry tests allowed to measure the silver content in the paper supports as well as the leaching of silver in an aqueous media. The Ag-functionalized paper supports showed strong antibacterial properties against *Staphylococcus aureus.*

Keywords

Cellulose

Bacterial cellulose

Cellulose functionalization

Lytic polysaccharide monooxygenases

SamLPMO10C

1. Introduction

The growing demand for sustainable and environmentally friendly materials is encouraging the development of new products based on renewable raw materials with improved properties. In this context, natural polymers, such as cellulose, have positioned themselves as one of the most important alternatives for the replacement of petroleum-derived materials, like plastics and other polluting polymers (Tanpichai et al. 2022). Cellulose is the most abundant polymer on Earth and is the main component of the plant cell wall. It is a biodegradable, renewable, and insoluble polymer in most solvents due to its hydrogen bonds and its crystallinity. It is composed of D-glucose units linked by O-glycosidic bonds β (1→4) forming long linear chains. Cellulose can be synthesized in plants (the most abundant source), algae, tunicate marine animals, and some bacteria (Klemm et al. 2005). The main advantage of using vegetable cellulose plant biomass-derived cellulose is its abundance, however, it is associated with hemicellulose and lignin so, before further use, a prior purification process is necessary. On the other hand, bacterial cellulose, BC hereinafter, initially reported by (Brown 1886), is a chemically equivalent structure to plant biomass-derived cellulose, but with a high chemical purity since it lacks hemicellulose and lignin. BC is a linear extracellular polysaccharide produced mainly by bacteria from the genera *Komagataeibacter* (Yamada et al. 2012) but also from other genera such as *Agrobacterium* (Matthysse et al. 2005), *Rhizobium* (Robledo et al. 2012), *Azotobacter*, *Pseudomonas*, *Salmonella*, *Sarcina ventriculi* (Torres et al. 2019) and, *Lactiplantibacillus plantarum* (Saleh et al. 2022). BC exhibits many excellent properties such as unique nanostructure, high water holding capacity (Lee et al. 2014), high degree of polymerization, high crystallinity (Klemm et al. 2011), high mechanical and tensile strength (Torres et al. 2019), high elasticity, and good biocompatibility (Shah et al. 2013). All these features make the BC an interesting matrix for various applications in life science and technology (Klemm et al. 2021).

Cellulose can act as support for compounds, so the new composite combines the mechanical and physical properties of cellulose and the properties of the added compound (Buruaga-Ramiro et al. 2020; Cabañas-Romero et al. 2020; Golonka et al. 2021; Onyszko et al. 2022). Also, cellulose can be chemically modified prior to combine with a compound, so cellulose improves its mechanical properties (Cichosz et al. 2021; Zhou et al. 2021) or gains new properties such as antibacterial capacity (Orlando et al. 2020). However, the use of chemicals to modify cellulose generates residues that are harmful to the environment, therefore, reducing its use is a necessary approach. The Laccase/TEMPO-mediated oxidation of BC performed by Morena et al. (2019) operated in milder conditions than the traditional oxidation by TEMPO/NaBr/NaClO so the use of chemicals was reduced. Therefore, exclusively enzymatic treatment of cellulose molecules to obtain new properties is an even more environmentally friendly strategy.

In this work, eucalyptus, a plant source for cellulose, and bacterial cellulose were enzymatically treated with a recently described type of enzyme, lytic polysaccharide monooxygenases (LPMOs). LPMOs are copper-dependent enzymes that cleave recalcitrant polysaccharides such as cellulose and chitin (Vaaje-Kolstad et al. 2017). Cellulose-active LPMOs oxidize either the C1 or the C4 carbon of the scissile glycosidic bond in cellulose while some LPMOs produce a mixture of C1- and C4-oxidized products (Quinlan et al. 2011; Horn et al. 2012). In the CAZy database, LPMOs are classified in the auxiliary activity (AA) families 9-11, and 13-16 (Drula et al. 2022), and their

abundance in the genomes of biomass-degrading organisms suggests the great importance of LPMOs in biomass processing. The use of LPMOs to help produce nanomaterials such as cellulose nanofibrils (NFC) and cellulose nanocrystals (CNN) has been reported and shows the potential applications of this enzyme to produce new nanomaterials (Buruaga-Ramiro et al. 2021; Hu et al. 2018; Moreau et al. 2019; Valenzuela et al. 2019).

In this work, SamLPMO10C, a LPMO from *Streptomyces ambofaciens* recently cloned and characterized in the research group, was used. SamLPMO10C, a cellulose-active LPMO, belongs to the AA10 family, which includes bacterial LPMOs, and presents a mechanism for breaking the glycosidic bond that links glucose to cellulose by oxidizing the C1 of glucose. This results in the formation of 1,5-δ-lactones that are spontaneously hydrated to aldonic acids (Valenzuela et al. 2017). The carboxyl functional groups created can help to introduce new substances (e.g., metal ions) endowing the cellulose matrix with new functionalities derived from the ligand. The purpose of this research was to evaluate the suitability of LPMO as an oxidizing enzymatic agent to increase the carboxyl groups contained in the cellulose matrices. Then, silver was incorporated, as a model ligand. Finally, the properties of the Ag-functionalized cellulose were investigated. The main novelty of this work is the use of an enzyme as the only oxidizing agent that increases the carboxyl content which would facilitate the subsequent incorporation of silver into the cellulosic matrix. This protocol could be used to create other environmentally friendly materials with other types of ligands.

2. Materials and methods

2.1 Substrates

The activity assays of the Lytic polysaccharide monooxygenase used in this work, SamLPMO10C from *S. ambofaciens*, were carried out first with phosphoric swollen acid cellulose (PASC) as a model substrate for the enzyme. PASC was prepared from Avicel® PH-101 (Fluka) by treatment with 70% of H_3PO_4 according to Wood (1988), using centrifugation for the sedimentation of the cellulose instead of decantation during the washing process. Bleached pulps of eucalyptus ECF were kindly provided by Teresa Vidal (Polytechnical University of Catalonia).

To produce BC, *Komagataeibacter intermedius* JF2 cells (Fernández et al. 2019) grown on Hestrin and Schramm (HS)-Agar were transferred into HS liquid medium. After vigorous shaking, the resulting cell suspension was used to inoculate (1:40) 10 cm Petri dishes containing 40 ml of HS liquid medium. They were incubated under static conditions for 7 days at room temperature.

After 7 days of incubation, the cellulose membranes formed in the air/liquid interface of the Petri dishes were washed with distilled water to remove the remains of the culture medium. The washed membranes were incubated overnight with 1% NaOH at 70 °C to eliminate the bacteria and, after this incubation, the membranes were washed with distilled water until reaching pH 7. Then, to obtain the bacterial cellulose pulp, the membranes were triturated with a blender (Philips HR3655- ProBlend 6) and homogenized using a homogenizer system (CAT Unidrive x 1000).

2.2 X-ray diffraction

X-ray diffraction patterns of dried BC and eucalyptus pulps were obtained with a PANalytical X'Pert PRO MPD Alpha1 powder diffractometer. The samples were analyzed at the radiation wavelength of 1.5418 Å and scanned from 2 ◦ to 50◦, 2θ range. Samples were fixed over a zero background Silicon single crystal sample holder (pw1817/32), and the ensembles were mounted in a PW1813/32 sample holder. The same Silicon holder was used to measure all the replicates of each sample. The Peak Height method, which has been previously employed (Segal et al. 1959), was used to calculate the crystallinity index (CI) of cellulose samples from the XRD spectra.

2.3 Production and purification of the enzyme

SamLPMO10C, previously cloned and expressed in *Escherichia coli* by (Valenzuela et al. 2017) was produced and purified according to the authors. Following this, the enzyme was incubated with $CuCl_2$ at room temperature for 30 minutes in a 1:4 molar ratio (LPMO: $CuCl_2$). The resulting protein concentration was measured via Nanodrop® 1000 spectrophotometer, using the molecular weight of 34,689 kDa and the extinction coefficient of 75,775 at 280 nm. The enzyme was stored at -20 °C until further use.

2.4 Oxidation of cellulosic substrates

Standard reactions were carried out in 50 mM ammonium acetate buffer pH 6.0, 2 mM ascorbic acid, and 2 µM of H_2O_2 at 50 °C and 250 rpm. Inactivation of the enzyme after the incubations were archived by boiling at 100 °C for 10 minutes unless indicated otherwise. The same reaction but without the enzyme was incubated as negative controls.

To evaluate the activity of the LPMO, 20 µg of SamLPMO10C was incubated with 1% of PASC in a final volume of 100 µL in 1.5 mL microcentrifuge tubes for 72h in an Eppendorf Thermomixer.

The oxidation of BC and eucalyptus pulp were carried out with 2 and 8 mg of SamLPMO10C respectively and incubation at 36 and 72h were performed in the same conditions as the incubation with PASC but the inactivation of the enzyme was archived by the addition of 3.5 mL of 0.5 M EDTA, and the final volume of the reactions was 50 and 40 mL respectively.

2.5 Activity analysis

For the initial confirmation of the activity of SamLPMO10C, soluble fractions generated in the degradation reactions of PASC, BC, and eucalyptus pulps were analyzed for the detection of oxidized products by matrix-assisted laser desorption/ionization-time of flight mass spectrometry (MALDI-TOF MS). Reaction samples (3 µl) were mixed with 7 µl of acetonitrile, and then 1 µl was mixed with 1 µl of matrix solution (10 mg/ml of 2,5-dihydroxybenzoic acid dissolved in acetonitrile-water [1:1, vol/vol], 0.1% [wt/vol] trifluoroacetic acid). 1 µl of the mixture was spotted in duplicated onto the MALDI-TOF MS plate and allowed to dry before the analysis. Positive mass spectra were collected with a 4800 Plus MALDI TOF/TOF (ABSciex 2010) spectrometer with an Nd: YAG 200-Hz laser operated at 355 nm.

Also, the quantification of the activity of SamLPMO10C on BC and eucalyptus pulp was analyzed by High-Performance Anion Exchange Chromatography with Pulsed Amperometric Detection (HPAEC-PAD). After

removing insoluble substrates by centrifugation, supernatants were centrifuged and diluted in water 1/40 and analyzed by HPAEC-PAD using Dionex GS50, gradient pump, Dionex AS50 Autosampler, and electrochemical detector Waters 2465 as described previously (Westereng et al. 2013) with some modification. In brief, 40 µL and 10 µL samples of eu-ox and BC-ox respectively were injected on a CarboPac PA1 2×250mm analytical column (Dionex). Cello-oligosaccharides were eluted at 0.25 ml/min using a stepwise linear gradient from 100% eluent A (0.1M NaOH) toward 10% eluent B (0.6M NaOAc in 0.1M NaOH) 10 min after injection and 40% eluent B 15 min after injection, followed by a 5 min exponential gradient to 100% B. The column was reconditioned between each run by running initial conditions for 10 min. Standards were generated using 1, 2, 4, and 8 µg/ml cellobiose and cellobionic acid.

2.6 Quantification of carboxyl groups

Carboxyl groups content of eucalyptus and BC oxidized and no oxidized were measured by conductometric titration according to the method originally developed by Katz and Beatson (1984) with some modifications: 55 ml of Milli-Q water and 5 ml of 0.01 M NaCl were added to 0.1 g dry-weight of each sample and then stirred overnight so a well-dispersed aqueous suspension was obtained. After that, 0.1 M HCl was added until pH 3.0 was reached. Then, 0.04 M NaOH was added at a rate of 0.1 mL/min until pH 11 was reached using a pH-stat. After one minute of each addition of the titrating agent, the conductivity value was recorded. The carboxyl content is determined from the conductivity curve (µS/cm) based on the volume of NaOH added. From the plotted curve of parabolic shape, the descending and ascending trend lines were added in an Excel spreadsheet (Microsoft 365) to define each linear region in the graph chart (Dang 2007). A line across the flat portion of the curve was plotted and the intersections of both trend lines with the flat line were obtained.

The carboxyl acid content of the pulp was calculated using equation 1:

$$RCOOH = \frac{(\mathrm{B} - \mathrm{A}) + [\mathrm{NaOH}]}{W} * \frac{100\mathrm{mmol}}{100\mathrm{dp}}$$

Where: B-A is the difference of the volume added in the flat portion, [NaOH] is the molar concentration of titrant agent added, W are the grams of dry paste of the sample that were used and, and dp refers to the weight of the dry pulp in grams. The experiments were performed in triplicate.

2.7 Production of Ag-paper supports

Once BC and eucalyptus pulps were oxidized by SamLPMO10C, a silver nitrate solution was added to 1 and 5 g (dry weight) of BC and eucalyptus pulps respectively, at a ratio of 10 mmol of silver nitrate per gram of dry pulp. Controls of BC and eucalyptus pulps without enzymatic treatment were also included. Each mixture was mechanically homogenized and incubated for 24 hours in dark conditions at room temperature. Each incubation was performed in duplicates.

After the incubation, the treated BC and eucalyptus pulps were filtered using a Büchner flask and Whatman® 3MM filters as support for the pulp. A vacuum was applied to remove water. The excess $AgNO_3$ was removed by adding

one volume of ethanol and then two volumes of water. The paper support formed was removed from the filter and allowed to dry at room temperature and vacuumed for 4 days. Finally, paper supports were cut into squares of 1 cm^2.

2.8 Thermal treatment of paper supports

Paper supports were treated with heat at 121 °C for 20 minutes. The paper supports generated this way for BC and eucalyptus but without enzymatic oxidation are referred to as BC/Ag/TT and eu/Ag/TT, respectively. When oxidation of the cellulosic substrates with LPMO was carried out as well as the addition of silver and thermal treatment the paper supports are referred to as BC-ox/Ag/TT for BC and eu-ox/Ag/TT for eucalyptus. Negative controls are BC paper for bacterial cellulose paper and eu paper for eucalyptus paper.

2.9 Characterization of paper supports

2.9.1 Scanning electron microscope (SEM) and energy-dispersive X-ray spectroscopy (EDS) analysis

The presence of silver in the paper supports was verified by SEM (JSM 7100 F) using a LED filter and a backscattered electron detector (BED). EDS analysis was carried out to verify the chemical composition of the paper supports. ImageJ software was used to measure the size of the silver particles.

2.9.2 Ag content and leaching

To measure the total silver content (Ag^0 + Ag^{+1}) of the samples, 1 cm^2 of paper support was digested with 1 ml of concentrated HNO_3, 5.5 M HNO_3 for paper support from eucalyptus, and 10 M HNO_3 for paper support from BC. This treatment was for 24 hours. The acid releases the total silver content from the paper support before the analysis by inductively coupled plasma-optical emission spectrometry (ICP-OES).

To test the leaching of silver from the different paper supports, 1 cm^2 of paper support was incubated with 1 ml of 0.3 mM H_3PO_3 for 24 h while shaking at 1000 rpm. After the incubation, the silver content of the samples was analyzed by Inductively coupled plasma mass spectrometry (ICP-MS) both before and after the addition of HNO_3 at a final concentration of 1%. The acid oxidized the elemental silver (Ag^0) of the NPs to silver cation (Ag^+), this allowed the measurement of elemental silver in the samples.

2.9.3 Antibacterial activity against Staphylococcus aureus assays

To test the antibacterial properties of the paper supports, the Gram-positive bacteria *Staphylococcus aureus* CECT 234 was used. The strain was grown overnight in Luria-Bertani (LB) broth at 37 °C in shaking conditions. Then, these cultures were centrifuged for 5 min at 14000 *g* and the pellets were resuspended in 0.3 mM KH_2PO_4 to remove the culture medium. Two tests were carried out: an antibacterial test by viable count and an antibacterial test by inhibition of metabolic activity with resazurin.

2.9.3.1 Dynamic Contact Condition Test.

This test was adapted from ASTM E2149-01 (Standard Test Method for determining the antimicrobial activity of Immobilized Antimicrobial Agents Under Dynamic Contact Conditions). Five 1 cm^2 pieces of the functionalized

paper support were immersed in 5 mL of a suspension of a known concentration of microorganisms and incubated at room temperature in shaking conditions. In each case, control was run with no functionalized paper support under the same conditions. The viable cells on the suspension were determined at 0, 1, and 24 hours by taking samples at each time, culturing, and counting the CFU/mL (colony former units/mL) by standard viable plate count in Tryptone soy agar (TSA) plates. The percentage of reduction of viability against the paper control at the same time of incubation was calculated.

2.9.3.2 Resazurin assay

Resazurin, blue and nonfluorescent, is reduced by electron transfer reactions associated with respiration, and therefore, cell viability, producing resorufin, pink and highly fluorescent, that can be measured by a fluorimeter (O'Brien et al. 2000). 1 cm^2 of paper was incubated with a suspension of *S. aureus* of known concentration in 0.3 mM KH_2PO_4. The metabolic activity of the cells in the bacterial suspension was determined at different times (0, 30, 60, and 120 minutes). For the assay, 50 μL of resazurin was added to 200 μL of suspension in a 96-well plate. The plate was incubated at room temperature in the dark for 15 minutes. Fluorescence was measured with a Varian Cary Eclipse fluorescence spectrophotometer (Varian Iberica, Spain). Suspension of *S. aureus* and incubation with no functionalized paper supports were used as controls.

3 Results and discussion

3.1 Production of purified and functional SamLPMO10C

Functional SamLPMO10C was expressed in *E. coli* BL21 (DE3) star and purified following the method developed previously (Valenzuela et al. 2017). A protein of approximately 40 kDa was obtained after the final step of purification (Fig. 1), in agreement with the theoretical molecular weight of the enzyme. The yield of the purified protein was 6 mg per liter of culture. The activity of the enzyme was initially verified by MALDI-TOF using PASC as substrate under standard conditions. This analysis showed peaks corresponding to oxidized cello-oligosaccharides of 4-7 degrees of polymerization (DP) (Fig. 1). Each product of the reaction can form adducts with Na +, K +, or both, so there is more than one peak for the same degree of polymerization. This is in concordance with the results of previous works for SamLPMO10C, confirming that this enzyme has a C1-oxidation pattern (Valenzuela et al. 2017).

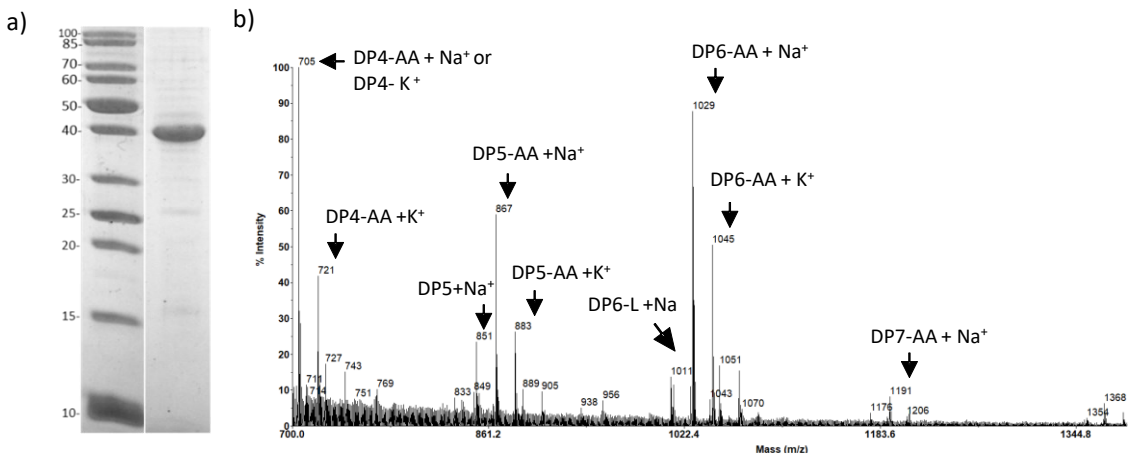

Fig. 1 Purification analysis of SamLPMO10C by SDS-PAGE (a) and MALDI-TOF screening of oxidized products released by the enzymatic oxidation of PASC after 72 h of reaction (b). DP—degree of polymerization. AA—Aldonic acid. L—Lactone. DP5—cellopentaose. DP4-OX—cellotetraonic acid, DP5-OX—cellopentaonic acid, DP6-OX—cellohexaonic acid and DP7-OX—celloeptaonic acid.

3.2 Enzymatic treatment of eucalyptus cellulose and bacterial cellulose

BC and eucalyptus pulps were treated with SamLPMO10C as summarized in S1 for 36 and 72 h in shaking conditions. The reactions stopped after the addition of EDTA.

The activity of the enzyme for each substrate was first verified by MALDI-TOF and then by HPAEC PAD analysis. The enzyme was active on both substrates as detected by the peaks observed by MALDI-TOF analysis (Fig. 2). For BC, oxidized cello-oligosaccharides of 5 to 7 degrees of polymerization can be observed. Meanwhile, for eucalyptus pulp, oxidized cello-oligosaccharides of 5 and 6 degrees of polymerization were found.

The second activity verification consisted of the quantification of aldonic acids by HPAEC-PAD, and the results are listed in Table 1 (chromatograms are attached in S2). For both substrates, the maximum amount of aldonic acids was found at 72 hours of reaction, which yielded an increase of 2 and 1.7 times for BC pulp and eucalyptus pulp respectively, regarding 36 hours of reaction. Consequently, the reaction time of 72 hours was chosen for further investigations. The values of total aldonic acids were in the same magnitude order as the cellobionic acid found for cotton linters (Valls et al. 2019). Previous studies have demonstrated a direct correlation between the oxidation rate of SamLPMO10C and the degree of substrate crystallinity (Valenzuela et al. 2019). In this work, BC had a crystallinity of 95% while eucalyptus exhibited a crystallinity degree of 84%. Therefore, the underlying reason for this differential activity can be attributed to the origin of the substrate and its crystallinity. It has been demonstrated that LPMOs target the most recalcitrant regions, facilitating subsequent access to other enzymes such as cellulases (Vaaje-Kolstad et al. 2010; Horn et al. 2012).

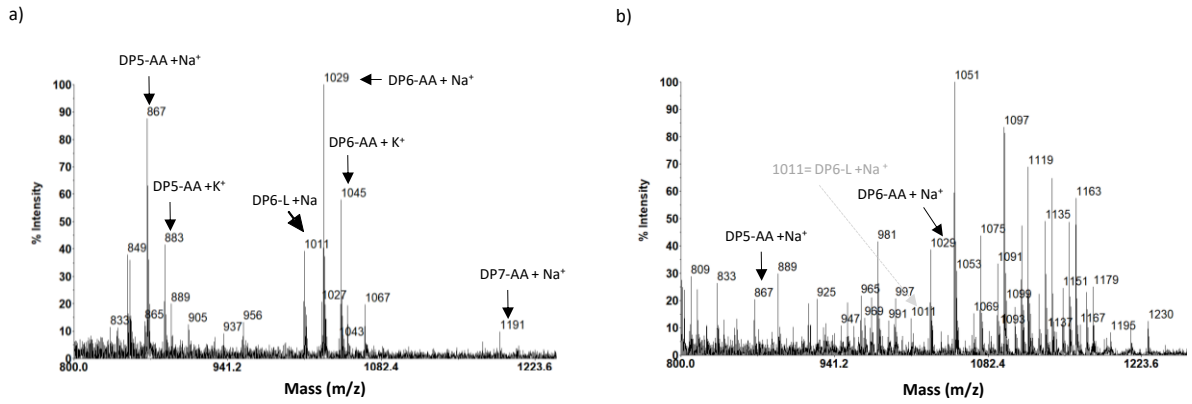

Fig. 2 MALDI-TOF analysis of oxidized products released by the enzymatic oxidation of SamLPMO10C on Bacterial cellulose (a) and eucalyptus pulp (b) after 72 h of reaction. DP—degree of polymerization. AA—Aldonic acid. L—Lactone. DP5-OX—cellopentaonic acid, DP6-OX—cellohexaonic acid.

The carboxyl content in the insoluble fraction of SamLPMO10C-oxidized pulps were also determined (Table 2) (Titration plots are attached in S3). The initial content of carboxyl groups in BC and eucalyptus pulp can be attributed to chemical modifications during their isolation and purification processes (Tolvaj and Faix 1995). These modifications can introduce carboxyl groups, and additional factors such as visible light and the bleaching process in eucalyptus pulp production can further contribute to the oxidation of the cellulose chain (Zhang et al. 1994). However, the carboxyl content values of the initial unoxidized pulps and the enzymatically oxidized pulps are high compared to those found in other works (see S4). However, it should be noted that the conductimetric method commonly used to measure the carboxyl content of cellulose is variable and dependent on experimental conditions, the presence of interferences, and the cellulose substrate that is analyzed. To compensate for this weakness, an unoxidized control that serves as a starting point for comparing the increase in carboxyl groups was included and it was found that after the enzymatic treatment with SamLPMO10C, BC and eucalyptus pulps increased their carboxyl groups 2.7 and 2.4 times, respectively. This degree of carboxyl increase is within the magnitude of carboxyl generated by LPMOs reported by other authors (Hu et al. 2018; Koskela et al. 2019; Solhi et al. 2022). It is noteworthy that SamLPMO10C showed more activity on BC than on eucalyptus, in accordance with the quantification of soluble oligosaccharides shown above. Previous results evaluating SamLPMO10C activity on cotton linters reported that carboxyl groups increased 1.6 times with respect to the initial carboxyl pulp content (Valls et al. 2019). In this work, SamLPMO10C successfully created carboxyl groups by oxidation of the hydroxyl group in the C1 position of the cellulose chain. Therefore, this enzyme is suitable to increase the carboxyl content in different cellulose substrates as this and previous studies have shown.

Table 1 Aldonic acid release produced by the enzymatic pretreatment

Pulp treatment	Enzymatic Pretreatment (h)	Aldonic acid release (mg/g pulp ± SD)
BC-ox	36	9.38 ± 0.10
BC-ox	72	19.03 ± 2.81
eu-ox	36	5.86 ± 1.64
eu-ox	72	9.87 ± 0.88

Table 2 Carboxyl content of substrates before and after SamLPMO10C oxidation

Pulp treatment	Enzymatic Pretreatment (h)	COO^- (mmol/Kg pulp)
BC	0	127 ± 12
BC-ox	72	347 ± 23
eu	0	153 ± 12
eu-ox	72	373 ± 46

3.3 Addition of silver and characterization of paper supports

After the oxidation of the cellulosic substrates, the addition of silver and the production of paper supports were carried out. The functionalized supports were analyzed by scanning electron microscopy (SEM), and energy-dispersive X-ray spectroscopy (EDS), and characterized in terms of silver content, leaching, and antibacterial capacity.

SamLPMO10C oxidized pulps were treated with 10 mmol $AgNO_3$/g of dry pulp as a source of silver ions. Non-oxidized pulps were used as controls. As described before, the hydroxyl groups present in the cellulose structure can attract the silver cations through dipole-ion interaction (Barud et al. 2008). Furthermore, the new negatively charged carboxyl groups (COO^-) created by the action of the enzyme were expected to attract Ag cations (Ag^+) by electrostatic interactions. Musino et al. (2021) showed that hydroxyl groups were the nucleation centers that attract the positively charged silver, and the COO- groups helped the dispersion state of the fibers and thereby, increased the access of the silver to the cellulose. After the treatment of pulps with $AgNO_3$, paper supports were produced and then subjected to thermal reduction. The heat is expected to cause a reduction of silver ions and triggers the formation of elemental silver nanoparticles (de Santa Maria et al. 2009; Morena et al. 2019).

The morphology of the surface of the paper supports was evaluated by scanning electron microscope (Fig. 3). Fig. 3a shows the typical network structure of bacterial cellulose fibers, approximately 70-100 nm wide and several micrometers long. These BC nanofibers have a high surface area which could help to stabilize the particles avoiding agglomerations. In Fig. 3c, corresponding to oxidized and silver-treated BC (BC-ox/Ag/TT), spherical particles

randomly distributed on the surface were observed with the BED-C filter in the same area as Fig. 3b, suggesting that these particles were composed of a high atomic weight element as was the case of silver. The size of these particles was relatively homogeneous with a diameter of 26 ± 3.21 nm. For oxidized and silver-treated eucalyptus paper supports (eu-ox/Ag/TT) a similar type of nanoparticles was observed (Fig. 3e and 3f). In this case, the diameter of the particles was 152 ± 43 nm, a larger diameter probably attributed to the also larger pore diameter in the matrix of eucalyptus cellulose compared to bacterial cellulose. Garza-Cervantes et al. (2020) also found a similar average size for their silver-cellulose composite. SEM images have not revealed Ag NPs in the BC/Ag/TT and eu/Ag/TT paper supports although it is highly likely that silver nanoparticles may also exist within these supports since OH groups act as nucleation centers for silver. The Ag NPs on the non-oxidized supports may be less evenly distributed in the matrix compared to the supports that have been previously oxidized. Therefore, it appears that the dispersion state induced by the increased carboxyl groups resulting from the enzymatic oxidation favors the formation of silver nanoparticles evenly distributed along the cellulosic support. As envisaged, no silver nanoparticles were found in controls without added silver.

The composition of these nanoparticles was analyzed by EDS, a qualitative technique that enables the determination of the atomic composition of the analyzed material. The EDS analysis (Fig. 4) shows a signal corresponding to silver and the peaks of carbon and oxygen that also appear in the spectrum corresponding to the components of the cellulose molecule.

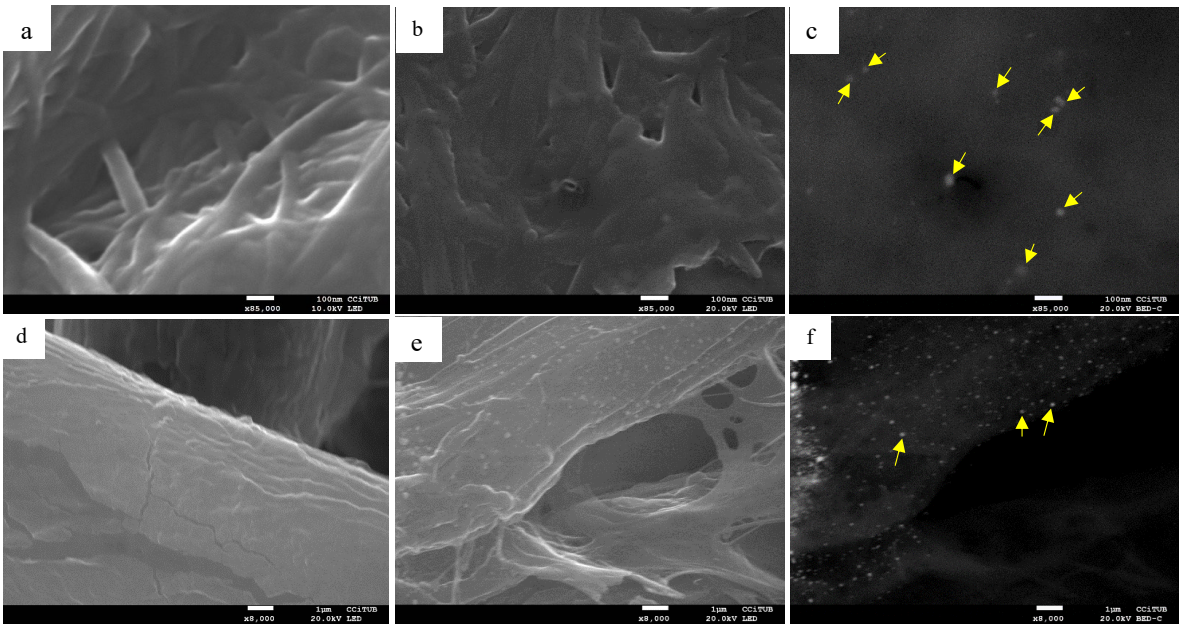

Fig. 3 SEM images of (a) BC paper support with an LED filter at 85,000x magnification. (b) BC-ox/Ag/TT paper support visualized with an LED filter at 85,000x magnification. (c) BC-ox/Ag/TT paper support with a BED-C filter at 85,000x magnification. (d) eu paper support with an LED filter at 8,000x magnification. (e) eu-ox/Ag/TT with an LED filter at 8,000x magnification. (f) eu-ox/Ag/TT with a BED-C filter at 8,000x magnification. The yellow

arrows point to silver nanoparticles detected on the paper supports. Note that in Fig. 3f, some, not all, nanoparticles are indicated.

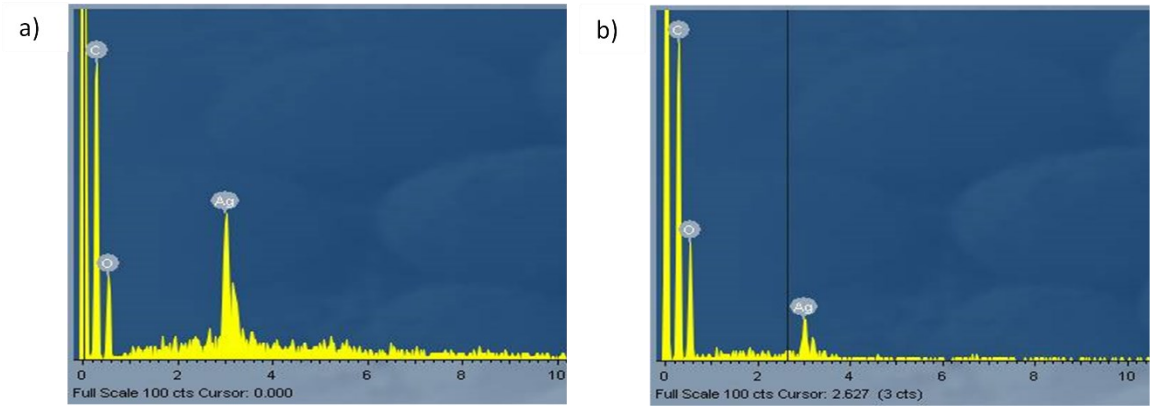

Fig. 4 Energy dispersive X-ray spectrometer (EDS) spectrum of silver nanoparticles in BC-ox/Ag/TT (a) and eu-ox/Ag/TT (b) paper supports.

To assess the total silver content ($Ag^0 + Ag^+$) incorporated into the paper supports Inductively Coupled Plasma (ICP) analysis was carried out. When comparing the BC and eucalyptus matrices, it was evident that eucalyptus incorporated more silver than BC (Fig. 5), which could be attributed to the larger size of eucalyptus pores observed by SEM images and to the fact that eucalyptus fibers form a looser network that is easier to penetrate. These results agree with those obtained for the size of the particles. When oxidizing the cellulose pulp, it can be expected that by incorporating more carboxyl groups, the negative charges on the surface will improve the dispersion state as suggested by Musino et al. (2021) so the hydroxyl groups, the real nucleation point for metallic nanoparticles, can attract more metal ions. This occurred with BC-ox/Ag/TT where this support incorporated, on average, 2.3 times more silver than the unoxidized silver-treated BC paper supports (BC/Ag/TT). On the contrary, in the case of silver functionalized eucalyptus, the oxidized eu-ox/Ag/TT supports contained less silver than the non-oxidized support (eu/Ag/TT), in this case, oxidation has not favored the incorporation of more silver ions. However, the oxidation of cellulose favored the generation of silver nanoparticles as previously explained.

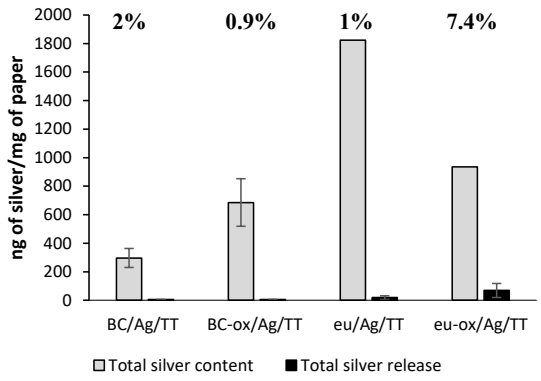

Fig. 5 Total silver content and silver leaching of functionalized paper supports. Percentages represent the fraction of silver released from each type of composite.

The leaching of silver from the different functionalized paper supports was also analyzed. For that purpose, 1 cm^2 of paper samples were immersed in an aqueous medium and shaking conditions for 24 h. Then, the silver content in the aqueous medium was analyzed by ICP-MS before and after the addition of HNO_3. When no HNO_3 was added to the cellulose substrates, only silver cations released were measured. When HNO_3 was added, the elemental silver was oxidized hence the total amount of silver released was measured. Table 3 shows the amount of silver ions and the total silver that migrated from the matrices to the aqueous media. The difference between the total amount of released silver and silver ions released corresponded to nanoparticles of elemental silver released to the aqueous medium. However, statistical analysis (t Student) showed that there were no significant differences, meaning that silver migrated from the matrices as ions and not as elemental silver. These results agree with the previous work of (Morena et al. 2019), where it is described, that silver also migrated from a bacterial cellulose matrix in the form of ions.

Table 3 Silver leaching from the paper supports

Paper support	**Ag^+ release Ag^+ng /mg of paper ±SD**	**Total silver release Ag^++Ag^0 ng/mg of paper**
BC/Ag/TT	4.3 ± 0.1	5.9 ± 0.8
BC-ox/Ag/TT	4.7 ± 0.1	6.4 ± 0.2
eu/Ag/TT	18.0 ± 12.9	18.9 ± 12.9
eu-ox/Ag/TT	64.5 ± 45.6	69.5 ± 49.6

By comparing the overall silver content in the paper supports with the amount released during leaching evaluation, it becomes evident that thermal treatment significantly contributes to the stabilization of silver within both matrices.

Most of the silver incorporated into functionalized paper supports had been retained (Fig. 5), especially in BC supports where the ligand diffusion was as low as 0.9% for BC-ox/Ag/TT and 2% for BC/Ag/TT, the fine network of BC fibers and thermal treatment helped stabilize and trap the NPs embedded in the matrix. For the eu supports the variability of silver uptake was higher and so was the leaching, 1% for eu/Ag/TT and 7.4% for eu-ox/Ag/TT. As pointed out above, eucalyptus cellulose has higher and more variable pore sizes and a looser structure so these features could influence silver leaching. The migration of the ligand incorporated into the cellulosic supports is an important characteristic for their future applications. On some occasions, the diffusion of the ligand is going to be a desirable feature (e.g., drug delivery) but on other occasions, the low diffusion is going to be necessary (e.g., sensors).

3.4 Antibacterial properties against Staphylococcus aureus of the paper supports

To determine the effect of Ag-NPs paper supports on cell viability, BC and eucalyptus silver-functionalized papers were incubated at room temperature with a suspension of a known concentration of *S. aureus*. Then, viable cells (CFU/mL) were determined after different times of incubation, and the percentage of inhibition was calculated with respect to the control of the untreated paper (Table 4).After one hour of incubation, there was 100% of inhibition for eu-ox/Ag/TT meanwhile, for BC-ox/Ag/TT, there was 83.3% of inhibition. The slower reduction in viability for BC-ox/Ag/TT may be because in this functionalized paper support the Ag NPs are trapped in the cellulose matrix more efficiently, BC-ox/Ag/TT showed only 0.9% leaching of silver against 7.4% for eu-ox/Ag/TT. The faster effect of the eucalyptus functionalized paper supports can also be attributed to the higher silver content in the paper as well as to the higher amount of silver migrated to the buffer media. The leaching of silver from the matrix favored the contact between silver and the microorganism, enhancing its toxic effect. Interestingly, there were no viable cells after 24 hours of contact with BC and eucalyptus functionalized papers. Silver salts have long been investigated for their inhibitory and bactericidal effects and potential application for burns (Fox, 1968; Moyer et al. 1965) but their mechanism of action is not quite elucidated. It has been reported that silver ions cause the loss of DNA´s replication ability (Feng et al. 2000). Also, silver ions bind to proteins´ thiol groups promoting the inactivation of bacterial proteins (Feng et al. 2000; Jung et al. 2008)

It is eye-catching that non-treated eu-paper also presented a decrease in the viable cell count indicating the antibacterial activity of eucalyptus cellulose itself. This characteristic was reported previously for flax cellulose, where a reduction of 17 % of *S. aureus* viability after 1 h of incubation was observed following the same standard method (Fillat et al. 2018). This antibacterial property of plant cellulose is due to the residual lignin and xylan that cannot be found in bacterial cellulose (Christakopoulos et al. 2003; Spasojević et al. 2016). The Kappa number, a measure of lignin content, and the carbohydrate content of eucalyptus (Beltramino-Heffes 2016) is provided in S5.

Table 4 Viable count (CFU/mL) and viability reduction percentage of *Staphylococcus aureus* in contact with paper supports containing AgNPs. BC and eucalyptus non-treated samples were used as controls

		CFU/mL	% Reduction		CFU/mL	% Reduction
t_0		$2.4 \cdot 10^6$	0		$2.94 \cdot 10^6$	0
t_1	**BC-paper**	$2.4 \cdot 10^6$	0	**eu-paper**	$1.73 \cdot 10^6$	32
t_{24}		$2.4 \cdot 10^6$	0		$7.0 \cdot 10^5$	72
t_0		$2.4 \cdot 10^6$	0		$2.94 \cdot 10^6$	0
t_1	**BC-ox/Ag/TT**	$3 \cdot 10^5$	83.3	**eu-ox/Ag/TT**		100
t_{24}		0	100			100

To test the effect of the functionalized paper supports on the metabolism of *S. aureus*, the BC and eucalyptus papers were immersed in a suspension of known concentration of the bacteria. The tubes were incubated at RT while shaking and the metabolic activity of the cells was determined after 0, 30, 60, and 120 minutes. The samples were incubated with resazurin, and then the fluorescence was measured as a measure of metabolic activity. For eu-ox/Ag/TT paper supports the reduction of metabolic activity occurred faster than for BC-ox/Ag/TT paper supports (Fig. 6). At 30 min there was a reduction of 89% of metabolic activity of *S. aureus* in contact with eu-ox/Ag/TT and a 24% reduction in the case of BC-ox/Ag/TT, in accordance with the higher silver content and leaching of eucalyptus matrices (Fig. 5). These results indicate that the amount of incorporated silver in the paper supports was toxic to *S. aureus*. On the other hand, for BC with silver NPs, the reduction of metabolic activity showed to be gradual over time and, only after 2 hours, a 74% reduction in bacterial activity was reached. This slower antimicrobial activity of BC/AgNPs fits with the cellular viability test previously explained.

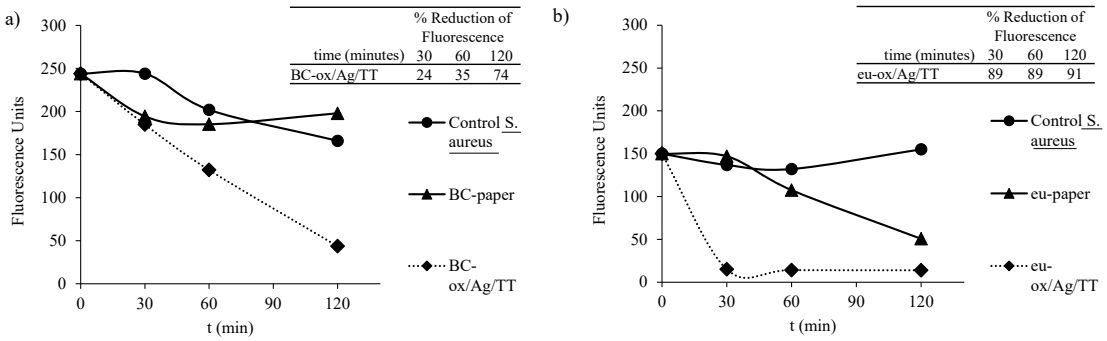

Fig. 6 Microbial activity (FU) of *Staphylococcus aureus* after being in contact with (a) BC and functionalized BC paper supports and, (b) eu and eu functionalized paper supports. Bacterial cellulose paper (BC-paper), silver-treated bacterial cellulose (BC-ox/Ag/TT). Eucalyptus paper (eu-paper), silver treated eucalyptus (eu-ox/Ag/TT). Control *S. aureus* refers to a suspension of *S. aureus* with no paper incubated.

Eucalyptus control samples showed antibacterial capacity that increased with time even though they did not contain silver, in good agreement with the previous result of reduction of cell viability. It is noteworthy that for BC-ox/Ag/TT there is an 83% reduction of viability after 60 minutes but only a 35% reduction of metabolic activity. This apparent difference in antibacterial capacity is because the two antimicrobial tests used provide different but complementary information. The results indicated that in the viability test, the cells were in an active but nonculturable state. For eu-ox/Ag/TT the same thing occurred, the viability was rapidly reduced to 100% after 60 minutes but the cells still showed metabolic activity, although reduced by 89%. This suggests that the silver caused *S. aureus* cells to reach an active but nonculturable state first and then eventually die, as suggested by Jung et al. (2008).

The two antibacterial tests assayed demonstrated that the eucalyptus and BC paper supports functionalized with silver had strong antibacterial capacity against *S. aureus* due to the contact of the paper support with the bacteria as well as the leaching of silver in the aqueous media. Cellulosic-based materials have demonstrated their great versatility for functionalization and can be used to add other types of ligands.

4 Conclusions

In this work, the production of silver functionalized BC and eu paper was achieved. Carboxyl groups generated by enzymatic oxidation of cellulose fibers with LPMO favored the generation of silver nanoparticles on these paper supports after thermal induction. The functionalized paper supports showed strong antibacterial activity against *Staphylococcus aureus*. It is foreseeable that enzymatically oxidized bacterial and eucalyptus celluloses could be functionalized with other metals, expanding the applications of the resulting paper supports which could be used for catalysis, filter membranes, and wearable devices such as sensors.

Authors´ contributions

LC conducted the experiments and wrote the manuscript. JM and SV took part in planning the study, supervised the experiments, checked the results, and revised the manuscript. All authors read and approved the final manuscript.

Funding statement

This work was supported by Scientific and Technological Research Council (MINECO, Spain), grant CTQ2017-84966-C2-2-R. Verónica Cabañas-Romero acknowledges a doctoral fellowship from Programa Nacional de Becas de Posgrado en el Exterior “Don Carlos Antonio López” del Ministerio de Hacienda del Paraguay.

Acknowledgments

We thank the Serveis Cientifico-Tècnics of the University of Barcelona (CCiTUB) for technical supportin scanning electron microscopy and HPAEC-PAD analysis.

Data availability
The data that support the findings of this study are available from the corresponding authors on reasonable request.

Competing of interest
There are no conflicts of interest to declare.

Consent for publication
All authors have read and commented on the study. All authors consented to the publication of this work.

Ethics and consent to participate approval
Not applicable.

Bibliography

ASTM Standard E2149–01. (2010). Standard test method for determining the antimicrobial activity of immobilized antimicrobial agents under dynamic contact conditions. ASTM International

Barud HS, Barrios C, Regiani T, Marques RFC, Verelst M, Dexpert-Ghys J, Messeddeq Y, Ribeiro SJL (2008) Self-supported silver nanoparticles containing bacterial cellulose membranes. Mater Sci Eng C 28: (4), 515-518. https://doi.org/10.1016/j.msec.2007.05.001

Beltramino-Heffes F (2016) Enzymatic-assisted preparation of nanocrystalline cellulose from non-wood fibers. Universitat Politècnica de Catalunya

Brown AJ (1886) XLIII. —On an acetic ferment which forms cellulose. J. Chem. Soc., Trans. 49:432–439. https://doi.org/10.1039/CT8864900432

Buruaga-Ramiro C, Fernández-Gándara N, Cabañas-Romero LV, Valenzuela SV, Pastor FIJ, Diaz P, Martinez, J (2022). Lytic polysaccharide monooxygenases and cellulases on the production of bacterial cellulose nanocrystals. Eur. Polym. J., 163 110939. https://doi.org/10.1016/j.eurpolymj. 163, 110939.

Buruaga-Ramiro C, Valenzuela SV, Valls C, Roncero MB, Pastor FIJ, Diaz P, Martinez J (2020) Development of an antimicrobial bioactive paper made from bacterial cellulose. Int. J. Biol. Macromol. 158:587–594. https://doi.org/10.1016/j.ijbiomac.2020.04.234

Cabañas-Romero LV, Valls C, Valenzuela SV, Roncero MB, Pastor FIJ, Diaz P, Martinez J (2020) Bacterial Cellulose-Chitosan Paper with Antimicrobial and Antioxidant Activities. Biomacromolecules 21:1568–1577. https://doi.org/10.1021/acs.biomac.0c00127

Christakopoulos P, Katapodis P, Kalogeris E, Kekos D, Macris BJ, Stamatis H, Skaltsa H (2003) Antimicrobial activity of acidic xylo-oligosaccharides produced by family 10 and 11 endoxylanases. Int. J. Biol. Macromol.31:171–175. https://doi.org/10.1016/S0141-8130(02)00079-X

Cichosz S, Masek A, Rylski A (2020) Cellulose Modification for Improved Compatibility with the Polymer Matrix: Mechanical Characterization of the Composite Material. Materials 13(23):5519. https://doi.org/10.3390/ma13235519

Dang Z (2007) The Investigation of Carboxyl Groups of Pulp Fibers during Kraft Pulping, Alkaline Peroxide Bleaching, and TEMPO-mediated Oxidation. Georgia Institute of Technology.

de Santa Maria LC, Santos ALC, Oliveira PC, Barud HS, Messaddeq Y, Ribeiro SJL (2009) Synthesis and characterization of silver nanoparticles impregnated into bacterial cellulose. Mater. Lett. 63(9-10):797–799. https://doi.org/10.1016/j.matlet.2009.01.007

Drula E, Garron ML, Dogan S, Lombard V, Henrissat B, Terrapon N (2022) The carbohydrate-active enzyme database: functions and literature. Nucleic Acids Res. 50(D1):D571–D577. https://doi.org/10.1093/nar/gkab1045

Feng QL, Wu J, Chen GQ, Cui FZ, Kim TN, Kim JO (2000) A mechanistic study of the antibacterial effect of silver ions on *Escherichia coli* and *Staphylococcus aureus*. J. Biomed. Mater. Res. 52(4):662–668. https://doi.org/10.1002/1097-4636(20001215)52:4<662::AID-JBM10>3.0.CO;2-3

Fernández J, Morena AG, Valenzuela SV, Pastor FIJ, Díaz P, Martinez, J (2019) Microbial Cellulose from a *Komagataeibacter intermedius* Strain Isolated from Commercial Wine Vinegar. J Polym Environ. 27:956–967. https://doi.org/10.1007/s10924-019-01403-4

Fillat A, Martínez J, Valls C, Cusola O, Rocero MB, Vidal T, Valenzuela SV, Diaz P, Pastor FIJ (2018) Bacterial cellulose for increasing barrier properties of paper products. Cellulose 25:6093–6105. https://doi.org/10.1007/s10570-018-1967-0

Fox CL (1968) Silver Sulfadiazine—A New Topical Therapy for *Pseudomonas* in Burns. Arch Surg 96(2):184-188. https://doi.org/10.1001/archsurg.1968.01330200022004

Garza-Cervantes JA, Mendiola-Garza G, de Melo EM, Dugmore TIJ, Matharu AS, Morones-Ramirez JR (2020) Antimicrobial activity of a silver-microfibrillated cellulose biocomposite against susceptible and resistant bacteria. Sci. Rep. 10(1):7281. https://doi.org/10.1038/s41598-020-64127-9

Golonka I, Greber KE, Oleksy-Wawrzyniak M, Paleczny J, Dryś A, Junka A, Sawicki W, Musiał W (2021) Antimicrobial and Antioxidative Activity of Newly Synthesized Peptides Absorbed into Bacterial Cellulose Carrier against *Acne vulgaris*. Int. J. Mol. Sci. 22(14):7466. https://doi.org/10.3390/ijms22147466

Horn SJ, Vaaje-Kolstad G, Westereng B, Eijsink V (2012) Novel enzymes for the degradation of cellulose. Biotechnol. Biofuels 5(1):1-13. https://doi.org/10.1186/1754-6834-5-45

Hu J, Tian D, Renneckar S, Saddler JN (2018) Enzyme mediated nanofibrillation of cellulose by the synergistic actions of an endoglucanase, lytic polysaccharide monooxygenase (LPMO) and xylanase. Sci. Rep. 8(1):1–8. https://doi.org/10.1038/s41598-018-21016-6

Jung WK, Koo HC, Kim KW, Shin S, Kim SH, Park YH (2008) Antibacterial Activity and Mechanism of Action of the Silver Ion in *Staphylococcus aureus* and *Escherichia coli*. Appl. Environ. Microbiol. 74(7):2171–2178. https://doi.org/10.1128/AEM.02001-07

Katz S, Beatson RP, Scallan AM (1984) The determination of strong and weak acidic groups in sulfite pulps. Svensk Papperstidning 87(6):R48–R53

Klemm D, Heublein B, Fink HP, Bohn A (2005) Cellulose: Fascinating biopolymer and sustainable raw material. Angew. Chem. Int. Ed. 44(22):3358–3393. https://doi.org/10.1002/anie.200460587

Klemm D, Kramer F, Moritz S, Lindstrom T, Ankerfors M, Gray D, Dorris A (2011) Nanocelluloses: A New Family of Nature-Based Materials. Angew. Chem. Int. Ed. 50(24):5438–5466. https://doi.org/10.1002/anie.201001273

Klemm D, Petzold-Welcke K, Kramer F, Ritcher T, Raddatz V, Fried W, Nietzsche S, Bellmann T, Fischer D (2021) Biotech nanocellulose: A review on progress in product design and today's state of technical and medical applications. Carbohydr. Polym. 254:117313. https://doi.org/10.1016/j.carbpol.2020.117313

Koskela S, Wang S, Xu D, Yang X, Li K, Berglund LA, McKee LS, Bulone V, Zhou Q (2019) Lytic polysaccharide monooxygenase (LPMO) mediated production of ultra-fine cellulose nanofibres from delignified softwood fibres. Green Chem. 21:5924–5933. https://doi.org/10.1039/C9GC02808K

Lee KY, Buldum G, Mantalaris A, Bismarck A (2014) More than Meets the Eye in Bacterial Cellulose: Biosynthesis, Bioprocessing, and Applications in Advanced Fiber Composites. Macromol Biosci 14(1):10–32. https://doi.org/10.1002/mabi.201300298

Matthysse AG, Marry M, Krall L, Kaye M, Ramey BE, Fuqua C, White AR (2005) The Effect of Cellulose Overproduction on Binding and Biofilm Formation on Roots by *Agrobacterium tumefaciens.* Mol. Plant Microbe Interact. 18(9):1002–1010. https://doi.org/10.1094/MPMI-18-1002

Moreau C, Tapin-Lingua S, Grisel S, Gimbert I, Le Gall S, Meyer V, Petit-Conil M, Berrin JG, Cathala B, Villares A (2019) Lytic polysaccharide monooxygenases (LPMOs) facilitate cellulose nanofibrils production. Biotechnol. Biofuels 12:1-13. https://doi.org/10.1186/s13068-019-1501-0

Morena AG, Roncero MB, Valenzuela SV, Valls C, Vidal T, Pastor FIJ, Diaz P, Martinez J (2019) Laccase/TEMPO-mediated bacterial cellulose functionalization: production of paper-silver nanoparticles composite with antimicrobial activity. Cellulose 26:8655–8668. https://doi.org/10.1007/s10570-019-02678-5

Moyer CA, Brentano L, Gravens D, Margraf HW, Monafo WW (1965) Treatment of Large Human Burns With 0.5% Silver Nitrate Solution. Arch Surg 90(6):812-867. https://doi.org/10.1001/archsurg.1965.01320120014002

Musino D, Rivard C, Landrot G, Novales B, Rabilloud T, Capron I (2021) Hydroxyl groups on cellulose nanocrystal surfaces form nucleation points for silver nanoparticles of varying shapes and sizes. J. Colloid Interface Sci. 584:360–371. https://doi.org/10.1016/j.jcis.2020.09.082

O'Brien J, Wilson I, Orton T, Pognan F (2000) Investigation of the Alamar Blue (resazurin) fluorescent dye for the assessment of mammalian cell cytotoxicity. Eur J Biochem 267(17):5421–5426. https://doi.org/10.1046/j.1432-1327.2000.01606.x

Onyszko M, Markowska-Szczupak A, Rakoczy R, Paszkiewicz O, Janusz J, Gorgon-Kuza A, Wenelska K, Mijowska E (2022) The cellulose fibers functionalized with star-like zinc oxide nanoparticles with boosted antibacterial performance for hygienic products. Sci. Rep. 12(1):1321 https://doi.org/10.1038/S41598-022-05458-7

Orlando I, Basnett P, Nigmatullin R, Wang W, Knowles J, Roy I (2020) Chemical Modification of Bacterial Cellulose for the Development of an Antibacterial Wound Dressing. Front. Bioeng. Biotechnol. *8*:1–19. https://doi.org/10.3389/fbioe.2020.557885

Quinlan RJ, Sweeney MD, Lo Leggio L, Otten H, Poulsen JCN, Johansen KS, Krogh KBRM, Jørgensen CI, Tovborg M, Anthonsen A, Tryfona T, Walter CP, Dupree P, Xu F, Davies GJ, Walton PH (2011) Insights into the oxidative degradation of cellulose by a copper metalloenzyme that exploits biomass components. Proc. Natl. Acad. Sci. U.S.A. 108(37):15079–15084. https://doi.org/10.1073/pnas.1105776108

Robledo M, Rivera L, Jiménez-Zurdo JI, Rivas R, Velázquez E, Martínez-Molina E, Hirsch AM, Mateos PF (2012) Role of *Rhizobium* endoglucanase CelC2 in cellulose biosynthesis and biofilm formation on plant roots and abiotic surfaces. Microb. Cell Factories 11(1):1-12. https://doi.org/10.1186/1475-2859-11-125

Saleh AK, El-Gendi H, Soliman NA, El-Zawawy WK, Abdel-Fattah Y (2022) Bioprocess development for bacterial cellulose biosynthesis by novel *Lactiplantibacillus plantarum* isolate along with characterization and antimicrobial assessment of fabricated membrane. Sci. Rep. 12(1):2181. https://doi.org/10.1038/s41598-022-06117-7

Segal L, Creely JJ, Martin AE, Conrad CM (1959) An Empirical Method for Estimating the Degree of Crystallinity of Native Cellulose Using the X-Ray Diffractometer. Text. Res. J. 29:786–794. https://doi.org/10.1177/004051755902901003

Shah N, Ul-Islam M, Khattak WA, Park JK (2013) Overview of bacterial cellulose composites: A multipurpose advanced material. Carbohydr. Polym. 98(2):1585–1598. https://doi.org/10.1016/j.carbpol.2013.08.018

Solhi L, Li J, Li J, Heyns NMI, Brumer H (2022) Oxidative enzyme activation of cellulose substrates for surface modification Green Chem. 24:4026–4040. https://doi.org/10.1039/D2GC00393G

Spasojević D, Zmejkoski D, Glamočlija J, Nikolić M, Soković M, Milošević V, Jarić I, Stojanović M, Marinković E, Barisani-Asenbauer T, Prodanović R, Jovanović M, Radotić K (2016) Lignin model compound in alginate hydrogel: a strong antimicrobial agent with high potential in wound treatment. Int. J. Antimicrob. Agents 48(6):732–735. https://doi.org/10.1016/j.ijantimicag.2016.08.014

Tanpichai S, Boonmahitthisud A, Soykeabkaew N, Ongthip L (2022) Review of the recent developments in all-cellulose nanocomposites: Properties and applications. Carbohydr. Polym. 286:119192. https://doi.org/10.1016/j.carbpol.2022.119192

Tolvaj L, Faix O (1995) Artificial Ageing of Wood Monitored by DRIFT Spectroscopy and CIE L*a*b* Color Measurements. 1. Effect of UV Light. Holzforschung 49(5):397–404. https://doi.org/10.1515/hfsg.1995.49.5.397

Torres FG, Arroyo JJ, Troncoso OP (2019) Bacterial cellulose nanocomposites: An all-nano type of material. Mater. Sci. Eng. *C* 98:1277–1293. https://doi.org/10.1016/j.msec.2019.01.064

Vaaje-Kolstad G, Forsberg Z, Loose JS, Bissaro B, Eijsink VG (2017) Structural diversity of lytic polysaccharide monooxygenases. Curr. Opin. Struct. Biol. 44:67–76. https://doi.org/10.1016/j.sbi.2016.12.012

Vaaje-Kolstad G, Westereng B, Horn SJ, Liu Z, Zhai H, Sertie M, Eijsink VGH (2010) An Oxidative Enzyme Boosting the Enzymatic Conversion of Recalcitrant Polysaccharides. Science (1979) 330:219–222. https://doi.org/10.1126/science.1192231

Valenzuela SV, Ferreres G, Margalef G, Pastor FIJ (2017) Fast purification method of functional LPMOs from *Streptomyces ambofaciens* by affinity adsorption. Carbohydr. Res. 448:205–211. https://doi.org/10.1016/j.carres.2017.02.004

Valenzuela SV, Valls C, Schink V, Sánchez D, Roncero MB, Diaz P, Martinez J, Pastor FIJ (2019) Differential activity of lytic polysaccharide monooxygenases on celluloses of different crystallinity. Effectiveness in the sustainable production of cellulose nanofibrils. Carbohydr. Polym. 207:59–67. https://doi.org/10.1016/j.carbpol.2018.11.076

Valls C, Pastor FIJ, Roncero MB, Vidal T, Diaz P, Martínez J, Valenzuela S (2019) Assessing the enzymatic effects of cellulases and LPMO in improving mechanical fibrillation of cotton linters. Biotechnol. Biofuels 12(1):1-14. https://doi.org/10.1186/s13068-019-1502-z

Westereng B, Agger JW, Horn SJ, Vaaje-Kolstad G, Aachmann FL, Stenstrøm YH, Eijsink VG (2013). Efficient separation of oxidized cello-oligosaccharides generated by cellulose degrading lytic polysaccharide monooxygenases. J. Chromatogr. A, 1271(1), 144-152.

Wood TM (1988) Preparation of crystalline, amorphous, and dyed cellulase substrates. Meth. Enzymol. 160:19-25. https://doi.org/10.1016/0076-6879(88)60103-0

Yamada Y, Yukphan P, Vu HTL, Muramatsu Y, Ochaikul D, Nakagaw Y (2012) Subdivision of the genus *Gluconacetobacter* Yamada, Hoshino and Ishikawa 1998: the proposal of *Komagatabacter* gen. nov., for

strains accommodated to the *Gluconacetobacter xylinus* group in the *α-Proteobacteria*. Ann. Microbiol. 62(2):849–859. https://doi.org/10.1007/s13213-011-0288-4

Zhang Y, Sjögren B, Engstrand P, Htun M (1994) Determination of Charged Groups in Mechanical Pulp Fibres and Their Influence on Pulp PropertiesJ. Wood Chem. Technol. 14:83–102. https://doi.org/10.1080/02773819408003087

Zhou L, Ke K, Yang M-B, Yang W (2021) Recent progress on chemical modification of cellulose for high mechanical-performance Poly(lactic acid)/Cellulose composite: A review. Compos. Commun. 23:100548. https://doi.org/10.1016/j.coco.2020.100548

4.1 4.2 Capítulo 2. Estrategias de expresión de Monooxigenasas líticas de polisacáridos (LPMOs) y estudio de los efectos que tienen estas enzimas sobre la celulosa.

4.1.1 Artículo 3: Lytic polysaccharide monooxygenases low-cost expression strategies and insights into the enzyme-substrate interactions

Estrategias de expresión de bajo costo para monooxigenasas de polisacáridos líticas y estudio sobre las interacciones enzima-sustrato

Las monooxigenasas líticas de polisacáridos (LPMOs) son enzimas dependientes de cobre que descomponen polisacáridos recalcitrantes y tienen un gran potencial para la producción su aplicación en biorefinerías y la producción de productos químicos base. En este estudio, dos LPMOs bacterianas, ShaLPMO10A y SamLPMO10C, fueron expresadas en *Escherichia coli* y *Streptomyces lividans*. Se obtuvieron grandes cantidades de enzimas activas que fueron secretadas mediante expresión homóloga en el hospedador *Streptomyces* evaluado. Se estudió el efecto de estas enzimas sobre la masa molar de la celulosa a lo largo de la reacción de oxidación, mostrando que la masa molar disminuye a medida que avanza la reacción. SamLPMO10C y ShaLPMO10A se unieron firmemente a la celulosa bacteriana, lo que mostró un cambio de masa debido a la actividad enzimática muy temprano al inicio de la reacción, como se mostró en el análisis de microbalanza de cristal de cuarzo con disipación (QCM-D, por sus siglas en inglés). Ambas LPMOs estudiadas en este trabajo mostraron actividad oxidativa en un amplio rango de temperaturas, lo que las convierte en candidatos interesantes para su uso en biorefinerías celulósicas.

UNIVERSITAT DE BARCELONA

Departament de Genètica, Microbiologia i Estadística
Secció de Microbiologías, Virologia i Biotecnología
Facultat de Biologia
Avinguda Diagonal 643
08028 Barcelona
Tel
+34934034675

Barcelona, 11th August 2023

Dear Editor

Please consider the enclosed manuscript entitled "Lytic polysaccharide monooxygenases low-cost expression strategies and insights into the enzyme-substrate interactions" for publication in the ACS Sustainable Chemistry & Engineering journal. The authors of this work are L. Verónica Cabañas-Romero, Carolina Buruaga-Ramiro, F.I. Javier Pastor, Ana Villares, Margaux Grellier, Ramón I. Santamaría, Margarita Díaz, and myself, Susana V. Valenzuela (corresponding author). Keywords: Lytic polysaccharide monooxygenases, Homologous expression, Heterologous expression, HPSEC-MALLs and QCM-D

This manuscript presents a study focused on the lytic polysaccharide monooxygenases (LPMOs), which are copper-dependent enzymes with immense potential in the cleavage of recalcitrant polysaccharides. The research investigates the expression of two bacterial LPMOs, ShaLPMO10A and SamLPMO10C, in *Escherichia coli* and *Streptomyces lividans*. Through homologous expression in the *Streptomyces* host, significant levels of active enzymes were successfully produced and secreted. The study delves into the effects of these enzymes on cellulose molar mass during the oxidation reaction, revealing a progressive decrease in molar mass. Particularly intriguing is the observation that SamLPMO10C and ShaLPMO10A exhibit firm binding to bacterial cellulose, leading to early mass changes indicative of enzymatic activity, as demonstrated by quartz crystal microbalance with dissipation (QCM-D) analysis. Furthermore, the remarkable oxidative activity exhibited by both LPMOs across a broad temperature range positions them as promising candidates for integration into cellulosic biorefineries.

UNIVERSITAT DE BARCELONA

Departament de Genètica, Microbiologia i Estadística
Secció de Microbiologías, Virologia i Biotecnología
Facultat de Biologia
Avinguda Diagonal 643
08028 Barcelona
Tel
+34934034675

This article examines the effects of LPMOs on cellulose, the most abundant biopolymer on Earth. By studying this interaction, the article underscores the implementation of a sustainable approach by working with a renewable resource like cellulose, thereby exemplifying the application of green principles in materials science and biochemistry in an innovative manner.

I firmly believe that our manuscript makes a significant contribution to the advancement of sustainable chemistry and engineering, particularly within the context of enzymatic cleavage of recalcitrant polysaccharides. Its originality, scientific merit, and environmental implications make it a strong fit for publication in ACS Sustainable Chemistry & Engineering.

Thank you for your time and consideration.

Sincerely,

Susana V. Valenzuela

UNIVERSITAT DE BARCELONA

Departament de Genètica, Microbiologia i Estadística
Secció de Microbiologías, Virologia i Biotecnología
Facultat de Biologia
Avinguda Diagonal 643
08028 Barcelona
Tel
+34934034675

AUTHORS INFORMATION

Corresponding author

Susana V. Valenzuela - *Department of Genetics, Microbiology, and Statistics, Faculty of Biology, Universitat de Barcelona, Av. Diagonal 643, 08028, Barcelona, Spain, and Institute of Nanoscience and Nanotechnology (IN^{2}UB), Universitat de Barcelona, Spain; orcid.org/0000-0002-1684-9514; Email: susanavalenzuela@ub.edu*

Authors

L. Verónica Cabañas-Romero - *Department of Genetics, Microbiology, and Statistics, Faculty of Biology, Universitat de Barcelona, Av. Diagonal 643, 08028, Barcelona, Spain, and Institute of Nanoscience and Nanotechnology (IN^{2}UB), Universitat de Barcelona, Spain; orcid.org/0000-0001-7512-8779; Email: veronica.cabanas@ub.edu*

Carolina Buruaga-Ramiro- *Department of Genetics, Microbiology, and Statistics, Faculty of Biology, Universitat de Barcelona, Av. Diagonal 643, 08028, Barcelona, Spain, and Institute of Nanoscience and Nanotechnology (IN^{2}UB), Universitat de Barcelona, Spain; orcid.org/0000-0002-0187-1399; Email: carolburuaga@gmail.com*

F.I. Javier Pastor- *Department of Genetics, Microbiology, and Statistics, Faculty of Biology, Universitat de Barcelona, Av. Diagonal 643, 08028, Barcelona, Spain, and Institute of Nanoscience and Nanotechnology (IN^{2}UB), Universitat de Barcelona, Spain; orcid.org/0000-0003-0326-2527; Email: fpastor@ub.edu*

Ana Villares-*UR1268 BIA, INRAE, F-44316 Nantes, France; orcid.org/0000-0001-5441-7299; Email: ana.villares@inrae.fr*

Margaux Grellier-*UR1268 BIA, INRAE, F-44316 Nantes, France; Email: margaux.grellier@inrae.fr*

Ramón I. Santamaría-*Instituto de Biología Funcional y Genómica (IBFG)/Departamento de Microbiología y Genética. Consejo Superior de Investigaciones Científicas (CSIC)/Universidad de Salamanca (USAL), C/ Zacarías González, nº 2, 37007-Salamanca, Spain; orcid.org/0000-0002-2181-6776; Email: santa@usal.es*

Margarita Díaz-*Instituto de Biología Funcional y Genómica (IBFG)/Departamento de Microbiología y Genética. Consejo Superior de Investigaciones Científicas (CSIC)/Universidad de Salamanca (USAL), C/ Zacarías González, nº 2, 37007-Salamanca, Spain; orcid.org/0000-0003-4286-1506; Email: mardi@usal.es*

Lytic polysaccharide monooxygenases low-cost expression strategies and insights into the enzyme-substrate interactions

L. Verónica Cabañas-Romero[†,‡] , Carolina Buruaga-Ramiro[†,‡], F.I. Javier Pastor[†, ‡], Ana Villares [§], Margaux Grellier [§], Ramón I. Santamaría [‖], Margarita Díaz [‖] and, Susana V. Valenzuela[* †, ‡]

[†] Department of Genetics, Microbiology, and Statistics, Faculty of Biology, Universitat de Barcelona, Av. Diagonal 643, 08028, Barcelona, Spain

[‡] Institute of Nanoscience and Nanotechnology (IN^{2}UB), Universitat de Barcelona, Spain

[§] UR1268 BIA, INRAE, F-44316 Nantes, France

[‖] Instituto de Biología Funcional y Genómica (IBFG)/Departamento de Microbiología y Genética. Consejo Superior de Investigaciones Científicas (CSIC)/Universidad de Salamanca (USAL), C/ Zacarías González, nº 2, 37007-Salamanca, Spain

∗ Corresponding author at Department of Genetics, Microbiology, and Statistics, Faculty of Biology, Universitat de Barcelona, Av. Diagonal 643, 08028, Barcelona, Spain.

susanavalenzuela@ub.edu

+34934034675

Abstract

Lytic polysaccharide monooxygenases (LPMOs) are copper-dependent enzymes that cleave recalcitrant polysaccharides and have great potential for biorefineries and platform chemicals production. In this study two bacterial LPMOs, ShaLPMO10A and SamLPMO10C, were expressed in *Escherichia coli* and *Streptomyces lividans.* High levels of active enzymes were produced and secreted by homologous expression in the *Streptomyces* host assayed. The effect of these enzymes on the molar mass of cellulose throughout the oxidation reaction was studied, showing that the molar mass decreases as the reaction progresses. SamLPMO10C and ShaLPMO10A bound firmly to bacterial cellulose which showed mass change due to the enzymatic activity very early at the beginning of the reaction, as showed by quartz crystal microbalance with dissipation (QCM-D) analysis. Both LPMOs studied in this work performed oxidative activity in a wide range of temperatures making these enzymes interesting candidates for use in cellulosic biorefineries.

Keywords

Lytic polysaccharide monooxygenases

Homologous expression

Heterologous expression

HPSEC-MALLs

QCM-D

INTRODUCTION

Concerns about climate change and the current global situation make the development of new fuel sources and new materials imperative. In this context, lignocellulosic biomass is recognized as a source of materials to replace, at some point, petroleum derivatives.[1] However, the main bottleneck for the use of lignocellulose is its recalcitrance. Currently, the disassembly of lignocellulose consists of thermochemical, chemical, or enzymatic treatments.[1,2]

Lytic polysaccharide monooxygenases (LPMOs) are copper-dependent enzymes discovered in 2010 [3] that cleave recalcitrant polysaccharides such as cellulose and chitin by a cleavage mechanism that involves oxidation through the insertion of oxygen in two alternative positions of the sugar rings. Oxidation at C1 results in the release of a lactone, followed by ring opening to form aldonic acid, while oxidation at C4 releases a 4-keto sugar at the non-reducing end. Some of these oxidative enzymes produce a mixture of C1- and C4-oxidized products.[3–7] LPMOs require an electron donor such as ascorbate, cellobiose dehydrogenase, phenols, glucose-methanol-choline oxidoreductases, or photosynthetic pigments such as chlorophylls.[8–10] The original catalytic scenario proposed is a monooxygenase reaction and involves the delivery of two electrons, two protons, and molecular oxygen (R-H + $2e^-$ + 2H+ O_2 => R-OH + H_2O). [3] More recently it has been proposed that LPMOs are peroxygenases (R-H + H2O2 => R-OH + H2O).[11]

LPMOs are currently classified into “Auxiliary Activity” families AA9−11 and AA13−17 in the Carbohydrate-Active enZYmes (CAZy) database.[12] The most widely studied LPMO families are AA9 and AA10. While AA9 LPMOs are only distributed in fungi, AA10 LPMOs are mainly found in bacteria. In nature, the main function of these enzymes is the deconstruction of biomass, an important step in the global carbon cycle. Among the bacterial kingdom, the *Streptomyces* genus is well known for its important role in biomass decomposition. Thereby the interest in investigating the cellulolytic systems of the different members of this genus for applications in biotechnology.[13,14] Garda et al. described two encoding genes from *Streptomyces halstedii* JM8, a cellulolytic strain isolated from straw: one protein, CelS2, was an endoglucanase, and, the other protein, named p40, did not show any clear hydrolytic activity against cellulosic or xylanosic compounds, although showed high affinity for Avicel (crystalline cellulose).[15] Subsequent bioinformatic studies suggested that p40 might be a LPMO.

The production of high levels of active enzymes is one of the main goals of biotechnology. *Pichia pastoris* for fungal LPMOs and *Escherichia coli* for bacterial LPMOs are examples of the preferred hosts.[10] Other bacterial hosts reported to express LPMOs are *Bacillus subtilis* and the cyanobacterium *Synechococcus elongatus.*[16,17] In the traditional *E. coli* system, frequently insoluble inclusion bodies are formed which makes downstream processing difficult. Also, the use of antibiotics raises cost production and increases concerns related to antibiotic resistance. In such cases, alternative production strategies are required, and microorganisms of the genus *Streptomyces* have been successfully applied for enzyme production such as amylases and xylanases.[18]

In this work, two bacterial LPMOs were studied: SamLPMO10C, previously cloned and expressed by Valenzuela et al. [19] and p40, renamed here as ShaLPMO10A. SamLPMO10C and ShaLPMO10A were expressed in *E. coli* and *Streptomyces lividans,* and the yield of the active enzymes was evaluated. To our knowledge, this is the first time that a *Streptomyces* strain is used as a host for LPMO expression. Furthermore, both enzymes were characterized in terms of activity at different temperatures, and the effect they had on the molar mass of bacterial cellulose. Finally, real-time interaction between bacterial cellulose and the LPMOs by quartz crystal microbalance with dissipation (QCM-D) analysis was carried out for the first time.

MATERIALS AND METHODS

Substrates

Phosphoric acid swollen cellulose (PASC) was obtained from crystalline cellulose Avicel ® PH-101 (Fluka) treated with 70 % of H_3PO_4 according to Wood [20], using centrifugation for the sedimentation of the cellulose instead of decantation during the washing process.

Bacterial cellulose, hereinafter referred to as BC in this work, was produced from *Komagataeibacter intermedius* JF2 according to Fernández et al*. K. intermedius* JF2 cells were initially cultivated on Hestrin and Schramm (HS)-Agar. Then, the cells were transferred into HS liquid medium and subjected to vigorous shaking. The resulting cell suspension was then utilized to inoculate 10 cm Petri dishes, each containing 40 mL of HS liquid medium, at a dilution of 1:40. [21]

The Petri dishes were left to incubate under static conditions for a duration of 7 days, at room temperature.

Following the 7-day incubation period, cellulose membranes formed at the air/liquid interface of the Petri dishes. To remove any remnants of the culture medium, the membranes were thoroughly washed with distilled water.

Next, the washed membranes were subjected to an overnight incubation with 1% NaOH at 70 °C, aiming to eliminate the bacteria. After this incubation, further washing with distilled water was carried out until reaching a pH level of 7.

To obtain the bacterial cellulose pulp, the membranes underwent trituration using a blender (Philips HR3655- ProBlend 6) and were subsequently homogenized with a homogenizer system (CAT Unidrive x 1000).

LPMOs cloning and expression

In S. lividans

The ShaLPMO10A and SamLPMO10C encoding genes were cloned under the control of the *S. lividans pstS* promoter after several cloning steps. [22] The final plasmids originated were denominated pNUF21 and pNUF22 respectively and transferred to *Streptomyces lividans* 1326 by protoplast transformation. Cultures in liquid YE medium + 5% fructose + neomycin 20 μg/mL were done in 250 mL baffled flasks containing 50 mL of media. [22] Ten flasks were used for the culture of each construction and the final cultures were done during 48 hours at 28 ºC and 200 rpm. As a negative control one culture of *S. lividans* containing the plasmid pN702Gem3 (the cloning vector used in the construction of the pNUF21 and pNUF22 plasmids) was used.[23] The supernatant of the cultures was obtained by centrifugation (10.000 *g* 10 minutes) and filtered through a 0.22 μm filters. The production of the proteins was observed in a denaturing polyacrylamide gel by loading 10 μL directly (without precipitation).

In E. coli

SamLPMO10C, previously cloned and expressed in *E. coli* by Valenzuela et al.[19] was produced according to the authors´ indications. The enzyme production was scaled up in a 50 L bioreactor.

The ShaLPMO10A encoding gene, on the other hand, was PCR amplified and cloned in the pLATE11 vector following the instructions provided by the supplier (Thermo Scientific). *E coli* DH5α was transformed with the recombinant plasmid by the $CaCl_2$ method.[24] Successful constructs were sequence verified and transformed into *E. coli* BL21 star (DE3). Recombinant cells were cultured overnight at 37 °C, 200 rpm in two tubes containing 5 mL of LB medium. Then each tube was inoculated into shake flasks with 500 mL of LB. Finally, the precultures were transferred and grown in a 50 L LB bioreactor until $O.D._{600}$ between ~06 ~0.8 was reached. At this point, the culture was induced at 21 ºC overnight using 1 mM Isopropyl beta-D-1-thiogalactopyranoside (IPTG) as the final concentration. In each step, the medium contained 100 μg/mL ampicillin.

After cultivation, cell pellets were collected by centrifugation at 4 °C and resuspended in 1/10 of the initial volume with 50 mM Tris-HCl pH 7. Then, cells were lysed using PANDA GEA 2000 homogenizer at 800 bars. Cell debris was removed by centrifugation and the soluble extract was analyzed by sodium dodecyl sulfate-polyacrylamide gel electrophoresis (SDS-PAGE). Afterward, 10 mL of soluble extract was incubated with $CuCl_2$ at room temperature for 30 min in a 1:4 molar ratio (LPMO: $CuCl_2$). Then, to remove the excess copper, the copper-saturated soluble extract was desalted with a PD-10 desalting column (GE Healthcare) equilibrated with 20 mM MES and analyzed by SDS-PAGE. The rest of the soluble extract without copper was further purified (see below) and the soluble extract was stored at -20 °C until further analysis.

Purification by polysaccharide-binding assay

The homologous and heterologous enzymes were purified by affinity adsorption to Avicel described by Valenzuela et al. [19] The supernatant with purified enzyme was analyzed by sodium SDS-PAGE. After the purification, LPMOs were incubated with $CuCl_2$ at room temperature for 30 min in a 1:4 molar ratio (LPMO: $CuCl_2$). The enzymes were then concentrated by centrifugation using Amicon ® centrifugal filter devices. To remove the copper and glucose excess PD-10 desalting columns (GE Healthcare) equilibrated with 20 mM MES buffer (pH 5.5) were used. The resulting protein concentration was measured at 280 nm via a Nanodrop® 1000 spectrophotometer, and using the molecular weights of SamLPMO10C and ShaLPMO10A, which were determined to be 34.69 kDa and 38.24 kDa, respectively. Their extinction coefficients (ε) were calculated as 75.78 and 78.76, which, like the molecular weights, were calculated using the ExPASy ProtParam tool (https://web.expasy.org/protparam/). 50 mM Tris-HCl pH 7 was added, and enzymes were stored at -20 °C until further use.

Oxidation of cellulosic substrates

Oxidation reactions contained 1 mg/mL of the enzyme, 1% of cellulosic substrates (Phosphoric acid swollen cellulose, PASC hereinafter, or BC), 2 mM ascorbic acid (Alfa aesar chemicals) as an electron donor and 2 μM of hydrogen peroxide (ITW reagents). These last two were freshly prepared for each set of reactions. Before the addition of ascorbic acid and H_2O_2 the enzyme was incubated for 30 min with the substrate. All reactions were carried out with 50 mM acetate buffer (pH 6). PASC oxidation was carried out in 200 μL of reaction mixtures prepared in 1.5 mL microcentrifuge tubes in an Eppendorf Thermomixer at 900 rpm. BC oxidation was performed in 10 mL of reaction mixtures prepared in 50 mL falcon tubes under mild agitation conditions. Inactivation of the enzyme after the incubations were achieved by boiling them at 100 °C for 10 min.

Control reactions without ascorbic acid, as well as control reactions with the enzyme only added at the boiling step and without the enzyme were included. All reactions were performed in duplicates at least two times.

Activity analysis

For the initial confirmation of LPMO activity, soluble fractions generated in the degradation reactions at 50 °C were analyzed by matrix-assisted laser desorption/ionization-time of flight mass spectrometry (MALDI-TOF MS) for the analysis of oxidized products. Reaction samples (3 μL) were mixed with 7 μL of acetonitrile. 1 μL of this solution was mixed with 1 μL of matrix solution (10 mg/mL of 2,5-dihydroxybenzoic acid dissolved in acetonitrile-water [1:1, vol/vol], 0.1% [wt/vol] trifluoroacetic acid). 0.1 μL of the mixture was spotted in duplicated onto the MALDI-TOF MS plate and allowed to dry before the

analysis. Positive mass spectra were collected with a 4800 Plus MALDI TOF/TOF (ABSciex 2010) spectrometer with an Nd: YAG 200-Hz laser operated at 355 nm.

Quantification of the degradation of PASC by the LPMOs in the soluble fraction was analyzed at 40, 50, and 60 °C at 2, 6, 24, 48, and 72 h according to the method developed by Keller et al.[25] Briefly, after removing the insoluble substrate by centrifugation, 100 µL of the supernatant containing the LPMO-oxidized oligosaccharides were overnight incubated with 5 U/mL of β-glucosidase from *Aspergillus niger* (Megazyme) in 50 mM citrate buffer (pH5) in a 200 µL final volume. The reaction was stopped by ebullition for 5 min. This way, the β-glucosidase hydrolyzed the oxidized oligosaccharides to glucose and gluconic acid. The last one was quantified using the Gluconic acid assay kit from Megazyme. Supernatants from oxidation reactions with the enzyme added at the boiling step were used as blanks.

High-performance size-exclusion chromatography coupled with multi-angle laser light scattering, viscometry, and refractive index detection (HPSEC-MALLS-VS-RI)

Molar mass determination of cellulose chains was determined as previously described. [26] Briefly, 40 mg of the freeze-dried BC and LPMOs-oxidized BC were filtered over sinter glass (porosity 16 - 40 µm) and then redispersed in anhydrous methanol (3 × 20 mL) followed by redispersion in anhydrous dimethylacetamide (3 × 20 mL). Then the DMAc-swollen fibers were added to 6 mL of DMAc/LiCl (9 % w/w) under magnetic string for 7 days at room temperature before 10-fold dilution with anhydrous DMAc. The solution was then filtered (PTFE 0.45 µm) and injected on a size exclusion chromatography system (OMNISEC Resolve, Malvern) with DMAc/LiCl (0.9 % w/v) as the eluent. The SEC columns used were Viscotek Tguard, LT4000L, LT5000L, and LT7000L. The system was equipped with a multi-angle laser light scattering Malvern SEC-MALS 20 and OMNISEC Reveal devices (Malvern). Calculations were performed with a dn/dc value of 0.136 mL/g and performed using OMNISEC software.

Quartz crystal microbalance with dissipation (QCM-D)

Gold-coated quartz crystals were cleaned in piranha solution H_2SO_4/H_2O_2 (7:3, v/v), rinsed exhaustively with Milli-Q water, and dried under a stream of nitrogen. BC surfaces were prepared by spin-coating. 500 µL from a 0.01 % BC dispersion was dropped on a pre-coated substrate with poly (allylamine hydrochloride) (PAH) dissolved in water and, after 10 min of adsorption, accelerated at 180 rpm to 3600 rpm for 60 s.

The QCM-D measurements were performed with a Q-Sense E4 instrument (AB, Sweden) using a piezoelectric AT-cut quartz crystal coated with gold electrodes on each side (QSX301, Q-Sense). All measurements were carried out at 40 °C using the QCM flow cell modules. The gold-coated crystals were excited through a driving voltage applied across the gold electrodes at its fundamental frequency (f_0 = 5

MHz) as well as at the 3rd, 5th, 7th, and 9th overtones (n = 3, 5, 7, and 9 respectively) corresponding to 15, 25, 35, and 45, MHz, respectively.

A baseline was first established by continuously flowing 50 mM Tris-HCl buffer (pH7) on the quartz crystal surface, then the frequency and dissipation signals were offset to zero just before injection of the LPMO in a continuous mode at a flow rate of 0.1 mL/min for 5 min. 30 min later, 2 mM ascorbic acid was injected at 0.1 mL/min into the QCM-D for 10 minutes. Data was collected overnight, then, a rinsing step of the surface with 50 mM Tris-HCl (pH 7) buffer was carried out at 0.1 mL/min for one hour. QCM-D experiments were carried out in duplicates at least twice.

RESULTS AND DISCUSSION

Primary analysis

Sequence analysis showed that SamLPMO10C and ShaLPMO10A are bimodular enzymes comprised of a catalytic AA10 domain and a carbohydrate-binding module of family CBM2. Figure 1A, B shows the 3D structure of the enzymes generated by AlphaFold2.[27] Pairwise sequence alignment indicated that the overall sequence identity and similarity between both enzymes were 76 % and 84 %, respectively. The predicted pI and molecular weight of the enzymes calculated using the ExPASy ProtParam tool (https://web.expasy.org/protparam/) are shown in Figure 1C.

Expression and verification of activity

Heterologous and homologous expression of SamLPMO10C and ShaLPMO10A were performed in *E. coli,* and *S. lividans*, respectively. Heterologous SamLPMO10C cloning and expression steps had been published elsewhere [19] and in this work is referred to as EC_SamLPMO10C. To obtain high expression of the heterologous LPMOs, and similarly to the expression strategy used previously, ShaLPMO10A encoding gene was cloned under the control of the strong T7 promoter in a pLATE vector and expressed in *E. coli* BL21 star (DE3). Heterologous ShaLPMO10A is referred to as EC_ShaLPMO10A. Constructs expressed the native enzymes including their signal peptide, without adding any tag. Both enzymes were obtained from the periplasm in soluble form and analyzed by sodium dodecyl sulfate-polyacrylamide gel electrophoresis (SDS-PAGE). A significant protein band was observed in the lysates of cells corresponding to the theoretical molecular weight SamLPMO10C and ShaLPMO10A (data not shown).

A)

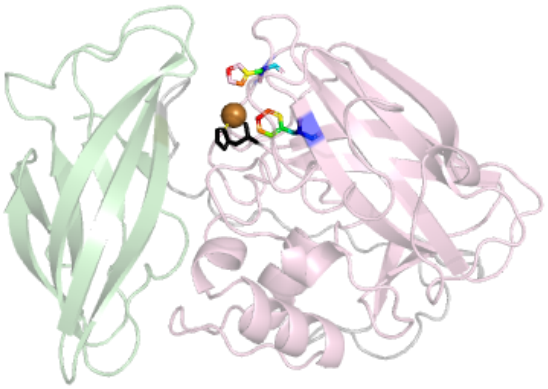

B)

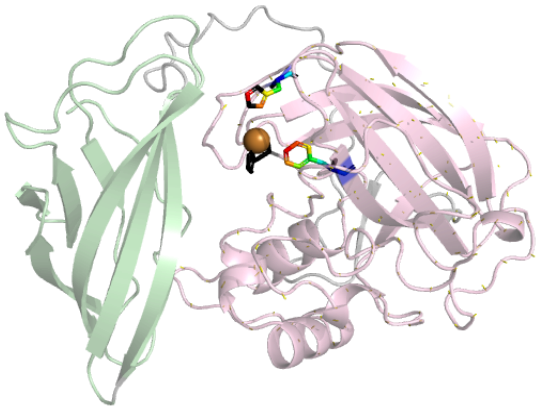

C)

Enzyme	Protein features				
	Size (AA)	pI	MW (kDa)	Substrate	Oxidation mechanism
SamLPMO10C*	364	5.03	34.69	Cellulose	C1
ShaLPMO10A	365	5.95	38.29	Cellulose	C1

Figure 1. A) Cartoon representation of SamLPMO10C and B) ShaLPMO10A using AlphaFold2. The enzymes are displayed in complex with copper. Catalytic N-terminal histidine residues are represented by black sticks, while the other two possible catalytic amino acids (histidine and phenylalanine) are shown in colored sticks. These residues are in the catalytic domain within 4 Å of their respective metal ions (measured by using PyMOL). The catalytic domains are depicted in pink, the CBM2 domains are displayed in green, and the linkers are in gray. The Predicted Aligned Error (PAE) plot is shown in S1. C) Features of the enzymes. * Extracted from Valenzuela et. al. [19]

After the successful expression of the enzymes, each cell lysate containing the unpurified enzyme was charged with copper, and its activity was verified by MALDI TOF using PASC as substrate under standard conditions. In the case of EC_SamLPMO10C, peaks corresponding to oxidized cello-oligosaccharides of 4 and 7 degrees of polymerization (DP) were found confirming that this enzyme has a C1-oxidation pattern.[19] Secondly, EC_ShaLPMO10A, characterized for the first time in this work generated C1-oxidized soluble products of 3 - 6 DP (Figure S2).

For the homologous expression, SamLPMO10C and ShaLPMO10A encoding genes were expressed in *S. lividans* and they are referred to as SL_SamLPMO10C and SL_ShaLPMO10A. The culture supernatants of the recombinant strains were harvested at 48 hours to avoid protein processing [15] and analyzed by SDS-PAGE. Prominent bands around 40 kDa, corresponding to the apparent molecular masses of SL_SamLPMO10C and SL_ShaLPMO10A, were observed in the supernatants (Figure S3). The oxidative activity of the homologous expressed LPMOs was evaluated on PASC. MALDI TOF analysis showed peaks corresponding to oxidized oligosaccharides confirming that both enzymes were active on this cellulose (Figure S3). Expression of the recombinant LPMOs in *S. lividans* yielded the

secretion of these enzymes to the extracellular media, a characteristic of the producing host that avoids the step of cell lysis in recombinant protein production. In addition, the supernatants containing the enzymes were embedded with a few proteins, so depending on future applications, the purification step may be avoided.

A binding assay of both enzymes to PASC and bacterial cellulose (crystalline cellulose) was also performed to evaluate the cellulose-binding ability of SamLPMO10C and ShaLPMO10A (Figure S4). This property had been used previously to purify SamLPMO10C by affinity adsorption to Avicel.[19] In this work, it proved to be suitable for ShaLPMO10A as well, when expressed in *E. coli*. However, it was less efficient to purify the LPMOs from *Streptomyces* supernatants. Purified or partially purified enzymes were concentrated and then analyzed by SDS PAGE (Figure 2).

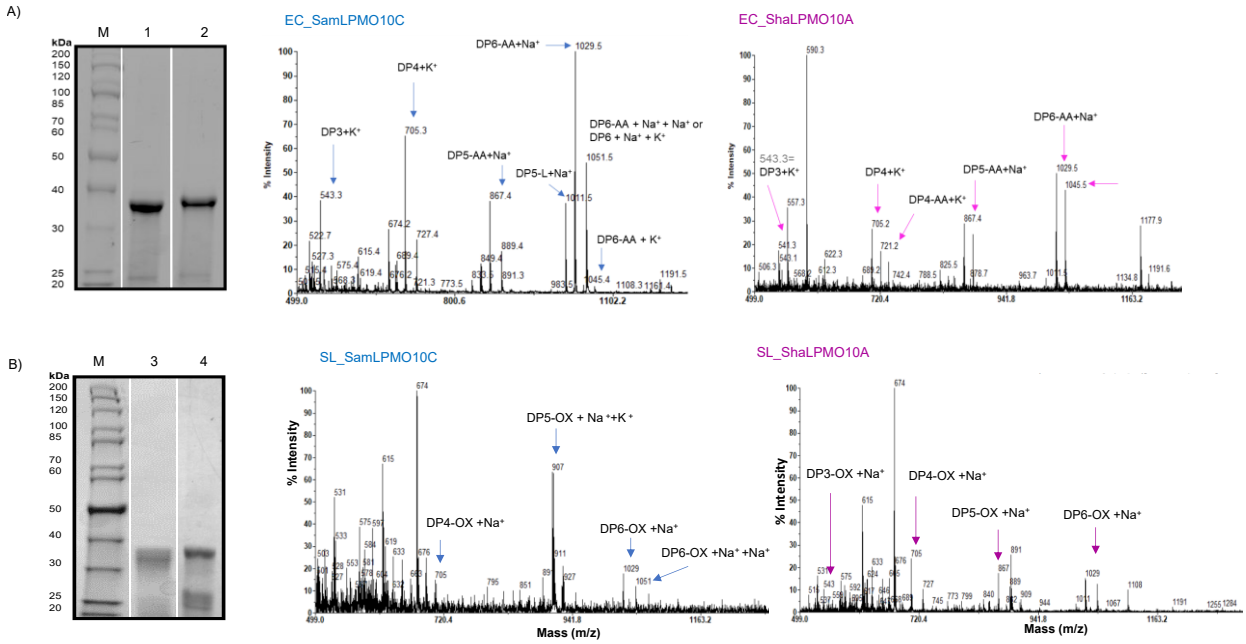

Figure 2. SDS-PAGE analysis representing: A) purified EC_SamLPMO10C (lane 1), and EC_ShaLPMO10A (lane 2) expressed in *E. coli*. B) partially purified SL_SamLPMO10C (lane 3) and SL_ShaLPMO10A (lane 4) expressed in *S. lividans.* The molecular mass ladder is shown as lane "M". The spectra next to the SDS-PAGE show MALDI-TOF MS analysis of products generated by purified A) EC_SamLPMO10C (left), EC_ShaLPMO10A (right). B) SL_SamLPMO10C (left), and SL_ShaLPMO10A (right).

The activity of purified enzymes on PASC was evaluated. The analysis showed that homologous and heterologous SamLPMO10C generated peaks corresponding to oxidized cello-oligosaccharides of DP 3 - 6 (Figure 2A). On the other hand, homologous and heterologous ShaLPMO10A, generated C1-oxidized soluble products of DP 3 - 6 (Figure 2B). The activity of both purified enzymes without removing the copper excess was also verified producing similar spectra (data not shown).

The yield for the heterologous enzyme EC_SamLPMO10C was 6 mg per liter of culture and for EC_ShaLPMO10A, 8 mg per liter of culture, which is in the same yield range when expressing others LPMOs in *E. coli*.[28,29] Meanwhile, the yield for the homologous expression, SL_SamLPMO10C was 125 mg per culture liter, and for SL_ShaLPMO10A was 90 mg per liter of culture, this is 21 and 11 times more than their heterologous counterpart showing that the homologous expression yielded a higher amount of active enzymes than traditional *E. coli* system. High levels of protein expression in *S. lividans* had been reported in other works and evidenced this strain as a promising expression system.[30–31] These high levels of active LPMOs produced by *Streptomyces* make this strain an interesting candidate to produce these enzymes and other commercially valuable biomolecules. Furthermore, this methodology reduces time and costs in comparison to conventional processes and the elimination of the purification step would simplify the production of enzymes and other biomolecules.

Purified EC_SamLPMO10C and EC_ShaLPMO10A were used for the rest of the analysis performed. To simplify the text, they were named SamLPMO10C and ShaLPMO10A in the following experiments.

The effect of temperature

To study the effect of temperature on the LPMOs´ activity, product formation from PASC was monitored over time at different incubation temperatures (Figure 3). To quantify oxidative cleavage of SamLPMO10C and ShaLPMO10A, the soluble oxidized cello-oligosaccharides released from PASC were followingly hydrolyzed by a β-glucosidase to glucose and gluconic acid. Afterwards, the gluconic acid generated was measured.

For SamLPMO10C there was product formation after 2 h of reaction at all temperatures assayed. At 40 °C, the formation of oxidized products increased gradually up to 24 h (125±6 mg/L) and then leveled out. At 50 and 60 °C there was a sharp increase in the first 6 hours of incubation (109±0.4, and 91±12 mg/L respectively), and then product formation stabilized. For ShaLPMO10A on the other hand, the effect of temperature on the enzyme´s activity was even more noteworthy. At all the temperatures tested the product formation was delayed but then reached higher levels. Maximal production was obtained in 24 h at 40 °C (233±19 mg/L). The overall yield of product formation was higher for ShaLPMO10A, nevertheless, both LPMOs showed to function in a wide range of temperatures, which can be useful in biorefineries and other industrial applications.[32–36]

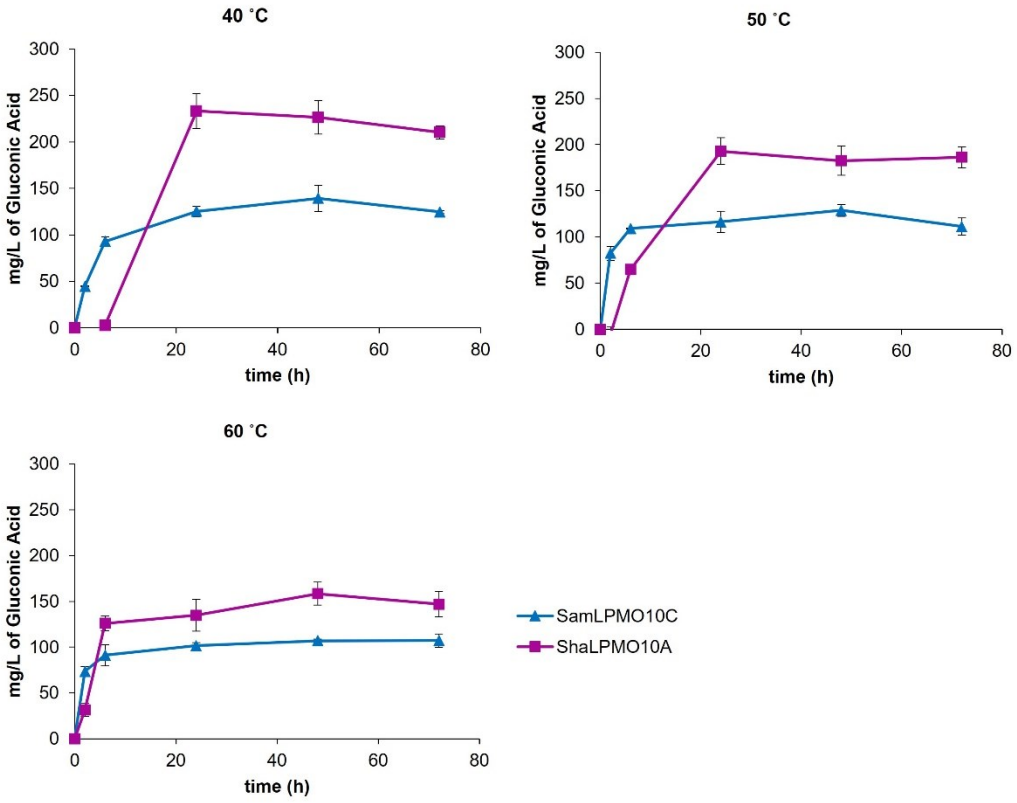

Figure 3. Activity of SamLPMO10C (blue curve) and ShaLPMO10A (magenta curve) at different temperatures. The graphs show progress curves for the degradation of 1% PASC in the presence of 2 mM ascorbic acid, and 2 μM H_2O_2 in 50 mM ammonium acetate buffer (pH 6). The reactions were carried out in Eppendorf Thermomixers at 900 rpm. Control reactions without ascorbic acid did not generate Gluconic acid.

Activity on bacterial cellulose

BC is a promising nanomaterial with extraordinary properties for its applications in technology and life sciences.[37] Recent reports show the effectiveness of SamLPMO10C in the production of nanomaterials from BC.[38] Continuing the search for BC-active LPMOs and understanding the effect they have on their substrate is of particular interest. For this reason, the activity of the two LPMOs on BC was thoroughly studied. The formation of oxidized cello-oligosaccharides from BC at 40 °C was monitored over 48 h. Both enzymes released reaction products gradually, but SamLPMO10C yielded more soluble oxidized cellooligosaccharides than ShaLPMO10A (Figure 4). The results suggest that the activity of the LPMOs depends on the substrate. While the amount of reaction products from PASC was higher for ShaLPMO10A, for BC, SamLPMO10C released a larger amount of soluble products.

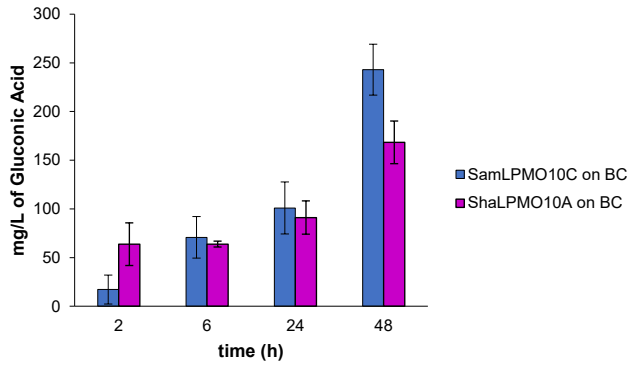

Figure 4. Activity of SamLPMO10C (blue) and ShaLPMO10A (magenta) on BC. Control reactions without ascorbic acid did not generate Gluconic acid.

High-performance size exclusion chromatography (HPSEC) coupled with multi-angle laser light scattering detection (MALLS) analysis of untreated and LPMO-treated bacterial cellulose

To further study the effect of SamLPMO10C and ShaLPMO10A on BC, the insoluble fraction of the LPMOs reactions on this substrate was analyzed by HPSEC-MALLS. Figure 5 shows the elution patterns of BC oxidized by SamLPMO10C and ShaLPMO10A, respectively. As the enzymatic reaction time increases, the elution patterns of oxidized BC changed little but they shifted slightly to higher retention volumes, suggesting that the enzymes caused partial depolymerization of cellulose chains.

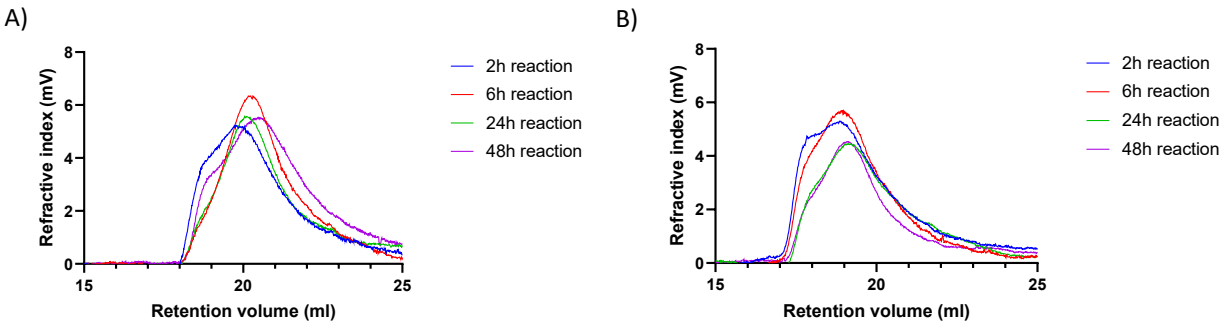

Figure 5. SEC-Elution patterns for bacterial cellulose oxidized at different incubation times (2, 6, 24, and 48 hours) by A) SamLPMO10C and B) ShaLPMO10A. Replicates and controls are attached in Figure S5.

To get more insight into the effect of LPMOs on bacterial cellulose´s molar mass, the M_w (weight average molar mass) and M_n (number average molar mass) of BC oxidized by LPMOs at different incubation times

were calculated. A wide range of BC´s molar mass can be found in the literature depending on the culture conditions and on the BC strain producer.[39,40] The results for M_w and M_n for the untreated BC used in this work were 897 ± 31 10^3 g/mol and 615 ± 43 10^3 g/mol, respectively. When BC was treated with SamLPMO10C or ShaLPMO10A, the cellulose chains´ length, expressed as M_w and M_n, decreased gradually after six hours of reaction (Figure 6 and 7). On the other hand, controls where the reducing agent was not added, controls where the enzyme was not added, and controls where the enzyme was added at the end of the incubation did not show substantial changes. All the values from the graph, including the controls with the added enzyme at the end of the incubation, which were not included in the graph for simplification, can be found in Figure S6. Earlier work showed that LPMOs create nicking points in the cellulose, therefore, weakening the cohesion of the cellulose architecture [41]. In our study, this effect may occur in the first hours of enzymatic action where little activity was quantified. Subsequently, the cleavage of cellulose chains increased over time, which is reflected in the reduction of M_w and M_n at the later phase of the reaction.

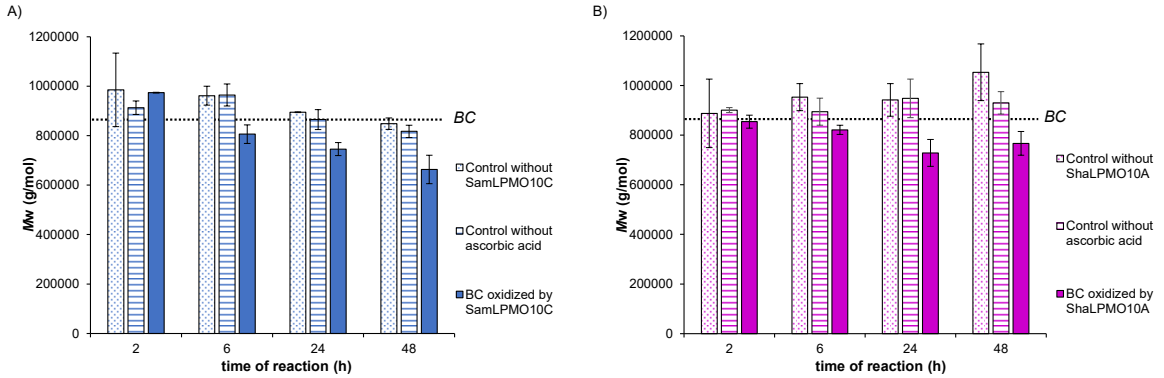

Figure 6. Weight average molar mass (*M*w) for BC treated with A) SamLPM10C and, B) ShaLPMO10A at 2, 6, 24, and 48 hours of reaction. Controls without the enzyme are represented with dotted bars and controls without ascorbic acid are represented with stripped bars. The dashed line corresponds to BC.

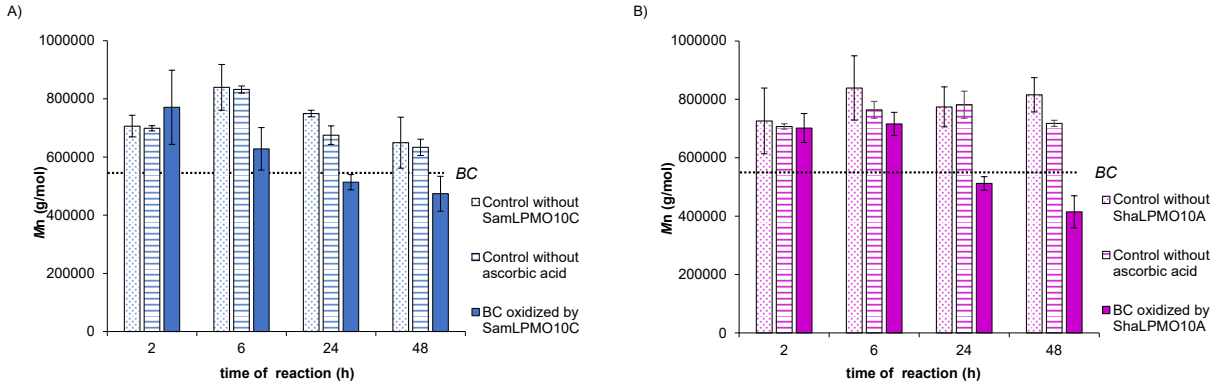

Figure 7. Number of average molar mass (*M*n) for BC treated with A) SamLPM10C and, B) ShaLPMO10A at 2, 6, 24, and 48 hours of reaction. Controls without the enzyme are represented with dotted bars and controls without ascorbic acid are represented with stripped bars. The dashed line corresponds to BC.

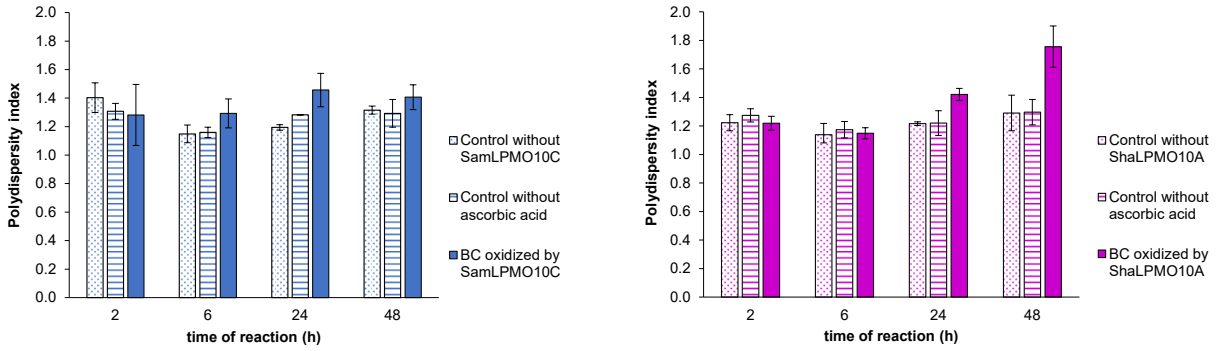

Figure 8. Polydispersity index (*M*w/*M*n)

The action of ShaLPMO10A on BC seemed to have more impact on M_n compared to SamLPMO10C. This was reflected by the increase of the polydispersity index (M_w/M_n), with reaction time, especially in BC oxidized by ShaLPMO10A (Figure 8). The high polydispersity could suggest a more "random" cleavage of cellulose chains.

Analysis of LPMO-cellulose interaction by quartz crystal microbalance with dissipation (QCM-D)

In order to give more insight into the mechanism of action of LPMO enzymes, their interaction with cellulose was assessed in real-time using a QCM-D. By monitoring changes in the resonance frequency ($\Delta f_n/n$) this method provides information about small mass changes. Thus, an increase in frequency indicates mass removal meanwhile the decrease in frequency shows mass uptake (adsorption or binding of molecules to the surface). Dissipation changes (ΔD_n) give information about the energy loss in the system: when the dissipation increases, the rigidity of the surface sensor decreases; meanwhile, when the dissipation decreases, the rigidity of the surface sensor increases.

Figure 9 shows the changes in frequency and dissipation signals during the analysis conducted with ShaLPMO10A (controls are attached in Figure S7). The results with this enzyme are shown as it yielded the most notable changes. The results obtained with SamLPMO10C are provided in Figure S8. The injection of ShaLPMO10A on the BC-coated gold sensors caused a sharp decrease in frequencies and increased dissipations (Figure 9B) indicating the adsorption of the enzyme onto the hydrated bacterial

cellulose. When the ascorbic acid was incorporated (Figure 9B) a small decline of frequencies and an increment of dissipations were noticed. Nonetheless, immediately, a gradual increase of frequencies was observed suggesting mass loss due to the enzyme activity. On the other hand, dissipation decreased which means the rigidity of surface increased. Note that these changes continued during the whole analysis but slowed down at approximately 70 minutes of analysis. The removal of cellulose by ShaLPMO10A action could result in stronger interaction between the remaining cellulose chains, and the subsequent release of water, which may increase the rigidity of the cellulose layer. Selig et al. found similar behavior for *Sc*LPMO10C, in this case, the mass loss stopped after one hour. [42] As a final step, rinsing with buffer for one hour was carried out (Figure 9A): the slight increase in frequencies and the small decrease in dissipations can be attributed to the removal of cellulose chains that were cut from the BC and remained loosely attached to its surface. Negative controls where no enzyme was injected (Figure S7), behaved differently, in this case when ascorbic acid was injected, frequencies increased, and dissipations decreased sharply and not gradually as in the sample with the LPMO. Additionally, with the rinsing step at the end of the analysis, the initial conditions were almost reached. Furthermore, the separation of frequency and dissipation overtones when the enzyme was injected (Figure S9) showed a different pattern compared to the corresponding control with no enzyme (Figure S7), suggesting that the changes observed could be due to the enzymatic activity.

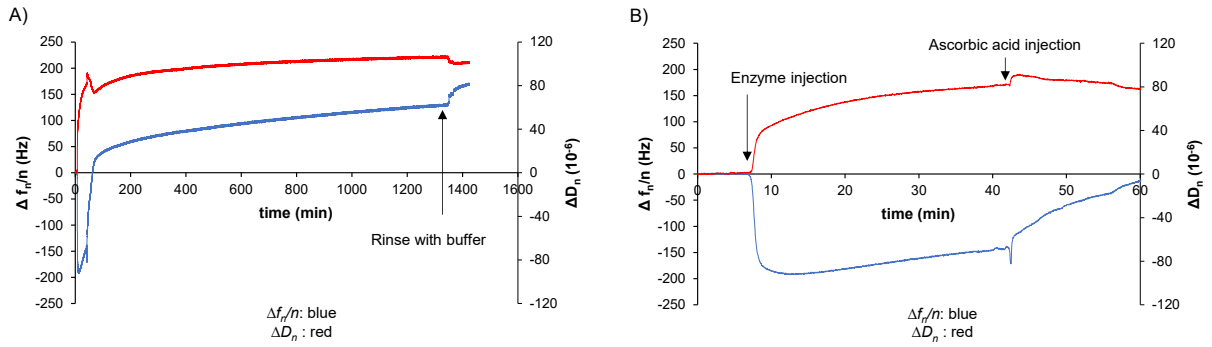

Figure 9. Frequencies ($\Delta f_n/n$) and dissipation (ΔD_n) changes for the overtone number $n = 3$ in the interaction among ShaLPMO10A and ascorbic acid with bacterial cellulose B) represents the first 60 minutes of the analysis. Controls are attached in Figure S7.

The buffer used in the rinsing elution from QCM-D experiments was collected for oxidized oligosaccharides screening by MALDI TOF. In the case of BC treated with ShaLPMO10A, no oxidized oligosaccharides were found (data not shown). SamLPMO10C interaction with BC analysis by QCM-D analysis results are attached in Figure S10 and in the rinse buffer, on the contrary to ShaLPMO10A results, soluble products of 4 and 5 DP were found. This suggests that the "random" cleavages induced

by ShaLPMO10A, as proposed in the preceding section, likely lead to the production of longer chains that are not detectable through MALDI-TOF when investigating the interaction between BC and the enzyme by QCM-D analysis.

All these results taken together suggest that SamLPMO10C and ShaLPMO10C, although similar in amino acid sequence, differ in terms of their preferences for substrates, SamLPMO10C is more active on BC and ShaLPMO10A on PASC, they also differ on the effect on the cellulosic chain, ShaLPMO10A generates more ¨random¨ cuts than SamLPMO10C, and, finally, the enzyme-substrate interaction is different for both enzymes.

CONCLUSIONS

In this work, two functional LPMOs from the AA10 family, SamLPMO10C and ShaLPMO10A, were expressed successfully in *E. coli* and *S. lividans*. The high levels of expression performed by *S. lividans* make this system an excellent candidate to express active LPMOs. The wide range of temperatures where these enzymes can act is interesting for sustainable applications in the industry where the operating conditions can vary. Insights on the effect of the LPMOs on BC´s chain length revealed that these enzymes decreased BC´s molar mass. Real-time analysis performed in this work gave more insights into the interaction between BC and LPMOs. Further studies on the real-time interaction between LPMOs and cellulose, as well as other substrates, can provide valuable insights into the mechanisms underlying the action of these enzymes. This, in turn, can facilitate the optimization of reaction conditions and lead to a reduction in costs, thereby expanding the potential range of applications for LPMOs.

ASSOCIATED CONTENT

SI Supporting information

MMSeqs2 multiple alignment results run on SamLPMO10C and ShaLPMO10A; Verification of unpurified heterologous LPMOs activity (MALDI-TOF MS spectra); SDS-PAGE analysis representing *Streptomyces lividans* supernatant containing SL_SamLPMO10C, and SL_ShaLPMO10A; Cellulose binding capacity of SamLPMO10C and ShaLPMO10A analyzed by SDS-PAGE; SEC-Elution patterns for bacterial cellulose oxidized by SamLPMO10C and ShaLPMO10A; Weight average molar mass (Mw), number average molar mass (Mn), polydispersity and yields of BC treated with SamLPMO10C and ShaLPMO10A; Frequencies ($\Delta f_n/n$) and dissipation (ΔD_n) changes of the control analyzed by QCM-D; Frequencies ($\Delta f_n/n$) and dissipation (ΔD_n) changes in the interaction among SamLPMO10C and ascorbic acid with bacterial cellulose; Frequencies ($\Delta f_n/n$) and dissipation (ΔD_n) changes in the interaction among ShaLPMO10A and

ascorbic acid with bacterial cellulose; MALDI-TOF MS spectra of soluble products (cello-oligosaccharides aldonic acids) generated by SamLPMO10C during the QCM-D experiments.

AUTHORS INFORMATION

Corresponding author

Susana V. Valenzuela - *Department of Genetics, Microbiology, and Statistics, Faculty of Biology, Universitat de Barcelona, Av. Diagonal 643, 08028, Barcelona, Spain, and Institute of Nanoscience and Nanotechnology (IN²UB), Universitat de Barcelona, Spain; orcid.org/0000-0002-1684-9514; Email: susanavalenzuela@ub.edu*

Authors

L. Verónica Cabañas-Romero - *Department of Genetics, Microbiology, and Statistics, Faculty of Biology, Universitat de Barcelona, Av. Diagonal 643, 08028, Barcelona, Spain, and Institute of Nanoscience and Nanotechnology (IN²UB), Universitat de Barcelona, Spain; orcid.org/0000-0001-7512-8779; Email: veronica.cabanas@ub.edu*

Carolina Buruaga-Ramiro- *Department of Genetics, Microbiology, and Statistics, Faculty of Biology, Universitat de Barcelona, Av. Diagonal 643, 08028, Barcelona, Spain, and Institute of Nanoscience and Nanotechnology (IN²UB), Universitat de Barcelona, Spain; orcid.org/0000-0002-0187-1399; Email: carolburuaga@gmail.com*

F.I. Javier Pastor- *Department of Genetics, Microbiology, and Statistics, Faculty of Biology, Universitat de Barcelona, Av. Diagonal 643, 08028, Barcelona, Spain, and Institute of Nanoscience and Nanotechnology (IN²UB), Universitat de Barcelona, Spain; orcid.org/0000-0003-0326-2527; Email: fpastor@ub.edu*

Ana Villares-*UR1268 BIA, INRAE, F-44316 Nantes, France; orcid.org/0000-0001-5441-7299; Email: ana.villares@inrae.fr*

Margaux Grellier-*UR1268 BIA, INRAE, F-44316 Nantes, France; Email: margaux.grellier@inrae.fr*

Ramón I. Santamaría-*Instituto de Biología Funcional y Genómica (IBFG)/Departamento de Microbiología y Genética. Consejo Superior de Investigaciones Científicas (CSIC)/Universidad de Salamanca (USAL), C/ Zacarías González, nº 2, 37007-Salamanca, Spain; orcid.org/0000-0002-2181-6776; Email: santa@usal.es*

Margarita Díaz-*Instituto de Biología Funcional y Genómica (IBFG)/Departamento de Microbiología y Genética. Consejo Superior de Investigaciones Científicas (CSIC)/Universidad de Salamanca (USAL), C/ Zacarías González, nº 2, 37007-Salamanca, Spain; orcid.org/0000-0003-4286-1506; Email: mardi@usal.es*

Authors´ contributions

LVCR: took part in planning the study, conducted most of the experimental work, analyzed data, and drafted the manuscript. CBR and JM: contributed to data interpretation and edited the manuscript. FIJP: acquired funding and edited the manuscript. AV: participated in planning the HPSEC-MALLS and QCM-D experiments, contributed to data interpretation, and edited the manuscript. MG: participated in planning and performed the HPSEC-MALLS experiments, contributed to data interpretation, and edited the manuscript. MD and RIS: conducted cloning and homologous expression of the enzymes and edited the manuscript. SV: supervised the experiments, checked the results, and revised the manuscript. All authors read and approved the final manuscript.

Notes

The authors declare no competing financial interest.

FUNDING STATEMENT

This work was supported by Scientific and Technological Research Council (MINECO, Spain), grant CTQ2017-84966-C2-2-R. L. Verónica Cabañas-Romero acknowledges a doctoral fellowship from Programa Nacional de Becas de Posgrado en el Exterior “Don Carlos Antonio López” from Ministry of Finance of Paraguay.

ACKNOWLEDGMENTS

We thank the Fermentation service from the University of Barcelona for technical support in the production of the enzymes in the 50 L bioreactor.

REFERENCES

(1) Himmel, M. E.; Ding, S. Y.; Johnson, D. K.; Adney, W. S.; Nimlos, M. R.; Brady, J. W.; Foust, T. D. Biomass Recalcitrance: Engineering Plants and Enzymes for Biofuels Production. *Science* **2007**, *315*, 804-807.

(2) McCann, M. C.; Carpita, N. C. Biomass Recalcitrance: A multi-scale, multi-factor, and conversion-specific property. *J Exp Bot* **2015**, *66* (14), 4109–4118.

(3) Vaaje-Kolstad, G.; Westereng, B.; Horn, S. J.; Liu, Z.; Zhai, H.; Sørlie, M.; Eijsink, V. G. H. An Oxidative Enzyme Boosting the Enzymatic Conversion of Recalcitrant Polysaccharides. *Science* **2010**, *330* (6001), 219–222.

(4) Vaaje-Kolstad, G.; Forsberg, Z.; Loose, J. S.; Bissaro, B.; Eijsink, V. G. Structural diversity of lytic polysaccharide monooxygenases. *Curr. Opin. Struct. Biol*. **2017**, *44*, 67–76.

(5) Aachmann, F. L.; Sørlie, M.; Skjåk-Bræk, G.; Eijsink, V. G. H.; Vaaje-Kolstad, G. NMR structure of a lytic polysaccharide monooxygenase provides insight into copper binding, protein dynamics, and substrate interactions. *Proc. Natl. Acad. Sci. U. S. A.* **2012**, *109* (46), 18779–18784.

(6) Quinlan, R. J.; Sweeney, M. D.; Lo Leggio, L.; Otten, H.; Poulsen, J.-C. N.; Johansen, K. S.; Krogh, K. B. R. M.; Jørgensen, C. I.; Tovborg, M.; Anthonsen, A.; Tryfona, T.; Walter, C. P.; Dupree, P.; Xu, F.; Davies, G. J.; Walton, P. H. Insights into the oxidative degradation of cellulose by a copper metalloenzyme that exploits biomass components. *Proc. Natl. Acad. Sci. U.S.A.* **2011**, *108* (37), 15079–15084.

(7) Forsberg, Z.; Vaaje-Kolstad, G.; Westereng, B.; Bunaes, A. C.; Stenstrøm, Y.; MacKenzie, A.; Sørlie, M.; Horn, S. J.; Eijsink, V. G. H. Cleavage of cellulose by a CBM33 protein. *Protein Sci.* **2011**, *20* (9), 1479–1483.

(8) Cannella, D.; Möllers, K. B.; Frigaard, N.-U.; Jensen, P. E.; Bjerrum, M. J.; Johansen, K. S.; Felby, C. Light-driven oxidation of polysaccharides by photosynthetic pigments and a metalloenzyme. *Nat. Commun.* **2016**, *7* (1), 11134.

(9) Kracher, D.; Scheiblbrandner, S.; Felice, A. K. G.; Breslmayr, E.; Preims, M.; Ludwicka, K.; Haltrich, D.; Eijsink, V. G. H.; Ludwig, R. Extracellular electron transfer systems fuel cellulose oxidative degradation. *Science* **2016**, *352* (6289), 1098–1102.

(10) Eijsink, V. G. H.; Petrovic, D.; Forsberg, Z.; Mekasha, S.; Røhr, Å. K.; Várnai, A.; Bissaro, B.; Vaaje-Kolstad, G. On the functional characterization of lytic polysaccharide monooxygenases (LPMOs). *Biotechnol. Biofuels* **2019**, *12* (1), 58.

(11) Bissaro, B.; Eijsink, V. G. H. Lytic polysaccharide monooxygenases: enzymes for controlled and site-specific Fenton-like chemistry. *Essays Biochem.* **2023**, *67* (3), 575-584

(12) Drula, E.; Garron, M.-L.; Dogan, S.; Lombard, V.; Henrissat, B.; Terrapon, N. The carbohydrate-active enzyme database: functions and literature. *Nucleic Acids Res* **2022**, *50* (D1), D571–D577.

(13) Pinheiro, G. L.; de Azevedo-Martins, A. C.; Albano, R. M.; de Souza, W.; Frases, S. Comprehensive analysis of the cellulolytic system reveals its potential for deconstruction of lignocellulosic biomass in a novel *Streptomyces sp*. *Appl. Microbiol. Biotechnol. 2017*, *101* (1), 301–319.

(14) Kirby, R. *Actinomycetes* and lignin degradation. *Adv. Appl. Microbiol.* **2005**, *58* (5), 125–168.

(15) Garda, A. L.; Fernández-Abalos, J. M.; Sánchez, P.; Ruiz-Arribas, A.; Santamaría, R. I. Two genes encoding an endoglucanase and a cellulose-binding protein are clustered and co-regulated by a TTA codon in *Streptomyces halstedii* JM8. *Biochem. Journal* **1997**, *324* (2), 403–411.

(16) Russo, D. A.; Zedler, J. A. Z.; Wittmann, D. N.; Möllers, B.; Singh, R. K.; Batth, T. S.; van Oort, B.; Olsen, J. V.; Bjerrum, M. J.; Jensen, P. E. Expression and secretion of a lytic polysaccharide monooxygenase by a fast-growing cyanobacterium. *Biotechnol. Biofuels* **2019**, *12* (1), 1-13.

(17) Yu, M. J.; Yoon, S. H.; Kim, Y. W. Overproduction and Characterization of a Lytic Polysaccharide Monooxygenase in *Bacillus subtilis* Using an Assay Based on Ascorbate Consumption. *Enzyme Microb. Technol.* **2016**, *93–94*, 150–156.

(18) Sevillano, L.; Díaz, M.; Santamaría, R. I. Development of an antibiotic marker-free platform for heterologous protein production in *Streptomyces*. *Microb. Cell Factories* **2017**, *16* (1), 1-13.

(19) Valenzuela, S. V.; Ferreres, G.; Margalef, G.; Pastor, F. I. J. Fast purification method of functional LPMOs from *Streptomyces ambofaciens* by affinity adsorption. *Carbohydr. Res.* **2017**, *448*, 205–211.

(20) Wood, T. M. Preparation of crystalline, amorphous, and dyed cellulase substrates. *Methods Enzymol.* **1988**, *160* (C), 19–25.

(21) Fernández, J.; Morena, A. G.; Valenzuela, S. V.; Pastor, F. I. J.; Díaz, P.; Martínez, J. Microbial Cellulose from a *Komagataeibacter intermedius* Strain Isolated from Commercial Wine Vinegar. *J. Polym. Environ.* **2019**, *27* (5), 956–967.

(22) Díaz, M.; Esteban, A.; Fernández-Abalos, J. M.; Santamaría, R. I. The high-affinity phosphate-binding protein PstS is accumulated under high fructose concentrations and mutation of the corresponding gene affects differentiation in *Streptomyces lividans*. *Microbiology* **2005**, *151* (8), 2583–2592.

(23) Fernández-Abalos, J. M.; Reviejo, V.; Díaz, M.; Rodríguez, S.; Leal, F.; Santamaría, R. I. Posttranslational processing of the xylanase Xys1L from *Streptomyces halstedii* JM8 is carried out by secreted serine proteases. *Microbiology* **2003**, *149* (7), 1623–1632.

(24) Cohen, S. N.; Chang, A. C. Y.; Hsu, L. Nonchromosomal Antibiotic Resistance in Bacteria: Genetic Transformation of *Escherichia coli* by R-Factor DNA. *Proceedings of the National Academy of Sciences* **1972**, *69* (8), 2110–2114.

(25) Keller, M. B.; Felby, C.; Labate, C. A.; Pellegrini, V. O. A.; Higasi, P.; Singh, R. K.; Polikarpov, I.; Blossom, B. M. A Simple enzymatic assay for the quantification of C1-specific cellulose oxidation by lytic polysaccharide monooxygenases. *Biotechnol. Lett.* **2020**, *42* (1), 93–102.

(26) Moreau, C.; Tapin-Lingua, S.; Grisel, S.; Gimbert, I.; Le Gall, S.; Meyer, V.; Petit-Conil, M.; Berrin, J.-G.; Cathala, B.; Villares, A. Lytic polysaccharide monooxygenases (LPMOs) facilitate cellulose nanofibrils production. *Biotechnol. Biofuels* **2019**, *12* (1), p156.

(27) Jumper, J.; Evans, R.; Pritzel, A.; Green, T.; Figurnov, M.; Ronneberger, O.; Tunyasuvunakool, K.; Bates, R.; Žídek, A.; Potapenko, A.; Bridgland, A.; Meyer, C.; Kohl, S. A. A.; Ballard, A. J.; Cowie, A.; Romera-Paredes, B.; Nikolov, S.; Jain, R.; Adler, J.; Back, T.; Petersen, S.; Reiman, D.; Clancy, E.; Zielinski, M.; Steinegger, M.; Pacholska, M.; Berghammer, T.; Bodenstein, S.; Silver, D.; Vinyals, O.; Senior, A. W.; Kavukcuoglu, K.; Kohli, P.; Hassabis, D. Highly accurate protein structure prediction with AlphaFold. *Nature* **2021**, *596* (7873), 583–589.

(28) Tuveng, T. R.; Jensen, M. S.; Fredriksen, L.; Vaaje-Kolstad, G.; Eijsink, V. G. H.; Forsberg, Z. A thermostable bacterial lytic polysaccharide monooxygenase with high operational stability in a wide temperature range. *Biotechnol Biofuels* **2020**, *13* (1), 1-16.

(29) Li, J.; Solhi, L.; Goddard-Borger, E. D.; Mathieu, Y.; Wakarchuk, W. W.; Withers, S. G.; Brumer, H. Four cellulose-active lytic polysaccharide monooxygenases from *Cellulomonas* species. *Biotechnol. Biofuels* **2021**, *14* (1), 1-19.

(30) Liu, L.; Yang, H.; Shin, H.; Li, J.; Du, G.; Chen, J. Recent advances in recombinant protein expression by *Corynebacterium*, *Brevibacterium*, and *Streptomyces*: from transcription and translation regulation to secretion pathway selection. *Appl. Microbiol. Biotechnol*. **2013**, *97* (22), 9597–9608.

(31) Díaz, M.; Ferreras, E.; Moreno, R.; Yepes, A.; Berenguer, J.; Santamaría, R. High-level overproduction of *Thermus enzymes* in *Streptomyces lividans*. *Appl. Microbiol. Biotechnol.* **2008**, *79* (6), 1001–1008.

(32) Berini, F.; Marinelli, F.; Binda, E. Streptomycetes: Attractive Hosts for Recombinant Protein Production. *Front. Microbiol.* **2020**, *11,* 1958.

(33) Agrawal, D.; Basotra, N.; Balan, V.; Tsang, A.; Chadha, B. S. Discovery and Expression of Thermostable LPMOs from Thermophilic Fungi for Producing Efficient Lignocellulolytic Enzyme Cocktails. *Appl. Biochem. Biotechnol.* **2020**, *191* (2), 463–481.

(34) Agrawal, D.; Kaur, B.; Kaur Brar, K.; Chadha, B. S. An innovative approach of priming lignocellulosics with lytic polysaccharide mono-oxygenases prior to saccharification with glycosyl hydrolases can economize second generation ethanol process. *Bioresour. Technol.* **2020**, *308*, 123257.

(35) Cannella, D.; Hsieh, C. C.; Felby, C.; Jørgensen, H. Production and effect of aldonic acids during enzymatic hydrolysis of lignocellulose at high dry matter content. *Biotechnol. Biofuels* **2012**, *5* (1), 26.

(36) Harris, P. V.; Welner, D.; McFarland, K. C.; Re, E.; Navarro P., J.-C.; Brown, K.; Salbo, R.; Ding, H.; Vlasenko, E.; Merino, S.; Xu, F.; Cherry, J.; Larsen, S.; Lo Leggio, L. Stimulation of Lignocellulosic Biomass Hydrolysis by Proteins of Glycoside Hydrolase Family 61: Structure and Function of a Large, Enigmatic Family. *Biochemistry* **2010**, *49* (15), 3305–3316.

(37) Klemm, D.; Petzold-Welcke, K.; Kramer, F.; Richter, T.; Raddatz, V.; Fried, W.; Nietzsche, S.; Bellmann, T.; Fischer, D. Biotech nanocellulose: A review on progress in product design and today's state of technical and medical applications. *Carbohydr. Polym.* **2021**, *254*, 117313.

(38) Buruaga-Ramiro, C.; Fernández-Gándara, N.; Cabañas-Romero, L. V.; Valenzuela, S. V.; Pastor, F. I. J.; Diaz, P.; Martinez, J. Lytic polysaccharide monooxygenases and cellulases on the production of bacterial cellulose nanocrystals. *Eur. Polym. J.* **2022**, *163*, 110939.

(39) Choi, C. N.; Song, H. J.; Kim, M. J.; Chang, M. H.; Kim, S. J. Properties of bacterial cellulose produced in a pilot-scale spherical type bubble column bioreactor. *Korean Journal of Chemical Engineering* **2009**, *26* (1), 136–140.

(40) Ono, Y.; Tanaka, R.; Funahashi, R.; Takeuchi, M.; Saito, T.; Isogai, A. SEC–MALLS analysis of ethylenediamine-pretreated native celluloses in LiCl/N,N-dimethylacetamide: softwood kraft pulp and highly crystalline bacterial, tunicate, and algal celluloses. *Cellulose* **2016**, *23* (3), 1639–1647.

(41) Villares, A.; Moreau, C.; Bennati-Granier, C.; Garajova, S.; Foucat, L.; Falourd, X.; Saake, B.; Berrin, J.-G.; Cathala, B. Lytic polysaccharide monooxygenases disrupt the cellulose fibers structure. *Sci. Rep.* **2017**, *7* (1), 40262.

(42) Selig, M. J.; Vuong, T. V.; Gudmundsson, M.; Forsberg, Z.; Westereng, B.; Felby, C.; Master, E. R. Modified cellobiohydrolase–cellulose interactions following treatment with lytic polysaccharide monooxygenase CelS2 (Sc*L*PMO10C) observed by QCM-D. *Cellulose* **2015**, 22 (4), 2263–2270.

Abstract Graphic Art

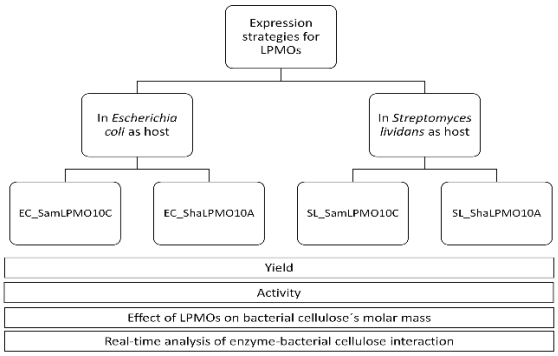

Sypnosis

Lytic polysaccharide monooxygenases (LPMOs) enhance polysaccharide breakdown, aiding biorefineries and sustainable platform chemical production. Our study explores efficient LPMO expression, cellulose degradation, and potential for eco-friendly biorefineries.

Supporting Information

Lytic polysaccharide monooxygenases low-cost expression strategies and insights into the enzyme-substrate interactions

L. Verónica Cabañas-Romero[†,‡] , Carolina Buruaga-Ramiro[†,‡], F.I. Javier Pastor[†, ‡], Ana Villares [§], Margaux Grellier [§], Ramón I. Santamaría [‖], Margarita Díaz [‖] and, Susana V. Valenzuela[* †, ‡]

[†] Department of Genetics, Microbiology, and Statistics, Faculty of Biology, Universitat de Barcelona, Av. Diagonal 643, 08028, Barcelona, Spain

[‡] Institute of Nanoscience and Nanotechnology (IN^{2}UB), Universitat de Barcelona, Spain

[§] UR1268 BIA, INRAE, F-44316 Nantes, France

[‖] Instituto de Biología Funcional y Genómica (IBFG)/Departamento de Microbiología y Genética. Consejo Superior de Investigaciones Científicas (CSIC)/Universidad de Salamanca (USAL), C/ Zacarías González, nº 2, 37007-Salamanca, Spain

∗ Corresponding author at Department of Genetics, Microbiology, and Statistics, Faculty of Biology, Universitat de Barcelona, Av. Diagonal 643, 08028, Barcelona, Spain.

Figure S1. MMSeqs2 multiple alignment results run on SamLPMO10C and ShaLPMO10A. (A). AlphaFold2 confidence measures: Average predicted Local Distance Difference Test-LDDT scores (B) and Predicted Aligned Error-PAE plots (C) for 5 different models. The model ranked as 1 was selected as the most confident among the others.

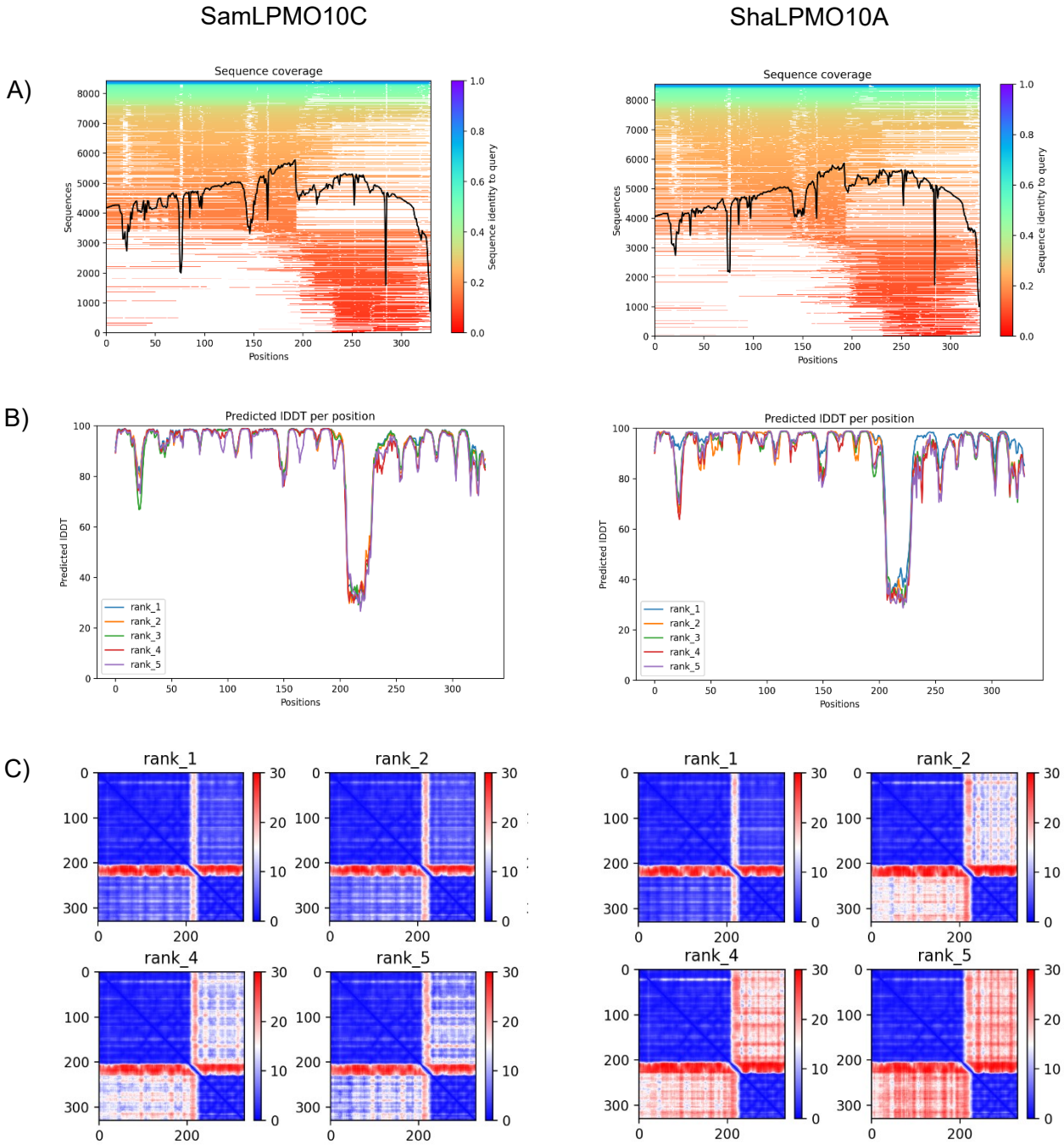

Figure S2. Verification of unpurified heterologous LPMOs activity. The spectra show MALDI-TOF MS analysis of products generated by 10 µL of *Escherichia coli´s* soluble cell extract containing: A) EC_SamLPMO10C and, B) EC_ShaLPMO10A.

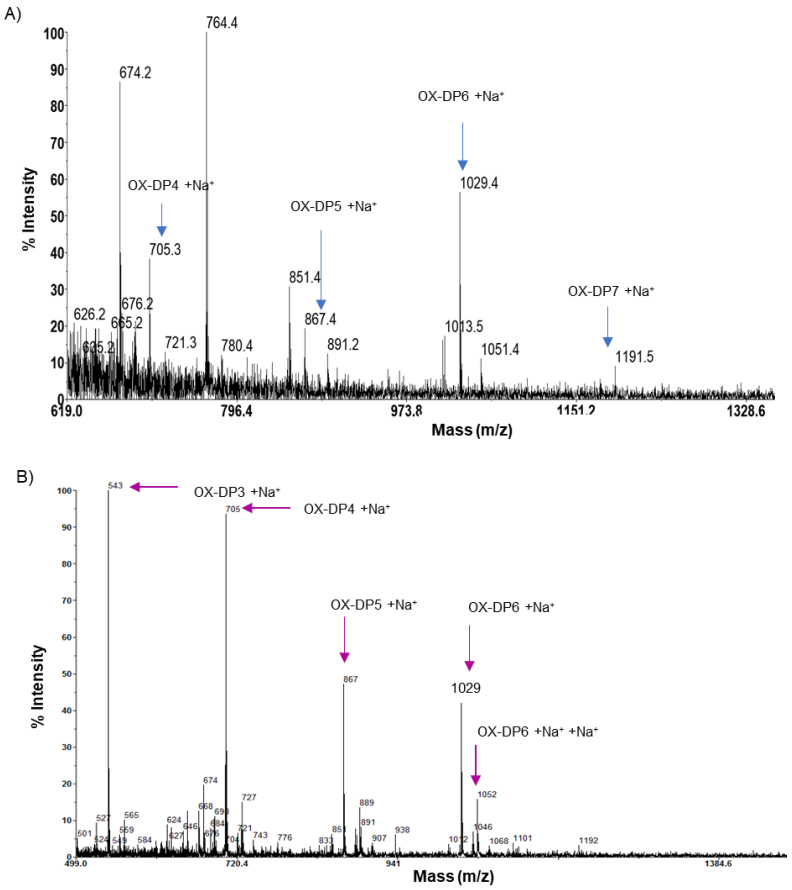

Figure S3. SDS-PAGE analysis representing *Streptomyces lividans* supernatant containing SL_SamLPMO10C (lane 1), and SL_ShaLPMO10A (lane 2). The molecular mass ladder is shown as lane "M". The spectra next to the SDS-PAGE show MALDI-TOF MS analysis of products generated by 10 µL of SL_SamLPMO10C (left), and SL_ShaLPMO10A (right). All reactions were carried out in the presence of 1% PASC, 2 mM ascorbic acid, and 2 µM H_2O_2, and incubated in shaking conditions at 900 rpm for 72h in 50 mM ammonium acetate buffer (pH 6).

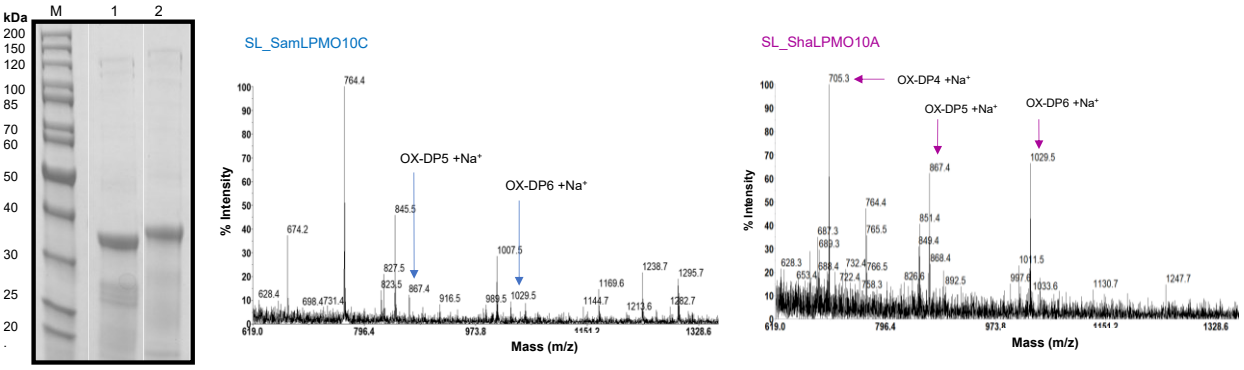

Figure S4. Cellulose binding capacity of SamLPMO10C (panel A: binding on PASC, panel B: binding on bacterial cellulose) and ShaLPMO10A (panel C: binding on PASC, panel D: binding on bacterial cellulose). Lane M: marker, lanes 1-3: fraction no bonded to cellulose after elution with 50 mM ammonium acetate buffer (pH 6), lane 4: elution with distilled water, lane 5: enzyme eluted with 10% SDS and ebullition. The microcentrifuge tubes contained 0.1 mg/ml of enzyme and 1% PASC or bacterial cellulose in 50 mM ammonium acetate buffer (pH 6) and were incubated at room temperature for 1 hour under mild agitation conditions. Lane 6: incubation of the enzyme without cellulose.

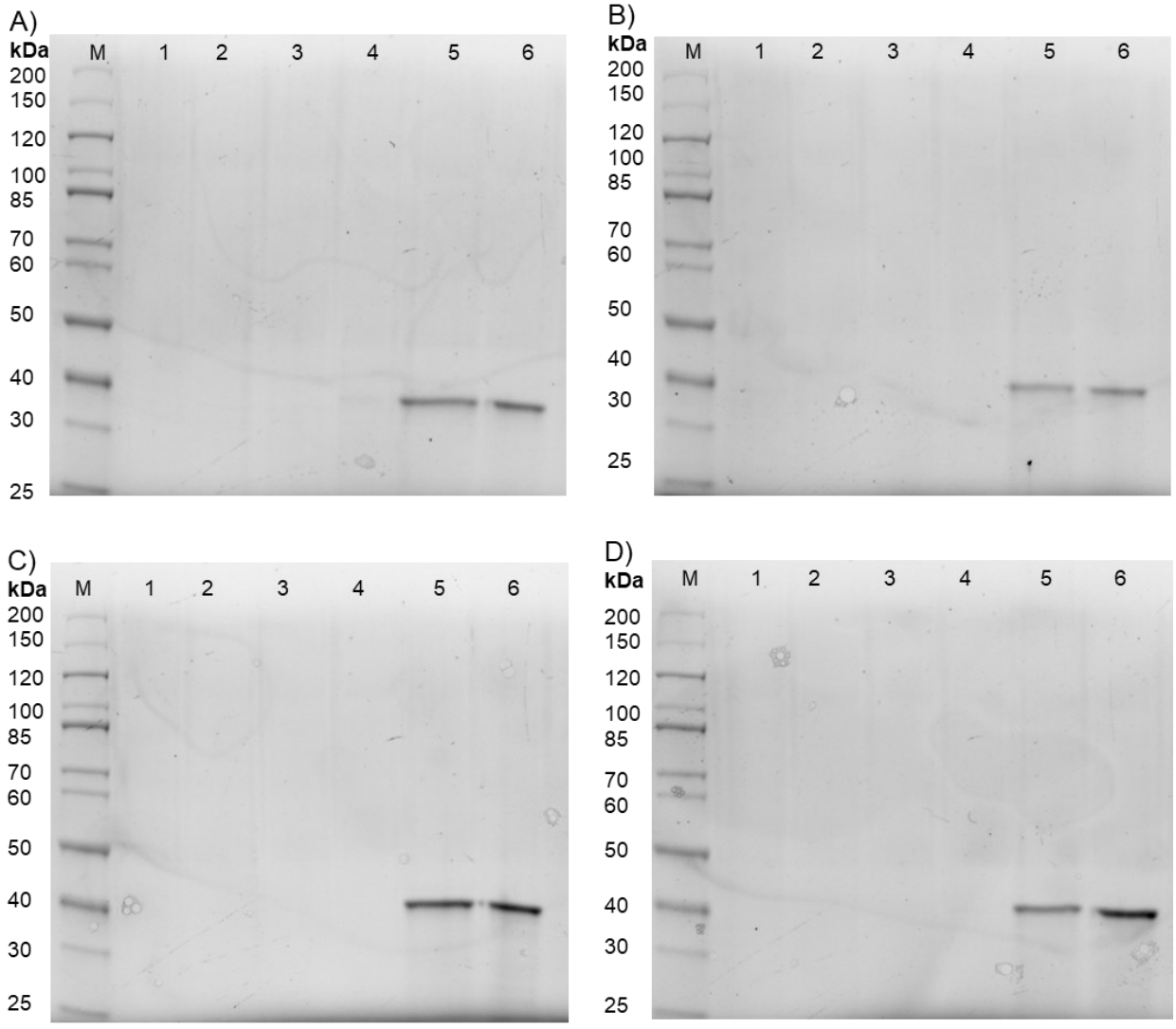

Figure S5. SEC-Elution patterns for bacterial cellulose oxidized by A) SamLPMO10C and B) ShaLPMO10A. Incubation times were 2, 6, 24, and 48 hours. C) Control with SamLPMO10C added at the end of the reaction, D) Control with ShaLPMO10A added at the end of the reaction, E) Control without ascorbic acid and with SamLPMO10C, F) Control without ascorbic acid and with ShaLPMO10A, G) Control without enzyme.

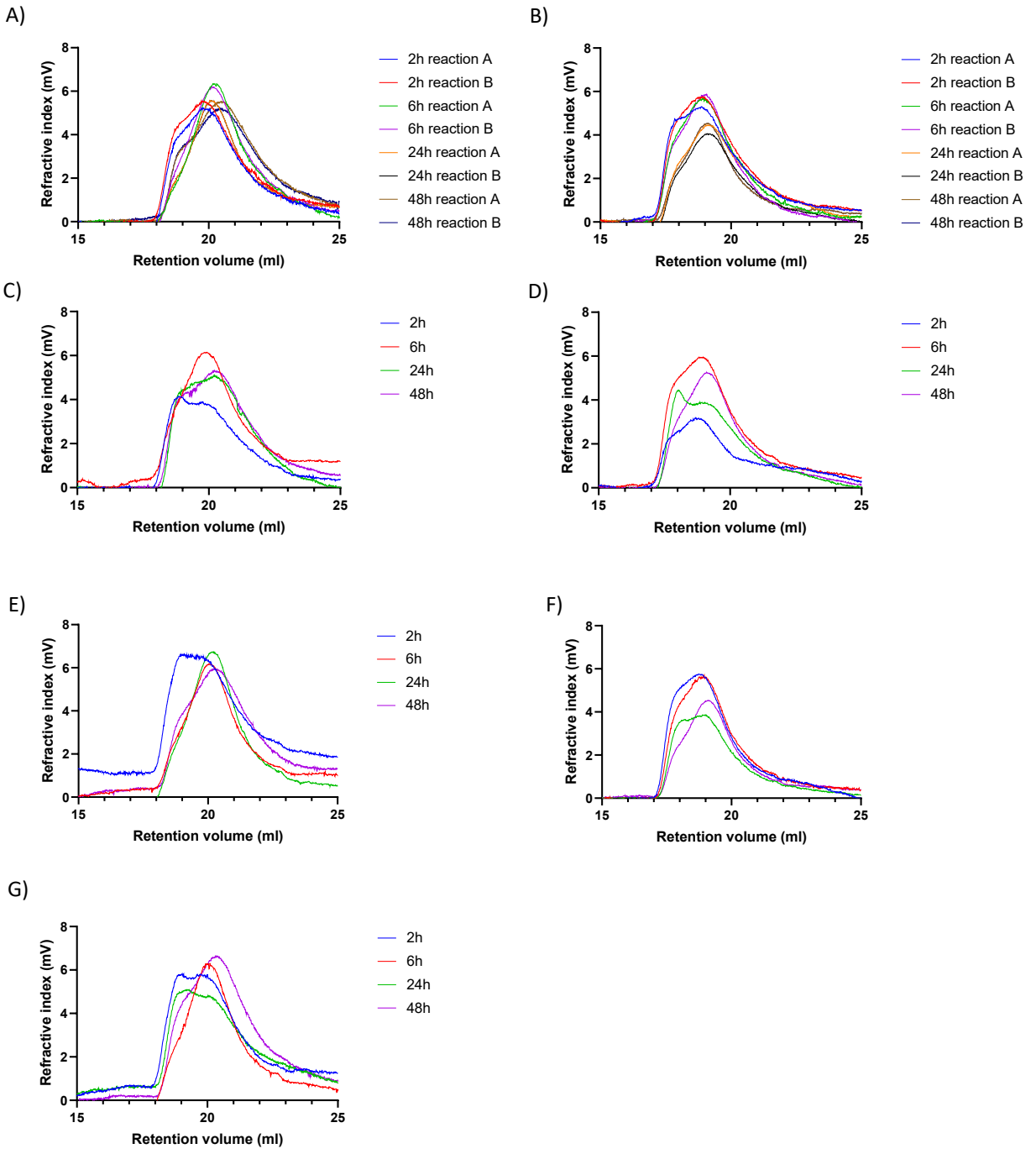

Figure S6. Weight average molar mass (*M*w), number average molar mass (*M*n), polydispersity and yields of the analysis of BC, controls and samples treated with SamLPMO10C and ShaLPMO10A.

	Sample	*M*w (g/mol)			*M*n (g/mol)			Polydispersity (*M*w/*M*n)			Yield		
	BC	8.97E+05	±	3.12E+04	6.15E+05	±	4.33E+04	1.46	±	0.05	88	±	9
2 h	BC oxidizied by SamLPMO10C	9.74E+05	±	1.62E+03	7.71E+05	±	1.28E+05	1.28	±	0.21	63	±	2
2 h	BC control without enzyme	9.85E+05	±	1.49E+05	7.06E+05	±	3.73E+04	1.40	±	0.28	77	±	14
2 h	BC control with enzyme	9.25E+05	±	7.99E+04	7.54E+05	±	1.28E+05	1.24	±	0.10	90	±	14
2 h	BC control without ascorbic acid	9.13E+05	±	2.71E+04	6.99E+05	±	9.14E+03	1.31	±	0.06	72	±	18
6 h	BC oxidizied by SamLPMO10C	8.06E+05	±	3.73E+04	6.28E+05	±	7.28E+04	1.29	±	0.10	83	±	4
6 h	BC control without enzyme	9.62E+05	±	3.84E+04	8.39E+05	±	7.85E+04	1.15	±	0.06	76	±	3
6 h	BC control with enzyme	8.70E+05	±	2.35E+04	6.82E+05	±	1.49E+04	1.28	±	0.06	83	±	8
6 h	BC control without ascorbic acid	9.65E+05	±	4.42E+04	8.32E+05	±	1.21E+04	1.16	±	0.04	71	±	8
24 h	BC oxidizied by SamLPMO10C	7.46E+05	±	2.63E+04	5.13E+05	±	2.63E+04	1.46	±	0.12	78	±	3
24 h	BC control without enzyme	8.95E+05	±	1.18E+03	7.49E+05	±	1.13E+04	1.19	±	0.02	64	±	10
24 h	BC control with enzyme	8.64E+05	±	1.90E+04	6.94E+05	±	2.58E+04	1.25	±	0.02	68	±	12
24 h	BC control without ascorbic acid	8.65E+05	±	4.06E+04	6.75E+05	±	3.20E+04	1.28	±	0.00	85	±	5
48 h	BC oxidizied by SamLPMO10C	6.63E+05	±	5.73E+04	4.74E+05	±	5.98E+04	1.41	±	0.09	78	±	4
48 h	BC control without enzyme	8.48E+05	±	2.30E+04	6.50E+05	±	8.76E+04	1.32	±	0.14	80	±	14
48 h	BC control with enzyme	8.25E+05	±	1.86E+04	6.54E+05	±	1.94E+02	1.26	±	0.03	78	±	4
48 h	BC control without ascorbic acid	8.17E+05	±	2.50E+04	6.33E+05	±	2.83E+04	1.29	±	0.10	78	±	2
2 h	BC oxidizied by ShaLPMO10A	8.55E+05	±	2.63E+04	7.02E+05	±	4.95E+04	1.22	±	0.05	76	±	2
2 h	BC control without enzyme	8.88E+05	±	1.38E+05	7.26E+05	±	8.94E+03	1.22	±	0.06	74	±	15
2 h	BC control with enzyme	8.11E+05	±	8.15E+04	5.84E+05	±	1.12E+05	1.40	±	0.24	73	±	39
2 h	BC control without ascorbic acid	9.01E+05	±	1.02E+04	7.07E+05	±	1.21E+04	1.27	±	0.05	68	±	12
6 h	BC oxidizied by ShaLPMO10A	8.21E+05	±	1.85E+04	7.16E+05	±	4.00E+04	1.15	±	0.04	77	±	2
6 h	BC control without enzyme	9.53E+05	±	5.47E+04	8.39E+05	±	2.88E+04	1.14	±	0.06	79	±	1
6 h	BC control with enzyme	9.02E+05	±	4.54E+04	7.70E+05	±	1.10E+05	1.18	±	0.08	78	±	0.1
6 h	BC control without ascorbic acid	8.95E+05	±	5.47E+04	7.64E+05	±	8.42E+04	1.17	±	0.06	76	±	1
24 h	BC oxidizied by ShaLPMO10A	7.28E+05	±	5.42E+04	5.12E+05	±	2.31E+04	1.42	±	0.04	70	±	5
24 h	BC control without enzyme	9.04E+05	±	7.52E+04	7.74E+05	±	4.64E+04	1.22	±	0.01	68	±	12
24 h	BC control with enzyme	9.42E+05	±	6.58E+04	7.25E+05	±	6.86E+04	1.25	±	0.01	72	±	1
24 h	BC control without ascorbic acid	9.49E+05	±	7.75E+04	7.82E+05	±	1.19E+05	1.22	±	0.09	75	±	9
48 h	BC oxidizied by ShaLPMO10A	7.67E+05	±	4.77E+04	4.15E+05	±	5.53E+04	1.76	±	0.14	82	±	8
48 h	BC control without enzyme	1.05E+06	±	1.15E+05	8.15E+05	±	1.02E+04	1.29	±	0.12	78	±	6
48 h	BC control with enzyme	1.02E+06	±	1.75E+05	7.55E+05	±	5.87E+04	1.35	±	0.13	73	±	4
48 h	BC control without ascorbic acid	9.30E+05	±	4.55E+04	7.18E+05	±	1.41E+04	1.30	±	0.09	69	±	11

Figure S7. A) Frequencies ($\Delta f_n/n$) and dissipation (ΔD_n) changes in the interaction between ascorbic acid and bacterial cellulose, instead of the LPMO, 50 Mm Tris HCl (pH 6) was injected. B) corresponds to the first 60 minutes of analysis.

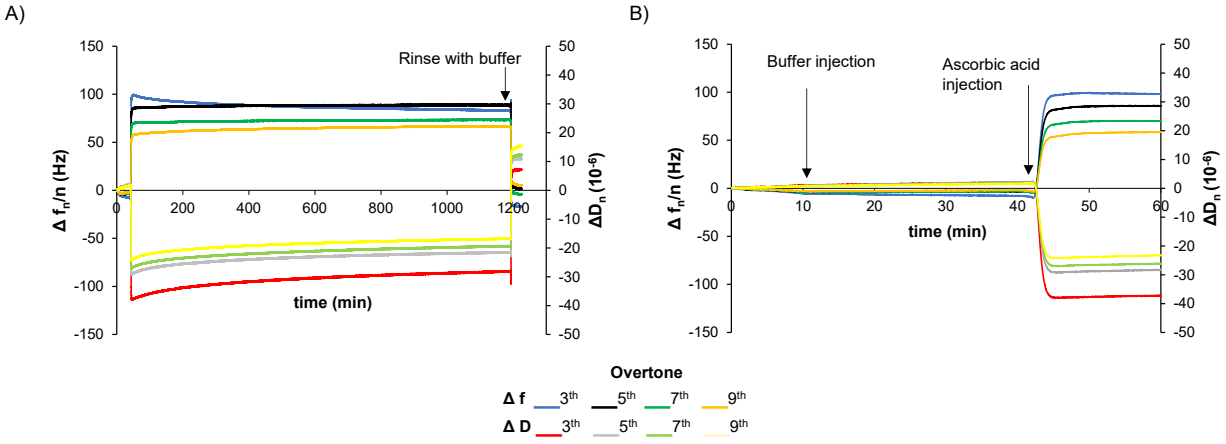

Figure S8. Frequencies ($\Delta f_n/n$) and dissipation (ΔD_n) changes in the interaction among SamLPMO10C and ascorbic acid with bacterial cellulose (A). (B) represents the first 60 minutes of the analysis.

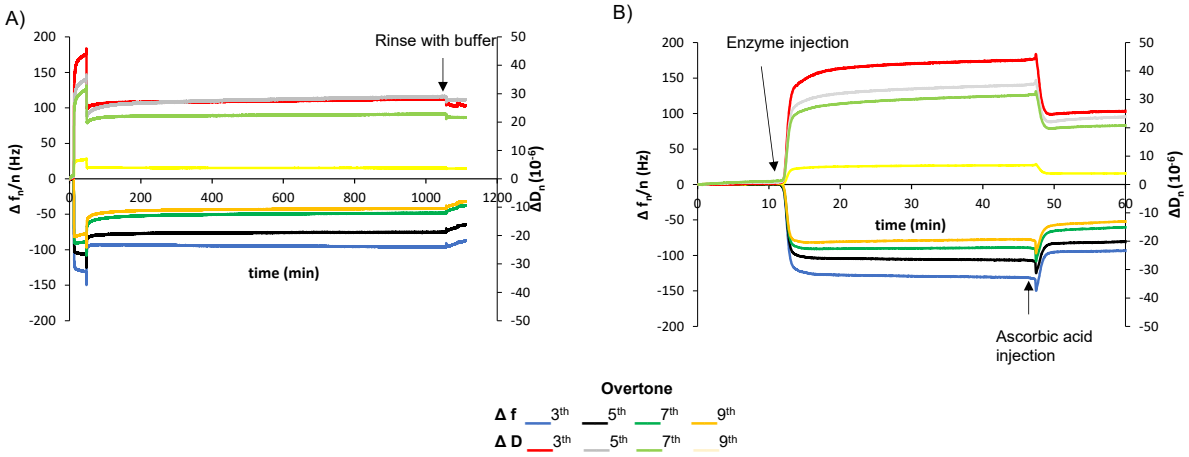

Figure S9. Frequencies ($\Delta f_n/n$) and dissipation (ΔD_n) changes in the interaction among ShaLPMO10A and ascorbic acid with bacterial cellulose (A). (B) represents the first 60 minutes of the analysis.

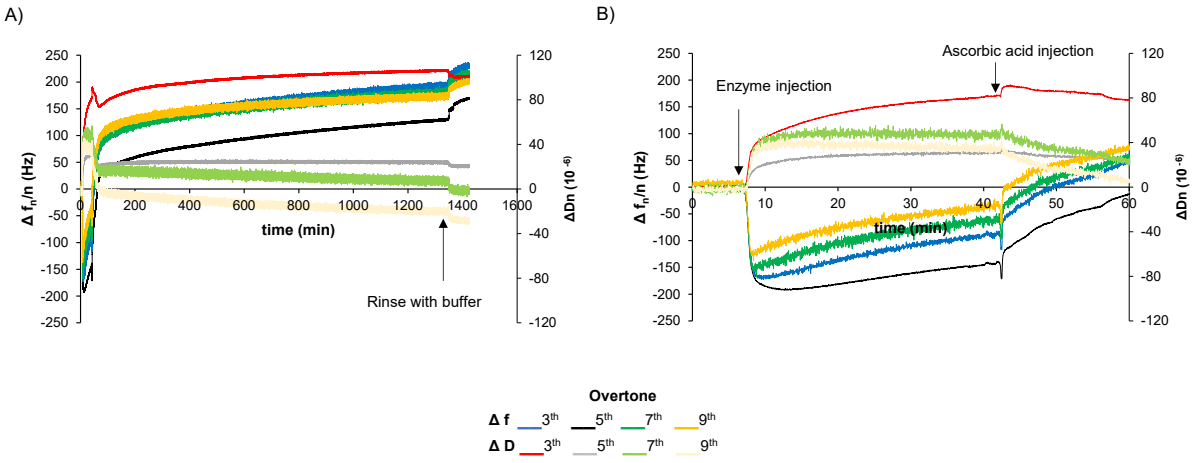

Figure S10. The spectra show MALDI-TOF MS analysis of soluble products (cello-oligosaccharides aldonic acids) generated by SamLPMO10C during the QCM-D experiments (A). Control without enzyme (B).

A)

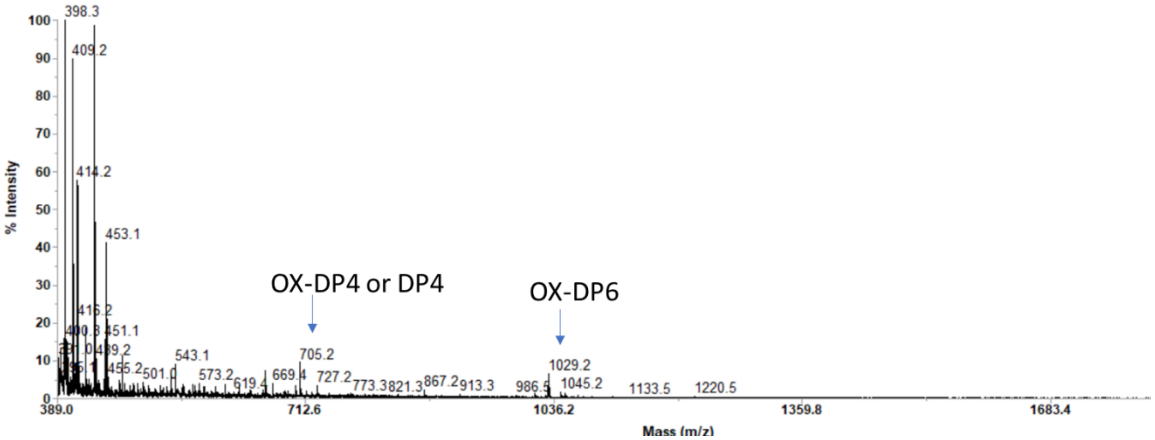

B)

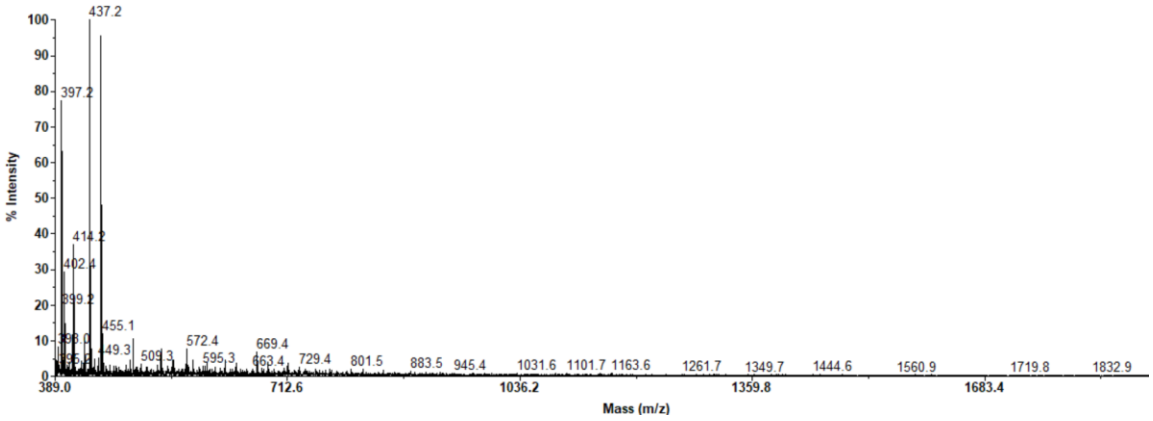

4.1 Capítulo 3. Evaluación de celulasas para el biorefino

4.1.2 Artículo 4: Flax biorefining for paper production

Biorefinado de lino para la producción de papel

En este trabajo, evaluamos el potencial de Cel6D, una exocelulasa recientemente reportada de *Paenibacillus barcinonensis*, como agente de biorefinado de la pasta de lino. Las fibras de lino se trataron con esta enzima, Cel9B (una endocelulasa que previamente se demostró que posee acción biorefinadora) y las dos en combinación. A continuación, las muestras de pasta de lino biorefinada se refinaron mecánicamente para obtener hojas de papel. Los tres tratamientos de biorefinado redujeron la permeabilidad al aire en las hojas de papel. Cel9B aumentó el índice de tracción y la resistencia al plegado, y la combinación Cel6D-Cel9B aumentó el índice de tracción y el índice de estallido, pero también resultó en una marcada disminución del índice de desgarro y la resistencia al plegado. Por otro lado, Cel6D aumentó el índice de tracción y el índice de estallido; también, lo que es más importante, disminuyó la resistencia al desgarro, aunque ligeramente, en relación con los otros dos tratamientos. Los resultados de este trabajo pueden ser útiles para comprender los efectos diferenciales de las exocelulasas y endocelulasas como herramientas de biorefinado y abrir nuevas vías para explorar su uso en otras aplicaciones biotecnológicas.

Barcelona, July 25th 2023

Dear Editor

I am writing to submit our article entitled "Flax biorefining for paper production" signed by Oriol Cusola, Carolina Buruaga-Ramiro, Cristina Valls, M. Blanca Roncero, Susana V. Valenzuela, and myself, L. Verónica Cabañas-Romero, for consideration for publication in your esteemed journal.

In our study, we evaluated an enzyme recently described, Cel6D from *Paenibacillus barcinonensis* as a potential biorefining agent for flax-derived cellulose pulp to produce paper and analyzed its mechanical properties. Additionally, we used Cel9B, a well-known enzyme, from the same strain. By combining both enzymes, we studied their impact on the paper's mechanical properties. We believe this research significantly advances the field by promoting the use of enzymes as greener alternatives in paper pulp biorefining.

The focus of our study on utilizing enzymes for pulp refining is of significant importance in the context of sustainable and eco-friendly paper production. Our findings offer valuable insights into the potential of enzymes as green alternatives in the paper manufacturing industry.

Hoping this manuscript meets the criteria for publication in Cellulose.

Yours sincerely,

L. Verónica Cabañas-Romero

Flax biorefining for paper production

L. Verónica Cabañas-Romero [*a], Oriol Cusola [b], Carolina Buruaga-Ramiro [a], Cristina Valls [b], M. Blanca Roncero [b] and Susana V. Valenzuela [a]

[a] Department of Genetics, Microbiology and Statistics, Faculty of Biology, Universitat de Barcelona, Av. Diagonal 643, 08028 Barcelona, Spain

[b] CELBIOTECH_Paper Engineering Research Group, Universitat Politècnica de Catalunya_BarcelonaTech, 08222 Terrassa, Spain

∗ Corresponding author at Department of Genetics, Microbiology, and Statistics, Faculty of Biology, Universitat de Barcelona, Av. Diagonal 643, 08028, Barcelona, Spain.

Abstract

In this work, we assessed the potential of Cel6D, a recently reported exocellulase from *Paenibacillus barcinonensis*, as a biorefining agent for flax pulp. Pulp fibers were treated with this enzyme, Cel9B (an endocellulase previously shown to possess biorefining action) and the two in combination. Samples of biorefined flax pulp were mechanically refined to obtain handsheets. All three biorefining treatments decreased air permeance in the handsheets. Cel9B increased tensile index and folding endurance, and the Cel6D−Cel9B combination increased tensile index and burst index but also resulted in markedly decreased tear index and folding endurance. On the other hand, Cel6D increased tensile index and burst index; also, more importantly, it decreased tear resistance, albeit slightly, relative to the other two treatments. The results of this work can be useful to understand the differential effects of exocellulases and endocellulases as biorefining tools and open up new avenues for exploring their use in other biotechnological applications.

Keywords: Biorefining, Cellulases, Cel9B, Cel6D, Flax pulp.

1. Introduction

Their abundance, availability and low processing costs have aroused growing interest in nonwood fibers lately, especially in countries with scant wood resources (Abd El-Sayed et al. 2020). The primary sources of nonwood cellulose fibers for the paper industry include bagasse, bamboo, straw, sisal, jute, abaca, cotton linters, reeds and flax (Ferdous et al. 2021; Manian et al. 2021). Flax (*Linum usitatissimum*) is an excellent candidate for manufacturing durable, lightweight sheets commonly used in the production of cigarettes, special book volumes and lightweight paper (del Río et al. 2011).

Most paper production processes involve pulping, stock preparation, sheet formation and a finishing step (Torres et al. 2012). Refining during stock preparation causes fibrillation, bursting of primary and secondary cell walls, formation of fines and a reduction in fiber length. In fact, fibrillation alters both external and internal fiber surfaces, and improves their binding properties by increasing their flexibility (Biermann 1996; Torres et al. 2012). Refining breaks primary and secondary fiber walls and removes them in part; in this way, it increases fiber surface areas and fiber−fiber bonding, thus leading to improved strength-related properties in the resulting handsheets. Refining additionally promotes the formation of fines and increases fiber length cut, thereby enhancing handsheet flexibility and density (Biermann 1996; Torraspapel 2009; Przybysz Buzała et al. 2016).

The paper industry is increasingly using cellulases to reduce production costs and environmental impacts. There are three basic types of cellulases, namely:

(a) Endoglucanases (EGs), which hydrolyze amorphous cellulose by randomly breaking internal links in cellulose chains to give oligosaccharides of variable size, thus causing new reducing and nonreducing chain ends to be formed for attack by the enzymes (Quiroz-Castañeda and Folch-Mallol 2013)

(b) Exoglucanases or cellobiohydrolases (CBHs), which act on the ends of cellulose chains to release cellobiose molecules as main products. Exoglucanases have proved specific toward cellulose ends. Thus, cellobiohydrolases act on the reducing ends of

cellulose chains (CBH I), whereas other exoglucanases target nonreducing ends (CBH II) (Koivula et al. 1998).

(c) β-D-glucosidases, which hydrolyze cellobiose and cellodextrins with a maximum degree of polymerization of 6 to produce glucose (Tomme et al. 1995).

Using enzymes that alter fiber surfaces can increase fiber−fiber cohesion and enhance the mechanical properties of paper as a result. For example, a cellulase-based pretreatment can facilitate subsequent mechanical refining and reduce energy costs as a result (Gil et al. 2009). Cellulases have proved widely differently efficient as refining aids. Thus, Pere et al. (1995) found endoglucanases from *Trichoderma reesei* to impair the mechanical properties of the resulting paper. In subsequent research into enzymes from *Trichoderma reesei* as biorefining agents, they found using cellobiohydrolase CBHI prior to refining to save energy by up to 20% and thermochemical pulp thus obtained to have improved strength-related properties (Pere et al. 2000). Research into the potential of cellulases of diverse origin for improving the mechanical properties of paper has led to contradictory outcomes (Kmiotek et al. 2021; Nagl et al. 2021). Thus, cellulases have shown biorefining potential, but their actual effect depends on the particular type of enzyme, substrate, conditions and application time. This has made identifying and developing new cellulases for altering cellulose fibers in order to obtain products with unique properties while saving energy and reducing the environmental impact a technological priority for the paper industry.

Previous studies on the use of endocellulase Cel9B from *Paenibacillus barcinonensis* before mechanical refining have shown it to considerably improve some mechanical properties including tensile strength and burst index in eucalyptus and flax sheets (García et al. 2002; Cadena et al. 2010; Garcia-Ubasart et al. 2013). Thus, Cel9B facilitates refining with substantial energy savings and provides paper with markedly improved mechanical properties. The emergence of Cel6D, which is a recently reported GH6 cellobiohydrolase from *Paenibacillus barcinonensis* (Cerda-Mejía et al. 2017), and the excellent results previously obtained with Cel9B, led us to explore the use of exocellulase Cel6D as a biorefining enzyme here.

The primary aim of this work was to examine the biomodifying effects of cellulases Cel6D, Cel9B and the two in combination on cellulose fibers from flax. The combination of Cel9B, which follows an endoprocessive mechanism, and the exocellulase Cel6D was expected to have a synergistic effect leading to improved mechanical properties of the resulting paper (i.e., the enzymes were expected to possess biorefining action). The starting hypothesis was checked by examining the effect of various enzymatic treatments on the refining process and the properties of the resulting paper.

2. Materials and Methods

2.1 Pulp

ECF flax pulp was supplied by CELESA (Tortosa, Spain) and pretreated by soft refining according to ISO 5264-1:1979 in a Valley mill for 10 min.

2.2 Enzymes

Purified Cel9B was obtained from *Escherichia coli* BLR(DE3)/pET28aCel9B clarified cell extracts by binding and elution from Avicel as described elsewhere (Chiriac et al. 2010). Clarified cell extracts from Cel6D-producing *E. coli* recombinant clones (Cerda-Mejía et al. 2017) were purified by using the same method and analyzed by sodium dodecyl sulfate−polyacrylamide gel electrophoresis (SDS-PAGE). Cel6D and Cel9B production were scaled up in a 50 L bioreactor.

Cel9B and Cel6D concentrations were determined according to Bradford (1976), using bovine serum albumin as standard. Also, proteins were quantified from their absorbance at 280 nm as measured with an ND-1000 spectrophotometer from NanoDrop Technologies (Thermo Fisher Scientific, Waltham, MA, USA). Proteins were analyzed by sodium dodecyl sulfate−polyacrylamide gel electrophoresis (SDS−PAGE).

2.3 Enzimatic treatments

The Cel9B used had an activity of 0.36 CMCase U/mg protein. Cellulase activity was determined by using the DNS method to measure the amount of reducing sugars released from carboxymethyl cellulose (Miller 1959). The assay mixture contained 1.5% carboxymethylcellulose (CMC) in a final volume of 100 µl of 50 mM acetate buffer (pH 5) and the mixture was incubated at 50 °C for 30 min. Color development was measured at 540 nm. One unit of enzymatic activity was defined as the amount of enzyme releasing 1 µmol of reducing sugar equivalent per minute under the assay conditions used.

Enzymes were dosed as protein [mg/g odp (oven-dry) pulp] into the solution prior to adding any pulp in order to allow them to disperse evenly in the pulp. Six different enzyme doses were used, namely: 1 mg Cel6D/g (odp), 1.5 mg Cel6D/g (odp), 3 mg Cel6D/g (odp), 1 mg Cel9B/g (odp), 1.5 mg Cel9B/g (odp) and 3 mg Cel9B/g (odp). A control treatment was also performed under identical conditions in the absence of enzyme.

The enzyme treatments were done in polyethylene bags that were placed in a laboratory water bath. An amount of 30 g (odp) pulp at 5% consistency in 50 mM sodium acetate buffer at pH 5 at 50 °C was treated with enzyme for 1 h (García et al. 2002; Cadena et al. 2010), the reaction being stopped by washing the pulp with deionized water in a porous glass filter funnel of porosity grade 3. The resulting liquors were recovered for analysis by thin-layer chromatography (TLC) spotted on silica gel plates (Kieselgel 20 F254 20 × 20 cm; Merck, Darmstadt, Germany), using 3:6:1 (v/v/v) chloroform/acetic acid/water as solvent. Oligosaccharides were detected by spraying the plates with a 95:5 (v/v) ethanol/concentrated sulfuric acid mixture and heating at 120 °C. Once the enzyme doses to be used were established, they were employed in further tests conducted under the same incubation conditions.

2.4 *Mechanical refining and handsheet properties*

Enzyme-treated and control pulp samples were refined at 1000 revolutions (rev) in a PFI mill from Hamjern Maskin a.s. (Hamar, Norway) according to ISO 5264. Pulp properties including drainage resistance (°SR, ISO 5267) and water retention value (WRV, ISO 23714) were measured. Fiber morphology was examined in a Kajaani FS300 fiber analyzer in terms of fiber length and content in fines according to ISO 16065-1:2001. Mechanical properties were determined according to ISO 5269-2:2004 in handsheets obtained with a Rapid-Köthen lab former. The enzyme doses to be used were found by using 100 g/m^2 handsheets. Then, 74 ± 6 g/m^2 paper was prepared according to ISO 5331 and tested mechanically under the following ISO standards: 1924 for tensile index, 2758 for burst index, 1974 for tear index, 5626 for folding endurance and 5636 for Bendtsen permeance. Handsheets made from enzyme-treated, unrefined flax pulp were included in all tests. They were designated Cel6D 0 rev, Cel9B 0 rev and Cel6D+Cel9B 0 rev according to whether the pulp had been treated with Cel6D, Cel9B or both enzymes, respectively. Likewise, the handsheets from pulp treated with Cel6D, Cel9B and both enzymes, and mechanically refined at 1000 revolutions, were designated Cel6D 1000 rev, Cel9B 1000 rev and (Cel6D+Cel9B) 1000 rev, respectively.

2.5 *Microscopy analysis*

An optical microscope (Olympus) was used to examine the appearance of the pulp samples. Also, small pieces of paper were analyzed by scanning electron microscopy with a JSM 7100 F thermal field microscope from JEOL (Tokyo, Japan) equipped with an LED filter.

3. Results and discussion

3.1 *Cellulase production*

Cellulases Cel9B (Chiriac et al. 2010) and Cel6D (Cerda-Mejía et al. 2017) from *Paenibacillus barcinonensis* were expressed and purified by affinity adsorption. The prominent bands observed corresponded to the theoretical molecular weight of the proteins (103 kDa for Cel9B and 84 kDa

for Cel6D; Fig. 1). This purification method is straightforward and inexpensive, so it is highly suitable for industrial use.

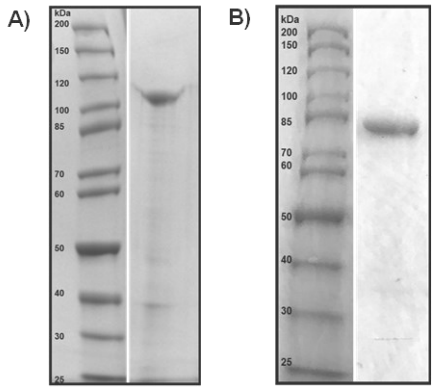

Fig. 1 Results of the SDS−PAGE analysis. A) Cel9B. B) Cel6D.

3.2 Optimum enzyme doses

Properly dosing cellulases is very important as too high a dose can dramatically impair the mechanical properties of the resulting pulp and paper. In this work, the optimum Cel6D and Cel9B dose were established by using thin-layer chromatography (S1) to analyze the liquors from their treatments. Paper properties were assessed in handsheets of 100 g/m^2 rather than the standard 75 g/m^2 in order to amplify the effects of the enzymes. The handsheets were tested for air permeance, density and tensile strength.

As can be seen from Table 1, Cel6D and Cel9B at any dose considerably reduced air permeance relative to the control samples. Also, they increased tensile strength. Specifically, a Cel6D dose of 1 mg enzyme/g odp increased tensile index by 18% and one of 1.5 or 3 mg/g odp increased it by 23%. On the other hand, a Cel9B dose of 1 mg/odp increased the index by 9%, whereas one of 1.5 mg/odp increased it by 18% —and, interestingly, a dose of 3 mg/g odp increased it by only 9%. Cel9B has a proven effect on various types of cellulose fibers that results in improved pulp and handsheet properties (García et al. 2002; Cadena et al. 2010; Garcia-Ubasart et al. 2013). An optimal dose of 1.5 mg/g odp was chosen for both enzymes.

Table 1. Properties of paper from flax pulp treated with Cel6D or Cel9B in variable doses.

Enzyme dose	Density (g/cm^3)	Air permeance (μm/Pa·s)	Tensile index (kN/m)
Control	0.419	28	22
1 mg Cel6D/odp	0.476	23	26
1.5 mg Cel6D/odp	0.472	22	27
3 mg Cel6D/odp	0.458	22	27
1 mg Cel9B/odp	0.470	29	24
1.5 mg Cel9B/odp	0.470	27	27
3 mg Cel9B/odp	0.500	31	24

3.3 *Analysis of liquors*

Flax fibers were treated as described under Materials and Methods. Analysis by thin layer chromatography of the liquors from the different enzymatic treatments showed both Cel9B and Cel6D to be active on flax pulp, both individually and in combination (Fig. 2). The only hydrolysis product for Cel6D was cellobiose, which confirmed its cellobiohydrolase activity. On the other hand, Cel9B, which is a processive endoglucanase, released cellobiose and cellotetraose in addition to small amounts of glucose. The major product of the treatment using the two enzymes in combination was cellobiose, accompanied by small amounts of cellotetraose and glucose (i.e., the liquor was similar in composition to those provided by the individual enzymes).

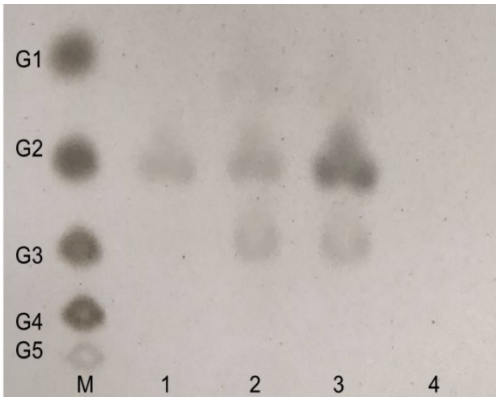

Fig. 2 Thin-layer chromatograms for the hydrolysis products of enzymatically treated flax pulp. Lane 1: Cel6D. Lane 2: Cel9B. Lane 3: Cel6D+Cel9B. Lane 4: negative control without enzyme. Lane M: markers containing glucose (G1), cellobiose (G2), cellotriose (G3), cellotetraose (G4) and cellopentaose (G5).

3.4 Effects of the enzymes on pulp fibers

Whether the enzymatic treatments altered the morphology of the fibers was checked by subjecting pulp treated with the optimum enzyme dose (1.5 mg/g odp) to optical and electron scanning microscopy (Fig. 3). Conditioning the starting pulp in the Valley mill caused the fibers to exhibit external fibrillation and cut. This was especially so with Cel6D1000rev and influenced the mechanical properties of the resulting handsheets. On the other hand, as was apparent in the optical microscopy images, Cel9B 1000rev contained more particles (fines) than did Control 1000rev.

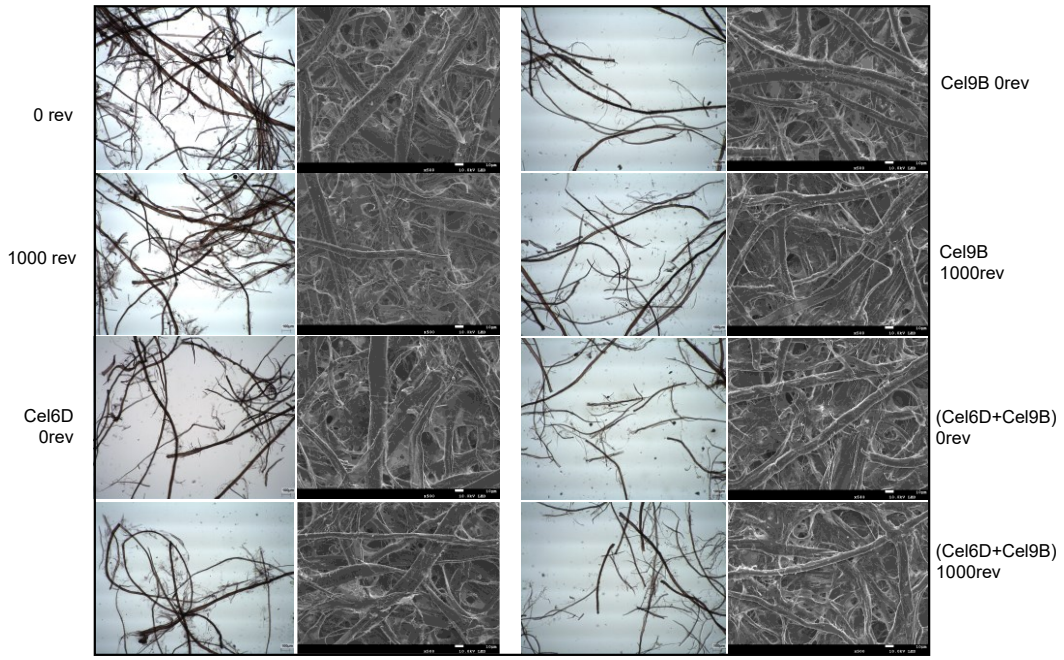

Fig. 3 Optical and SEM images of handsheets obtained from enzymatically treated and untreated (control) pulp.

Table 2 shows the drainage resistance and water retention value of the pulp samples. As can be seen, refining Cel9B raised drainage resistance by 17%, which is consistent with the results of studies using Cel9B on various cellulose substrates (García et al. 2002; Cadena et al. 2010). The three enzymatic treatments markedly increased WRV (by 7, 9 and 10% with Cel6D, Cel9B and Cel6+Cel9B, respectively); therefore, the enzymes caused softening and/or delamination of the outer walls of cellulose fibers.

Table 2. Effect of biorefining with cellulases and mechanical refining on pulp properties.

Pulp	Drainage resistance (°SR)	Water retention value (WRV)
0 rev	40 ± 4	1.11 ± 0.02
1000 rev	48 ± 1	1.15 ± 0.01
Cel6D 0 rev	40	1.11 ± 0.02
Cel6D + 1000 rev	46 ± 3	1.23 ± 0.01
Cel9B 0 rev	39 ± 2	1.13 ± 0.01
Cel9B + 1000 rev	56	1.25 ± 0.05
(Cel6D+Cel9B) 0 rev	40 ± 1	1.07 ± 0.02
(Cel6D+Cel9B) + 1000 rev	47 ± 2	1.27 ± 0.04

3.5 Effect of the enzymes on handsheet density and air permeance

Once the effect of the enzymatic treatments on the physical properties of flax pulp was examined, the samples were used to form handsheets for mechanical and optical analysis. As can be seen from Fig. 4, all enzymatic treatments decreased air permeance and density to a similar extent, which suggests that the enzymes resulted in more compact handsheets that were thus less permeable to air. As expected, combining the enzymatic treatments with mechanical refining further decreased air permeability relative to unrefined samples. Interestingly, however, all handsheets —control, refined samples treated with no enzyme included— were similar in air permeability. Cel6D and the enzyme combination slightly increased handsheet density, the increase being especially marked in the handsheets from mechanically refined pulp treated with either Cel9B or the Cel9B+Cel6D combination —which suggests that density and air permeability changes were induced to a greater extent by Cel9B than they were by Cel6D.

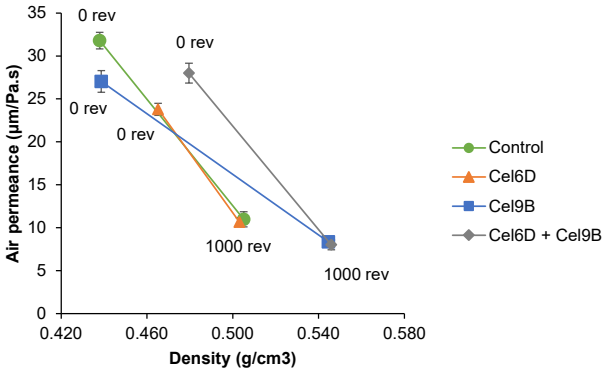

Fig. 4 Air permeance vs density plot.

The light scattering coefficient is a measure of interfiber bonding, with which it is inversely related (Retulainen 1996; Mansfield et al. 2002). As can be seen from Fig 5, the coefficient decreased slightly in the sequence 1000 rev > Cel6D 1000 rev > 1000 rev Cel9B. Interestingly, the (Cel9B+Cel6D) 0 rev handsheets exhibited a marked decrease —seemingly, the individual effects of Cel6D and Cel9B resulted in greater fiber−fiber contact in the sheets.

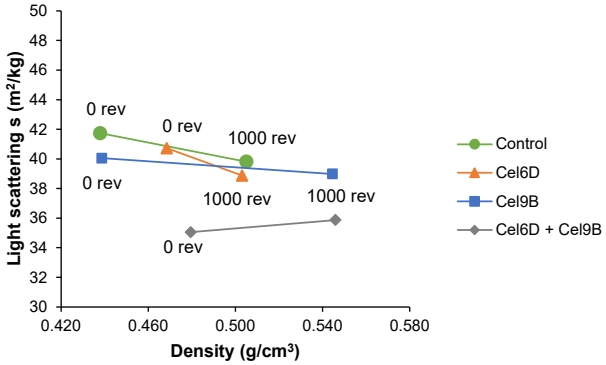

Fig. 5 Light scattering coefficient vs density plot.

3.6 *Effect of the enzymes on the mechanical properties of the handsheets*

As can be seen from Fig. 6, the three enzymatic treatments modified the tensile strength and tear index of the handsheets. Thus, Cel6D 0 rev exhibited a tensile index 9% higher, and Cel9B 0 rev and (Cel6D+Cel9B) 0 rev one 22% and 26% higher, respectively, than that of the handsheets from pulp treated with no enzyme (0 rev). Also, the enzyme−mechanical refining combination

increased tensile strength by 9% in Cel6D 1000 rev, and 12% in Cel9B 1000 rev, relative to the handsheets from pulp that was mechanically refined only (1000 rev). Combining Cel6D+Cel9B and mechanical refining at 1000 rev led to a 12% increase in tensile index. Taken together, these results testify to the clear influence of Cel9B on handsheet tensile strength.

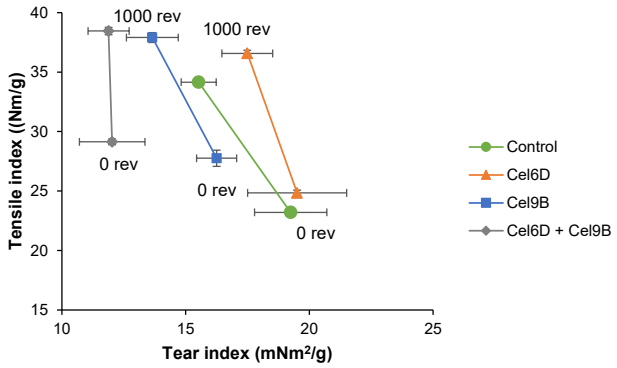

Fig. 6 Tensile index vs tear index plot.

With conventional refining, the mechanical properties of paper develop through a gradual increase in tensile strength and a gradual decrease in tear resistance. However, Cel6D 0 rev handsheets exhibited a slightly increased tear index (Fig. 6). Conversely, Cel9B 0 rev exhibited a tear index 26% lower than that of 0 rev handsheets. Interestingly, the handsheets from (Cel6D+Cel9B) 0 rev pulp exhibited a drastic decrease in tear resistance (37%) whereas those from (Cel6D +Cel9B) 1000 rev pulp retained the tear resistance of its unrefined counterpart. As expected, combining the enzymatic treatments with mechanical refining (Cel6D 1000 rev and Cel9B 1000 rev handsheets) decreased tear strength even further. Tear strength in the handsheets from Cel9B 1000 rev and (Cel6D+Cel9B) 1000 rev was lower than it was in the control handsheets (1000 rev). However, Cel6D 1000 rev handsheets exhibited slightly higher tear strength than the control samples. Therefore, Cel6D led to the best mechanical properties in the handsheets.

The tear index is strongly influenced by both the length of fibers and the proportion of fines (fiber length ≤ 0.2 mm) in handsheets (Ferreira et al. 1999). Figure 7A is a plot of tear

index against the content in fines. As can be seen, 0 rev and Cel6D 0 rev handsheets, and their mechanically refined counterparts, had a similar content in fines. However, Cel9B increased such a content and decreased tear index as a result. The effect of this enzyme was enhanced by its combination with Cel6D, which increased fines and decreased tear resistance. The effect of Cel9B on fiber length (Fig. 7B) was especially apparent in Cel9B 1000 rev, which exhibited a decreased length. Further proof of the synergistic action of Cel9B and Cel6D was provided by the fact that (Cel6D+Cel9B) 1000 rev exhibited a markedly decreased fiber length. This result suggests that a combination of biorefining and mechanical refining at 1000 revolutions had an especially strong effect, so refining at lower revolutions is one way of enhancing the physical and mechanical properties of the handsheets without compromising tear index.

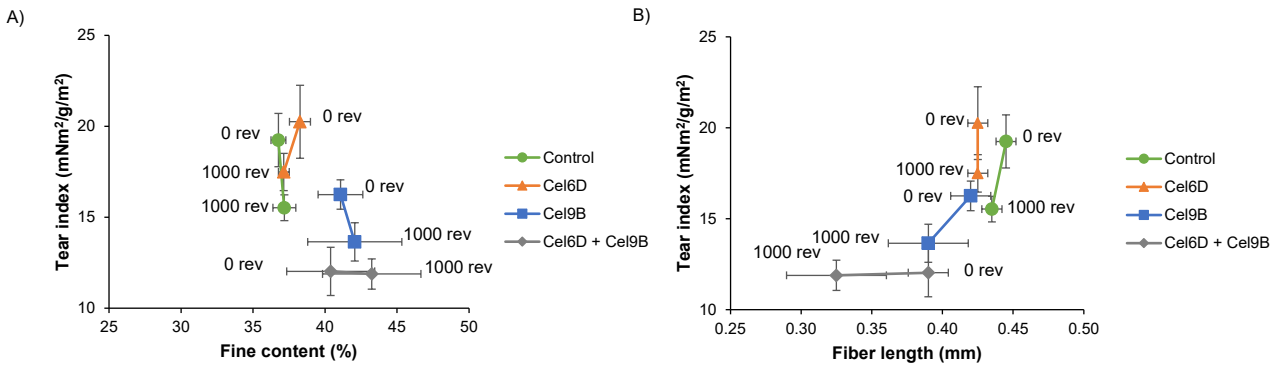

Fig. 7 Tear index as a function of the content in fines (A) and fiber length (B).

Cel6D altered neither fiber length nor the content in fines, so it had a less marked effect on tear resistance. This result is interesting since a decrease in tear strength is a logical consequence of refining and there is great interest in developing technological tools to avoid a reduction in tear strength when refining.

Table 3. Effect of the enzymatic treatments and mechanical refining on burst index and folding endurance

Pulp	Burst index (kN/g)	Folding endurance
0 rev	1.37 ± 0.16	1.38 ± 0.16
1000 rev	1.92 ± 0.02	1.98 ± 0.02
Cel6D 0 rev	1.71 ± 0.44	1.63 ± 0.11
Cel6D + 1000 rev	2.13 ± 0.03	1.94 ± 0.03
Cel9B 0 rev	1.49 ± 0.11	1.58 ± 0.11
Cel9B + 1000 rev	1.89 ± 0.05	2.16 ± 0.05
(Cel6D+Cel9B) 0 rev	1.49 ± 0.15	1.50 ± 0.15
(Cel6D+Cel9B) + 1000 rev	2.12 ± 0.07	1.63 ± 0.07

As can be seen from Table 3, Cel6D, Cel9B and (Cel6D+Cel9B) increased burst index relative to 0 rev handsheets. The increase was especially marked in Cel6D 0 rev (25 %). After mechanical refining, all handsheets exhibited an increased burst strength, the increase being less marked in Cel9B 1000 rev handsheets than in the others. The folding endurance of Cel6D 0 rev, Cel9B 0 rev and (Cel6D+Cel9B) 0 rev was similar to that of the control 0 rev handsheets. Interestingly, with refining, Cel6D 1000 rev and (Cel6D+Cel9B) 1000 rev exhibited a decrease in folding endurance by 2 and 18 %, respectively, relative to 1000 rev handsheets, which once again suggests that the combination of biorefining and mechanical refining at 1000 revolutions was excessive. By contrast, Cel9B 1000 rev handsheets exhibited a folding endurance 9% higher than that of 1000 rev handsheets, a result that testifies to the advantages of this enzyme for enhancing this mechanical property.

4. Conclusions

In this work, we assessed the effect of purified cellulases Cel6D, Cel9B and Cel6D+Cel9B on flax pulp and compared it with that of mechanical refining. The enzymatic treatments by themselves decreased air permeance in the resulting handsheets. As regards mechanical properties, Cel9B increased tensile index and, in combination with mechanical refining, folding endurance as well. Cel6D failed to alter fiber length, so it decreased tear strength to a lesser extent than in the control samples; also, it increased burst index. Finally, a combination of Cel9B

and Cel6D considerably decreased tear strength and folding endurance in the handsheets, which suggests that both enzymes weakened pulp fibers. The enzyme combination increased tensile strength and burst index, but the improvements were due to the individual effects of either enzyme rather than to a synergistic action. The results testify to the potential of Cel9B as a biorefining agent and suggest that Cel6D can also be useful for industrial biorefining of paper. Either enzyme is useful for a specific purpose, but Cel6D has a proven biotechnological potential for application to other types of cellulose fibers.

Acknowledgments

The authors thank the Fermentation Service of the University of Barcelona for technical support in preparing the enzymes in a 50 L bioreactor.

Authors' contributions

LC conducted most of the experiments, collected the data and wrote the manuscript draft. OC took part in the planning of the study, supervised the experiments and checked the results, CB produced the enzymes and contributed to the writing of the manuscript, CV took part in the planning of the study, supervised the experiments and checked the results, MR took part in the planning of the study, supervised the experiments, checked the results and contributed to the writing of the manuscript, SV took part in the planning of the study, supervised the experiments, checked the results and revised the manuscript draft. All authors read and approved the final manuscript.

Funding statement

This work was funded by Spain's Scientific and Technological Research Council (MINECO) through grant CTQ2017-84966-C2-2-R. Verónica Cabañas-Romero acknowledges additional funding in the form of a doctoral fellowship from the Programa Nacional de Becas de Posgrado en el Exterior "Don Carlos Antonio López" of Paraguay's Ministry of Finance.

Data availability

The data supporting the findings of this study are available from the corresponding authors on reasonable request.

Competing interests

The authors have no conflicts of interest to declare.

Consent for publication

All authors have read and commented on the study. Also, all consent to the publication of this work.

Ethics and consent to participate approval

Not applicable.

Human and animal rights statement

This research did not involve any Human Participants and/or Animals.

References

Abd El-Sayed ES, El-Sakhawy M, El-Sakhawy MA-M (2020) Non-wood fibers as raw material for pulp and paper industry. Nord Pulp Paper Res J 35:215–230. https://doi.org/10.1515/npprj-2019-0064

Biermann CJ (1996) Handbook of pulping and papermaking, Elsevier

Bradford MM (1976) A rapid and sensitive method for the quantitation of microgram quantities of protein utilizing the principle of protein-dye binding. Anal Biochem 72:248–54. https://doi.org/10.1006/abio.1976.9999

Cadena EM, Chriac AI, Pastor FIJ, Pastor FIJ, Diaz P, Vidal T, Torres A (2010) Use of cellulases and recombinant cellulose binding domains for refining TCF kraft pulp. Biotechnol Prog 26:960–7. https://doi.org/10.1002/btpr.411

Cerda-Mejía L, Valenzuela SV, Frías C, Diaz P, Pastor FIJ (2017) A bacterial GH6 cellobiohydrolase with a novel modular structure. Appl Microbiol Biotechnol 101:2943–2952. https://doi.org/10.1007/s00253-017-8129-4

Chiriac AI, Cadena EM, Vidal T, Torres AL, Diaz P, Pastor FIJ (2010) Engineering a family 9 processive endoglucanase from *Paenibacillus barcinonensis* displaying a novel architecture. Appl Microbiol Biotechnol 86:1125–1134. https://doi.org/10.1007/s00253-009-2350-8

del Río JC, Rencoret J, Gutiérrez A, Nieto L, Jiménez-Barbero J, Martínez AT (2011) Structural Characterization of Guaiacyl-rich Lignins in Flax (*Linum usitatissimum*) Fibers and Shives. J Agric Food Chem 59:11088–11099. https://doi.org/10.1021/jf201222r

Ferdous T, Ni Y, Quaiyyum MA, Uddin MN, Jahan MS (2021) Non-Wood Fibers: Relationships of Fiber Properties with Pulp Properties. ACS Omega 6:21613–21622. https://doi.org/10.1021/acsomega.1c02933

Ferreira PJ, Matos S, Figueiredo MM (1999) Size Characterization of Fibres and Fines in Hardwood Kraft Pulps. Particle & Particle Systems Characterization 16:20–24. https://doi.org/10.1002/(SICI)1521-4117(199905)16:1<20::AID-PPSC20>3.0.CO;2-M

García O, Torres AL, Colom JF, Pastor FIJ, Diaz P, Vidal T (2002) Effect of cellulase-assisted refining on the properties of dried and never-dried eucalyptus pulp. Cellulose 9(2):115–125. https://doi.org/10.1023/A:1020191622764

Garcia-Ubasart J, Torres AL, Vila C, Pastor FIJ, Vidal T (2013) Biomodification of cellulose flax fibers by a new cellulase. Ind Crops Prod 44:71–76. https://doi.org/10.1016/j.indcrop.2012.10.019

Gil N, Gil C, Amaral ME, Costa A, Duarte AP (2009) Use of enzymes to improve the refining of a bleached *Eucalyptus globulus* kraft pulp. Biochem Eng J 46:89–95. https://doi.org/10.1016/j.bej.2009.04.011

Kmiotek M, Dybka-Stępień K, Karmazyn A (2021) Mild enzymatic treatment of bleached pulp for tissue production. Bioresources 16(2):4221–4236. https://doi.org/10.15376/biores.16.2.4221-4236

Koivula A, Linder M, Teeri T. Structure-function relationships in *Trichoderma* cellulolytic enzymes. In Harman GE, Kubicek CP, editors, *Trichoderma* and *Gliocladium*. Vol. 2. LondonBristol: Taylor & Francis. 1998. p. 3-23

Manian AP, Cordin M, Pham T (2021) Extraction of cellulose fibers from flax and hemp: a review. Cellulose 28:8275–8294. https://doi.org/10.1007/s10570-021-04051-x

Mansfield SD, Gilkes NR, Warren RAJ, Kilburn DG (2002) The Effects of Recombinant *Cellulomonas fimi* β-1,4-glycanases on Softwood Kraft Pulp Fibre and Paper Properties. In: Progress in Biotechnology. pp 301–310

Miller GL (1959) Use of Dinitrosalicylic Acid Reagent for Determination of Reducing Sugar. Anal Chem 31:426–428. https://doi.org/10.1021/ac60147a030

Nagl M, Haske-Cornelius O, Skopek L, Pellis A, Bauer W, Nyanhongo GS, Guebitz G (2021) Biorefining: the role of endoglucanases in refining of cellulose fibers. Cellulose 28(12):7633–7650. https://doi.org/10.1007/s10570-021-04022-2

Pere J, Siika-aho M, Buchert J, Viikari L (1995) Effects of purified *Trichoderma reesei* cellulases on the fiber properties of kraft pulp. Tappi J 78(6):71–78

Pere J, Siika-Aho M, Viikari L (2000) Biomechanical pulping with enzymes: Response of coarse mechanical pulp to enzymatic modification and secondary refining. Biotechnology 83(5):1–8

Przybysz Buzała K, Przybysz P, Kalinowska H, Derkowska M (2016) Effect of Cellulases and Xylanases on Refining Process and Kraft Pulp Properties. PLoS One 11:e0161575. https://doi.org/10.1371/journal.pone.0161575

Quiroz-Castañeda RE and Folch-Mallol JL (2013) Hydrolysis of biomass mediated by cellulases for the production of sugars. Sustainable degradation of lignocellulosic biomass techniques, applications and commercialization. InTech, pp119-155.

Retulainen E (1996) Fiber properties as control variables in papermaking?: Part 1. Fiber properties of key importance in the network. Paperi ja puu 78:187–194

Tomme P, Warren RAJ and Gilkes NR (1995). Cellulose hydrolysis by bacteria and fungi. Adv Microb Physiol *37*:1-81.

Torraspapel (2009) Formación Fabricación de papel. Torraspapel 4–57

Torres CE, Negro C, Fuente E, Blanco A (2012) Enzymatic approaches in paper industry for pulp refining and biofilm control. Appl Microbiol Biotechnol 96:327–344. https://doi.org/10.1007/s00253-012-4345-0

Flax biorefining for paper production

SUPPLEMENTARY INFORMATION

L. Verónica Cabañas-Romero [*a], Oriol Cusola [b], Carolina Buruaga-Ramiro [a], Cristina Valls [b], M. Blanca Roncero [b] and Susana V. Valenzuela [a]

[a] Department of Genetics, Microbiology and Statistics, Faculty of Biology, Universitat de Barcelona, Av. Diagonal 643, 08028 Barcelona, Spain

[b] CELBIOTECH_Paper Engineering Research Group, Universitat Politècnica de Catalunya_BarcelonaTech, 08222 Terrassa, Spain

∗ Corresponding author at Department of Genetics, Microbiology, and Statistics, Faculty of Biology, Universitat de Barcelona, Av. Diagonal 643, 08028, Barcelona, Spain.

S1. Thin-layer chromatograms of hydrolysis products from flax pulp treated with Lane 1: 1 mg Cel9B /odp, Lane 2: 1.5 mg Cel9B/odp, Lane 3: 3 mg Cel9B/odp, Lane 4: negative control without enzyme, Lane 5: 1 mg Cel6D/odp, Lane 6: 1.5 mg Cel6D/odp, Lane 7: 3 mg Cel6D/odp and, Lane 8: negative control without enzyme. Lane M: markers that contain glucose (G1), cellobiose (G2), cellotriose (G3), cellotetraose (G4), and cellopentaose (G5).

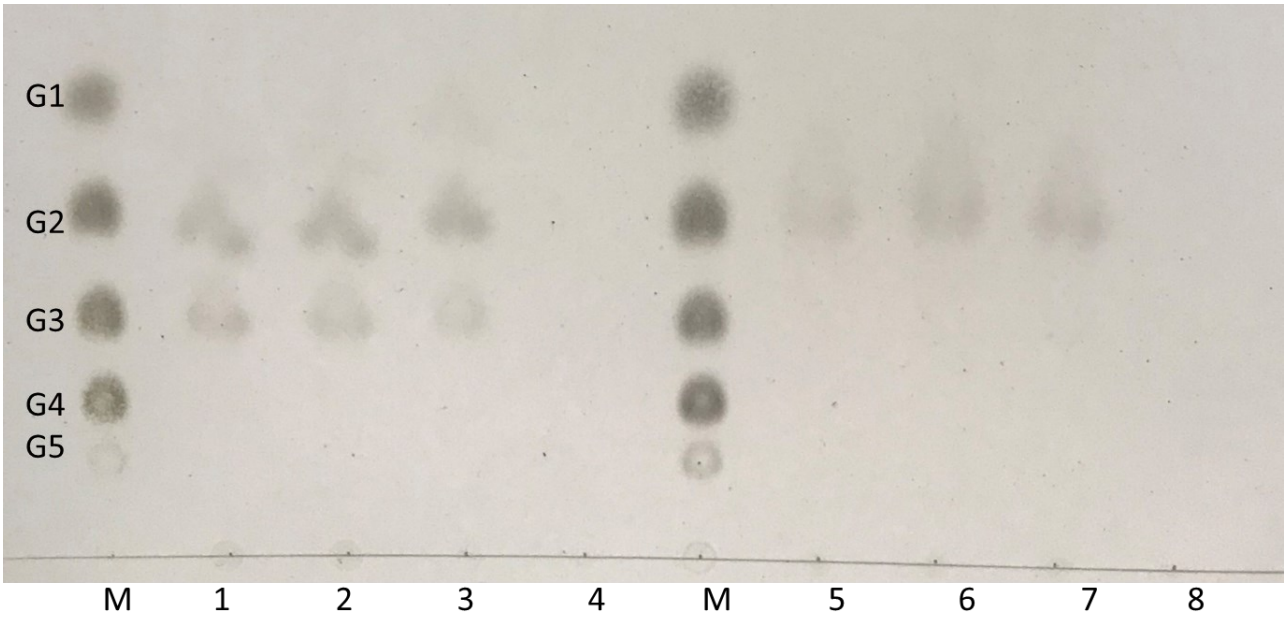

5. DISCUSIÓN GENERAL

5.1 Funcionalización de la celulosa

El primer capítulo se ha centrado en la funcionalización de la celulosa para conferirle nuevas características y, por consiguiente, revalorizar la biomasa celulósica. En este contexto, la celulosa tiene muchas excelentes propiedades que pueden aprovecharse para producir materiales que pueden ser utilizados como dispositivos médicos, *food packaging* u otros bienes de alto valor.

En el primer artículo se describe la obtención de un *nanocomposite* de CB con quitosano. La mezcla de polímeros para producir materiales compuestos con nuevas propiedades ha recibido mucha atención como estrategia para producir nuevos soportes (Bonilla *et al*., 2014; Fortunati *et al*., 2017, 2019). El quitosano y la celulosa tienen estructuras moleculares muy similares, y la mezcla de ambos se facilitaría gracias a la interacción dipolo-dipolo de los grupos amino del quitosano con los grupos hidroxilo de la celulosa.

Para obtener los *nanocomposites* de CB con quitosano, se siguieron dos enfoques: la formación de papel de CB seguida de impregnación por inmersión de hojas de papel con quitosano (BC-ChI); y la impregnación en masa de la pulpa de CB con quitosano seguido de la formación de hojas de papel (BC-ChM). La cantidad de quitosano en los *nanocomposites* se estimó restando la concentración de quitosano en la solución antes y después del procedimiento de impregnación. La proporción de CB-Ch fue de aproximadamente 10:1 y sugería que el quitosano se incorporó a las nanofibras de la red de celulosa. En el proceso de impregnación en masa, las fibras de CB estaban suspendidas en agua, lo que habría facilitado el acceso del quitosano, favoreciendo su interacción con las moléculas de celulosa. En cambio, en la impregnación por inmersión, la accesibilidad del quitosano a las moléculas de celulosa habría sido menor ya que las fibras de CB fueron compactadas y secadas durante el proceso de elaboración del papel. Sin embargo, no se encontraron diferencias significativas en la cantidad de quitosano en los nanocompuestos de CB-Ch, lo que sugiere que el quitosano en los compuestos BC−ChI no solo recubrieron la superficie del papel, sino que también penetró en la matriz porosa de las fibras de CB. Se analizaron los *nanocomposites* por FTIR (*Fourier-transform infrared spectroscopy*) y, aunque los respectivos espectros están dominados por el componente de la celulosa, pequeños picos atribuibles a los grupos amino y amida del quitosano fueron detectados.

Con el fin de determinar si los dos tipos de compuestos presentaban capacidades de retención diferentes, se llevó a cabo un análisis de la migración del quitosano desde las matrices

celulósicas a un medio acuoso y se estimó que más del 90% del quitosano incorporado quedó retenido en ambos *nanocomposites* BC-Ch. Se ha propuesto el uso de membranas de CB-Ch para cubrir heridas ya que la migración progresiva de quitosano hacia la piel tiene propiedades antimicrobianas (Lin *et al*., 2013). Sin embargo, en este trabajo se elaboró un tipo diferente de matriz, el papel, donde la fuerte interacción entre el quitosano y la matriz de CB aseguraría la inmovilización del ligando y, en consecuencia, minimizaría la fuga de las moléculas bioactivas. En la industria del embalaje, una de las propiedades más apreciadas es la retención de aditivos, impidiendo la transferencia de estos compuestos desde el envase hasta el producto. Además, dado que el quitosano es biocompatible y no tóxico, los *nanocomposites* BC-Ch biodegradables podrían ser interesantes para aplicaciones que tienen que estar en contacto con alimentos o productos farmacéuticos.

En cuanto a las propiedades físicas de los nanocomposites no se observaron diferencias significativas entre los resultados obtenidos para los nanocomposites BC−ChI y BC−ChM, lo que sugiere que los dos enfoques para obtener los papeles de BC−Ch generaron matrices similares. Sin embargo, algunas diferencias entre los *nanocomposites* BC-Ch y los papeles de CB fueron observadas: aumento del gramaje y la densidad de los *nanocomposites* BC-Ch respecto a la CB debido a la incorporación del quitosano, disminución de la permeancia al aire y ligero aumento de la lisura de los nanocomposites de BC-Ch. La capacidad de absorción de agua (WAC) de nanocomposites BC−Ch fue menor que la de los papeles de CB, probablemente por la interacción entre los grupos amino del quitosano y los grupos hidroxilo de la celulosa. En consecuencia, habría menos grupos hidroxilo disponibles para interactuar con las moléculas de agua, lo que afectaría el comportamiento de absorción de los nanocomposites.

La elección del quitosano como ligando de la CB se debe a sus propiedades antimicrobianas y antioxidantes (Abd El-Hack *et al*., 2020). Por consiguiente, la capacidad antimicrobiana de los nanocomposites fue evaluada en cuanto a la capacidad de inhibir el crecimiento y capacidad de reducir la viabilidad de *Staphylococcus aureus*, *Pseudomonas aeuroginosa* y *Candida albicans* como modelos de bacterias gram-positiva, gram-negativa y levaduras, respectivamente. Con respecto a la capacidad de inhibir el crecimiento microbiano, la levadura *C. albicans* mostró menos sensibilidad al quitosano que las cepas bacterianas. Además, el quitosano fue más activo contra la bacteria gram-positiva que la gram-negativa. Estas diferencias dependerían de varios factores como son el mecanismo de acción del quitosano y la estructura del microorganismo en sí. Sin embargo, el mecanismo exacto de la acción antimicrobiana del

quitosano no se comprende totalmente. Factores como el peso molecular, el grado de acetilación del quitosano y el pH del medio pueden influir en su acción antimicrobiana (Abd El-Hack *et al*., 2020). Los resultados sugirieron que la membrana lipídica externa en gram-negativos podría conferir cierta protección, dificultando el acceso del quitosano a la célula. Sin embargo, en la literatura no existe un acuerdo general en cuanto al grado de susceptibilidad de los grampositivos, gramnegativos y levaduras al quitosano (Li and Zhuang, 2020). En cuanto a las diferencias entre los nanocomposites BC-Ch, BC-ChI mostró ser más efectiva para inhibir el crecimiento microbiano. Para complementar estos estudios se evaluó además la capacidad de los nanocomposites de BC-Ch de reducir la viabilidad de las células microbianas al sumergir los nanocomposites en una solución de concentración microbiana conocida. Los resultados indicaron que los nanocomposites de BC−Ch no sólo inhibieron el crecimiento microbiano, sino también demostraron una fuerte actividad biocida frente a las cepas ensayadas. Además, la eficacia antimicrobiana de los dos tipos de nanocomposites fue similar, sugiriendo que esta propiedad no dependía del procedimiento seguido para la producción de los BC-Ch.

La CB es una matriz de gran resistencia mecánica y no se desintegra en el agua, lo que permite su reutilización. Una característica interesante de los nanocomposites producidos fue saber si después de sumergirlos en un medio acuoso durante un periodo de tiempo retendrían su actividad antimicrobiana. Para ello, muestras de BC−ChM y BC-ChI que fueron incubadas en agua y secadas fueron empleadas para medir su capacidad de inhibir el crecimiento de *S. aureus*. Ambos nanocomposites mantuvieron su capacidad antibacteriana en un 63% y 51% respectivamente.

Continuando con la caracterización de los *nanocomposites* BC-Ch se evaluó su potencial de inhibir la formación de biofilms. Los biofilms son comunidades microbianas incrustadas en una matriz de polímeros extracelulares fuertemente unidos a la superficie de materiales orgánicos e inorgánicos (Tuon *et al*., 2022). Estos biofilms aumentan la resistencia de los microorganismos a los antimicrobianos y son difíciles de erradicar con agentes de limpieza (Costerton *et al*., 1999; Flemming and Wingender, 2010) por lo que la prevención de su formación es una estrategia importante para tener en cuenta cuando se desarrollan nuevos materiales para aplicaciones biomédicas, farmacéuticas o de envasado. La capacidad de prevenir el crecimiento en los nancomposites de BC-Ch de *P. aeruginosa*, una conocida cepa productora de biofilm, fue estudiada. Las imágenes de microscopía electrónica de barrido revelaron que sobre los papeles de CB había una capa que cubría casi por completo a las fibras de CB, compatible con el crecimiento de células de *P. aeruginosa* y probablemente con el biofilm

producido por el mismo. En los *nanocomposites* BC-Ch esta misma capa también se encontró, pero en menor medida. Para complementar este estudio se evaluó la actividad metabólica de las células que sobre los nanocomposites se habían formado y se detectó menor actividad metabólica atribuible al menor crecimiento de *P. aeruginosa* en los nanocomposites BC-Ch respecto a los papeles de CB, en concordancia con las imágenes obtenidas por SEM (microscopía electrónica de barrido). La reducción de la actividad fue del 68% para BC−ChI y 81% para el BC−ChM respecto a la CB. Estos resultados estuvieron de acuerdo con la inhibición del crecimiento de *P. aeruginosa* comentada más arriba. Los resultados de las imágenes obtenidas por SEM y la actividad microbiana medida sugieren que el quitosano incorporado en los nanocomposites BC−Ch tuvo un fuerte efecto negativo en la formación de biofilm en su superficie. El quitosano se ha estudiado como inhibidor de la formación de biofilms por lo que su aplicación en el campo de la medicina o la industria alimentaria es bastante prometedora (Campana *et al*., 2018; Martinez *et al*., 2010).

Una de las características que hacen que el quitosano sea interesante para aplicaciones en medicina o en la industria del envasado de alimentos es su actividad antioxidante, debida a su grupo amino y sus dos hidroxilos, que pueden reaccionar con los radicales libres (Abd El-Hack *et al*., 2020). Los papeles de CB mostraron una ligera actividad antioxidante que se atribuye a los grupos hidroxilo de la celulosa (Fernandes *et al*., 2020). Por otro lado, cuando se añadió quitosano a la CB, aumentó la actividad antioxidante en ambos tipos de nanocomposites (BC-ChI y BC-ChM). BC−ChI mostró mayor actividad antioxidante que BC−ChM, probablemente debido a que el método de inmersión habría provocado una mayor carga de quitosano en la superficie del compuesto, favoreciendo su exposición al medio ambiente circundante.

Estos resultados tomados en su conjunto sugirieron que la CB es una matriz adecuada para producción de *nanocomposites* de BC-Ch probablemente debido a su elevada área superficial, porosidad y a la red tridimensional de la CB que facilita que los ligandos queden atrapados en dicha red. El quitosano que queda embebido en esta matriz confiere al nuevo material capacidad antimicrobiana y antioxidante.

Otra manera de funcionalizar la celulosa es mediante el cambio en su estructura a través de procedimientos químicos o enzimáticos. Las enzimas pueden modificar las fibras de celulosa de forma más amigable con el medio ambiente que los tratamientos químicos y físicos, confiriendo propiedades novedosas a la celulosa y al papel, siendo herramientas fundamentales para la obtención de nuevos materiales a partir de restos agrícolas y en general de fibras celulósicas. Aunque actualmente existen en el mercado numerosas enzimas con

actividad sobre las fibras, tales como celulasas y xilanasas, el gran potencial de biomodificación enzimática de las fibras conduce a la búsqueda de enzimas con nuevas actividades y al desarrollo de nuevos biocatalizadores para la mejora y valorización de los productos celulósicos. En 2010 se identificó y se caracterizó un nuevo tipo de enzimas: las monooxigenasas líticas de polisacáridos (LPMO), que despolimerizan los polisacáridos por ruptura oxidativa generando grupos carboxílicos, cambiando el paradigma de enzimas disruptoras de polisacáridos (Vaaje-Kolstad *et al*., 2010). Desde su descubrimiento numerosas investigaciones se han llevado a cabo para comprender su mecanismo de acción y desde luego, posibles aplicaciones biotecnológicas.

En el segundo artículo del primer capítulo se desarrolla el estudio de la SamLPMO10C, una enzima clonada en *Escherichia coli* y expresada anteriormente en este grupo de investigación, como herramienta biotecnológica. La enzima se utilizó para funcionalizar las cadenas de celulosa incrementando el contenido de grupos carboxilo. Seguidamente, en un segundo nivel de funcionalización, se introdujo nitrato de plata como fuente de iones de plata que posteriormente fueron reducidos térmicamente a plata elemental produciendo nanopartículas. Finalmente, tras ambas funcionalizaciones se evaluó la capacidad antibacteriana de los soportes celulósicos elaborados.

Primeramente, la enzima recombinante fue producida exitosamente en *E. coli* y purificada a través de su adsorción a Avicel, un protocolo rápido y económico desarrollado con anterioridad en el grupo de investigación. El rendimiento fue de 6 mg/L de cultivo, dentro del rango de rendimiento respecto a otras LPMOs expresadas en *E. coli* (Li *et al*., 2021; Tuveng *et al*., 2020). Posteriormente se verificó la actividad de la enzima, mediante MALDI TOF, sobre PASC (*Phosphoric acid swollen cellulose*) y a continuación sobre otros tipos de sustratos celulósicos: pulpa de eucalipto y celulosa bacteriana. Un aspecto de suma relevancia en el contexto de los tratamientos con LPMOs, es el período de incubación, dado que, si la reacción se lleva a cabo por un tiempo insuficiente, es posible que el rendimiento oxidativo sea bajo. Sin embargo, es posible que se presente una situación en la cual períodos de incubación más prolongados no se traduzcan en una mayor actividad enzimática por lo que un tiempo de incubación más breve podría resultar en un ahorro significativo de tiempo. Por tal razón se ensayaron dos tiempos de reacción enzimática en condiciones estándar de incubación, 36 y 72 horas, cuantificando los productos oxidados solubles liberados por SamLPMO10C. Para ambos sustratos analizados, se observó que la máxima cantidad de ácidos aldónicos fue alcanzada después de 72 horas de reacción. En comparación con el período de reacción de 36 horas, se obtuvo un aumento de

ácidos aldónicos de 2 veces para la pulpa BC y de 1.7 veces para la pulpa de eucalipto. Por consiguiente, se determinó que el tiempo de reacción óptimo para futuras investigaciones sería de 72 horas. Cabe destacar que los valores de ácidos aldónicos totales obtenidos estuvieron dentro del mismo rango que los reportados para el ácido celobiónico en *linters* de algodón (Valls *et al.*, 2019). Los *linters* de algodón son fibras cortas y suaves que se encuentran en la superficie de la semilla de algodón después de que se ha eliminado la fibra principal (Morais *et. al*., 2013). La diferencia en cuanto a productos oxidados solubles provenientes de la CB y eucalipto se debe a que SamLPMO10C tiene preferencia por sustratos cristalinos, tal y como se recoge en un trabajo previo (Valenzuela *et al.*, 2019).

Como el primer objetivo de este estudio fue evaluar el potencial de SamLPMO10C de introducir más grupos carboxilo por acción enzimática, el siguiente paso fue el de la cuantificación de dichos grupos funcionales. Los resultados obtenidos fueron satisfactorios ya que los grupos carboxilo aumentaron en 2.7 y 2 veces para las pastas de CB y eucalipto respectivamente. Valls *et al*., 2019 observaron que los grupos carboxilo de los *linters* de algodón aumentaron en 1.6 veces respecto a la muestra no tratada enzimáticamente. SamLPMO10C logró aumentar con éxito el contenido de grupos carboxilo mediante la oxidación del grupo hidroxilo en la posición C1 de la cadena de celulosa. Por lo tanto, esta enzima sería adecuada para aumentar el contenido de carboxilo en diferentes sustratos celulósicos.

A estos mismos sustratos celulósicos oxidados enzimáticamente y a los controles sin oxidar se añadió una solución de nitrato de plata de concentración conocida como fuente de iones Ag^{+}. Posteriormente estas pastas celulósicas fueron sometidas a lavados para eliminar el exceso de Ag^{+}. Seguidamente se elaboraron los soportes de papel y, a través de tratamiento térmico los iones Ag^{+} se redujeron a Ag^{0}. Los soportes funcionalizados se analizaron mediante SEM y espectroscopía de rayos X de dispersión de energía (EDS), y se caracterizaron en términos de contenido de plata, lixiviación y capacidad antibacteriana.

Las imágenes de microscopía electrónica de barrido revelaron que sobre la superficie de los soportes de papel hechos a partir de la pulpa oxidada con SamLPMO10C y con plata añadida se formaron nanopartículas (NPs). El análisis a través de EDS determinó que estas esferas redondeadas eran NPs de plata (Ag-NPs). En los soportes de CB oxidadas con SamLPMO10C estas Ag-NPs parecían estar embebidas en la matriz de fibras celulósicas, una red tridimensional con poros mucho más pequeños que los presentes en los soportes de eucalipto. Probablemente, esto condicionaría que las Ag-NPs generadas en los soportes de CB (soporte de papel de BC-ox/Ag/TT) sean menores (26 ± 3.21 nm) que las de los soportes de eucalipto

(soporte de papel de eu-ox/Ag/TT) donde se observaron Ag-NPs más grandes (152 ± 43 nm). Por otro lado, en los soportes de papel elaborados a partir de pulpas de celulosa sin oxidar enzimáticamente BC/Ag/TT y eu/Ag/TT no se encontraron Ag-NPs, aunque es muy probable que también existan nanopartículas de plata dentro de estos soportes, ya que los grupos OH actúan como centros de nucleación para la plata (Musino ***et al***., 2021). Las Ag-NPs en los soportes no oxidados podrían estar distribuidas de manera menos uniforme en la matriz en comparación con los soportes que han sido previamente oxidados. Por lo tanto, parece que el estado de dispersión inducido por los grupos carboxilo como resultado de la oxidación enzimática favorece la formación de nanopartículas de plata distribuidas de manera más uniforme en el soporte celulósico.

Este protocolo de oxidación enzimática y posterior adición de un ligando (en este caso plata) podría replicarse para la elaboración de otros tipos de materiales celulósicos funcionalizados con otros metales u otro tipo de sustancia o compuesto de acuerdo con las propiedades que se deseen incorporar a la matriz celulósica.

El contenido de plata de los soportes de CB y eucalipto, así como la migración de este ligando desde sus soportes correspondientes fueron estudiados. Los soportes de papel de eucalipto, tanto, eu/Ag/TT como eu-ox/Ag/TT incorporaron más plata que los soportes de papel de CB (BC/Ag/TT y BC-ox/Ag/TT). Esta diferencia de contenido de plata entre ambos soportes puede deberse a que la red de fibras de celulosa del eucalipto tiene poros más permeables que los soportes de CB. Al oxidar enzimáticamente la pulpa de celulosa de CB y eucalipto se esperó que al incorporar más grupos carboxilo, las cargas negativas en la superficie mejoren el estado de dispersión, como sugieren Musino ***et al.***, 2021, y así, los grupos hidroxilo, los verdaderos puntos de nucleación de las nanopartículas metálicas, pueden atraer más iones metálicos. Esto ha ocurrido con los soportes de CB donde BC-ox/Ag/TT ha incorporado 2.3 veces más plata que su contraparte BC/Ag/TT. Sin embargo, en cuanto a los soportes de eucalipto se ha dado el caso contrario, es decir, eu/Ag/TT ha incorporado más plata que eu-ox/Ag/TT.

Respecto a la migración de la plata, al incubar los soportes en un medio acuoso, la mayoría de la plata incorporada en los soportes de papel funcionalizados se mantuvo retenida, especialmente en los soportes de CB, donde la difusión del ligando fue tan baja como 0.9% para BC-ox/Ag/TT y 2% para BC/Ag/TT. La fina red de fibras de la CB y el tratamiento térmico ayudaron a estabilizar y atrapar las nanopartículas incrustadas en la matriz. En el caso de los soportes de eu, la migración de plata fue mayor que la de los soportes de CB, siendo del 1% para eu/Ag/TT y del 7.4% para eu-ox/Ag/TT. Por tanto, el tipo de soporte celulósico

condicionaría no solo el tamaño de las partículas que se forman si no también la cantidad de ligando y la migración de éste al medio. La difusión del ligando incorporado en los soportes celulósicos es una característica importante para sus futuras aplicaciones. En algunas ocasiones, la difusión del ligando será una característica deseable (por ejemplo, en la difusión de medicamentos), pero en otras ocasiones, una baja difusión será necesaria (por ejemplo, en sensores).

Se conoce desde hace tiempo que la plata tiene propiedades antimicrobianas (Sim ***et al***., 2018) y esa es la razón por la que se ha escogido a este metal como ligando modelo para la elaboración de soportes celulósicos con propiedades antimicrobianas. Para evaluar la capacidad antimicrobiana de los soportes de papel con plata contra *S. aureus* se llevaron a cabo dos tipos de pruebas que se complementan entre sí: una basada en la reducción de la viabilidad de las células y otra basada en la inhibición de la actividad metabólica bacteriana.

En el caso de la evaluación de la reducción de la viabilidad celular, tanto los soportes BC-ox/Ag/TT como eu-ox/Ag/TT inhibieron la viabilidad de *S. aureus*, aunque la reducción de la primera fue más lenta que la del soporte de eucalipto. El efecto más rápido de los soportes de papel funcionalizados de eucalipto se puede atribuir a su mayor contenido de plata. Además, en los soportes de BC-ox/Ag/TT las nanopartículas de plata estarían atrapadas en la matriz de celulosa de manera más eficiente y migrarían en menor cantidad, es decir, para eu-ox/Ag/TT, la difusión de la plata desde esta matriz favoreció el contacto entre la plata y el microorganismo, incrementando su efecto tóxico. Es interesante observar que después de 24 horas de contacto con los papeles funcionalizados con CB y eucalipto, no se contabilizaron células viables.

Por otro lado, se midió el efecto de los soportes de papel funcionalizados sobre el metabolismo de *S. aureus*. Para los soportes de papel eu-ox/Ag/TT, la reducción de la actividad metabólica ocurrió más rápido que para los soportes de papel BC-ox/Ag/TT. A los 30 minutos hubo una reducción del 89% de la actividad metabólica de *S. aureus* en contacto con eu-ox/Ag/TT y una reducción del 24% en el caso de BC-ox/Ag/TT. Estos resultados indicaron que la cantidad de plata incorporada en los soportes de papel fue tóxica para *S. aureus*. Para BC-ox/Ag/TT, la reducción de la actividad metabólica mostró ser gradual en el tiempo y, solo después de 2 horas, se alcanzó un 74% de reducción de la actividad microbiana. Esta actividad antimicrobiana más lenta de BC-ox/Ag/TT es complementaria al ensayo de viabilidad celular explicada anteriormente. Cabe destacar que para BC-ox/Ag/TT hubo un 83 % de reducción de la viabilidad después de 60 minutos, pero solo un 35 % de reducción de la actividad metabólica. Esta aparente diferencia en la capacidad antibacteriana se debe a que las dos pruebas

antimicrobianas utilizadas brindan información diferente pero complementaria. En la prueba de viabilidad, detectan las células que se encontraban en un estado activo, pero no cultivable. Para eu-ox/Ag/TT ocurrió lo mismo, la viabilidad se redujo rápidamente al 100% después de 60 minutos, pero las células aún mostraban actividad metabólica, aunque reducida en un 89%. Esto sugiere que la plata hizo que las células de *S. aureus* se mantuvieron primero en un estado activo, pero no cultivable y luego, finalmente, murieron.

Curiosamente el eucalipto sin tratar también presentó una disminución en el recuento de células viables y actividad metabólica, lo que indica la actividad antimicrobiana de la celulosa de eucalipto en sí misma. Esta característica se ha informado anteriormente para el lino, otra fuente de celulosa vegetal, donde se observó una reducción del 17% en la viabilidad de *S. aureus* después de 1 hora de incubación siguiendo el mismo método estándar ensayado en esta tesis (ASTM International, 2010; Fillat *et al*., 2012). La capacidad antimicrobiana de la celulosa vegetal se debe al xylano y a la lignina residual, que contiene fenoles naturales que no se encuentran en la celulosa bacteriana (Christakopoulos *et al*., 2003; Spasojević *et al*., 2016).

El estudio presentado en esta sección indicó que se pueden obtener soportes de papel tanto de CB como de celulosa de eucalipto funcionalizados por métodos enzimáticos. En este caso, tras la oxidación enzimática y con la adición de plata se consiguieron soportes con capacidad antimicrobiana contra *S. aureus*. Es previsible que se puedan obtener otras funcionalidades por la unión de otros metales. Éstos u otros ligandos pueden facilitar la unión de otro tipo de moléculas, como enzimas, ampliando así la aplicabilidad de estos soportes como papeles bioactivos. A las matrices celulósicas se pueden incorporar otros tipos de ligandos con capacidad antimicrobiana, por ejemplo, EDTA (Li *et al*., 2022).

Los materiales bioactivos, como los descritos en este capítulo son de interés por su potencial participación en el diseño de dispositivos sensores. Algunos envases de última generación son conocidos como "*active packaging*" ya que incorporan componentes o materiales activos con el objetivo de proporcionar funciones adicionales más allá de la simple protección y contención del producto. Estos componentes activos o sensores están diseñados para interactuar con el entorno o el producto envasado con el fin de mejorar su seguridad y vida útil.

5.1 Estrategias de expresión de Monooxigenasas líticas de polisacáridos (LPMOs) y estudio de los efectos que tienen estas enzimas sobre la celulosa.

SamLPMO10C ha demostrado su capacidad de oxidar diferentes tipos de sustratos celulósicos y demostró ser una herramienta interesante para futuras aplicaciones biotecnológicas. Sin embargo, hasta ahora no se la había estudiado en profundidad. En el segundo capítulo de esta tesis se describe, por un lado, la caracterización de SamLPMO10C y otra enzima de la misma familia, ShaLPMO10A, en términos de actividad a diferentes temperaturas y el efecto que tienen sobre la CB como modelo de sustrato cristalino y, por otro lado, el estudio, por primera vez, de la interacción entre la CB y las LPMO en tiempo real. Además, estas enzimas fueron expresadas en *E. coli* y *S. lividans*, esta última como alternativa para producir grandes cantidades de enzimas, uno de los retos biotecnológicos para su aplicación a nivel industrial.

SamLPMO10C y ShaLPMO10A son enzimas bimodulares compuestas por un dominio catalítico AA10 y un módulo de unión a carbohidratos de la familia CBM2. El alineamiento de secuencias reveló que la identidad de secuencia global y la similitud entre ambas enzimas eran del 76 % y el 84 %, respectivamente. Tanto SamLPMO10C como ShaLPMO10A oxidan el C1 de la cadena de celulosa por tanto la cadena oxidada resultante será un ácido aldónico. Ambas enzimas fueron expresadas exitosamente de manera heteróloga en *E. coli* y tras el proceso de purificación por adsorción a Avicel se obtuvieron proteínas activas purificadas con un rendimiento de 6 y 8 mg proteína/Litro de cultivo para SamLPMO10C y ShaLPMO10A respectivamente. Este rendimiento se encuentra en el rango de otras LPMOs expresadas en *E. coli* (Tuveng *et al*., 2020).

Para la expresión homóloga, los genes que codifican SamLPMO10C y ShaLPMO10A se expresaron en *S. lividans*, SL_SamLPMO10C y SL_ShaLPMO10A de aquí en adelante. En los sobrenadantes se observaron bandas prominentes de alrededor de 40 kDa, correspondientes a las masas moleculares aparentes de estas enzimas. A continuación, se evaluó su actividad oxidativa sobre PASC. El análisis MALDI TOF MS mostró picos correspondientes a oligosacáridos oxidados que confirmaron que ambas enzimas eran activas. La expresión de los LPMO recombinantes en *S. lividans* produjo la secreción de estas enzimas al medio extracelular, una característica del hospedador productor que evita el paso de la lisis celular en la producción de proteínas recombinantes. Aunque los respectivos sobrenadantes contenían otras proteínas minoritarias, dependiendo de futuras aplicaciones, se podría utilizar el sobrenadante crudo y evitarse el paso de la purificación.

Los sobrenadantes que contenían SL_SamC y SL_ShaLPMO10A fueron purificados mediante su afinidad a Avicel, aunque el método resultó ser menos eficiente para purificar las LPMO de los sobrenadantes de *S. lividans* en comparación con la homogeneidad lograda con las proteínas heterólogas: en los geles de SDS-PAGE, tras el proceso de purificación, se observaron otras bandas proteicas además de las correspondientes a las LPMOs. Un desafío para próximos trabajos es optimizar el proceso de purificación para estas enzimas expresadas homólogamente. El rendimiento fue de 125 y 90 mg por litro de cultivo para SL_SamLPMO10C y SL_ShaLPMO10A, respectivamente. Este alto rendimiento se ha obtenido con otras enzimas (Berini *et al*., 2020), pero hasta la fecha y según nuestro mejor conocimiento, ninguna LPMO ha sido expresada en *Streptomyces*. Por tanto, *S. lividans* es una candidata interesante para producir LPMOs y otras biomoléculas comercialmente valiosas. Además, esta metodología reduce tiempo y costes en comparación con los procesos convencionales, y la eliminación del paso de purificación simplificaría la producción de enzimas y otras biomoléculas.

El estudio de la actividad sobre PASC de SamLPMO10C y ShaLPMO10A a varias temperaturas reveló que, sobre este sustrato, SamLPMO10C libera oligosacáridos oxidados solubles desde las dos horas de incubación a todas las temperaturas ensayadas. La máxima formación de producto se dio a 40 °C. Para ShaLPMO10A, por otro lado, a todas las temperaturas ensayadas, la formación del producto fue más lenta pero luego la enzima alcanzó niveles más altos de productos de oxidación que SamLPMO10C. La producción máxima se obtuvo también a 40 °C y el rendimiento general de la formación del producto fue mayor para ShaLPMO10A que para SamLPM10C; sin embargo, ambas LPMO demostraron funcionar en un amplio rango de temperaturas, lo que puede ser útil en biorefinerías y otras aplicaciones industriales.

Los prometedores resultados obtenidos con las LPMOs sobre PASC motivaron estudiar la actividad de éstas sobre CB como modelo de sustrato cristalino. La formación de oligosacáridos oxidados solubles a partir de la CB se estudió durante 48 h a 40 °C. Ambas enzimas liberaron productos gradualmente, a las 24 h de reacción la misma cantidad de productos solubles fue detectada, pero finalmente, a las 48 h de reacción, SamLPMO10C produjo más oligosacáridos oxidados solubles que ShaLPMO10A. Estos resultados, tomados en conjunto, demuestran que la actividad de las LPMOs depende, entre otros factores, del tipo de sustrato celulósico. Mientras que la cantidad de productos de reacción sobre PASC fue mayor para ShaLPMO10A, sobre la CB, SamLPMO10C liberó una mayor cantidad de cadenas celulósicas oxidadas solubles.

Para estudiar más a fondo el efecto de SamLPMO10C y ShaLPMO10A sobre la CB, se analizó la fracción insoluble de las reacciones enzimáticas mediante cromatografía de exclusión por tamaño de alta resolución (HPSEC, por sus siglas en inglés). Esta técnica es utilizada para separar y analizar las moléculas en función de su tamaño en una muestra. Acoplado al HPSEC, se encuentra el detector de dispersión de luz láser de múltiples ángulos (MALLS) el cual se basa en la dispersión de la luz láser en diferentes ángulos para obtener información sobre el tamaño y la estructura de las moléculas analizadas y permite, a su vez, determinar la masa molar y la distribución de tamaños de las macromoléculas. Un primer análisis de los patrones de elución de las muestras oxidadas por las enzimas señaló un ligero desplazamiento de los picos de la CB conforme se incrementaba el tiempo de incubación sugiriendo la despolimerización parcial de las cadenas celulósicas. Para obtener más información sobre el efecto de las LPMOs en la masa molar de la CB, se calcularon la *M*w y la *M*n de la CB oxidada por las LPMOs en diferentes tiempos de incubación. *M*w se refiere a la masa molar promedio ponderada y se calcula teniendo en cuenta tanto el peso de cada molécula como su abundancia relativa en la muestra. Las moléculas de mayor tamaño tienen un mayor impacto en el valor de *M*w, ya que su peso se tiene en cuenta de manera proporcional. Por lo tanto, *M*w tiende a ser mayor que *M*n cuando la distribución de tamaños de las moléculas está sesgada hacia las moléculas más grandes. *M*n, por otro lado, se refiere a la masa molar promedio en número y se calcula sumando las masas molares individuales de cada molécula y dividiendo por el número total de moléculas en la muestra. *M*n da una medida del tamaño promedio de las moléculas sin tener en cuenta su peso relativo. Si las moléculas tienen tamaño similar, *M*n y *M*w tendrán valores semejantes. Sin embargo, si hay una amplia variedad de tamaños moleculares, *M*n será menor que *M*w. En la literatura se puede encontrar un amplio rango de masa molar de CB dependiendo de las condiciones de cultivo y de la cepa productora de celulosa (Choi *et al*., 2009; Ono *et al*., 2016). Los resultados de *M*w y *M*n para la CB utilizada en este trabajo fueron 897 ± 31 10^3 g/mol y 615 ± 43 10^3 g/mol, respectivamente. Cuando la CB fue oxidada enzimáticamente con SamLPMO10C o ShaLPMO10A, la longitud de las cadenas de celulosa, expresadas como *M*w y *M*n, disminuyeron gradualmente a partir de 6h de reacción (*M*w = 806 ± 37 10^3 g/mol, *M*n= 628 ± 73 10^3 g/mol para SamLPMO10C y *M*w = 821 ± 19 10^3 g/mol, *M*n= 716 ± 40 g/mol). Las LPMOs crean puntos de corte en la celulosa, por lo tanto, debilitan la cohesión de la arquitectura de ésta (Villares *et al*., 2017), y, en el caso de este estudio, este efecto de debilitamiento parecería ocurrir en las primeras horas de incubación con la enzima ya que poca actividad oxidativa fue cuantificada. Esto permite que la escisión de las cadenas de celulosa aumente conforme se incrementan las horas de incubación alcanzando

valores de *M*w= 663 ± 57 10^3 g/mol, *M*n= 474 ± 60 10^3 g/mol para SamLPMO10C y *M*w= 767 ± 48 10^3 g/mol, *M*n= 415 ± 55 10^3 g/mol para ShaLPMO10A luego de 48 h de reacción enzimática.

La acción de ShaLPMO10A sobre la CB pareció tener más impacto en *M*n en comparación con SamLPMO10C. Esto se reflejó en el índice de polidispersidad (*M*w/*M*n), que aumentó con el tiempo de reacción. El aumento de la polidispersidad causada por esta última enzima sugiere un mecanismo de escisión más "aleatorio" de las cadenas de celulosa. Esto no sucede con SamLPMO10C, en este caso, el índice de polidispersidad aumenta solo ligeramente.

Finalmente, para obtener más información sobre el mecanismo de acción de las LPMOs, se evaluó su interacción con la CB en tiempo real utilizando una microbalanza de cristal de cuarzo con disipación (QCM-D). Mediante el control de cambios en la frecuencia de resonancia ($\Delta f_n/n$), este método proporciona información sobre pequeños cambios de masa. Por lo tanto, un aumento en la frecuencia indica eliminación de masa, mientras que una disminución en la frecuencia muestra adsorción de masa (adsorción o unión de moléculas a la superficie). Los cambios de disipación (ΔD_n) dan información sobre la pérdida de energía en el sistema: cuando aumenta la disipación, la rigidez del sensor de superficie disminuye; mientras tanto, cuando la disipación disminuye, la rigidez del sensor de superficie aumenta.

La inyección de ShaLPMO10A en los sensores de oro recubiertos con CB provocó una notable disminución de las frecuencias y un aumento de las disipaciones, lo que indica la adsorción de la enzima a la CB. Al añadir el ácido ascórbico se notó una pequeña disminución de las frecuencias y un incremento de las disipaciones. Sin embargo, inmediatamente se observó un aumento gradual en las frecuencias lo que sugería una pérdida de masa debido a la actividad enzimática. Por otro lado, disminuyeron las disipaciones lo que significa que aumentó la rigidez de la superficie. Estos cambios continuaron durante el análisis, pero se ralentizaron aproximadamente a los 70 minutos. Resultados similares han sido observados en estudios anteriores (Selig *et. al*., 2017). La eliminación de celulosa por acción de ShaLPMO10A podría dar como resultado una interacción más fuerte entre las cadenas de celulosa restantes y la posterior liberación de agua, lo que puede aumentar la rigidez de la capa de celulosa, de ahí la disminución de disipaciones. Como paso final, se realizó un lavado con buffer durante una hora: el ligero aumento en las frecuencias y la pequeña disminución en las disipaciones se pueden atribuir a las cadenas de celulosa que fueron cortadas anteriormente y quedaron sueltas, pobremente adheridas a su superficie y luego fueron eliminadas con el lavado. Los controles negativos donde no se inyectó enzima, se comportaron de manera diferente, en este caso

cuando se inyectó ácido ascórbico, las frecuencias aumentaron y las disipaciones disminuyeron bruscamente y no gradualmente como en la muestra con la LPMO. En estos controles, con el lavado al final del análisis casi se alcanzaron las condiciones iniciales. Además, la separación de armónicos de frecuencia y disipación cuando se inyectó la enzima mostró un patrón diferente en comparación con el control correspondiente sin enzima, lo que sugiere que los cambios observados en las muestras podrían deberse a la actividad enzimática. El buffer (Tris-HCl pH 6) utilizado en el paso de lavado se recogió para el cribado por MALDI TOF de productos solubles resultado de la escisión enzimática. En el caso de la CB tratada con ShaLPMO10A, no se encontraron productos solubles.

La interacción de SamLPMO10C-CB analizada por QCM-D revela que los cambios son mucho más agudos (no graduales) que en el caso de ShaLPMO10A sugiriendo algún mecanismo de acción/interacción diferente a ésta última. El aumento de frecuencias ha sido menor que la de ShaLPMO10A indicando menor pérdida de masa de CB. El buffer de lavado al final del análisis fue cribado por MALDI TOF y reveló la presencia de oligosacáridos solubles de 4 y 5 grados de polimerización, productos de la acción enzimática.

El análisis de la fracción soluble de las reacciones enzimáticas con CB comentado anteriormente reveló que a las 24 h de reacción (tiempo aproximado de reacción de los análisis por QCM-D) hay cantidades similares de productos oxidados solubles para ambas enzimas, sin embargo, en los análisis QCM-D, sólo se han encontrado productos solubles para la reacción con SamLPMO10C. Es más, los cambios de frecuencias y disipaciones han sido menores para SamLPMO10C. Los resultados de la cuantificación de la fracción soluble y los análisis por QCM-D no son exactamente comparables ya que para el análisis por QCM-D no se añadió H_2O_2 como cosustrato. Se sabe que el peróxido de hidrógeno estimula la actividad de las LPMOs, sin embargo, para estos experimentos no se utilizó H_2O_2 para no añadir una variable más a esta técnica tan sensible que detecta cambios de masa a nanoescala.

De todas maneras, en los análisis con QCM-D hay diferencias en los perfiles de SamLPMO10C y ShaLPMO10A. Una hipótesis para explicar este fenómeno teniendo en cuenta todos los resultados en conjunto es que ShaLPMO10A podría ser una enzima procesiva, es decir, sin disociarse del sustrato (esto se reflejaría en la disminución de $\Delta f_n/n$ del análisis QCM-D cuando la enzima inicialmente se une a la CB) cortaría la cadena de CB (reflejado en el aumento $\Delta f_n/n$ y disminución de (ΔD_n)) generando cadenas de diferentes tamaños, (reflejado en el aumento del índice de polidispersidad y aumento de viscosidad intrínseca de la celulosa comentada anteriormente). Cuando la enzima se ¨desprende¨ de la celulosa es posible que cause la

disrupción, a su vez, de aquellas cadenas inicialmente cortadas lo cual explicaría los productos solubles encontrados en la evaluación de actividad sobre CB y no en los análisis con QCM-D ya que en la incubación para los primeros las condiciones de incubación fueron de agitación lo cual favorecería el ¨desprendimiento¨ de la enzima mientras que con el análisis QCM-D, la incubación fue estática por los requerimientos de la técnica. Para probar o desmentir esta hipótesis podría realizarse experimentos como el perfil de oligosacáridos por HPAEC-PAD a diferentes tiempos y en condiciones estándar de incubación que en esta tesis no se realizó por limitaciones de equipo y tiempo. Otra posibilidad sería prolongar los tiempos de incubación en los análisis por QCM-D y llevar a cabo un perfil de los productos solubles para complementar los datos obtenidos. Además, incorporar H_2O_2 como cosustrato de la reacción, aunque el uso de peróxido de hidrógeno puede ser de ¨doble filo¨ ya que un exceso del mismo causa desactivación de la LPMO por lo que un cuidadoso diseño experimental es necesario (Eijsink *et al*., 2019). Todos estos resultados, tomados en su conjunto, sugieren que, aunque SamLPMO10C y ShaLPMO10A son similares en secuencia aminoacídica, presentan diferencias en cuanto a su preferencia por sustratos y parece ser que difieren en cuanto al mecanismo de corte de la cadena celulósica. Estudios adicionales sobre la interacción en tiempo real entre las LPMO y la celulosa bacteriana, así como otros sustratos celulósicos, pueden proporcionar información valiosa sobre los mecanismos subyacentes a la acción de estas enzimas. Esto, a su vez, puede facilitar la optimización de las condiciones de reacción y conducir a una reducción de costes, ampliando así la gama de aplicaciones de estas enzimas.

5.3 Evaluación de celulasas para el biorefinado

Otro tipo de enzimas de interés biotecnológico son las celulasas. El tercer y último capítulo de la tesis se ha enfocado en el estudio de las celulasas Cel6D y Cel9B de *Paenibacillus barcinonensis* como potenciales agentes biorefinadores. El interés en este tipo de enzimas en la industria papelera está aumentando debido a su potencial para reducir los costes de producción y conseguir un menor impacto medioambiental, así como en la mejora de propiedades del papel.

El refino convencional consiste en un tratamiento mecánico que provoca fibrilación de las fibras celulósicas, ruptura de las paredes celulares primarias y secundarias, formación de finos y disminución de la longitud de las fibras debido al corte. La fibrilación consiste en una modificación de la superficie de las fibras, tanto externa como interna, y aumenta la flexibilidad

de las fibras y mejora sus propiedades de unión. Con el refinado, las paredes primaria y secundaria de la fibra se rompen y se eliminan parcialmente, por lo tanto, se mejoran las uniones fibra a fibra, el área superficial de las fibras aumenta. Todo esto se traduce en mejores propiedades de resistencia del papel. Finalmente, con la formación de finos y el corte de la longitud de la fibra, aumenta la flexibilidad y la densidad del papel, ésta última propiedad causa a su vez, la disminución de la porosidad y la permeancia al aire (Biermann, 1996; Buzala *et al*., 2016). Con el refino convencional se mejora el índice de tracción, estallido y plegado debido al incremento del área superficial de las fibras y a los enlaces que éstas establecen entre sí. Una propiedad que habitualmente se ve disminuida es el índice de desgarro debido a la disminución de la longitud de las fibras.

El biorefinado, un proceso asistido por enzimas, puede ser una opción respetuosa con el medio ambiente para mejorar las propiedades mecánicas del papel. Diversos estudios han descrito que el tratamiento previo de las pastas con celulasas permite reducir el consumo energético (García *et al*., 2002; Pere and Viikari, 2000). Las mejoras introducidas por las enzimas dependen del sustrato, condiciones y tiempo de aplicación y de la enzima misma (Kmiotek *et al*., 2021; Mansfield *et al*., 2002; Nagl *et al*., 2021; Pere *et al*., 1995; Pere and Viikari, 2000). Por ello, la identificación y desarrollo de nuevas celulasas que modifiquen las fibras celulósicas y mejoren las propiedades de los productos papeleros es de gran importancia biotecnológica.

Los estudios sobre la aplicación de la endoglucanasa Cel9B de *P. barcinonensis* antes del refinado mecánico revelaron un aumento notable en las propiedades mecánicas (índice de tracción y explosión) de los papeles hechos a partir de pulpas de eucalipto y lino (Cadena *et al*., 2010; García *et al*., 2002; Garcia-Ubasart *et al*., 2013). Los resultados obtenidos con Cel9B mostraron que, a dosis bajas, la enzima facilita el proceso de refinado, permitiendo un importante ahorro energético, además de mejorar notablemente las propiedades mecánicas del papel. Sin embargo, dosis altas de la enzima debilitaron el papel teniendo por tanto un efecto negativo. Los excelentes resultados obtenidos con Cel9B motivaron el estudio del uso de la exocelulasa Cel6D (Cerda-Mejía *et al*., 2017) como agente biorefinador.

En este trabajo, las celulasas Cel9B y Cel6D fueron expresadas en *E. coli* y purificadas por adsorción a Avicel. Este sencillo método de purificación es económico y fácil de realizar, lo que resulta muy útil y apropiado para aplicaciones industriales. El método se basa en el mismo principio utilizado para purificar las LPMOs estudiadas en el capítulo anterior.

La dosificación de celulasas es muy importante, debido que, si la dosis es muy alta, las propiedades mecánicas del papel pueden verse afectadas drásticamente. Por tanto, se probaron diferentes dosis de Cel6D y Cel9B, aplicadas por separado, para optimizar la dosificación enzimática. Para evaluar el impacto de ambas celulasas sobre su sustrato, se fabricaron papeles con un gramaje ligeramente mayor que los papeles estándar (100 g/m^2 en vez de 75 g/m^2) para visualizar mejor los efectos de las enzimas. Se midieron las siguientes propiedades del papel: permeabilidad al aire, densidad e índice de tracción. El tratamiento enzimático con Cel6D o Cel9B, en todas las dosis ensayadas, condujo a un aumento en la densidad de las fibras, lo que indica que las enzimas hidrolizaron efectivamente las fibras de celulosa y dieron como resultado papeles más compactos. Se determinó una dosis óptima de 1,5 mg/odp (*oven dry pulp*) para ambas enzimas ya que fue la mínima dosis de enzima necesaria para conseguir los mejores resultados de las propiedades ensayadas.

Una vez decidida la dosis enzimática, se aplicaron tres tratamientos con: Cel9B, Cel6D y la combinación de ambas enzimas. Como hipótesis de trabajo se consideró que como la primera es una endoglucanasa procesiva y la segunda, una exoglucanasa, era posible que la sinergia entre ambas se reflejase en la mejora de las propiedades del papel. A otras porciones de pasta de lino con los mismos tratamientos enzimáticos se aplicó además el refinado mecánico.

El efecto de los tres tratamientos enzimáticos es notable en el WRV de las pastas que además fueron refinadas mecánicamente. El aumento de 7, 9 y 10 % para las pastas tratadas con Cel6D, Cel9B y Cel6+Cel9B, respectivamente, indica que las enzimas causan ablandamiento y/o delaminación de las paredes exteriores de las fibras de celulosa.

Las enzimas y el refinado mecánico también causaron cambios en las propiedades del papel. La permeabilidad al aire, únicamente con los tratamientos enzimáticos, disminuyó considerablemente sugiriendo que se obtuvieron papeles más compactos y, por tanto, menos permeables al aire. Cuando se combinó el biorefinado con el refinado mecánico, la permeabilidad al aire se redujo aún más. Los tratamientos enzimáticos produjeron mejoras en las propiedades ópticas (coeficiente *light scattering*) que están ligadas directamente con la forma y tamaño de las fibras e indican la capacidad de unión fibra a fibra. El valor del coeficiente *light scattering* y el grado de unión entre fibras están inversamente relacionados. Curiosamente, los papeles hechos a partir de pasta biorefinada con ambas enzimas y sin el refinado convencional causaron una disminución significativa en este coeficiente indicando que solamente los tratamientos enzimáticos con Cel6D y Cel9B causaron un mayor contacto fibra-fibra en el papel. Sin embargo, al combinar este tratamiento con el refino mecánico, este valor

aumenta ligeramente por lo que es posible que combinación de Cel6D y Cel9B haya resultado excesiva provocando el debilitamiento de las fibras celulósicas.

En cuanto a las propiedades mecánicas, la resistencia a la tracción de los papeles mejoró con los tres tratamientos enzimáticos aplicados siendo la combinación de Cel9B y Cel6D el tratamiento que mejor resultado obtuvo. Cuando se aplicó el refinado mecánico el índice de tracción también mejoró para las tres condiciones. El aumento progresivo de la resistencia a la tracción suele ir acompañado de una disminución gradual de la resistencia al desgarro. Esto no sucede con el biorefinado con Cel6D donde se observó un aumento de la resistencia a la tracción con un ligero detrimento de la resistencia al desgarro. En cambio, los tratamientos con Cel9B y Cel9B+Cel6D causaron una notable disminución de esta propiedad, especialmente cuando las dos enzimas actúan juntas. Cuando se aplicó el refinado mecánico el mismo patrón se repitió, por tanto, Cel6D mejoraría la resistencia a la tracción del papel sin causar una disminución significativa en la resistencia al desgarro. La resistencia al desgarro se ve afectada tanto por la longitud de las fibras como por la proporción de finos y éstos no se vieron mayormente afectados con el tratamiento con Cel6D. Este resultado es interesante ya que la disminución de la resistencia al desgarro es inherente al refinado, y existe mucho interés en desarrollar herramientas tecnológicas para evitar la reducción de la resistencia al desgarro durante este proceso.

No se sabe si la mejora de las propiedades mecánicas del papel se debe al mecanismo de acción de las enzimas (endo o exo celulasas), a la familia de éstas o a la cepa de origen ya que diversos resultados se encuentran en la literatura. En el caso de celulasas de *Cellulomonas fimi* Cel5A y Cel6A, ambas β-1,4-endoglucanasas causaron daños significativos a la resistencia del papel, por otro lado, Cel6B y Cel48C, son dos celobiohidrolasas provenientes de la misma bacteria, pero solamente Cel48C mejoró el índice de tracción del papel (Mansfield *et al*., 2002). En esta tesis se confirma a Cel9B como agente biorefinador y se introduce a Cel6D como otra enzima potencial para tener en cuenta en la industria papelera. La combinación de Cel9B y Cel6D es también muy interesante y abre la puerta para el desarrollo de cócteles enzimáticos que podrían utilizarse como coadyuvantes del proceso de refinado de pastas de lino y porque no, de otras pastas papeleras.

6. Conclusiones

La celulosa se presenta como un destacado candidato para reemplazar derivados del petróleo en diversas aplicaciones. Su abundancia en fuentes renovables, como plantas y residuos agrícolas, la convierte en una opción atractiva desde el punto de vista sostenible. Además, la celulosa ofrece una amplia gama de posibilidades de funcionalización, lo que permite adaptar sus propiedades según las necesidades específicas de cada industria. En este contexto, se han llevado a cabo investigaciones exitosas que han probado diferentes métodos de funcionalización, abriendo así puertas para obtener materiales con propiedades mejoradas y aplicaciones más versátiles. Esto impulsa la transición hacia un mundo más sostenible, donde la utilización de recursos renovables y la disminución de la dependencia de los derivados del petróleo conducen a una sociedad responsable con el medio ambiente.
En particular en el presente trabajo concluimos lo siguiente:

- Se han obtenido *nanocomposites* de CB-Ch a través de dos métodos (impregnación, BC-ChI e inmersión, BC-ChM).
- Los dos métodos de impregnación permitieron una unión estable del quitosano a la matriz de CB.
- Los *nanocomposites* BC-Ch demostraron tener propiedades antimicrobianas y antioxidantes.
- Los *nanocomposites* BC−Ch tienen la consistencia y rigidez de papel y mostraron una gran durabilidad, conservando sus propiedades durante mucho tiempo sin necesidad de un almacenamiento especial.
- Se ha logrado incrementar en 2.7 y 2.4 veces los grupos carboxilo de la CB y celulosa vegetal, (eucalipto), respectivamente, mediante oxidación enzimática con SamLPMO10C.
- Los resultados sugieren que los grupos carboxilo generados por oxidación enzimática de las fibras de celulosa facilitaron la dispersión de éstas por lo que la generación de nanopartículas de plata tras inducción térmica de los soportes de papel a los que se añadió plata ha dado lugar a nanopartículas de plata bien distribuidas.

- Los soportes de papel funcionalizados (BC-ox/Ag/TT y eu-ox/Ag/TT) mostraron una fuerte actividad antibacteriana contra *S. aureus*.
- Se ha obtenido un sistema económico para la expresión homóloga y eficiente de LPMOs activas en *Streptomyces* que prescinde de la purificación estándar.
- SamLPMO10C y ShaLPMO10A son operativas en un amplio rango de temperaturas y difieren en los sustratos óptimos, lo cual es interesante para aplicaciones sostenibles en la industria donde las condiciones de operación pueden variar.
- SamLPMO10C y ShaLPMO10A disminuyen gradualmente la masa molar (tanto M_w como M_n) de las cadenas de celulosa.
- El análisis en tiempo real de la interacción entre CB y SamLPMO10C y ShaLPMO10A sugiere que estas enzimas tienen un mecanismo de interacción con el sustrato diferente una de otra.
- El uso de Cel9B, Cel6D y la combinación de ambas enzimas sobre la pasta de lino, combinado con el refino mecánico causa un aumento del WRV (valor de retención de agua) indicando que estos tratamientos cambian la estructura de las fibras de celulosa, por tanto, actúan como agentes biorefinadores.
- Únicamente con la aplicación de tres tratamientos enzimáticos, Cel9B, Cel6D y Cel9B+Cel6D, se consigue la disminución de la permeancia al aire de los papeles.
- La resistencia a la tracción mejora con los tres tratamientos enzimáticos ensayados, sin embargo, la resistencia al desgarro disminuye notablemente, excepto en los papeles tratados con Cel6D.
- Estos estudios han confirmado el potencial de Cel9B como un agente de biorefinado e introducen a Cel6D como otra enzima biorefinadora a considerar en la industria papelera. Dependiendo de las propiedades deseadas, se puede utilizar una u otra enzima. Cel6D ha demostrado su potencial biotecnológico, el cual puede ser estudiado en otros tipos de fibras de papel.

7. Referencias bibliográficas

Aachmann, F. L., Sørlie, M., Skjåk-Bræk, G., Eijsink, V. G. H. and Vaaje-Kolstad, G. (2012) ¨NMR structure of a lytic polysaccharide monooxygenase provides insight into copper binding, protein dynamics, and substrate interactions¨, *Proceedings of the National Academy of Sciences of the United States of America*, *109*(46), pp. 18779-18784. doi.org/10.1073/pnas.1208822109

Abd El-Hack, M. E., El-Saadony, M. T., Shafi, M. E., Zabermawi, N. M., Arif, M., Batiha, G. E., Khafaga, A. F., Abd El-Hakim, Y. M. and Al-Sagheer, A. A. (2020) ¨Antimicrobial and antioxidant properties of chitosan and its derivatives and their applications: A review¨, *International Journal of Biological Macromolecules*, *164*, pp. 2726-2744. doi.org/10.1016/j.ijbiomac.2020.08.153

Abd El-Sayed, E. S., El-Sakhawy, M. and El-Sakhawy, M. A.-M. (2020) ¨Non-wood fibers as raw material for pulp and paper industry¨, *Nordic Pulp & Paper Research Journal*, *35*(2), pp. 215-230. doi.org/10.1515/npprj-2019-0064

Agger, J. W., Isaksen, T., Várnai, A., Vidal-Melgosa, S., Willats, W. G. T., Ludwig, R., Horn, S. J., Eijsink, V. G. H. and Westereng, B. (2014) ¨Discovery of LPMO activity on hemicelluloses shows the importance of oxidative processes in plant cell wall degradation¨, *Proceedings of the National Academy of Sciences of the United States of America*, *111*(17), pp. 6287-6292. doi.org/10.1073/pnas.1323629111

Álvarez, A. and de Santos, E. (Julio de 2022) ¨*Aspapel presenta el informe anual del sector de la celulosa y el papel*¨. ASPAPEL. http://www.aspapel.es/content/aspapel-presenta-el-informe-anual-del-sector-de-la-celulosa-y-el-papel-2

Antar, M., Lyu, D., Nazari, M., Shah, A., Zhou, X., and Smith, D. L. (2021) ¨Biomass for a sustainable bioeconomy: An overview of world biomass production and utilization¨, *Renewable and Sustainable Energy Reviews*, *139*, p. 110691. doi.org/10.1016/j.rser.2020.110691

Ashokkumar, V., Venkatkarthick, R., Jayashree, S., Chuetor, S., Dharmaraj, S., Kumar, G., Chen, W.-H., and Ngamcharussrivichai, C. (2022) ¨Recent advances in lignocellulosic biomass for biofuels and value-added bioproducts - A critical review¨, *Bioresource technology*, *344*, p. 126195. doi.org/10.1016/j.biortech.2021.126195

Askarian, F., Uchiyama, S., Masson, H., Sørensen, H. V., Golten, O., Bunæs, A. C., Mekasha, S., Røhr, Å. K., Kommedal, E., Ludviksen, J. A., Arntzen, M. Ø., Schmidt, B., Zurich, R. H., van Sorge, N. M., Eijsink, V. G. H., Krengel, U., Mollnes, T. E., Lewis, N. E., Nizet, V. and Vaaje-Kolstad, G. (2021) ¨The lytic polysaccharide monooxygenase CbpD promotes *Pseudomonas aeruginosa* virulence in systemic infection¨, *Nature Communications*, *12*(1), p. 1230. doi.org/10.1038/s41467-021-21473-0

ASTM Standard E2149–01. (2010). Standard test method for determining the antimicrobial activity of immobilized antimicrobial agents under dynamic contact conditions. ASTM International

Attia, M. A. and Brumer, H. (2021) "New Family of Carbohydrate-Binding Modules Defined by a Galactosyl-Binding Protein Module from a *Cellvibrio japonicus* Endo-Xyloglucanase", *Applied and environmental microbiology*, *87*(5), p. e0263420. doi.org/10.1128/AEM.02634-20

Berini, F., Marinelli, F. and Binda, E. (2020) ¨Streptomycetes: Attractive Hosts for Recombinant Protein Production¨, *Frontiers in Microbiology*, *11*, p. 1958 doi.org/10.3389/fmicb.2020.01958

Bhat, M. K. and Bhat, S. (1997) "Cellulose degrading enzymes and their potential industrial applications", *Biotechnology Advances*, *15*(3-4), pp. 583-620. doi.org/10.1016/S0734-9750(97)00006-2

Biermann, C. J. (1996). Handbook of pulping and papermaking. *Elsevier*, pp.158-185.

Bissaro, B. and Eijsink, V. G. H. (2023) ¨Lytic polysaccharide monooxygenases: enzymes for controlled and site-specific Fenton-like chemistry¨, *Essays in Biochemistry*, p. 20220250. doi.org/10.1042/EBC20220250

Bissaro, B., Røhr, Å. K., Müller, G., Chylenski, P., Skaugen, M., Forsberg, Z., Horn, S. J., Vaaje-Kolstad, G. and Eijsink, V. G. H. (2017) ¨Oxidative cleavage of polysaccharides by monocopper enzymes depends on H_2O_2¨, *Nature chemical biology*, *13*(10), pp. 1123-1128. doi.org/10.1038/nchembio.2470

Blanco, A., Díaz, P., Martínez, J., Vidal, T., Torres, A. L. and Pastor, F. I. (1998) ¨Cloning of a new endoglucanase gene from *Bacillus* sp. BP-23 and characterisation of the enzyme. Performance in paper manufacture from cereal straw¨, *Applied microbiology and biotechnology*, *50*(1), pp. 48-54. doi.org/10.1007/s002530051255

Blanco, A. and Pastor, F. I. J. (1993). ¨Characterization of cellulase-free xylanases from the newly isolated *Bacillus* sp. strain BP-23¨, *Canadian Journal of Microbiology*, *39*(12), pp. 1162-1166. doi.org/10.1139/m93-175

Blanco, A., Vidal, T., Colom, J. F. and Pastor, F. I. J. (1995) ¨Purification and properties of xylanase A from alkali-tolerant *Bacillus* sp. strain BP-23¨, *Applied and Environmental Microbiology*, *61*(12), pp. 4468-4470. doi.org/10.1128/aem.61.12.4468-4470.1995

Bonilla, J., Fortunati, E., Atarés, L., Chiralt, A. and Kenny, J. M. (2014) ¨Physical, structural and antimicrobial properties of poly vinyl alcohol-chitosan biodegradable films¨, *Food Hydrocolloids*, *35*, pp. 463-470. doi.org/10.1016/j.foodhyd.2013.07.002

Boraston, A. B., Bolam, D. N., Gilbert, H. J. and Davies, G. J. (2004) "Carbohydrate-binding modules: fine-tuning polysaccharide recognition", *The Biochemical journal*, *382*(3), pp. 769-781. doi.org/10.1042/BJ20040892

Bordenave, N., Grelier, S. and Coma, V. (2010) ¨Hydrophobization and antimicrobial activity of chitosan and paper-based packaging material¨, *Biomacromolecules*, *11*(1), pp. 88-96. doi.org/10.1021/bm9009528

Bornhorst, J. A. and Falke, J. J. (2000) ¨[16] Purification of proteins using polyhistidine affinity tags¨, *Methods in enzymology,* 326, pp. 245-254.

Brown, A.J. (1886) ¨XLIIL-On an acetic ferment which form cellulose¨, *Journal of the Chemical Society, Transactions*, (*49*), pp. *432*-439

Buruaga-Ramiro, C., Fernández-Gándara, N., Cabañas-Romero, L. V., Valenzuela, S. V., Pastor, F. I. J., Diaz, P., and Martinez, J. (2022) ¨Lytic polysaccharide monooxygenases and cellulases on the production of bacterial cellulose nanocrystals¨, *European Polymer Journal*, *163*, p. 110939. doi.org/10.1016/j.eurpolymj.2021.110939

Buzala, K. P., Przybysz, P., Kalinowska, H., & Derkowska, M. (2016) ¨Effect of cellulases and xylanases on refining process and kraft pulp properties¨, *PLoS ONE*, *11*(8), pp. 1-14. doi.org/10.1371/journal.pone.0161575

Cadena, E. M., Chriac, A. I., Pastor, F. I. J., Diaz, P., Vidal, T. and Torres, A. L. (2010) ¨Use of Cellulases and Recombinant Cellulose Binding Domains for Refining TCF Kraft Pulp¨, *Biotechnology progress,* pp. 3-10. doi.org/10.1002/btpr.411

Campana, R., Biondo, F., Mastrotto, F., Baffone, W. and Casettari, L. (2018) ¨Chitosans as new tools against biofilms formation on the surface of silicone urinary catheters¨, *International Journal of Biological Macromolecules*, *118*, pp. 2193-2200. doi.org/10.1016/j.ijbiomac.2018.07.088

Cannella, D., Möllers, K. B., Frigaard, N.-U., Jensen, P. E., Bjerrum, M. J., Johansen, K. S. and Felby, C. (2016) ¨Light-driven oxidation of polysaccharides by photosynthetic pigments and a metalloenzyme¨, *Nature Communications*, *7*(1), p. 11134. doi.org/10.1038/ncomms11134

Cerda, L. A., Valenzuela, S. V., Diaz, P. and Pastor, F. I. J. (2016) ¨New GH16 β-glucanase from *Paenibacillus barcinonensis* BP-23 releases a complex pattern of mixed-linkage oligomers from barley glucan¨, *Biotechnology and Applied Biochemistry*, *63*(1), pp. 51-56. doi.org/10.1002/bab.1348

Cerda-Mejía, L., Valenzuela, S. V., Frías, C., Diaz, P. and Pastor, F. I. J. (2017) ¨A bacterial GH6 cellobiohydrolase with a novel modular structure¨, *Applied Microbiology and Biotechnology*, *101*(7), pp. 2943-2952. doi.org/10.1007/s00253-017-8129-4

Chakraborty, S., Gupta, R., Jain, K. K., Hemansi, S. G. and Kuhad, R. C. (2016) "Cellulases: Application in Wine and Brewery Industry", *New and Future Developments in Microbial Biotechnology and Bioengineering*, pp. 193-200. Elsevier. doi.org/10.1016/B978-0-444-63507-5.00017-4

Chen, R. (2012) ¨Bacterial expression systems for recombinant protein production: *E. coli* and beyond¨, *Biotechnology Advances*, *30*(5), pp. 1102-1107. doi.org/10.1016/j.biotechadv.2011.09.013

Chiriac, A. I., Cadena, E. M., Vidal, T., Torres, A. L., Diaz, P. and Javier Pastor, F. I. (2010) ¨Engineering a family 9 processive endoglucanase from *Paenibacillus barcinonensis* displaying a novel architecture¨, *Applied Microbiology and Biotechnology*, *86*(4), pp. 1125-1134. doi.org/10.1007/s00253-009-2350-8

Christakopoulos, P., Katapodis, P., Kalogeris, E., Kekos, D., Macris, B. J., Stamatis, H. and Skaltsa, H. (2003) ¨Antimicrobial activity of acidic xylo-oligosaccharides produced by family 10 and 11 endoxylanases¨, *International Journal of Biological Macromolecules, 31*(4-5), pp. 171-175.

Chiu, E., Hijnen, M., Bunker, R. D., Boudes, M., Rajendran, C., Aizel, K., Oliéric, V., Schulze-Briese, C., Mitsuhashi, W., Young, V., Ward, V. K., Bergoin, M., Metcal, P. and Coulibaly, F. (2015) ¨Structural basis for the enhancement of virulence by viral spindles and their *in vivo* crystallization¨, *Proceedings of the National Academy of Sciences of the United States of America*, *112*(13), pp. 3973-3978. doi.org/10.1073/pnas.1418798112

Choi, C. N., Song, H. J., Kim, M. J., Chang, M. H. and Kim, S. J. (2009) ¨Properties of bacterial cellulose produced in a pilot-scale spherical type bubble column bioreactor¨, *Korean Journal of Chemical Engineering*, *26*(1), pp. 136-140. doi.org/10.1007/s11814-009-0021-1

Chylenski, P., Bissaro, B., Sørlie, M., Røhr, Å. K., Várnai, A., Horn, S. J. and Eijsink, V. G. H. (2019) ¨Lytic Polysaccharide Monooxygenases in Enzymatic Processing of Lignocellulosic Biomass¨, *ACS Catalysis*, *9*(6), pp. 4970-4991. doi.org/10.1021/acscatal.9b00246

Ciano, L., Davies, G. J., Tolman, W. B. and Walton, P. H. (2018) ¨Bracing copper for the catalytic oxidation of C–H bonds¨, *Nature Catalysis*, *1*(8), pp. 571-577. doi.org/10.1038/s41929-018-0110-9

Colom P., J. F., García H., J. A., and Torres L., A.L. (1984). Introducción histórica a la fabricación del papel y pastas. *Escuela Técnica Superior de Ingenieros Industriales*. *Departamento de Industria Papelera y Gráfica*.

Cosgrove, D. J., Li, L. C., Cho, H. T., Hoffmann-Benning, S., Moore, R. C. and Blecker, D. (2002) ¨The growing world of expansins¨, *Plant and Cell Physiology*, *43*(12), pp. 1436-1444. doi.org/10.1093/pcp/pcf180

Costerton, J. W., Stewart, P. S. and Greenberg, E. P. (1999) ¨Bacterial biofilms: A common cause of persistent infections¨, *Science*, *284*(5418), pp. 1318-1322. doi.org/10.1126/science.284.5418.1318

Crouvisier-Urion, K., Bodart, P. R., Winckler, P., Raya, J., Gougeon, R. D., Cayot, P., Domenek, S., Debeaufort, F. and Karbowiak, T. (2016) ¨Biobased Composite Films from Chitosan and Lignin: Antioxidant Activity Related to Structure and Moisture¨, *ACS Sustainable Chemistry & Engineering*, *4*(12), pp. 6371-6381. doi.org/10.1021/acssuschemeng.6b00956

Davies, G. and Henrissat, B. (1995) "Structures and mechanisms of glycosyl hydrolases", *Structure*, *3*(9), pp. 853-859. doi.org/10.1016/S0969-2126(01)00220-9

del Río, J. C., Rencoret, J., Gutiérrez, A., Nieto, L., Jiménez-Barbero, J. and Martínez, Á. T. (2011) ¨Structural characterization of guaiacyl-rich lignins in flax (*Linum usitatissimum*) fibers and shives¨, *Journal of agricultural and food chemistry*, *59*(20), pp. 11088-11099. doi.org/10.1021/jf201222r

Deligey, F., Frank, M. A., Cho, S. H., Kirui, A., Mentink-Vigier, F., Swulius, M. T., Nixon, B. T., and Wang, T. (2022) ¨Structure of *In Vitro* -Synthesized Cellulose Fibrils Viewed by Cryo-Electron Tomography and ^{13}C Natural-Abundance Dynamic Nuclear Polarization Solid-State NMR¨, *Biomacromolecules*, *23*(6), pp. 2290-2301. doi.org/10.1021/acs.biomac.1c01674

Dhiman, T. R., Zaman, M. S., Gimenez, R. R., Walters, J. L. and Treacher, R. (2002) "Performance of dairy cows fed forage treated with fibrolytic enzymes prior to feeding", *Animal Feed Science and Technology*, *101*(1-4), pp. 115-125. doi.org/10.1016/S0377-8401(02)00177-3

Díaz, M., Ferreras, E., Moreno, R., Yepes, A., Berenguer, J. and Santamaría, R. (2008) ¨High-level overproduction of *Thermus* enzymes in *Streptomyces lividans¨, Applied Microbiology and Biotechnology*, *79*(6), pp. 1001-1008. doi.org/10.1007/s00253-008-1495-1

Drula, E., Garron, M. L., Dogan, S., Lombard, V., Henrissat, B. and Terrapon, N. (2022) "The carbohydrate-active enzyme database: functions and literature", *Nucleic acids research*, *50*(D1), pp. D571-D577.

Eijsink, V. G. H., Petrovic, D., Forsberg, Z., Mekasha, S., Røhr, Å. K., Várnai, A., Bissaro, B. and Vaaje-Kolstad, G. (2019) ¨On the functional characterization of lytic polysaccharide monooxygenases (LPMOs)¨, *Biotechnology for Biofuels*, *12*(1), pp. 1-17. doi.org/10.1186/s13068-019-1392-0

Fernandes, I. de A. A., Pedro, A. C., Ribeiro, V. R., Bortolini, D. G., Ozaki, M. S. C., Maciel, G. M., and Haminiuk, C. W. I. (2020). ¨Bacterial cellulose: From production optimization to new applications¨, *International Journal of Biological Macromolecules*, *164*, pp. 2598-2611. doi.org/10.1016/j.ijbiomac.2020.07.255

Fernández-Ábalos, J. M., Sánchez, P., Coll, P. M., Villanueva, J. R., Pérez, P. and Santamaría, R. I. (1992) ¨Cloning and nucleotide sequence of celA1, and endo-beta-1, 4-glucanase-encoding gene from *Streptomyces halstedii* JM8¨, *Journal of bacteriology, 174*(20), pp. 6368-6376.

Fillat, A., Martínez, J., Valls, C., Cusola, O., Roncero, M. B., Vidal, T., Valenzuela, S.V., Díaz, Pilar and Pastor, F.I.J. (2018) ¨Bacterial cellulose for increasing barrier properties of paper products¨, *Cellulose, 25,* pp. 6093-6105.

Flemming, H.-C. and Wingender, J. (2010) ¨The biofilm matrix¨, *Nature Reviews Microbiology*, *8*(9), pp. 623-633. doi.org/10.1038/nrmicro2415

Forsberg, Z., Mackenzie, A. K., Sørlie, M., Røhr, Å. K., Helland, R., Arvai, A. S., Vaaje-Kolstad, G. and Eijsink, V. G. H. (2014) ¨Structural and functional characterization of a conserved pair of bacterial cellulose-oxidizing lytic polysaccharide monooxygenases¨, *Proceedings of the National Academy of Sciences*, *111*(23), pp. 8446-8451. doi.org/10.1073/pnas.1402771111

Forsberg, Z., Vaaje-kolstad, G., Westereng, B., Bunsæ, A. C., Stenstrøm, Y., Mackenzie, A., Sørlie, M., Horn, S. J. and Eijsink, V. G. H. (2011) ¨Cleavage of cellulose by a CBM33 protein¨, *Protein Science*, *20*(9), pp. 1479-1483. doi.org/10.1002/pro.689

Fortunati, E., Giovanale, G., Luzi, F., Mazzaglia, A., Kenny, J. M., Torre, L. and Balestra, G. M. (2017) ¨Effective postharvest preservation of kiwifruit and romaine lettuce with a chitosan hydrochloride coating¨, *Coatings*, *7*(11), p. 196. doi.org/10.3390/coatings7110196

Fortunati, E., Mazzaglia, A. and Balestra, G. M. (2019) ¨Sustainable control strategies for plant protection and food packaging sectors by natural substances and novel nanotechnological approaches¨ *Journal of the Science of Food and Agriculture*, *99*(3), pp. 986-1000. doi.org/10.1002/jsfa.9341

Frommhagen, M., Sforza, S., Westphal, A. H., Visser, J., Hinz, S. W. A., Koetsier, M. J., van Berkel, W. J. H., Gruppen, H. and Kabel, M. A. (2015) ¨Discovery of the combined oxidative cleavage of plant xylan and cellulose by a new fungal polysaccharide monooxygenase¨, *Biotechnology for Biofuels*, *8*(1), pp. 4-15. doi.org/10.1186/s13068-015-0284-1

Gallardo, Ó., Pastor, F. I. J., Polaina, J., Diaz, P., Łysek, R., Vogel, P., Isorna, P., González, B. and Sanz-Aparicio, J. (2010) ¨Structural Insights into the Specificity of Xyn10B from *Paenibacillus barcinonensis* and Its Improved Stability by Forced Protein Evolution¨, *Journal of Biological Chemistry*, *285*(4), pp. 2721-2733. doi.org/10.1074/jbc.M109.064394

García, O., Torres, A. L., Colom, J. F., Pastor, F. I. J., Díaz, P. and Vidal, T. (2002) ¨Effect of cellulase-assisted refining on the properties of dried and never-dried eucalyptus pulp¨, *Cellulose*, *9*(2), pp. 115-125. doi.org/10.1023/A:1020191622764

García Hortal, J. A. (1986) ¨Fibras papeleras de origen natural¨, *Escuela Técnica Superior de Ingenieros Industriales. Departamento de Industria Papelera y Gráfica*.

Garcia-Ubasart, J., Torres, A. L., Vila, C., Pastor, F. I. J. and Vidal, T. (2013) ¨Biomodification of cellulose flax fibers by a new cellulase¨, *Industrial Crops and Products*, *44*, pp. 71-76. doi.org/10.1016/j.indcrop.2012.10.019

Garda, A. L., Fernández-Ábalos, J. M., Sánchez, P., Ruiz-Arribas, A. and Santamaría, R. (1997) ¨Two genes encoding an endoglucanase and a cellulose-binding protein are clustered and co-regulated by a TTA codon in *Streptomyces halstedii* JM8¨, *Biochemical journal*, *324*(*2),* pp. 403-411.

Geyer, R., Jambeck, J. R., & Law, K. L. (2017) ¨Production, use, and fate of all plastics ever made¨, Science advances, 3(7), p. e1700782. https://doi.org/10.1126/sciadv.1700782

Gharehkhani, S., Sadeghinezhad, E., Kazi, S. N., Yarmand, H., Badarudin, A., Safaei, M. R. and Zubir, M. N. M. (2015) ¨Basic effects of pulp refining on fiber properties—A review¨, *Carbohydrate Polymers*, *115*, pp. 785-803. doi.org/10.1016/j.carbpol.2014.08.047

Gil, N., Gil, C., Amaral, M. E., Costa, A. P. and Duarte, A. P. (2009) "Use of enzymes to improve the refining of a bleached *Eucalyptus globulus* kraft pulp", *Biochemical Engineering Journal*, *46*(2), pp. 89-95. doi.org/10.1016/j.bej.2009.04.011

Hangasky, J. A., Iavarone, A. T. and Marletta, M. A. (2018). ¨Reactivity of O_2 versus H_2O_2 with polysaccharide monooxygenases¨, *Proceedings of the National Academy of Sciences*, *115*(19), pp. 4915-4920. doi.org/10.1073/pnas.1801153115

Hemsworth, G. R., Ciano, L., Davies, G. J. and Walton, P. H. (2018) ¨Production and spectroscopic characterization of lytic polysaccharide monooxygenases¨, *Methods in Enzymology, 613*, pp. 63-90. doi.org/10.1016/bs.mie.2018.10.014

Hestrin, S., and Schramm, M. (1954) ¨Synthesis of cellulose by *Acetobacter xylinum*. 2. Preparation of freeze-dried cells capable of polymerizing glucose to cellulose¨, *The Biochemical journal*, *58*(2), pp. 345-352. doi.org/10.1042/bj0580345

Horn, S. J., Vaaje-Kolstad, G., Westereng, B. and Eijsink, V.G.H. (2012) ¨Novel enzymes for the degradation of cellulose¨, Biotechnology *for Biofuels*, *5*(1), p. 45. doi.org/10.1186/1754-6834-5-45

Hu, S.-Q., Gao, Y.-G., Tajima, K., Sunagawa, N., Zhou, Y., Kawano, S., Fujiwara, T., Yoda, T., Shimura, D., Satoh, Y., Munekata, M., Tanaka, I., and Yao, M. (2010) ¨Structure of bacterial cellulose synthase subunit D octamer with four inner passageways¨, *Proceedings of the National Academy of Sciences of the United States of America*, *107*(42), pp. 17957-17961. doi.org/10.1073/pnas.1000601107

Infanzón, B., Valenzuela, S. V., Fillat, A., Pastor, F. I. J. and Diaz, P. (2014) ¨Unusual carboxylesterase bearing a GGG(A)X-type oxyanion hole discovered in *Paenibacillus barcinonensis* BP-23¨, *Biochimie*, *104*(1), pp. 108-116. doi.org/10.1016/j.biochi.2014.06.003

Ishihara, M., Matsunaga, M., Hayashi, N., and Tišler, V. (2002) ¨Utilization of d-xylose as carbon source for production of bacterial cellulose¨, *Enzyme and Microbial Technology*, *31*(7), pp. 986-991. doi.org/10.1016/S0141-0229(02)00215-6

Jacek, P., Dourado, F., Gama, M., and Bielecki, S. (2019) ¨Molecular aspects of bacterial nanocellulose biosynthesis¨, *Microbial Biotechnology*, *12*(4), pp. 633-649. doi.org/10.1111/1751-7915.13386

Jordan, D. B., Bowman, M. J., Braker, J. D., Dien, B. S., Hector, R. E., Lee, C. C., Mertens, J. A., and Wagschal, K. (2012) ¨Plant cell walls to ethanol¨, *The Biochemical journal*, *442*(2), pp. 241-252. doi.org/10.1042/BJ20111922

Keshk, S. M. (2014) ¨Bacterial Cellulose Production and its Industrial Applications¨, *Journal of Bioprocessing & Biotechniques*, *04*(02), p. 150. doi.org/10.4172/2155-9821.1000150

Kirby, R. (2005) ¨Actinomycetes and lignin degradation¨, *Advances in Applied Microbiology*, *58*(05), pp. 125-168. doi.org/10.1016/S0065-2164(05)58004-3

Klemm, D., Heublein, B., Fink, H.-P., and Bohn, A. (2005) ¨Cellulose: fascinating biopolymer and sustainable raw material¨, *Angewandte Chemie International edition*, *44*(22), pp. 3358-3393. doi.org/10.1002/anie.200460587

Klemm, D., Petzold-Welcke, K., Kramer, F., Richter, T., Raddatz, V., Fried, W., Nietzsche, S., Bellmann, T., and Fischer, D. (2021) ¨Biotech nanocellulose: A review on progress in product design and today's state of technical and medical applications¨, *Carbohydrate Polymers*, *254*, p. 117313. doi.org/10.1016/j.carbpol.2020.117313

Kmiotek, M., Dybka-Stępień, K., and Karmazyn, A. (2021) "Mild enzymatic treatment of bleached pulp for tissue production", *BioResources*, *16*(2), pp. 4221-4236. doi.org/10.15376/biores.16.2.4221-4236

Kommedal, E. G., Angeltveit, C. F., Klau, L. J., Ayuso-Fernández, I., Arstad, B., Antonsen, S. G., Stenstrøm, Y., Ekeberg, D., Gírio, F., Carvalheiro, F., Horn, S. J., Aachmann, F. L. and Eijsink, V. G. H. (2023) ¨Visible light-exposed lignin facilitates cellulose solubilization by lytic polysaccharide monooxygenases¨, *Nature Communications*, *14*(1), p.1063. doi.org/10.1038/s41467-023-36660-4

Kracher, D., Scheiblbrandner, S., Felice, A. K. G., Breslmayr, E., Preims, M., Ludwicka, K., Haltrich, D., Eijsink, V. G. H. and Ludwig, R. (2016) ¨Extracellular electron transfer systems fuel cellulose oxidative degradation¨, *Science*, *352*(6289), pp. 1098-1101. doi.org/10.1126/science.aaf3165

Kucharska, K., Rybarczyk, P., Hołowacz, I., Łukajtis, R., Glinka, M. and Kamiński, M. (2018) "Pretreatment of Lignocellulosic Materials as Substrates for Fermentation Processes", *Molecules*, *23*(11), p. 2937. doi.org/10.3390/molecules23112937

Lam, E., Male, K. B., Chong, J. H., Leung, A. C. W., and Luong, J. H. T. (2012) ¨Applications of functionalized and nanoparticle-modified nanocrystalline cellulose¨, *Trends in Biotechnology*, *30*(5), pp. 283-290. doi.org/10.1016/j.tibtech.2012.02.001

Lee, K.-Y., Buldum, G., Mantalaris, A., and Bismarck, A. (2014) ¨More than meets the eye in bacterial cellulose: biosynthesis, bioprocessing, and applications in advanced fiber composites¨, *Macromolecular bioscience*, *14*(1), pp. 10-32. doi.org/10.1002/mabi.201300298

Lewis, G. E., Hunt, C. W., Sanchez, W. K., Treacher, R., Pritchard, G. T. and Feng, P. (1996) "Effect of Direct-Fed Fibrolytic Enzymes on the Digestive Characteristics of a Forage-Based Diet Fed to Beef Steers", *Journal of Animal Science*, *74*(12), pp. 3020-3028. doi.org/10.2527/1996.74123020x

Li, J., Solhi, L., Goddard-Borger, E. D., Mathieu, Y., Wakarchuk, W. W., Withers, S. G. and Brumer, H. (2021) ¨Four cellulose-active lytic polysaccharide monooxygenases from *Cellulomonas* species¨, *Biotechnology for Biofuels*, *14*(1), p. 29. doi.org/10.1186/s13068-020-01860-3

Li, J. and Zhuang, S. (2020) ¨Antibacterial activity of chitosan and its derivatives and their interaction mechanism with bacteria: Current state and perspectives¨, *European Polymer Journal*, *138*, p. 109984. doi.org/10.1016/j.eurpolymj.2020.109984

Li, R., Liu, K., Huang, X., Li, D., Ding, J., Liu, B. and Chen, X. (2022) ¨Bioactive Materials Promote Wound Healing through Modulation of Cell Behaviors¨, *Advanced Science*, *9*(10), pp. 1-22. doi.org/10.1002/advs.202105152

Lin, W.-C., Lien, C.-C., Yeh, H.-J., Yu, C.-M. and Hsu, S. (2013) ¨Bacterial cellulose and bacterial cellulose-chitosan membranes for wound dressing applications¨, *Carbohydrate polymers*, *94*(1), pp. 603-611. doi.org/10.1016/j.carbpol.2013.01.076

Lin, X., Wu, Z., Zhang, C., Liu, S. and Nie, S. (2018) ¨Enzymatic pulping of lignocellulosic biomass¨, *Industrial Crops and Products*, *120*, pp. 16-24. doi.org/10.1016/j.indcrop.2018.04.033

Liu, S., Qamar, S. A., Qamar, M., Basharat, K., and Bilal, M. (2021) ¨Engineered nanocellulose-based hydrogels for smart drug delivery applications¨, *International Journal of Biological Macromolecules*, *181*, pp. 275-290. doi.org/10.1016/j.ijbiomac.2021.03.147

Lumiainen, J. (2000) ¨Refining of chemical pulp¨, *Papermaking – Part 1(8)*, pp. 87-121.

Manan, S., Ullah, M. W., Ul-Islam, M., Shi, Z., Gauthier, M., and Yang, G. (2022) ¨Bacterial cellulose: Molecular regulation of biosynthesis, supramolecular assembly, and tailored structural and functional properties¨, *Progress in Materials Science*, *129*, p. 100972. doi.org/10.1016/j.pmatsci.2022.100972

Mansfield, S. D., Gilkes, N. R., Warren, R. A. J. and Kilburn, D. G. (2002) ¨The Effects of Recombinant Cellulomonas fimi β-1,4-glycanases on Softwood Kraft Pulp Fibre and Paper Properties¨, *Progress in Biotechnology,* 21(C), pp. 301-310. doi.org/10.1016/S0921-0423(02)80033-8

Martinez, L. R., Mihu, M. R., Han, G., Frases, S., Cordero, R. J. B., Casadevall, A., Friedman, A. J., Friedman, J. M. and Nosanchuk, J. D. (2010) ¨The use of chitosan to damage *Cryptococcus neoformans* biofilms¨, *Biomaterials*, *31*(4), pp. 669-679. doi.org/10.1016/j.biomaterials.2009.09.087

Matthysse, A. G., Marry, M., Krall, L., Kaye, M., Ramey, B. E., Fuqua, C., and White, A. R. (2005) ¨The effect of cellulose overproduction on binding and biofilm formation on roots by *Agrobacterium*

tumefaciens¨, Molecular Plant-Microbe Interactions, *18*(9), pp. 1002-1010. doi.org/10.1094/MPMI-18-1002

Merino, S. T. and Cherry, J. (2007) ¨Progress and challenges in enzyme development for biomass utilization¨, *Advances in Biochemical Engineering/Biotechnology*, *108*, pp. 95-120. doi.org/10.1007/10_2007_066

Moon, M., Lee, J. P., Park, G. W., Lee, J. S., Park, H. J. and Min, K. (2022) ¨Lytic polysaccharide monooxygenase (LPMO)-derived saccharification of lignocellulosic biomass¨, *Bioresource Technology*, *359*, p. 127501. doi.org/10.1016/j.biortech.2022.127501

Moon, R. J., Martini, A., Nairn, J., Simonsen, J., and Youngblood, J. (2011) ¨Cellulose nanomaterials review: structure, properties and nanocomposites¨, *Chemical Society reviews*, *40*(7), pp. 3941-3994. doi.org/10.1039/c0cs00108b

Morena, A. G., Roncero, M. B., Valenzuela, S. V., Valls, C., Vidal, T., Pastor, F. I. J., Diaz, P. and Martínez, J. (2019) ¨Laccase/TEMPO-mediated bacterial cellulose functionalization: production of paper-silver nanoparticles composite with antimicrobial activity¨, *Cellulose*, *26*(16), pp. 8655-8668. doi.org/10.1007/s10570-019-02678-5

Morais, J. P. S., de Freitas Rosa, M., Nascimento, L. D., Do Nascimento, D. M. and Cassales, A. R. (2013) ¨Extraction and characterization of nanocellulose structures from raw cotton linter¨, *Carbohydrate polymers, 91*(1), pp. 229-235.

Musino, D., Devcic, J., Lelong, C., Luche, S., Rivard, C., Dalzon, B., Landrot, G., Rabilloud, T. and Capron, I. (2021) ¨Impact of physico-chemical properties of cellulose nanocrystal/silver nanoparticle hybrid suspensions on their biocidal and toxicological effects¨, *Nanomaterials*, *11*(7), p. 1862. doi.org/10.3390/nano11071862

Nagl, M., Haske-Cornelius, O., Skopek, L., Pellis, A., Bauer, W., Nyanhongo, G. S. and Guebitz, G. (2021) "Biorefining: the role of endoglucanases in refining of cellulose fibers", *Cellulose*, *28*(12), pp. 7633-7650. doi.org/10.1007/s10570-021-04022-2

Omadjela, O., Narahari, A., Strumillo, J., Mélida, H., Mazur, O., Bulone, V., and Zimmer, J. (2013) ¨BcsA and BcsB form the catalytically active core of bacterial cellulose synthase sufficient for in vitro cellulose synthesis¨, *Proceedings of the National Academy of Sciences*, *110*(44), pp. 17856-17861. doi.org/10.1073/pnas.1314063110

Ono, Y., Tanaka, R., Funahashi, R., Takeuchi, M., Saito, T. And Isogai, A. (2016) ¨SEC–MALLS analysis of ethylenediamine-pretreated native celluloses in LiCl/N,N-dimethylacetamide: softwood kraft pulp and highly crystalline bacterial, tunicate, and algal celluloses¨, *Cellulose*, *23*(3), pp. 1639-1647. doi.org/10.1007/s10570-016-0948-4

Panyella, I. (2005) "El papiro egipcio: el primer libro de la historia", *Asnabi*, *34*(17), pp. 17-23.

Payen, A. (1838) ¨Mémoire sur la composition du tissu propre des plantes et du ligneux¨, *Comptes rendus*, 7, pp. 1052-1056

Pedersen, G. B., Blaschek, L., Frandsen, K. E. H., Noack, L. C., and Persson, S. (2023) ¨Cellulose synthesis in land plants¨, *Molecular Plant*, *16*(1), pp. 206-231. doi.org/10.1016/j.molp.2022.12.015

Pere, J., Siika-aho, M., Buchert, J. and Viikari, L. (1995) "Effects of purified *Trichoderma reesei* cellulases on the fiber properties of kraft pulp", *Tappi journal*, *78*(6), pp. 71-78.

Pere, J., Sikka-Aho, Matti and, Viikari, L. (2000) "Biochemical pulping with enzymes: Response of coarse mechanical pulp to enzymatic modification and seconday refining", *Tappi Journal*, *83*(5), pp. 1-8.

Pinheiro, G. L., de Azevedo-Martins, A. C., Albano, R. M., de Souza, W. and Frases, S. (2017) ¨Comprehensive analysis of the cellulolytic system reveals its potential for deconstruction of lignocellulosic biomass in a novel *Streptomyces* sp.¨, *Applied Microbiology and Biotechnology*, *101*(1), pp. 301-319. doi.org/10.1007/s00253-016-7851-7

Polko, J. K., and Kieber, J. J. (2019) ¨The Regulation of Cellulose Biosynthesis in Plants¨ *The Plant Cell*, *31*(2), pp. 282-296. doi.org/10.1105/tpc.18.00760

Postek, M. T., Vladár, A., Dagata, J., Farkas, N., Ming, B., Wagner, R., Raman, A., Moon, R. J., Sabo, R., Wegner, T. H. and Beecher, J. (2011) ¨Development of the metrology and imaging of cellulose nanocrystals¨, *Measurement Science and Technology*, *22*(2), p. 024005. doi.org/10.1088/0957-0233/22/2/024005

Prim, N., Blanco, A., Martínez, J., Pastor, F. I. J. and Diaz, P. (2000) ¨estA, a gene coding for a cell-bound esterase from *Paenibacillus* sp. BP- 23, is a new member of the bacterial subclass of type B carboxylesterases¨, *Research in Microbiology*, *151*(4), pp. 303-312. doi.org/10.1016/S0923-2508(00)00150-9

Quinlan, R. J., Sweeney, M. D., Lo Leggio, L., Otten, H., Poulsen, J.-C. N., Johansen, K. S., Krogh, K. B. R. M., Jørgensen, C. I., Tovborg, M., Anthonsen, A., Tryfona, T., Walter, C. P., Dupree, P., Xu, F., Davies, G. J. and Walton, P. H. (2011) ¨Insights into the oxidative degradation of cellulose by a copper metalloenzyme that exploits biomass components¨, *Proceedings of the National Academy of Sciences of the United States of America*, *108*(37), pp. 15079-15084. doi.org/10.1073/pnas.1105776108

Reeve, D. W. (2012) ¨Chlorine Dioxide Bleaching¨, *TAPPI Notes*, pp. 135-165. doi.org/10.1016/B978-0-444-59421-1.00006-5

Revin, V., Liyaskina, E., Nazarkina, M., Bogatyreva, A. and Shchankin, M. (2018) ¨Cost-effective production of bacterial cellulose using acidic food industry by-products¨, *Brazilian Journal of Microbiology*, *49*, pp. 151-159. doi.org/10.1016/j.bjm.2017.12.012

Robledo, M., Rivera, L., Jiménez-Zurdo, J. I., Rivas, R., Dazzo, F., Velázquez, E., Martínez-Molina, E., Hirsch, A. M., and Mateos, P. F. (2012) ¨Role of *Rhizobium* endoglucanase CelC2 in cellulose biosynthesis and biofilm formation on plant roots and abiotic surfaces¨, *Microbial Cell Factories*, *11*, pp. 1-12. doi.org/10.1186/1475-2859-11-125

Rol, F., Belgacem, M. N., Gandini, A., and Bras, J. (2019) ¨Recent advances in surface-modified cellulose nanofibrils¨, *Progress in Polymer Science*, *88*, pp. 241-264. doi.org/10.1016/j.progpolymsci.2018.09.002

Roman, M., Dong, S., Hirani, A. and Lee Y.W. (2009) ¨Cellulose Nanocrystals for Drug Delivery¨, *ACS Symposium Series,* 1017, pp. 81–91. doi: 10.1021/bk-2009-1017.ch004.

Römling, U., and Galperin, M. Y. (2015) ´Bacterial cellulose biosynthesis: diversity of operons, subunits, products, and functions¨ *Trends in Microbiology*, *23*(9), pp. 545-557. doi.org/10.1016/j.tim.2015.05.005

Roncero, M. B. and Vidal T. (2007) ¨Optimización del tratamiento con ozono en el blanqueo TCF de pastas para papel¨, *Afinidad : órgano de la Asociación de Químicos del Instituto Químico de Sarría.*, *64*(529), pp. 420-428.

Rosano, G. L. and Ceccarelli, E. A. (2014) ¨Recombinant protein expression in *Escherichia coli*: Advances and challenges¨, *Frontiers in Microbiology*, *5*, pp. 1-17. doi.org/10.3389/fmicb.2014.00172

Rosenboom, J.-G., Langer, R., and Traverso, G. (2022) ¨Bioplastics for a circular economy¨, *Nature Reviews Materials*, *7*(2), pp. 117-137. doi.org/10.1038/s41578-021-00407-8

Ross, P., Mayer, R., and Benziman, M. (1991) ¨Cellulose biosynthesis and function in bacteria¨, *Microbiological reviews*, *55*(1), pp. 35-58. doi.org/10.1128/mr.55.1.35-58.1991

Roukas, T. and Kotzekidou, P. (2022) ¨From food industry wastes to second generation bioethanol: a review¨ *Reviews in Environmental Science and Bio/Technology*, *21*(1), pp. 299-329. doi.org/10.1007/s11157-021-09606-9

Russo, D. A., Zedler, J. A. Z., Wittmann, D. N., Möllers, B., Singh, R. K., Batth, T. S., van Oort, B., Olsen, J. V., Bjerrum, M. J. and Jensen, P. E. (2019) ¨Expression and secretion of a lytic polysaccharide monooxygenase by a fast-growing cyanobacterium¨, *Biotechnology for Biofuels*, *12*(1), p. 74. doi.org/10.1186/s13068-019-1416-9

Sabbadin, F., Hemsworth, G. R., Ciano, L., Henrissat, B., Dupree, P., Tryfona, T., Marques, R. D. S., Sweeney, S. T., Besser, K., Elias, L., Pesante, G., Li, Y., Dowle, A. A., Bates, R., Gomez, L. D., Simister, R., Davies, G. J., Walton, P. H., Bruce, N. C. and McQueen-Mason, S. J. (2018) ¨An ancient family of lytic polysaccharide monooxygenases with roles in arthropod development and biomass digestion¨, *Nature Communications*, *9*(1), pp. 756. doi.org/10.1038/s41467-018-03142-x

Sainz-Polo, M. A., González, B., Menéndez, M., Pastor, F. I. J. and Sanz-Aparicio, J. (2015) ¨Exploring Multimodularity in Plant Cell Wall Deconstruction¨, *Journal of Biological Chemistry*, *290*(28), pp. 17116-17130. doi.org/10.1074/jbc.M115.659300

Saleh, A. K., El-Gendi, H., Soliman, N. A., El-Zawawy, W. K., and Abdel-Fattah, Y. R. (2022) ¨Bioprocess development for bacterial cellulose biosynthesis by novel *Lactiplantibacillus plantarum* isolate along with characterization and antimicrobial assessment of fabricated membrane¨, *Scientific Reports*, *12*(1), pp. 1-17. doi.org/10.1038/s41598-022-06117-7

Sánchez, M. M., Fritze, D., Blanco, A., Spröer, C., Tindall, B. J., Schumann, P., Kroppenstedt, R. M., Diaz, P. and Pastor, F. I. J. (2005) ¨*Paenibacillus barcinonensis* sp. nov., a xylanase-producing bacterium isolated from a rice field in the Ebro River delta¨, *International Journal of Systematic and Evolutionary Microbiology*, *55*(2), pp. 935-939. doi.org/10.1099/ijs.0.63383-0

Sánchez, M. M., Pastor, F. I. J. and Diaz, P. (2003) ¨Exo-mode of action of cellobiohydrolase Cel48C from *Paenibacillus* sp. BP-23. A unique type of cellulase among Bacillales¨*, European Journal of Biochemistry*, *270*(13), pp. 2913-2919. doi.org/10.1046/j.1432-1033.2003.03673.x

Selig, M. J., Vuong, T. V., Gudmundsson, M., Forsberg, Z., Westereng, B., Felby, C. and Master, E. R. (2015) ¨Modified cellobiohydrolase–cellulose interactions following treatment with lytic polysaccharide monooxygenase CelS2 (Sc LPMO10C) observed by QCM-D¨, *Cellulose, 22,* pp. 2263-2270

Sevillano, L., Díaz, M. and Santamaría, R. I. (2017) ¨Development of an antibiotic marker-free platform for heterologous protein production in *Streptomyces*¨, *Microbial Cell Factories*, *16*(1), pp. 1-13. doi.org/10.1186/s12934-017-0781-y

Sewsynker-Sukai, Y., David, A.N. and Kana, E. B.G. (2020) ¨Recent developments in the application of kraft pulping alkaline chemicals for lignocellulosic pretreatment: Potential beneficiation of green liquor dregs waste¨, *Bioresource Technology*, *306*, p. 123225. doi.org/10.1016/j.biortech.2020.123225

Sharma, N., Bhardwaj, N. K. and Singh, R. B. P. (2020) ¨Environmental issues of pulp bleaching and prospects of peracetic acid pulp bleaching: A review¨, *Journal of Cleaner Production*, *256*, p. 120338. doi.org/10.1016/j.jclepro.2020.120338

Sianidis, G., Pozidis, C., Becker, F., Vrancken, K., Sjoeholm, C., Karamanou, S., Takamiya-Wik, M., van Mellaert, L., Schaefer, T., Anné, J. and Economou, A. (2006) ¨Functional large-scale production of a novel *Jonesia* sp. xyloglucanase by heterologous secretion from *Streptomyces lividans*¨, *Journal of biotechnology*, *121*(4), pp. 498-507. doi.org/10.1016/j.jbiotec.2005.08.002

Sidar, A., Albuquerque, E. D., Voshol, G. P., Ram, A. F. J., Vijgenboom, E. and Punt, P. J. (2020) "Carbohydrate Binding Modules: Diversity of Domain Architecture in Amylases and Cellulases From Filamentous Microorganisms", *Frontiers in Bioengineering and Biotechnology*, *8*(5), p. 871. doi.org/10.3389/fbioe.2020.00871

Sim, W., Barnard, R., Blaskovich, M. A. T. and Ziora, Z. (2018) ¨Antimicrobial Silver in Medicinal and Consumer Applications: A Patent Review of the Past Decade (2007–2017) ¨, *Antibiotics*, *7*(4), p. 93. doi.org/10.3390/antibiotics7040093

Singh, A., Bajar, S., Devi, A. and Pant, D. (2021) "An overview on the recent developments in fungal cellulase production and their industrial applications", *Bioresource Technology Reports*, *14*, p. 100652. doi.org/10.1016/j.biteb.2021.100652

Skals, P. B., Krabek, A., Nielsen, P. H. and Wenzel, H. (2008) "Environmental assessment of enzyme assisted processing in pulp and paper industry", *The International Journal of Life Cycle Assessment*, *13*(2), pp. 124-132. doi.org/10.1065/lca2007.11.366

Spasojević, D., Zmejkoski, D., Glamočlija, J., Nikolić, M., Soković, M., Milošević, V., Jarić, I., Stojanović, M., Marinković, E., Barisani-Asenbauer, T., Prodanović, R., Jovanović, M. and Radotić, K. (2016) ¨Lignin model compound in alginate hydrogel: a strong antimicrobial agent with high potential in wound treatment¨, *International Journal of Antimicrobial Agents, 48*(6), pp. 732–735. https://doi.org/10.1016/j.ijantimicag.2016.08.014

Sukharnikov, L. O., Cantwell, B. J., Podar, M. and Zhulin, I. B. (2011) ¨Cellulases: Ambiguous nonhomologous enzymes in a genomic perspective¨, *Trends in Biotechnology*, 29(10), pp. 473-479. doi.org/10.1016/j.tibtech.2011.04.008

Sukumaran, R. K., Singhania, R. R. and Pandey, A. (2005) "Microbial cellulases - Production, applications and challenges", *Journal of Scientific and Industrial Research*, *64*(11), pp. 832-844.

Tanpichai, S., Boonmahitthisud, A., Soykeabkaew, N., and Ongthip, L. (2022) ¨Review of the recent developments in all-cellulose nanocomposites: Properties and applications¨, *Carbohydrate Polymers*, *286*, p. 119192. doi.org/10.1016/j.carbpol.2022.119192

Tennakoon, P., Chandika, P., Yi, M., and Jung, W.-K. (2023) ¨Marine-derived biopolymers as potential bioplastics, an eco-friendly alternative¨ *iScience*, *26*(4), p. 106404. doi.org/10.1016/j.isci.2023.106404

Torraspapel. (2009). Formación Fabricación de papel. Torraspapel, pp. 4–57.

Torres, C. E., Negro, C., Fuente, E. and Blanco, A. (2012) ¨Enzymatic approaches in paper industry for pulp refining and biofilm control¨, *Applied Microbiology and Biotechnology*, *96*(2), pp. 327-344. doi.org/10.1007/s00253-012-4345-0

Torres, F. G., Arroyo, J. J., and Troncoso, O. P. (2019) ¨Bacterial cellulose nanocomposites: An all-nano type of material¨, *Materials Science and Engineering: C*, *98*, pp. 1277-1293. doi.org/10.1016/j.msec.2019.01.064

Tuon, F. F., Ramon D., L., Suss, P. H. and Ribeiro, V.S.T. (2022) ¨Pathogenesis of the *Pseudomonas aeruginosa* Biofilm: A Review¨, *Pathogens*, *11*(3), p. 300. doi.org/10.3390/pathogens11030300

Tuveng, T. R., Jensen, M. S., Fredriksen, L., Vaaje-Kolstad, G., Eijsink, V. G. H. and Forsberg, Z. (2020) ¨A thermostable bacterial lytic polysaccharide monooxygenase with high operational stability in a wide temperature range¨, *Biotechnology for Biofuels*, *13*(1), pp. 1-16. doi.org/10.1186/s13068-020-01834-5

UNE Norma española (2014) ¨Papel, cartón, pastas y términos relacionados. Vocabulario. Parte 5: Propiedades de la pasta, el papel y el cartón¨ (UNE 4046-14).

UNE Norma española (2005) ¨Pastas. Preparación de hojas de laboratorio para ensayos físicos. Parte 2: Método Rapid-Köthen¨ (UNE-EN ISO 5269-2:2005).

Vaaje-Kolstad, G., Forsberg, Z., Loose, J. S., Bissaro, B. and Eijsink, V. G. (2017) ¨Structural diversity of lytic polysaccharide monooxygenases¨, *Current Opinion in Structural Biology*, *44*, pp. 67-76. doi.org/10.1016/j.sbi.2016.12.012

Vaaje-Kolstad, G., Horn, S. J., van Aalten, D. M. F., Synstad, B. and Eijsink, V. G. H. (2005) ¨The non-catalytic chitin-binding protein CBP21 from *Serratia marcescens* is essential for chitin degradation¨, *Journal of Biological Chemistry*, *280*(31), pp. 28492-28497. doi.org/10.1074/jbc.M504468200

Vaaje-Kolstad, G., Westereng, B., Horn, S. J., Liu, Z., Zhai, H., Sørlie, M. and Eijsink, V. G. H. (2010) ¨An Oxidative Enzyme Boosting the Enzymatic Conversion of Recalcitrant Polysaccharides¨, *Science*, *330*(6001), pp. 219-222. doi.org/10.1126/science.1192231

Valenzuela, S. V., Diaz, P. and Pastor, F. I. J. (2012) ¨Modular glucuronoxylan-specific xylanase with a family CBM35 carbohydrate-binding module¨, *Applied and environmental microbiology*, *78*(11), pp. 3923-3931. doi.org/10.1128/AEM.07932-11

Valenzuela, S. V., Valls, C., Roncero, M. B., Vidal, T., Diaz, P. and Pastor, F. I. J. (2014a) ¨Effectiveness of novel xylanases belonging to different GH families on lignin and hexenuronic acids removal from specialty sisal fibres¨, *Journal of Chemical Technology & Biotechnology*, *89*(3), pp. 401-406. doi.org/10.1002/jctb.4132

Valenzuela, S. V., Diaz, P. and Pastor, F. I. J. (2014b) ¨Xyn11E from *Paenibacillus barcinonensis* BP-23: A LppX-chaperone-dependent xylanase with potential for upgrading paper pulps¨, *Applied Microbiology and Biotechnology*, *98*(13), pp. 5949-5957. doi.org/10.1007/s00253-014-5565-2

Valenzuela, S. V., Ferreres, G., Margalef, G. and Pastor, F. I. J. (2017) ¨Fast purification method of functional LPMOs from *Streptomyces ambofaciens* by affinity adsorption¨, *Carbohydrate Research*, *448*, pp. 205-211. doi.org/10.1016/j.carres.2017.02.004

Valenzuela, S. V., Lopez, S., Biely, P., Sanz-Aparicio, J. and Pastor, F. I. J. (2016) ¨The Glycoside Hydrolase Family 8 Reducing-End Xylose-Releasing Exo-oligoxylanase Rex8A from *Paenibacillus barcinonensis* BP-23 Is Active on Branched Xylooligosaccharides¨, *Applied and Environmental Microbiology*, *82*(17), pp. 5116-5124. doi.org/10.1128/AEM.01329-16

Valenzuela, S. V., Valls, C., Schink, V., Sánchez, D., Roncero, M. B., Diaz, P., Martínez, J. and Pastor, F. I. J. (2019) ¨Differential activity of lytic polysaccharide monooxygenases on celluloses of different crystallinity. Effectiveness in the sustainable production of cellulose nanofibrils¨, *Carbohydrate Polymers*, *207*, pp. 59-67. doi.org/10.1016/j.carbpol.2018.11.076

Valls, C., Pastor, F. I. J., Roncero, M. B., Vidal, T., Diaz, P., Martínez, J. and Valenzuela, S. V. (2019) ¨Assessing the enzymatic effects of cellulases and LPMO in improving mechanical fibrillation of cotton linters¨, *Biotechnology for Biofuels*, *12*(1), p. 161. doi.org/10.1186/s13068-019-1502-z

Vandhana, T. M., Reyre, J.-L-., Sushmaa, D., Berrin, J.-G., Bissaro, B. and Madhuprakash, J. (2022) ¨On the expansion of biological functions of lytic polysaccharide monooxygenases¨, *New Phytologist*, *233*(6), pp. 2380-2396. doi.org/10.1111/nph.17921

Vasconcelos, N. F., Andrade, F. K., de Araújo P.V., L., Vieira, R. S., Vaz, J. M., Chevallier, P., Mantovani, D., Borges, M. de F. and Rosa, M. de F. (2020) ¨Oxidized bacterial cellulose membrane as support for enzyme immobilization: properties and morphological features¨, *Cellulose*, *27*(6), pp. 3055-3083. doi.org/10.1007/s10570-020-02966-5

Viana, R. M., Sá, N. M. S. M., Barros, M. O., Borges, M. de F., and Azeredo, H. M. C. (2018) ¨Nanofibrillated bacterial cellulose and pectin edible films added with fruit purees¨, *Carbohydrate Polymers*, *196*, pp. 27-32. doi.org/10.1016/j.carbpol.2018.05.017

Villares, A., Moreau, C., Bennati-Granier, C., Garajova, S., Foucat, L., Falourd, X., Saake, B., Berrin, J. G., and Cathala, B. (2017) ¨Lytic polysaccharide monooxygenases disrupt the cellulose fibers structure¨, *Scientific Reports*, *7*, pp. 1-9. doi.org/10.1038/srep40262

Vrancken, K. and Anné, J. (2009) ¨Secretory production of recombinant proteins by *Streptomyces*¨. *Future microbiology*, *4*(2), pp. 181-188. doi.org/10.2217/17460913.4.2.181

Vu, V. V., Beeson, W. T., Span, E. A., Farquhar, E. R. and Marletta, M. A. (2014) ¨A family of starch-active polysaccharide monooxygenases¨, *Proceedings of the National Academy of Sciences of the United States of America*, *111*(38), pp. 13822-13827. doi.org/10.1073/pnas.1408090111

Wahid, F., Hu, X.-H., Chu, L.-Q., Jia, S.-R., Xie, Y.-Y. and Zhong, C. (2019) ¨Development of bacterial cellulose/chitosan based semi-interpenetrating hydrogels with improved mechanical and antibacterial properties¨, *International journal of biological macromolecules*, *122*, pp. 380-387. doi.org/10.1016/j.ijbiomac.2018.10.105

Yamada, Y., Yukphan, P., Vu, H. T. L., Muramatsu, Y., Ochaikul, D., and Nakagawa, Y. (2012) ¨Subdivision of the genus *Gluconacetobacter* Yamada, Hoshino and Ishikawa 1998: the proposal of *Komagatabacter* gen. nov., for strains accommodated to the *Gluconacetobacter xylinus* group in the *α-Proteobacteria*¨, *Annals of Microbiology*, *62*(2), pp. 849-859. doi.org/10.1007/s13213-011-0288-4

Yang, H., and Kubicki, J. D. (2020) ¨A density functional theory study on the shape of the primary cellulose microfibril in plants: effects of C6 exocyclic group conformation and H-bonding¨, *Cellulose*, *27*(5), pp. 2389-2402. doi.org/10.1007/s10570-020-02970-9

Yano, H., Sugiyama, J., Nakagaito, A. N., Nogi, M., Matsuura, T., Hikita, M., and Handa, K. (2005) ¨Optically Transparent Composites Reinforced with Networks of Bacterial Nanofibers¨, *Advanced Materials*, *17*(2), pp. 153-155. doi.org/10.1002/adma.200400597

Yu, M.-J., Yoon, S.-H. and Kim, Y.-W. (2016) ¨Overproduction and characterization of a lytic polysaccharide monooxygenase in *Bacillus subtilis* using an assay based on ascorbate consumption¨ *Enzyme and microbial technology*, *93-94*, pp. 150-156. doi.org/10.1016/j.enzmictec.2016.08.014

Zhang, Z.-X., Nong, F.-T., Wang, Y.-Z., Yan, C.-X., Gu, Y., Song, P. and Sun, X.-M. (2022) ¨Strategies for efficient production of recombinant proteins in *Escherichia coli*: alleviating the host burden and enhancing protein activity¨, *Microbial Cell Factories*, *21*(1), p. 191. doi.org/10.1186/s12934-022-01917-y